HARNESSING INTERSPECIES ANTAGONISM TO ENHANCE ANTIBIOTIC EFFICACY

Lauren Christine Radlinski

A dissertation submitted to the faculty at the University of North Carolina at Chapel Hill in partial fulfillment of the requirements for the degree of Doctor in Philosophy in the Department of Microbiology and Immunology.

Chapel Hill
2020

Approved by:

Brian P. Conlon

Matthew C. Wolfgang

Peggy A. Cotter

Rita Tamayo

Nathaniel J. Moorman

ABSTRACT

Lauren Christine Radlinski:
Harnessing interspecies antagonism to enhance antibiotic efficacy
(Under the direction of Thomas H. Kawula and Brian P. Conlon)

Beyond genetically encoded mechanisms of resistance, the factors that contribute to antibiotic treatment failure within the host are poorly understood. Traditional susceptibility assays fail to account for extrinsic determinants of antibiotic susceptibility present during infection and are therefore poor predictors of treatment outcome. To maximize the reach of current therapeutics, we must develop a more sophisticated understanding of antibiotic efficacy in the infection environment. Here we demonstrate that interspecies interactions between two important opportunistic pathogens, *Pseudomonas aeruginosa* and *Staphylococcus aureus*, alters *S. aureus* response to antibiotics. We show that the *P. aeruginosa*-produced endopeptidase LasA potentiates lysis of *S. aureus* by vancomycin, rhamnolipids facilitate proton-motive force-independent aminoglycoside uptake, and that small molecule 4-hydroxy-2-heptylquinoline-N-oxide (HQNO) induces multidrug tolerance in *S. aureus* through respiratory inhibition and reduction of cellular ATP. We further demonstrate rhamnolipid-mediated potentiation of aminoglycoside uptake and killing of *S. aureus* restores susceptibility to otherwise tolerant persister, biofilm, small colony variant, anaerobic, and resistant *S. aureus* populations.

Furthermore, bacterial pathogens that replicate within the intracellular niche are protected from antibiotics that cannot penetrate the eukaryotic membrane. Identifying and disrupting the pathways used by these pathogens to modify the intracellular niche in order to survive is an alternative strategy for limiting bacterial proliferation. Here, we use *Francisella tularensis* as a model intracellular bacterial pathogen to identify and describe the bacterial metabolic pathways and host-derived nutrients necessary for intracellular and *in vivo* growth. These findings reveal potential new therapeutic targets for disrupting bacterial nutrient acquisition that may be broadly applicable for treating other important intracellular pathogens.

Overall, the findings presented here suggest that antibiotic susceptibility is contingent on a multitude of factors including interspecies interaction and the physiological replicative niche. Further elucidation of key antibiotic susceptibility determinants *in vivo,* as well as of strategies to overcome barriers to antibiotic efficacy may lead to a more holistic and personalized approach to therapy that will aid in the resolution of persistent infection.

ACKNOWLEDGEMENTS

First, I would like to acknowledge my advisors Thomas H. Kawula and Brian P. Conlon for their patient and enthusiastic support over the years. Thanks to Tom for guiding my development as an independent scientist during the first two tumultuous years of graduate school. Thanks to Brian for agreeing to take me on and giving me the opportunity to learn from him as he established his research program at UNC. Overall I am incredibly grateful that my graduate education allowed for the opportunity to learn from both of these amazing mentors and scientists. Next, thank you to the Kawula and Conlon lab members who have supported these projects through lively discussion and help at the bench. In particular, I want to acknowledge Sarah E. Rowe for her contribution to Chapter 2 and Jason Brunton and Shaun Steele for their work on Chapter 4. Further, I want to acknowledge the members of my committee for providing much insightful discussion and encouragement. I would also like to collectively thank all the members of the UNC Microbiology and Immunology Department, in particular those willing to stay out late for even more lively and insightful discussions. Lastly, I want to thank my family and my partner Thuvi for all the love and support over the years. I would never have gotten this far without you.

TABLE OF CONTENTS

LIST OF TABLES

LIST OF FIGURES

LIST OF ABBREVIATIONS

ADEP	acyldepsipeptide
AICAR	5-amnoimidazole-4-carboxamide ribonucleotide
AME	aminoglycoside-modifying enzyme
AMP	adenosine monophosphate
AMPK	AMP-dependent protein kinase
AMPs	antimicrobial peptides
$AsKO_2$	potassium arsenate
ATGL	adipose triglyceride lipase
ATP	adenosine triphosphate
AI-2	autoinducer-2
BAL	bronchoalveolar lavage
BHI	brain heart infusion
BMDM	bone marrow-derived macrophage
BSA	bovine serum albumin
Cam	chloramphenicol
CCCP	carbonyl cyanide 3-chlorophenylhydrazone
CDM	Chamberlain's defined media
CEAAs	cell envelope-acting agents
CF	cystic fibrosis
CFU	colony-forming units
Cip	ciprofloxacin
C_{max}	maximum serum concentration

Da	Dalton
DMEM	Dulbecco's modified Eagle medium
Erm	erythromycin
F6P	fructose 6-phosphate
FBP	fructose 1,6-bisphosphate
FICI	fractional inhibitory concentration index
G3P	glycerol-3 phosphate
Gent	gentamicin
GFP	green fluorescent protein
GdhA	glutamate dehydrogenase
GlpA	glycerol-3P dehydrogenase
GlpK	glycerol kinase
GlpX	1,6-bisphosphatase
GML	glycerol monolaurate
HGT	horizontal gene transfer
HI	heat inactivated
HCN	hydrogen cyanide
HQNO	2-heptyl-4-hydroxyquinoline *N*-oxide
Kan	kanamycin
LB	Luria-Bertani broth
LC-MS/MS	liquid chromatography tandem mass spectrometry
MaeA	malate dehydrogenase
MFI	mean fluorescence intensity

MIC	minimum inhibitory concentration
MHB	Mueller-Hinton broth
MMH	modified Mueller-Hinton broth
MOI	multiplicity of infection
MRSA	methicillin-sensitive *Staphylococcus aureus*
MSSA	methicillin-resistant *Staphylococcus aureus*
NaCN	sodium cyanide
NO	nitric oxide
NO_3	nitrate
O_2	molecular oxygen
OD	optical density
PBS	phosphate-buffered saline
PckA	phosphoenol pyruvate carboxykinase
PCR	polymerase chain reaction
PEP	phosphoenol pyruvate
PfkA	phosphofructokinase
PPAR-γ	peroxisome proliferator-activated receptor gamma
PK/PD	pharmacokinetic/pharmacodynamics
PMB	polymyxin B
PMF	proton motive force
PpdK	pyruvate-phosphate dikinase
PYO	pyocyanin
qRT-PCR	quantitative reverse transcription polymerase chain reaction

QS	quorum sensing
RL	rhamnolipid
RLU	relative luminescence units
RNS	reactive nitrogen species
ROS	reactive oxygen species
SCV	small colony variant
SD	standard deviation
TA	toxin/antitoxin
Tob	tobramycin
TSB	tryptic soy broth
Vanc	vancomycin
WT	wild-type

CHAPTER 1
ANTIMICROBIAL STRATEGIES FOR THE COMPLEX INFECTION ENVIRONMENT[1]

Since the discovery of penicillin in 1928, antibiotics have become an essential component of modern healthcare. They have made once life-threatening infections readily treatable, greatly prolonged the lives of immunocompromised individuals, and made possible the routine undertaking of invasive surgical procedures. Currently, however, we are facing a growing crisis as resistance to antibiotics continues to spread, while the discovery of new antibiotics has stagnated[1,2]. For these reasons, it is more important than ever to use current antibiotics as effectively and appropriately as possible, and to develop novel strategies to eradicate difficult-to-treat bacterial populations before they evolve resistance. As part of this effort, we must develop a more sophisticated understanding of antibiotic efficacy in the infection environment. This task involves identifying the extrinsic factors that directly potentiate or antagonize antibiotic action during treatment, understanding how antagonistic and synergistic interactions can be overcome and exploited to enhance antibiotic efficacy, and to develop novel strategies for targeting bacterial populations that are refractory to current therapeutics. Approaching patient treatment from a holistic point of view that considers the physiological state of an infecting organism as well as the external determinants of antibiotic susceptibility within the patient may improve our understanding of why

[1]Adapted and expanded from: Radlinski LC, Conlon BP. 2017. Antibiotic efficacy in the complex infection environment. *Current Opinion in Microbiology.*

antibiotic treatment failure occurs, and reveal opportunities for improving treatment outcome to promote patient health.

PART I. ANTICIPATING AND AVOIDING ANTIBIOTIC TREATMENT FAILURE

Antibiotic treatment failure: resistance vs. tolerance

Antibiotic treatment failure is most commonly associated with resistance. Antibiotic resistance occurs when a bacterium acquires a genetically heritable trait, typically through chromosomal mutation or horizontal gene transfer, that allows the organism to grow in increasing concentrations of an antibiotic. Resistance-conferring mutations include those resulting in target site alteration, induction of drug efflux, metabolic bypass of the drug's target, or direct enzymatic inactivation of the antibiotic[3]. An increase in resistance corresponds with an increase in the minimum inhibitory concentration (MIC) of an antibiotic necessary to stop the growth of a bacterium. Resistance becomes life threatening when the MIC of a resistant isolate surpasses the maximum achievable concentration of antibiotic deliverable to the site of infection, as the drug will no longer inhibit growth of the pathogenic bacterial population within the host. Antibiotic resistance represents an increasingly urgent threat to public health as highlighted by a 2019 report by the Centers for Disease Control (CDC) that stated that more than 2.8 million cases of antibiotic resistant infections occur each year leading to over 35,000 deaths in the US alone[4].

Paradoxically, clinical isolates often exhibit full sensitivity to the administered antibiotics as measured through *in vitro* MIC assay*,* suggesting that treatment failure cannot be fully explained by the acquisition of resistance. Instead, there is a growing appreciation for the contribution of antibiotic tolerance to treatment failure[5–7].

Antibiotic tolerance is a phenotypic switch, usually to a metabolically quiescent state, that allows a subpopulation of bacteria to survive transient exposure to lethal antibiotic concentrations (Figure 1.1). As a tolerant population does not grow in the presence of antibiotic, this phenomenon is not associated in a change in MIC and thus tolerant bacterial populations often go undetected by *in vitro* clinical susceptibility assays[8]. Upon removal of the antibiotic, a tolerant population that has survived treatment will resume replication, and progeny of that population are equally susceptible to antibiotic killing relative to the parental cells. In the context of patient health, a tolerant bacterial population that has survived antibiotic therapy by entering a dormant state can resuscitate and resume growth upon the cessation of treatment, thus contributing to chronic and relapsing disease[9–11].

Though antibiotic tolerance and resistance are distinct phenomena, the two are clinically and conceptually related. Poor adhesion to antibiotic therapy regimens has long been associated with the rise of antibiotic resistance, as intermittent antibiotic exposure selects for the outgrowth of resistant subpopulations. In a similar way, recent *in vitro* studies with *Escherichia coli* have demonstrated that intermittent exposure to ampicillin selects for bacterial populations that are highly tolerant to ampicillin killing[12]. These tolerant populations acquire mutations that prolong population lag time without changing the MIC. Though these mutations are genetically heritable, this is not considered a mechanism of resistance, as the tolerant mutants are equally susceptible to antibiotic killing once the population enters exponential growth. However, Levin-Reisman *et al.* recently demonstrated that antibiotic tolerance precedes resistance, suggesting that extended periods of antibiotic tolerance may facilitate the evolution of

antibiotic resistance [13]. Further, Liu *et al* demonstrated that during the treatment of clinical isolates with combinational antibiotics, tolerance preceded the emergence of resistance[14]. Thus, within the host, incomplete clearance of a bacterial population during antibiotic therapy likely increases the frequency of antibiotic tolerance and drives the evolution of resistance.

Antibiotic tolerance was also recently implicated in the spread of antibiotic resistance mechanisms among bacterial species through horizontal gene transfer. The facultative intracellular enteric pathogen *Salmonella enterica* serovar Typhimurium (*S.* Typhimurium) colonizes both the lumen of the intestinal tract and within the cells of various host tissues. Luminal populations of *S.* Typhimurium are rapidly cleared by antibiotics[15]. However, tissue-associated, intracellular *S.* Typhimurium can tolerate antibiotic therapy for extended periods of time[16,17]. Following cessation of treatment, tolerant *S.* Typhimurium cells that have survived treatment resuscitate and migrate to the luminal space of the colon[18]. *In vivo* studies by Bakkeren *et al.* showed that these tissue-associated *S.* Typhimurium populations act as a bacterial reservoir for plasmids encoding clinically relevant mechanisms of resistance including β-lactamase activity[15]. After re-seeding the lumen of the gut, these cells can act as donors or recipients to facilitate the spread of resistance plasmids among various Enterobacteriaceae species, thus fostering the spread of antibiotic resistance among various members of the microbiota.

Antibiotic tolerance is associated with ATP depletion

Antibiotics can be divided into two broad categories, bacteriostatic and bactericidal, based on their ability to inhibit growth or kill bacteria, respectively. As

tolerance describes the capacity of a population to specifically survive antibiotic killing, persistence is defined only for bactericidal and not bacteriostatic antibiotics. Bactericidal antibiotics kill bacteria by corrupting active cellular processes[19]. Binding of aminoglycosides to the 30S subunit of the ribosome, for instance, does not inhibit protein synthesis, but instead facilitates mistranslation through incorporation of incorrect amino acids into the elongating peptide strand[20]. These misfolded proteins then proceed to wreak havoc on cell membrane permeability and other important functions, and eventually lead to cell death[19]. Similarly, quinolone antibiotics bind bacterial topoisomerase-DNA complexes to prevent strand rejoining following DNA cleavage. This essentially converts the topoisomerase into an endopeptidase that generates lethal double-stranded breaks in the bacterial chromosome[21]. Translation, DNA replication, and most other antibiotic targets are ATP-dependent processes, thus a reduction in intracellular ATP that occurs during metabolic dormancy is associated with a reduction in the number of active targets available for antibiotic action and an increase in antibiotic tolerance. Metabolic dormancy is associated with the induction of multidrug tolerance, suggesting that ATP depletion protects cells from multiple mechanisms of antibiotic killing.

In 1944 the microbiologist Joseph Bigger observed that a small sub-population of genetically susceptible *Staphylococcus aureus* cells survive intensive penicillin treatment[22]. Bigger termed this distinct subpopulation of cells ‘persisters.’ As with tolerance, persisters survive lethal antibiotic challenge without a change in MIC. The terms ‘tolerance’ and ‘persistence’ are often used interchangeably, however persistence is specifically defined as a special case of tolerance wherein a subpopulation of cells

survive antibiotic activity much better than the larger overall population (Figure 1.1) [23]. This phenomenon is readily observed *in vitro* and is characterized by a biphasic killing pattern where the bulk of the susceptible population succumbs to antibiotic killing at a much faster rate than the subpopulation of persister cells[8].

In all bacterial species tested, a small subset of cells (typically 0.001-1% of the population) stochastically enters an antibiotic-tolerant persister state, regardless of culture environment or growth phase[24,25]. To date, the precise mechanism(s) that facilitate the persister cell formation within an unstressed, exponentially growing culture are poorly understood. In *S. aureus* and *E. coli,* persister cells are associated with stochastic entrance into a stationary-phase-like state accompanied by a drop in intracellular ATP concentration[26,27]. Indeed, a population-wide state of tolerance can be induced in *S. aureus* through exposure to arsenate, which depletes intracellular ATP through futile cycling of ADP-As[26,28]. These findings support a “low-energy” hypothesis of persister cell formation, which proposes that ATP depletion is responsible for the induction of antibiotic tolerance. We recently demonstrated that within a growing culture, *S. aureus* cells with low expression of TCA cycle enzymes, and thus low levels of ATP generation, are tolerant to antibiotic killing[29]. This finding led to the hypothesis that stochastic fluctuation in TCA cycle enzymes may represent a prominent mechanism of persister cell formation in *S. aureus*.

Regardless of the specific mechanism responsible for persister cell formation, the frequency of antibiotic tolerant cells within a population can be increased through exposure to environmental stressors, including nutrient limitation[30], high cell density[31], and exposure to reactive oxygen species[32]. Many of these factors

influence the metabolic state of the bacterial population. For instance, as cultures of *S. aureus* approach stationary phase, nutrients become scarce and population density increases exponentially. Subsequently, *S. aureus* entrance into stationary phase is associated with a drop in ATP and a population-wide state of tolerance[26]. Similarly, in *E. coli* biofilm*,* amino acid starvation precipitates a significant increase in tolerance to ofloxacin challenge[33]. In general, nutrient starvation and subsequent persister cell formation has been attributed as a primary contributing factor to the refractory nature of bacterial biofilms to antibiotic activity[10,33,34].

Though metabolic dormancy often induces antibiotic tolerance, single cell analysis of tolerant populations has led researchers to appreciate that tolerance does not always require ATP depletion. Recent work by Stapels *et al.* demonstrated that *Salmonella* Typhimurium persisters within macrophages maintain metabolic activity[35]. Non-growing, intracellular *S.* Typhimurium persisters are transcriptionally and translationally active, and reprogram infected macrophages to drive M2 polarization and dampen the pro-inflammatory immune response [35]. Similarly, Pontes *et al.* demonstrated that treating *Salmonella* cultures with the bacteriostatic antibiotic chloramphenicol induces tolerance to ciprofloxacin and cefotaxime, despite the fact that inhibiting protein synthesis increases population-wide ATP levels[36]. Here the authors suggest that in this instance antibiotic tolerance is dependent on growth rate alone, and occurs independently of ATP. These studies raise interesting questions about the precise relationship linking bacterial ATP levels, antibiotic target activity, and tolerance.

Other factors that contribute to antibiotic treatment failure

Antibiotics must access a site of infection to kill or inhibit the growth of a pathogen population. Pharmacokinetic/pharmacodynamics (PK/PD) studies determine the maximum serum concentration (C_{max}) of an antibiotic achievable within the serum of the host. For simplicity, maximum serum concentrations are often substituted for antibiotic C_{max} concentrations at specific tissue or organ sites where most bacterial infections actually occur. Penetration of the antibiotic from serum to target tissue site depends on several factors including the molecular characteristics of the drug, the type of tissue infected, and the degree of inflammation[37]. Penetration occurs more rapidly in highly vascularized tissues, such as the liver. Poorly vascularized infection sites frequently reach lower antibiotic concentrations and are more difficult to target with antibiotics[38]. Osteomyelitis, for instance, is notoriously difficult to resolve through antibiotic therapy, and inadequate drug penetration due to low tissue vascularization may be partially responsible. A recent systematic review by Thabit *et al.* compiled data from a number of pharmacokinetic studies assessing the extent of antibiotic penetration into bone and joint tissues[39]. The range, peak (C_{max}), or mean concentrations of over 30 different antibiotics were contrasted with MIC for the most common Gram-positive bacterial species associated with osteomyelitis. Quinolones, macrolides and linezolids penetrated bone and joint tissue well, meeting or exceeding the MIC_{90} values for most pathogens tested, however penicillins and cephalosporins poorly penetrated the infection site[38]. Inadequate drug concentrations may contribute to antibiotic treatment failure by selecting for the outgrowth of resistant strains[40]. Further, exposure to sublethal antibiotic concentrations can induce a state of tolerance, as was recently

demonstrate in *P. aeruginosa*[41]. Thus, the factors that control drug penetration must be considered when selecting an appropriate therapeutic approach.

Furthermore, antibiotics often must access specific molecular target sites on the bacterium to facilitate death. Vancomycin is a frontline glycopeptide antibiotic used for the treatment of methicillin-resistant *S. aureus* (MRSA). Despite its widespread use, vancomycin treatment failure for endocarditis, bacterial pneumonia, or bacteremia range from 37-50%[42]. Vancomycin is hydrophilic molecule with a high molecular weight (over 1,400 Da) that readily binds plasma protein, resulting in poor tissue penetration[37]. Upon reaching infected tissue, vancomycin must specifically bind to D-Ala-D-Ala residues of bacterial lipid II peptidoglycan precursor during cell wall biosynthesis to elicit bactericidal activity[43]. Vancomycin also binds peptidoglycan of the mature cell wall, but this interaction does not kill the bacterium and instead contributes to treatment failure as dense populations with excess non-lethal binding sites prevent vancomycin from accessing target lipid II[44]. For this reason, vancomycin fares poorly against stationary and biofilm associated *S. aureus* because these dense populations with thick cell walls contain many decoy D-Ala-D-Ala binding targets that limit vancomycin bactericidal activity[45,46]. Newly developed cell wall-acting antibiotics circumvent this obstacle by specifically binding lipid II at the *S. aureus* septum without binding mature peptidoglycan, and are thus much more effective against bacterial populations at high cell densities[47,48]

Similar to vancomycin, aminoglycoside failure is often attributed to the inability of these drugs to access bacterial ribosomal targets. Aminoglycoside antibiotics are hydrophilic, positively charged, and typically around 400 Da in size[37]. Due to their size

and charge, aminoglycosides do not readily penetrate eukaryotic membranes through passive diffusion[49]. Instead, eukaryotic uptake of aminoglycoside antibiotics likely results from active cellular mechanisms such as pinocytosis, and consequently intracellular aminoglycoside accumulation is a slow process that typically takes 48-72 hours to reach detectable levels[49]. For this reason, prolonged aminoglycoside therapy is often necessary for resolving infections caused by intracellular pathogens.

Even against extracellular bacteria, aminoglycoside efficacy is hindered by poor membrane penetration. Bacterial aminoglycoside uptake occurs through proton motive force (PMF)-mediated passive diffusion[50]. In bacterial populations that are non-respiring, the PMF often falls below the threshold necessary for drug uptake. External factors that induce a phenotypic non-respiring state eventually select for genetically heritable aminoglycoside resistance. For instance, long-term exposure to subinhibitory concentrations of tobramycin selects for highly resistant *S. aureus* small colony variants (SCVs)[51]. Clinically isolated *S. aureus* SCVs are often auxotrophic for various electron transport components required for respiration such as menaquinone (e.g. *menD*), or hemin biosynthesis (e.g. *hemB*)[52]. However, aminoglycoside exclusion can occur without genetic mutation, as the absence of a terminal electron acceptor (e.g. O_2, NO_3) or the presence of a respiration inhibitor (e.g. hydrogen cyanide) can select for a SCV phenotype *in vivo*[53]. In these cases, facultative anaerobic species such as *S. aureus* can tolerate high concentrations of aminoglycoside antibiotics by switching to a non-respiring, fermentative metabolism[53]. Interestingly, this is considered an example of an ATP-independent mechanism of antibiotic tolerance, as *S. aureus* can readily

maintain adequate energy levels for growth and replication through fermentative metabolism in the presence of sufficient glycolytic carbon substrates.

Antibiotic susceptibility assays are poor predictors of treatment outcome

Current clinical antibiotic susceptibility testing consists primarily of *in vitro* diagnostic assays (e.g. MIC assay) that measure the ability of an antibiotic to inhibit growth of a pure bacterial culture grown under artificial conditions. However, these assays do not assess the ability of a drug to eradicate an existing bacterial population, and fail to account for extrinsic determinants of antibiotic susceptibility present in the complex infection milieu. Further, while MIC assays are important for characterizing the resistance profiles of infectious isolates, they do not assess the capacity of those isolates to tolerate the presence of the antibiotic. Indeed, several studies have demonstrated poor correlation between clinical antibiotic susceptibility testing and subsequent treatment outcome[54,55]. This poor correlation is particularly problematic in the case of deep-seated, chronic infections that fail to respond to prolonged antibiotic therapy despite apparent drug susceptibility. This suggests that environmental factors present within the host may influence a pathogen's susceptibility to antibiotic killing.

During infection, host-pathogen interactions, interspecies microbial interactions and metabolic heterogeneity in the infection environment can contribute to the success or failure of antibiotic therapy in patients (Figure 1.2). Identification and consideration of the factors present within the infection environment that impact the ability of an antibiotic to inhibit bacterial growth and/or kill bacterial cells will improve our ability to predict

efficacy in patients, reduce the duration of antibiotic therapy and decrease the risk of treatment failure, thereby minimizing the development and spread of antibiotic resistance.

Host-microbe interactions that influence antibiotic susceptibility

Inhibition of bacterial growth by bacteriostatic antibiotics gives the host immune system a chance to contain and eliminate an infectious bacterial population. Similarly, while bactericidal antibiotics facilitate cell death, even powerful bactericidal agents fail to completely eradicate bacterial populations, as antibiotic tolerant persister cells can survive in the presence of the antibiotic for long periods of time[22,56]. Hence, both bacteriostatic and bactericidal antibiotics rely on cooperation with the immune system to fully clear an infection. In some cases, this cooperation may simply be additive, whereas an antibiotic inhibits growth or kills a portion of the population and the immune system then eliminates the survivors. On the other hand, specific host-bacterial interactions may specifically inhibit or potentiate antibiotic efficacy. Such antagonistic or synergistic interactions are only recently coming to light and their impact on *in vivo* efficacy is yet to be fully appreciated.

By comparing antibiotic efficacy in the presence or absence of host factors, Sakoulas *et al.* observed that β-lactam antibiotics synergize with the host immune response to potentiate bactericidal activity. Specifically, they found that ampicillin treatment can kill “ampicillin resistant” populations of *Enterococcus faecium* by altering cell surface charge and increasing the pathogen’s sensitivity to the action of host antimicrobial peptides (AMPs)[57]. Similarly, *Staphylococcus aureus* populations,

considered β-lactam resistant by MIC testing, were sensitized to killing by various host factors following β-lactam exposure[58]. Furthermore, in a murine model of intratracheal infection, it was found that the macrolide antibiotic, azithromycin, synergizes with the host cathelicidin antimicrobial peptide, LL-37, resulting in bactericidal activity against *Pseudomonas aeruginosa, Klebsiella pneumoniae*, *Acinetobacter baumannii* and more recently *Stenotrophomonas maltophilia*, despite an apparent lack of susceptibility to azithromycin by MIC testing[59,60]. It is likely that other as yet unidentified interactions with host factors synergize with commonly used antibiotics to promote efficacy within a patient.

Interactions with the host may also be inhibitory to certain antibiotic activities. For instance, innate defenses can induce phenotypic resistance to the last-line antibiotic colistin in *Enterobacter cloacae* via activation of the histidine kinase PhoQ[61]. Importantly, in this study Band *et al.* demonstrate that an *E. cloacae* isolate described as colistin-susceptible via common clinical susceptibility testing can proliferate in the presence of colistin *in vivo,* leading to treatment failure and host death. Host-produced nitric oxide (NO) can inhibit PMF-dependent uptake of aminoglycoside antibiotics by inhibiting bacterial respiration and thus PMF generation in *Salmonella, P. aeruginosa,* and *S. aureus* [62], and DNA damage from exposure to reactive oxygen species (ROS) can induce persister cell formation in *E. coli* via the upregulation of toxin and drug efflux pump expression[63].

The clearest example of the potentially antagonistic relationship between the host immune response and antibiotic activity is the ability of numerous pathogens to survive within phagocytic cells, where the adoption of an intracellular lifestyle often

correlates with decreased antibiotic sensitivity[64–66]. Within this niche, bacteria are often physically protected from certain antibiotics, such as aminoglycosides, that penetrate poorly into host cells[67]. However, poor drug penetrance cannot fully explain treatment failure in this environment, suggesting that other factors may contribute to the refractory nature of intracellular pathogens to antibiotic therapy[65,68,69]. Within the phagosome, bacteria face a variety of stressors including phagosome acidification, nutrient sequestration, and exposure to reactive oxygen and nitrogen species[70]. For *Salmonella* Typhimurium, vacuolar acidification and nutrient deprivation induces antibiotic-tolerant persister cell formation through toxin-antitoxin module activation[17]. Similarly, nitrosative stress within the phagosome induces antibiotic tolerance of internalized *Mycobacterium tuberculosis*[71].

Recent appreciation for the capacity of *S. aureus* to persist within macrophages has led the hypothesis that infected macrophages may act as an important reservoir and mechanism of dissemination during infection[68]. Intracellular *S. aureus* is highly tolerant to killing by antibiotics, even against antibiotics that penetrate well into the intracellular space[32]. We recently demonstrated that ROS produced during respiratory burst induce a highly antibiotic tolerant state in *S. aureus*[32]. Within the phagosome, host-produced ROS attack *S. aureus* iron-sulfur cluster-containing proteins, including TCA cycle enzymes, to inhibit respiration and reduce bacterial ATP levels[32]. This was demonstrated to contribute to antibiotic treatment failure in a murine model of systemic *S. aureus* infection. Together, these findings suggest that a primary component of the innate immune response may be inadvertently antagonistic to antibiotic activity against *S. aureus* and potentially other intracellular pathogens.

These examples represent a microcosm of the many host-microbe interactions that influence antibiotic efficacy during infection. An improved understanding of how host factors mediate antibiotic susceptibility will improve our ability to predict antibiotic efficacy *in vivo*. Furthermore, consideration of these factors may lead to novel antimicrobial strategies with enhanced activity within the complex host environment.

Interspecies interaction during polymicrobial infection alters antibiotic susceptibility

Rather than existing in isolation, invading microorganisms frequently encounter a complex polymicrobial community within the host, where interactions with the resident microbiota or co-infecting pathogens can directly influence the overall structure and dynamics of the community. Antibiotic susceptibility within this complex environment may vary dramatically from that of the same organism grown in pure culture[72]. An excellent example of community based antibiotic resistance can be seen in the deactivation of an antibiotic by a single bacterial species, extracellularly or intracellularly, leading to *de facto* antibiotic resistance of the entire community[73,74]. In this case, antibiotic sensitive pathogens may elude antibiotic killing due to the activities of a co-existing organism[73]. As microbial expression of resistance factors such as antibiotic-modifying enzymes come with a fitness cost, during such instances of social "cheating" an antibiotic susceptible pathogen population can escape antibiotic action without the associated fitness or virulence cost[75,76].

In addition to antibiotic deactivation, interspecies interactions can alter microbial metabolism and physiology to induce transient resistance or tolerance to antibiotics. For instance, production of the respiratory toxin 2-heptyl-4-hydroxyquinoline *N*-oxide

(HQNO) by *P. aeruginosa* elicits aminoglycoside tolerance in *S. aureus* by inhibiting the electron transport chain and depleting *S. aureus* cellular PMF, a necessary pre-requisite for aminoglycoside uptake[53]. *P. aeruginosa*-produced HQNO has also been shown to induce vancomycin tolerance in *S. aureus* by shifting *S. aureus* into a fermentative lifestyle[77]. As these pathogens frequently co-exist within the cystic fibrosis lung and in chronic wound infections, these interactions may represent an important determinant of antibiotic treatment outcome. Intraspecies quorum sensing (QS) has also been associated with changes in the susceptibility of a population to antibiotic killing. Production of the QS molecules CSP and acyl-homoserine lactone mediate multidrug-tolerant persister cell formation within populations of *Streptococcus mutans* and *P. aeruginosa*, respectively[78,79]. In an interesting example of interspecies crosstalk, indole production by the native commensal *E. coli* was demonstrated to induce antibiotic tolerance in pathogenic *Salmonella enterica* Typhimurium[80]. Similarly, interception of *Haemophilus influenzae* autoinducer-2 (AI-2) by *Moraxella catarrhalis* significantly increases *M. catarrhalis* tolerance to antibiotics through the induction of *M. catarrhalis* biofilm formation[81]. Indeed, biofilm-associated infections have long been associated with antibiotic treatment failure, and these infections are often polymicrobial in nature[82]. Biofilm matrix production by one microbial species may induce antibiotic tolerance in another. In a recent example, it was demonstrated that *C. albicans* extracellular matrix production during dual-species biofilm formation protects *S. aureus* from antibiotic killing *in vivo*[83].

In all, studying bacterial pathogenesis outside of artificial monoculture is not only more representative of the conditions encountered during infection, but also reveals

instances where factors produced by one species can inadvertently influence the susceptibility of another to antimicrobial activities. Interspecies interactions can induce antibiotic resistance or tolerance, which may have a deleterious impact on antibiotic efficacy[72]. It is also likely that synergistic interactions occur that increase antibiotic efficacy, though only a few instances have been reported so far [84,85]. Identifying the determinants of antibiotic susceptibility in complex communities rather than relying on potentially misleading information garnered from monoculture susceptibility assays is essential for improving our ability to efficiently treat polymicrobial infection.

Physiological determinants of antibiotic susceptibility

Currently, antibiotic susceptibility is measured in nutrient rich media, under aerobic conditions, free of most stressors typically encountered during infection. However, the complex “macro-ecosystem” of a host is composed of a variety of physiologically distinct microenvironments subject to bacterial colonization. Nutrient availability and overall physiological states within these distinct niches can vary drastically, and promote stark differences in bacterial metabolism. Even within the same spatial niche there often exists a significant degree of environmental heterogeneity, with aerobic, microaerophilic and anaerobic microniches in close proximity. Such is the case in late stage CF patients, where decreased mucociliary clearance promotes the formation of mucus plugs within the alveoli of the lungs, creating anoxic microenvironments within the aerobic lung[86]. Oxygen penetration is also often severely hampered in wound infections and abscesses[87,88]. Indeed, obligate anaerobes are frequently isolated from the CF lung as well as from polymicrobial wound

infections, implying that anoxic microenvironments exist within these infection sites[86,89]. Within the heterogeneous infection environment, facultative anaerobes such as *S. aureus, E. coli or Streptococcus pneumoniae* can colonize both aerobic and anaerobic niches to cause disease, and life within these niches requires specific metabolic adaptation.

Physiologic heterogeneity in the infection environment may play a significant role in dictating antibiotic susceptibility. Indeed, certain antibiotic classes are active only against either aerobically or anaerobically growing bacteria. Metranidozole, for instance, is a prodrug that must be reduced by intracellular bacterial nitroreductases in order to exhibit bactericidal activity, which only occur in anaerobically growing bacteria[90]. Conversely, PMF-dependent uptake of aminoglycosides generally restricts their activity to aerobically respiring bacteria[50,91]. Active cellular respiration has also been linked to the lethality of other bactericidal antibiotics[92]. Respiration is a more efficient ATP generating process than fermentation, thus, actively respiring cells under oxygen rich conditions are expected to be higher in energy and more susceptible to antibiotic killing than cells in anoxic environments undergoing fermentation. In support of this hypothesis, frequently acquired mutations that result in defective electron transport in *S. aureus* are commonly associated with persistent infection, as the SCVs that result are highly resistant to antibiotic killing activity[93]. SCVs are selected for by oxidative stress and low pH as well as through interaction with small molecules produced by *P. aeruginosa* populations, further exemplifying how host and interspecies interaction can alter antibiotic susceptibility[94,95].

As bacteria compete both with other microorganisms and the host for nutrient sequestration during pathogenesis, nutrient availability undoubtedly plays a role in determining antibiotic susceptibility *in vivo* as well. Antibiotic tolerance increases significantly during periods of nutrient limitation or diauxic carbon-source transition, and starving bacteria of specific nutrients during *in vitro* growth markedly increases antibiotic tolerance[30,96,97]. Biofilm-associated growth represents a major source of metabolic heterogeneity during infection, as nutrient and oxygen consumption by cells at the periphery of the biofilm coupled with limited nutrient diffusion can result in a starvation-induced state of dormancy for cells at the center of the biofilm that is associated with increased tolerance to antibiotic killing[98]. Supplying biofilms with limiting nutrients can restore bacterial susceptibility to antibiotic killing suggesting that starvation induced antibiotic tolerance may be responsible for the recalcitrance of biofilm infections to antimicrobial treatment[30,99,100].

Staphylococcus aureus **adaptive metabolism contributes to its recalcitrance to antibiotic therapy**

S. aureus is a major human pathogen responsible for numerous chronic and relapsing infections[101]. *S. aureus* stably colonizes the anterior nares and skin of approximately one-third of the human population[102]. Typically this co-habitation is harmless, however colonization of immunocompromised individuals or physical disruption of the epithelial barrier in a healthy host can lead to subsequent dissemination of *S. aureus* through the blood to infect virtually any organ tissue in the body[103]. Life-threatening *S. aureus* infections include osteomyelitis, endocarditis,

necrotizing pneumonia and sepsis[104]. The rate of antibiotic treatment failure for these infections can reach 50%, and is often not associated with the emergence of antibiotic resistance[10,105–108]

As a facultative anaerobe, *S. aureus* can be found in a variety of physiologically distinct niches within a host. *S. aureus* encodes an extensive network of metabolic pathways that promote bacterial replication under a plethora of physiological conditions[109]. Under aerobic conditions, *S. aureus* can catabolize a wide range of sugars and amino acids through glycolysis, acetogenesis, and TCA pathways to generate ATP and reducing equivalents to power cellular respiration[110]. In the absence of a terminal electron acceptor (O_2, NO_3^-, etc.) or during respiration inhibition, *S. aureus* switches to fermentative lifestyle, typically fermenting glucose or other carbohydrates to a variety of fermentative end products including lactate, formate, ethanol, and potentially 2,3-butanediol[111–113]. This extensive metabolic network permits colonization of a wide range of niches within the complex host environment, and may explain the capacity of *S. aureus* to cause such a broad variety of infections[114]. Metabolic versatility makes systemic *S. aureus* infections difficult to resolve with antibiotic therapy, as broad-spectrum antibiotics are not always effective at targeting *S. aureus* in distinct physiological niches. For instance, aminoglycosides that require active respiration for bacterial uptake may eradicate respiring, planktonic *S. aureus* within the blood, but will be ineffective against non-respiring *S. aureus* deep within an abscess. Similarly, although vancomycin is considered a front-line antibiotic for resolving *S. aureus* infection, it is extremely ineffective at clearing dense, biofilm-associated *S. aureus* populations[115].

We propose that *S. aureus* represents an ideal model organism for studying how the extrinsic factors present during infection alter bacterial antibiotic susceptibility. This idea is explored further in Chapters 2 and 3. An improved understanding of how and why antibiotics fail to clear *S. aureus* populations within different niches of the host will not only aid in resolving recalcitrant *S. aureus* infection, but will also likely be broadly applicable for the resolution of other important pathogens responsible for chronic and relapsing infections.

PART II. EXPLOITING SYNERGISTIC INTERACTIONS TO IMPROVE TREATMENT OUTCOME

Targeting antibiotic tolerant populations.

Identifying the underlying causes of antibiotic treatment failure is a futile pursuit if we lack the therapeutic means to target these difficult-to-treat populations. How do we target dormant populations when most of our current antibiotic arsenal requires active bacterial targets to function? After discovering persisters, Bigger himself proposed that pulse-dosing cultures with antibiotics to allow persisters time to revive between treatments and would eventually result in complete clearance of the population[22]. The plausibility of this hypothesis is supported by mathematical modeling and *in vitro* experimentation[116–118]. However, this strategy is clinically impractical because it inherently selects for resistance. Perhaps the simplest approach is to maintain antibiotic pressure until the tolerant population can no longer maintain a low-energy, quiescent state. However, *in vitro* studies have demonstrated that an antibiotic-tolerance can be maintained for extensive periods of time among persisters [119]. Furthermore, long-term

treatment is challenging as it requires strict adherence to antibiotic regimens, often in the face of uncomfortable or even debilitating side-effects that reduce patient compliance[120]. This is particularly apparent during *Mycobacterium tuberculosis* treatment. *M. tuberculosis* is a slow-growing bacterial pathogen that replicates within the phagosome of alveolar macrophages[121]. Within this environment, host-mediated stressors including nutrient sequestration and nitrosative stress support suboptimal growth conditions and growth arrest of *M. tuberculosis,* rendering the pathogen tolerant to antibiotic killing [71]. Current guidelines for the treatment of drug-susceptible *M. tuberculosis* begins with a four-drug regimen of isoniazid, rifampin, pyrazinamide, and either ethambutanol or streptomycin that lasts for at least two months[122]. Not only is this intensive treatment regimen impractical for underdeveloped countries with poor access to healthcare, but harmful side effects make patient non-adherence common even in developed countries[123]. This has led to a rise in multi-drug resistant *M. tuberculosis* strains that necessitate even more extensive and crippling antibiotic regimens. Indeed, *M. tuberculosis* recently surpassed Human Immunodeficiency Virus (HIV) as the leading cause of death from infectious disease[124].

Clearly, extending antibiotic treatment duration is insufficient for combating treatment failure. Instead, researchers are pursing novel means for enhancing antibiotic efficacy against metabolically quiescent, tolerant populations that persist within infected hosts. These include combining antibiotics to target heterogeneous populations, physically disrupting cellular integrity, identifying susceptible targets in dormant populations, and reviving persisters prior to antibiotic exposure.

Combinational antibiotic therapy

Antibiotic synergy testing assesses the efficacy of a combinational antibiotic therapy against a bacterial population *in vitro*. The effect of a two-compound combinational therapy can be additive, where the cumulative antimicrobial effect is simply the sum of both individual therapies; synergistic, where the combinatorial activity of two compounds exceeds the sum of each compound alone; or antagonistic, where the effects of one compound decreases the antimicrobial effect of the other[125].

Over 50% of patients treated for septicemia and between 25-50% of patients with surgical site or pneumonia infections receive a combination of two or more antibiotics in an attempt to resolve the infection[126–128]. Prescription of multiple antibiotics with different spectra of activity may increase empiric coverage and efficacy of treatment, particularly when the susceptibility of infecting organism is unknown or there is heterogeneity in antibiotic susceptibility [128]. Combinational therapy may also slow the rise in resistance, and synergistic interactions can occur when two antibiotics with different mechanisms of action act on a single organism[129]. For instance, several *in vitro* studies have suggested that treating *P. aeruginosa* with a cell wall-acting β-lactam antibiotic during aminoglycoside therapy improves aminoglycoside penetrance and efficacy to improve bactericidal activity [130,131]. However, clinical investigations into the translational applications of these *in vitro* observations are conflicting, and our understanding of these molecular interactions is in its infancy[128]. Similarly, the practicality of using combinational therapies to slow the rise of resistance is controversial, as it has been suggested that this practice may actually select for multidrug resistant strains and speed the spread of resistance[128,132].

A second approach to combinational therapy focuses on antibiotic “sensitizers” or adjuvants. These are compounds that improve the efficacy of co-administered antibiotics, usually without demonstrating antimicrobial activity on their own[133]. Typically, adjuvants function by reversing mechanisms of resistance in naturally sensitive strains (e.g. combining an antibiotic with an antibiotic efflux pump inhibitor), or by sensitizing intrinsically resistant bacterial populations to killing (e.g. dispersion of antibiotic-tolerant biofilm)[133]. Clavulanic acid and amoxicillin for instance, make up a widely successful antibiotic cocktail that has been patented and commercialized as Augmentin®. Clavulanic acid inhibits the function of bacterial β-lactam-degrading β-lactamases during amoxicillin therapy, restoring the efficacy of amoxicillin against β-lactam-resistant populations[134]. One benefit of using antibiotic adjuvants is that a number of putative antimicrobial drugs that were shelved in the past for having low efficacy or a high intrinsic rate of resistance generation have been resurrected as promising adjuvant candidates. As researchers have only recently begun exploring potential antibiotic/adjuvant combinations, there may be a number of compounds with the capacity to significantly improve antibiotic lethality that have yet to be applied as such.

Disrupting cellular integrity to target antibiotic tolerant populations

As discussed above, the bulk of our antibiotic arsenal is composed of drugs that corrupt active cellular processes to facilitate bacterial killing. The requirement of an active cellular target for bactericidal activity lends to the association between antibiotic tolerance and metabolic dormancy. For this reason, many researchers have turned their

attention to developing compounds that directly target bacterial cellular integrity, as this approach may permit eradication of dormant populations that are inherently tolerant to current therapeutics. Cell envelope integrity represents a promising but underdeveloped target for antibiotic action. Recent attention has focused on the applicability of using antimicrobial fatty acids, peptides, or other naturally occurring and synthetic compounds that physically disrupt the phospholipid bilayer as potential therapeutics, either alone in combination with a secondary antibiotic[59,135–137]. The primary draw of this approach is that membrane integrity is essential for the survival and virulence of all bacteria, regardless of metabolic state. Interaction with the membrane does not require ATP, thus tolerant persister populations are theoretically as susceptible to killing as metabolically active cells. Another attractive feature is that it is often more difficult for bacteria to evolve resistance to compounds that disrupt membrane integrity, as these compounds typically interact with multiple targets within the membrane. Indeed, results from *in vitro* studies show that *de novo* mutations that confer resistance to lipopeptides, antimicrobial peptides, and small molecules are exceedingly rare[138].

The primary drawback of targeting the membrane stability is that compounds that disrupt bacterial membranes may be cytotoxic to host cells for the same reason. However, there are distinct physiological differences between bacterial and mammalian membrane composition, which may make it possible to specifically target bacterial membrane during treatment. Relative to mammalian membranes, bacteria lack cholesterol, and are dominated by negatively charged (phosphatidylglycerol, cardiolipin) and zwitterionic (phosphatidylethanolamine) phospholipids[139]. The clinical success of several membrane targeting antibiotics indicates that select targeting of bacterial

membrane is feasible and effective[138]. The antibiotic daptomycin, for instance, binds the surface of negatively charged bacterial membrane and oligomerizes to form pores and depolarize the membrane, leading to cell death[140,141]. As a membrane-acting agent, daptomycin often exhibits greater efficacy against non-growing *S. aureus* persister populations than traditional antibiotics[119]. Similarly, there are a number of membrane-acting compounds that have been recognized as safe by the United States Food and Drug Administration (FDA) for human consumption that exhibit antimicrobial activity[135,142,143]. Further, antimicrobial peptides and lipids constitute an important component of the human innate immune system, implying that these compounds may be safely administered to patients at concentrations that are bactericidal[144,145]. There may even be an opportunity to exploit synergistic interaction between naturally occurring antimicrobial lipids or peptides and antibiotics within the host to improve treatment outcome[59].

Targeting and resuscitating dormant populations

Others have pursued more creative ways to re-sensitize ATP-depleted populations to antibiotic killing by commandeering and manipulating normal cellular processes during treatment. For instance, Conlon *et al.* used the antibiotic acyldepsipeptide (ADEP) to target dormant persisters[146]. ADEP binds to and activates ClpP, a bacterial protease that normally degrades misfolded proteins in the presence of ATP[147,148]. While bound to ADEP, ClpP remains in the active form, independent of intracellular ATP levels, leading to unchecked proteolysis within the cell. The activation of non-specific protein degradation in ATP-depleted cells makes ADEP

an exciting candidate for targeting dormant bacterial populations, as ADEP-treated cells essentially degrade themselves to death in an energy-independent manner. The authors further demonstrated that combining ADEP4 with rifampicin facilitated the eradication of persister populations *in vitro* and in a deep-seated murine biofilm infection model[146].

Chemically resuscitating dormant cells prior to antibiotic exposure by providing nutrients may also improve persister eradication *in vitro* and *in vivo*. Eradication of *E. coli* and *S. aureus* persisters can be achieved through supplementation with glycolytic sugar molecules that enhance aminoglycoside uptake through PMF generation[149]. Similarly, supplementing cultures with glucose increases daptomycin efficacy against *S. aureus* persisters, and supplementation with nitrate or arginine potentiates tobramycin and ciprofloxacin killing of *P. aeruginosa* biofilm[99,150]. Though these *in vitro* studies support the idea of reviving antibiotic tolerant persisters to improve therapeutic outcome, the clinical practicality and potential negative repercussions from providing pathogens with excess nutrients during treatment has yet to be evaluated.

The widespread onset of multidrug-resistant pathogenic strains, coupled with an evaporating pipeline of new antibiotics reaching market emphasizes the importance of maximizing the efficacy of current antibiotics. Identifying instances where combinational antibiotic therapy can improve the rate and capacity of an antibiotic to clear recalcitrant bacterial populations will reduce the duration of antibiotic tolerance and slow the rise of resistance. Importantly, however, synergistic interactions observed *in vitro* are not always indicative of the *in vivo* outcome of combinational therapy and there are potential negative repercussions to combinational therapies that must be considered. Further

investigation is necessary to identify new opportunities for exploiting pathogen vulnerabilities during antibiotic therapy, as well as to assess the practicality and efficacy of implementing these therapies in patients.

PART III. IDENTIFYING THERAPEUTIC TARGETS FOR INTRACELLULAR PATHOGENS

The case for narrow-spectrum antibiotics

Broad-spectrum antibiotics act on both Gram-positive and negative bacterial species by targeting common cellular processes such as DNA replication (fluoroquinolones), transcription (rifamycins), translation (aminoglycosides), and cell wall biosynthesis (β-lactams) that are essential for bacterial replication and survival. With the discovery of penicillin, broad-spectrum antibiotics were the first developed, and remain the most commonly applied antimicrobial strategies used today for resolving bacterial infection. These drugs allow clinicians to quickly treat patients when a bacterial infection is suspected but the pathogen is unknown, they can also be used prophylactically to prevent infection during invasive surgery and during labor[151], and can resolve polymicrobial infection when more than one pathogen is causing disease.

While undoubtedly useful, there are several drawbacks to the widespread use of broad-spectrum antibiotic therapy. Their overuse can select for resistance in both pathogenic and non-pathogenic (commensal) species within the host and inadvertently generate a reservoir of resistance genes that can propagate through horizontal gene transfer to dangerous pathogens[152]. The primary advantage of these drugs (their broad specificity) additionally leads to indiscriminate targeting of both pathogen and

host commensal species that render a patient susceptible to subsequent infection. This is particularly apparent during nosocomial *Clostridioides difficile* infection, where colonization follows antibiotic-mediated clearance of the host microbial flora[153]. Finally, while broad-spectrum antibiotics are effective at targeting extracellular bacterial pathogens, they are often ineffective against bacterial species that replicate within the cytoplasm or vacuolar space of host cells due to poor intracellular penetrance[67]. Many important antibiotic classes cannot enter the host cell cytosol and thus cannot gain access to the target bacterial population within[67]. Aminoglycosides, for instance, are the frontline therapy of choice for the facultative intracellular pathogen, *Francisella tularensis,* despite the fact that these antibiotics poorly penetrate the host cell[67]. As *F. tularensis* is among several bacterial species that can disseminate via cell-to-cell transmission mechanisms without exposure to the extracellular space[154], extensive treatment periods that last several weeks are often necessary to treat this organism.

Recently, much attention has focused on the development of narrow-spectrum antibiotics that target specific genus, species, or physiological states of bacteria with the goal of addressing the issues posed by broad-spectrum antibiotic use[155]. Targeted therapies that specifically act on bacterial populations replicating within the intracellular environment without inadvertently decimating the host microbiome would be invaluable for preventing the spread of important diseases. However, implementation of this approach requires identification of antimicrobial targets that reduce pathogen viability without harming the host. In order to establish an infection, invading pathogens must actively modify the host metabolic activity to derive sufficient nutrients and reduce host

antimicrobial responses. Understanding and inhibiting these active microbial processes may prevent niche modification and restrict pathogen proliferation.

Disrupting niche modification to target recalcitrant pathogen populations

Preventing pathogens from cultivating an environment that supports replication within the host is a promising alternative to antibiotic therapy. During dysbiotic *Proteobacteria* expansion, enteric pathogens actively modify their environment to establish a replicative niche[156]. The enteric pathogen *Citrobacter rodentium,* for instance, actively drives metabolic reprogramming of epithelial cells away from β-oxidation and towards aerobic glycolysis by triggering colonic crypt hyperplasia[157]. This change in host cell metabolism increases oxygenation at the mucosal surface and drives aerobic expansion of pathogenic Enterobacteriaceae[156]. Inhibiting colonic crypt hyperplasia during *C. rodentium* infection with the γ-secretase inhibitor, dibenzazepine, reduced the ability of *C. rotentium* to colonize this environment[157]. Similarly, treating mice with a PPAR-γ agonist (rosiglitazone) significantly reduced *E. coli* luminal expansion by restoring epithelial β-oxidation and reducing luminal abundance of nitrate[158]. Recent clinical study of ulcerative colitis patients revealed that treatment with a PPAR-γ agonist that acts topically on the colonic epithelium (mesalazine) reduced *Proteobacteria* abundance in the colon, suggesting that this method may be effective for reducing pathogen expansion in human hosts[159]. Together, these studies demonstrate that inhibiting pathogen proliferation indirectly by targeting the host factors that support growth is an effective way to resolve infection, provided that we can first identify those factors.

An ideal therapy for intracellular pathogens would prevent pathogen-mediated niche modification of the intracellular space. For professional phagocytic cells this would allow for the host to eliminate pathogens through the normal innate immune response (phagosome acidification, ROS generation, etc.). Within non-phagocytic cells, disrupting pathogen-mediated niche modification would likely reduce nutrient availability and slow bacterial proliferation. However, in most cases the means by which these organisms compete with the hosts own metabolic demands to derive metabolites from the intracellular environment are unclear. An improved understanding of how intracellular bacterial pathogens modify the intracellular niche to obtain sufficient nutrients for replication and dissemination is likely to reveal novel therapeutic avenues for combating these important pathogens. Furthermore, targeting bacterial growth by altering host cell metabolism may circumvent issues concerning drug penetration, as host-targeting therapeutics act on infected host cells and not the bacteria replicating within that environment.

Targeting bacterial metabolism to inhibit proliferation

Prior to replication, virulence factor production, or dissemination, bacterial pathogens must secure sufficient nutrients to survive within the host. As an energy-starved pathogen cannot cause disease, cutting off a pathogen's food supply represents an enticing therapeutic avenue. Indeed, interfering with pathogen-specific metabolic pathways such as peptidoglycan synthesis, LPS synthesis, etc. has long been pursued as means for suppressing pathogen growth[160–162], and several studies have shown that inhibiting import or synthesis of a single essential metabolite significantly reduces

the virulence of otherwise virulent bacterial species[163,164]. However, for most pathogens the metabolic pathways and host-derived nutrients necessary for *in vivo* growth are poorly defined.

Extracellular pathogens are subject to a constant flux of available nutrients within the host. By contrast, intracellular pathogens encounter more stable growth conditions within the cytoplasm or vacuolar space within the host cell. The relative simplicity of the intracellular environment has prompted significant strides in understanding the metabolic requirements of intracellular pathogens[165]. Within this niche, bacteria have access only to nutrients they can scavenge from this compartment. Recent studies suggest that the intracellular environment is not simply an open buffet of freely available metabolites left over from host metabolic processes[165]. Instead, most intracellular nutrients are stored within complex structures and not immediately available to intracellular pathogens[165]. To grow, intracellular bacteria must either harvest newly imported nutrients or direct the degradation of resident complex storage structures into their constituents (fatty acids, carbohydrates and amino acids). Successful intracellular pathogens have evolved the means for manipulating the intracellular environment to obtain sufficient carbon and trace elements necessary for replication[166–170]. As a reward, these pathogens are shielded from the innate immune system, competing microorganisms, and certain antibiotics that cannot access the intracellular space. Further, pathogens that can survive within motile macrophages and neutrophils may commandeer these cells as mode of protected dissemination through the host[69,171,172].

Francisella tularensis as a model for studying intracellular carbon catabolism

F. tularensis is a Gram-negative, facultative intracellular bacterial pathogen and one of the most virulent organisms known. *F. tularensis* infects over 250 susceptible organisms, including humans[173]. Within these hosts, *F. tularensis* replicates within a variety of cell and tissue types including macrophages, epithelial cells, hepatocytes, neutrophils, fibroblasts and erythrocytes[174–177]. Following intracellular invasion, *F. tularensis* escapes the phagosome to replicate within the host cell cytosol[178]. A hallmark of *F. tularensis* pathogenesis is the bacterium's ability to reach extreme densities within this niche, often replicating 1,000-fold within 24 hours to fill 60% of host cytosolic volume with bacterial mass (unpublished data). This remarkable rate of growth demonstrates that *F. tularensis* is adept at harvesting and utilizing host cell nutrients in an environment that does not inherently contain sufficient free carbon to support the levels of replication observed. *F. tularensis* must actively modulate the host metabolic processes to amass sufficient carbon to support growth and dissemination. We previously demonstrated that *F. tularensis* commandeers host cell autophagy to break down macromolecules and derive a source of free amino acids [179]. However, *F. tularensis* replicates to a considerable degree even in the absence of autophagy, demonstrating that this organism further exploits host metabolic processes to derive sufficient nutrients[179].

F. tularensis poses a severe risk to public health and is considered a potential agent for bioterrorism because of the bacterium's low infectious dose and the high rate of mortality associated with tularemia [180–182]. Its broad host range and capacity to replicate to extreme densities within the intracellular space demonstrates that *F.*

tularensis is adept at modulating host cell metabolism to fuel replication. Furthermore, as a facultative intracellular pathogen, *F. tularensis* contains a small and decaying genome that encodes a relatively simple set of carbon catabolic pathways that support intracellular replication[183]. For these reasons, we propose that *F. tularensis* is an excellent model for studying intracellular niche modification and carbon metabolism, and that doing so will reveal new insights into how we can improve antimicrobial targeting of recalcitrant intracellular pathogens. This topic is explored further in Chapter 4.

In all, though antibiotic susceptibility is traditionally examined in simple homogenous conditions *in vitro*, more and more studies are revealing the dynamic and complex nature of antibiotic efficacy in the infection environment (Figure 1.2). The administration of antibiotics without consideration of these environmental factors may result in treatment failure, exacerbated disease progression, and the rise of resistant microorganisms. Moreover, we propose that pathogen sensitivity to antibiotic killing is contingent not only on genotype, but also the pathogen's metabolic state, and on interactions that occur with the host and co-infecting microorganisms. Further elucidation of key determinants of efficacy *in vivo* may lead to a more sophisticated and personalized approach to antibiotic therapy in order to eradicate infection as efficiently as possible. Doing so will reduce the likelihood of treatment failure and the incidence and spread of antibiotic resistance.

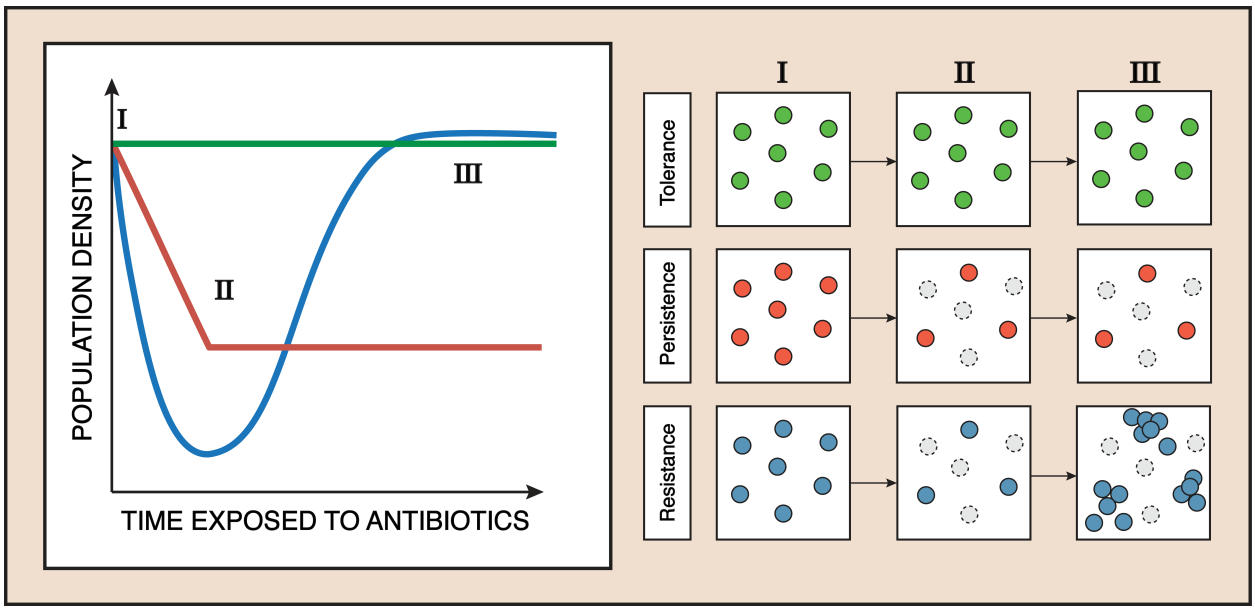

Figure 1.1. Antibiotic tolerance, persistence, and resistance are related but distinct phenomena that contribute to treatment failure. The effects of antibiotic tolerance, persistence and resistance on bacterial population density are contrasted. Antibiotic tolerance (green) refers to the survival of an entire population to lethal antibiotic exposure. A tolerant population neither grows, nor dies in the presence of antibiotic. Persister populations (red) reference a subpopulation of tolerant bacteria within a larger susceptible population. Following antibiotic challenge, the sensitive population succumbs to antibiotic killing. Persisters tolerate the antibiotic but are unable to grow in the presence of antibiotic. This leads to the biphasic kill curve illustrated above with a rapid exponential death phase followed by the formation of a stable persister plateau. If a heterogeneous population contained a resistant mutant (blue) capable of inactivating or overcoming the activity of the applied antibiotic, outgrowth of that resistant mutant subpopulation would follow an initial reduction in viable cells as the susceptible strain succumbs to antibiotic killing, followed by growth of the resistant population in the presence of the antibiotic.

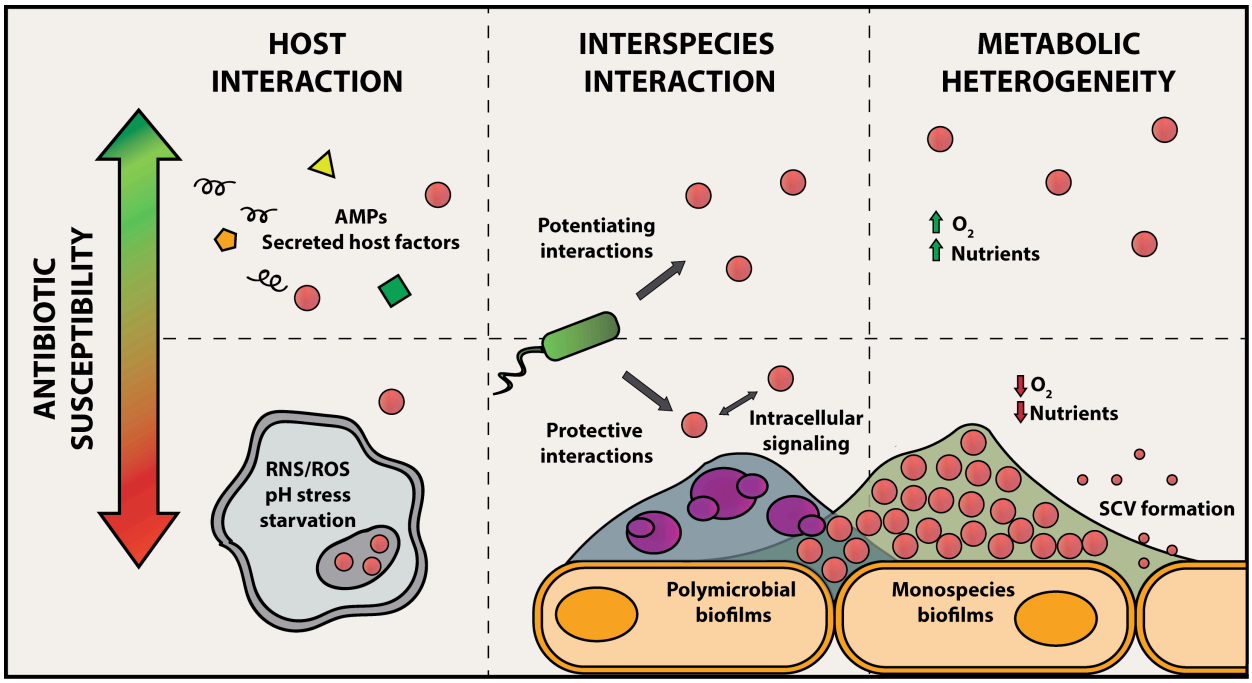

Figure 1.2. Overview of extrinsic factors influencing antibiotic susceptibility within the host. Environmental factors can antagonize or potentiate antibiotic efficacy killing of a pathogen. Antimicrobial peptides (AMPs) can synergize with antibiotics to increase killing of pathogens. Conversely, pathogen engulfment by phagocytic cells can inhibit antibiotic killing by preventing drug access to the pathogen or by directly influencing pathogen metabolism and physiology through production of reactive oxygen or nitrogen species (ROS/RNS), vacuole acidification or nutrient sequestration. Inter- and intraspecies interactions can positively and negatively impact a pathogen's susceptibility to antibiotic killing either through signaling processes or via direct interaction, such is the case in polymicrobial biofilms. Finally, heterogeneity in oxygen or nutrient concentration within the infectious environment can influence bacterial metabolism with significant consequences for antibiotic susceptibility.

CHAPTER 2
PSEUDOMONAS AERUGINOSA EXOPRODUCTS DETERMINE ANTIBIOTIC EFFICACY AGAINST *STAPHYLOCOCCUS AUREUS*[1]

Chronic co-infections of *Staphylococcus aureus* and *Pseudomonas aeruginosa* frequently fail to respond to antibiotic treatment, leading to significant patient morbidity and mortality. Currently, the impact of interspecies interaction on *S. aureus* antibiotic susceptibility remains poorly understood. In this study, we utilize a panel of *P. aeruginosa* burn wound and cystic fibrosis (CF) lung isolates to demonstrate that *P. aeruginosa* alters *S. aureus* susceptibility to bactericidal antibiotics in a variable, strain-dependent manner and further identify three independent interactions responsible for antagonizing or potentiating antibiotic activity against *S. aureus*. We find that *P. aeruginosa* LasA endopeptidase potentiates lysis of *S. aureus* by vancomycin, rhamnolipids facilitate proton-motive force-independent tobramycin uptake, and 2-heptyl-4-hydroxyquinoline *N*-oxide (HQNO) induces multidrug tolerance in *S. aureus* through respiratory inhibition and reduction of cellular ATP. We find that the production of each of these factors varies between clinical isolates, and corresponds to the capacity of each isolate to alter *S. aureus* antibiotic susceptibility. Furthermore, we demonstrate that vancomycin treatment of a *S. aureus* mouse burn infection is potentiated by the presence of a LasA producing *P. aeruginosa* population.

[1] Radlinski LC, Rowe SE, Kartchner LB, Maile R, Cairns BA, Vitko NP, Gode CJ, Lachiewicz AM, Wolfgang MC, Conlon BP. *Pseudomonas aeruginosa* exoproducts determine antibiotic efficacy against *Staphylococcus aureus. PLoS Biology.* 2017 Nov 27;15(11):e2003981

These findings demonstrate that antibiotic susceptibility is complex and dependent not only upon the genotype of the pathogen being targeted, but also on interactions with other microorganisms in the infection environment. Consideration of these interactions will improve the treatment of polymicrobial infections.

IMPORTANCE

Accurate prediction of antimicrobial efficacy is essential for successful treatment of bacterial infection. Beyond genetically encoded mechanisms of resistance, the specific determinants of antibiotic susceptibility during infection remain poorly understood. Here we show that a single interspecies interaction between *S. aureus* and *P. aeruginosa* can completely transform the antibiotic susceptibility profile of *S. aureus.* Through multiple distinct mechanisms, *P. aeruginosa* can antagonize or potentiate the efficacy of multiple classes of antibiotics against *S. aureus.* We identify the exoproducts responsible for altering *S. aureus* susceptibility to antibiotic killing, and furthermore demonstrate that these compounds are produced at varying levels in *P. aeruginosa* clinical isolates, with dramatic repercussions for *S. aureus* antibiotic susceptibility. Finally, we use a mouse model of *P. aeruginosa, S. aureus* co-infection to demonstrate that the presence of *P. aeruginosa* significantly alters the outcome of *S. aureus* antibiotic therapy in a host. These findings indicate that the efficacy of antibiotic treatment in polymicrobial infection is determined on the community level with interspecies interaction playing an important, and as yet unappreciated role.

INTRODUCTION

S. aureus is responsible for numerous chronic and relapsing infections such as osteomyelitis, endocarditis, and infections of the cystic fibrosis (CF) lung, as well as many penetrating trauma and burn infections, venous leg ulcers, pressure ulcers, and diabetic foot ulcers. These infections are notoriously difficult to treat, despite isolates frequently exhibiting full sensitivity to administered antibiotics, as measured *in vitro* using a Minimum Inhibitory Concentration (MIC) assay. This suggests that environmental factors present *in vivo* may influence the pathogen's susceptibility to antibiotic killing. While these factors can include physical barriers to antibiotic activity, such as tissue necrosis and low vascularization at a site of infection, or bacterial replication within host phagocytes, treatment failure cannot be fully explained by poor drug penetration[10]. Instead, environmental determinants, such as interactions with the host, can induce phenotypic responses or genetic adaptations in bacteria that reduce antibiotic sensitivity[184,185].

Similarly, within complex polymicrobial communities, such as those encountered in chronic skin infections, burn wound infections and chronic colonization of the CF lung, inter- and intra- species interactions can influence the pathogenicity and antibiotic susceptibility of individual organisms[53,186,187]. The presence of the fungal pathogen *Candida albicans,* for instance, can induce *S. aureus* biofilm formation and thus decrease the bacterium's susceptibility to antibiotic killing[186]. Furthermore, antibiotic deactivation by resistant organisms within a population can lead to de facto resistance of all members of the community[73,188–190].

In such polymicrobial infections, *S. aureus* is commonly co-isolated with the opportunistic pathogen *P. aeruginosa*[191]. These co-infections are generally more virulent and/or more difficult to treat than infections caused by either pathogen alone[192–194]. The interaction between these two organisms is complex, with *P. aeruginosa* producing a number of molecules that interfere with *S. aureus* growth, metabolism, and cellular homeostasis. These molecules include the secondary metabolites 4-hydroxy-2-heptylquinoline-*N*-oxide (HQNO), pyocyanin, and hydrogen cyanide, all of which inhibit *S. aureus* respiration[195–197]. Additionally, *P. aeruginosa* produces rhamnolipids, biosurfactants that interfere with the *S. aureus* cell membrane, and an endopeptidase, LasA, that cleaves pentaglycine bridges in *S. aureus* peptidoglycan[198–200].

These anti-staphylococcal compounds allow *P. aeruginosa* to quickly eliminate *S. aureus* during *in vitro* co-culture but do not prevent co-colonization *in vivo*. Recent findings suggest that within the CF lung, *P. aeruginosa* strains evolve to be less competitive with *S. aureus* resulting in more stable co-infection of the same spatial niche[201]. Additionally, work by Wakeman *et al.* has shown that the presence of the abundant innate immune protein, calprotectin, induces a phenotypic switch in *P. aeruginosa* that promotes stable *P. aeruginosa* and *S. aureus* interaction through the chelation of zinc and manganese ions at the site of infection. This in turn represses *P. aeruginosa* metabolic toxin production, resulting in significantly less HQNO and pyocyanin[202]. Similarly, Smith *et al.* recently demonstrated that *S. aureus* can tolerate *in vitro* co-culture with *P. aeruginosa* in the presence of serum albumin through the inhibition of *P. aeruginosa lasR* quorum sensing and thus LasA expression[203].

Despite these findings, *P. aeruginosa* LasA, rhamnolipids, HQNO and pyocyanin are routinely detected at significant concentrations in burn wounds and in CF sputum samples and thus likely influence *S. aureus* physiology[204–208].

We hypothesized that interaction with *P. aeruginosa* may antagonize or potentiate *S. aureus* antibiotic susceptibility and could explain the frequent occurrence of treatment failure in infections involving otherwise drug-susceptible strains. Furthermore, we hypothesized that such interactions could be exploited to improve antibiotic treatment outcome. Here we demonstrate that secreted *P. aeruginosa* factors dramatically alter *S. aureus* susceptibility to killing by multiple antibiotic classes, and identify several mediators of *S. aureus* antibiotic antagonism or potentiation. Importantly, the production of these molecules is highly strain dependent, thus implicating the genotype of co-infecting *P. aeruginosa* strains as critical determinants of antibiotic treatment outcomes for *S. aureus* infections. Ultimately, we demonstrate in a mouse model of *S. aureus, P. aeruginosa* co-infection that the presence of *P. aeruginosa* can significantly alter the outcome of *S. aureus* antibiotic treatment. Overall this work highlights the importance of considering the microbial context of the infection environment during the treatment of polymicrobial infection.

RESULTS

Pseudomonas aeruginosa alters *S. aureus* susceptibility to antibiotic killing

To investigate the impact of *P. aeruginosa* on *S. aureus* antibiotic susceptibility, we measured the bactericidal activity of three antibiotics against *S. aureus* in the presence of supernatants from 12 *P. aeruginosa* clinical isolates; 7 from the lungs of CF

patients and 5 from burn wounds, as well as two laboratory strains; PAO1 and PA14. We were interested in examining how *P. aeruginosa*-secreted exoproducts can impact the susceptibility of *S. aureus* to vancomycin, tobramycin and ciprofloxacin. Vancomycin is the frontline antibiotic for the treatment of MRSA. Ciprofloxacin and tobramycin are commonly used to treat *P. aeruginosa* during co-infection.

S. aureus strain HG003 was grown to exponential phase and treated with 500µL of sterile supernatant from overnight (18h) cultures of HG003 (control) or one of the 14 *P. aeruginosa* strains prior to antibiotic challenge. After 24h, cells were washed and plated to enumerate survivors. We found that the individual bactericidal activities of all three antibiotics against *S. aureus* were affected by *P. aeruginosa* supernatants. More specifically, we observed three *P. aeruginosa* isolates that significantly protected *S. aureus* from killing by tobramycin (BC239, BC312 and BC252) and one *P. aeruginosa* isolate (BC310) induced over a ten-fold increase in tobramycin killing of *S. aureus* (Figure 2.1A). We also observed that the majority of *P. aeruginosa* supernatants were antagonistic towards ciprofloxacin killing (Figure 2.1B). Furthermore, supernatants from 8 *P. aeruginosa* strains (PAO1, PA14, BC238, BC310, BC249, BC250, BC251 and BC252) dramatically potentiated vancomycin killing of *S. aureus,* resulting in 100-1000 times more killing than the control culture (Figure 2.1C). These data highlight the variable and strain-dependent influence of *P. aeruginosa* on the susceptibility of *S. aureus* to different antibiotics, however the mechanism(s) by which *P. aeruginosa* alters *S. aureus* antibiotic susceptibility remained unclear.

Rhamnolipids increase tobramycin uptake and efficacy against *S. aureus*

Previous studies have shown that during co-culture the presence of *P. aeruginosa* results in increased *S. aureus* resistance to tobramycin through the activity of HQNO[53]. In agreement with this, we observed that supernatants from BC239 and BC312 and BC252 protected *S. aureus* from tobramycin killing (Figure 2.1A). Paradoxically, however, we observed that the majority of our clinical isolates had no significant impact on tobramycin bactericidal activity. Even more striking, isolate BC310 appeared to potentiate tobramycin bactericidal activity against *S. aureus* (Figure 2.1A). We hypothesized that the impact of *P. aeruginosa* on *S. aureus* tobramycin susceptibility was multi-factorial, with an unidentified factor increasing tobramycin bactericidal activity.

Tobramycin uptake is dependent on proton-motive force (PMF)[209]. *P. aeruginosa* HQNO collapses *S. aureus* PMF by inhibiting electron transport, thus abolishing tobramycin uptake into the cell[53]. To explore the possibility that an additional factor within *P. aeruginosa* supernatant may influence the bactericidal activity of tobramycin against *S. aureus*, we examined *S. aureus* susceptibility to tobramycin in the presence of supernatant from a PA14 *ΔpqsLphzShcnC* strain. This strain cannot produce the respiratory toxins HQNO, pyocyanin or hydrogen cyanide, all of which inhibit *S. aureus* respiration and deplete PMF. Strikingly, we found that PA14 *ΔpqsLphzShcnC* mutant supernatant led to the rapid eradication of a *S. aureus* population following tobramycin treatment (Figures 2.2A, 2.3A). Heat-inactivation of *P. aeruginosa* PA14 supernatant had no impact on its ability to alter tobramycin activity, ruling out heat-labile proteins as potentiators of tobramycin killing (Figure 2.3B).

P. aeruginosa produces surfactant molecules called rhamnolipids that inhibit growth of competing Gram-positive bacteria. These amphiphilic molecules increase cell permeability by interacting with the plasma membrane[210]. We hypothesized that rhamnolipid interaction with the membrane may facilitate tobramycin entry into otherwise tolerant, PMF-depleted persister sub-populations. To investigate this possibility, we deleted the *rhlA* gene in PA14, which is essential for rhamnolipid biosynthesis. Supernatant from a PA14 *ΔrhlA* mutant conferred full protection to *S. aureus* against tobramycin killing (Figures 2.2A, 2.3A). Furthermore, during tobramycin treatment, the exogenous addition of a 50-50 mix of purified *P. aeruginosa* mono- and di-rhamnolipids at 30μg/ml facilitated the rapid eradication of the *S. aureus* population, and decreased the MIC of tobramycin for *S. aureus* 8-fold (Figure 2.2A)(Table 2.2). This concentration is within the physiological range of rhamnolipids likely encountered by *S. aureus* during co-infection with *P. aeruginosa*, as previous work by Bjarnsholt *et al*. found that clinical isolates produce a range of 2.4μg/ml to 72.8μg/ml rhamnolipids when grown *in vitro* and Read *et al.* reported rhamnolipid concentrations as high as 64 μg/ml in a CF lung explant[204,211]. At the concentrations used in this study, rhamnolipids did not display antibacterial activity in the absence of antibiotic (Figure 2.3C). Further, incubation with a similar concentration of L-rhamnose, the glycosyl head constituent of rhamnolipids, had no effect on tobramycin killing, ruling out metabolite-stimulated PMF generation as the mechanism of tobramycin potentiation (Figure 2.3D). Finally, we found that 30μg/ml purified *P. aeruginosa* rhamnolipids led to increased uptake of Texas Red-conjugated tobramycin as determined by flow cytometry (Figure 2.2B).

We next measured the relative amount of HQNO and rhamnolipids produced by each *P. aeruginosa* isolate using mass spectrometry[212] and a drop-collapse assay, respectively[213]. We observed a large variance in the production of both HQNO (Table 2.1) and rhamnolipids between isolates (Figure 2.2C). Importantly, the potentiator of tobramycin activity, BC310, was the only strain shown to be a high rhamnolipid producer without detectable HQNO production. In contrast, strain BC239, the strongest tobramycin antagonist, was among the highest HQNO producers, and did not produce rhamnolipids. Together, these data show that *P. aeruginosa* has the capacity to both positively and negatively influence *S. aureus* tobramycin uptake and bactericidal activity through the action of rhamnolipids and respiratory toxins, respectively. The presence of these two opposing factors may be responsible for the apparent disconnect between the *P. aeruginosa*-mediated increase in tobramycin resistance reported previously[53], and lack of protection from tobramycin killing following treatment with supernatant from the majority of *P. aeruginosa* strains observed in this study. Indeed, deletion of either *P. aeruginosa* respiratory toxins or rhamnolipids in a *P. aeruginosa* laboratory strain resulted in supernatants that facilitate complete sterilization or protection of *S. aureus* cultures, respectively (Figure 2.2A). Furthermore, similar trends were observed when *S. aureus* MRSA strain JE-2 was challenged with tobramycin following treatment with *P. aeruginosa* supernatant, supporting the relevance of this phenomenon in the clinical treatment of *S. aureus* infection (Figure 2.4A).

P. aeruginosa induces multidrug tolerance in *S. aureus* through respiratory inhibition

In addition to the ability of HQNO to inhibit uptake of aminoglycosides, we made an interesting and somewhat unexpected observation during our investigation. HQNO production in *P. aeruginosa* isolates correlated perfectly with protection against ciprofloxacin killing (Figure 2.1B)(Table 2.1). As ciprofloxacin uptake is PMF-independent, we wondered if *P. aeruginosa* HQNO was conferring ciprofloxacin tolerance in *S. aureus* via an alternate mechanism.

Antibiotic tolerance generally refers to a population-wide decrease in antibiotic susceptibility, often following exposure to external mediators of bacterial metabolism or physiology. In contrast, persister cells are generally described as antibiotic-tolerant sub-populations that form stochastically in an otherwise susceptible population. We recently demonstrated that both phenomena are specifically associated with cells entering a low ATP state[26,27]. Sub-populations of low energy cells give rise to persisters, while changes in the environment can lead to a low energy antibiotic tolerant state in the entire population. HQNO inhibits respiration, the most efficient mechanism for ATP generation in *S. aureus*. We hypothesized that *P. aeruginosa* inhibition of *S. aureus* respiration induces a low ATP, multidrug tolerant state of the entire population. In support of this, no protection from antibiotic killing was observed following pre-treatment with PA14 supernatant during anoxic growth (Figure 2.5A). We then cloned the fermentation-specific promoter for pyruvate acetyltransferase *(pflB)* from *S. aureus* upstream of *gfp* in a low-copy plasmid. Expression of *pflB* only occurs under anaerobic conditions or when respiration is inhibited[113]. We found that transcription of the *pflB*

promoter was activated in response to supernatant from all of the *P. aeruginosa* strains with the exception of PA14 *ΔpqsLphzShcnC* (negative control) and 4 of the clinical isolates, BC236, BC308, BC310, and BC251. Importantly, these were the only clinical isolates that did not induce significant protection from ciprofloxacin killing (Figure 2.1B). Activation of *pflB* during aerobic growth demonstrates that respiration is inhibited in these conditions (Figures 2.6A, 2.7). Direct intracellular ATP quantification of cultures treated with *P. aeruginosa* or *S. aureus* supernatant revealed that *P. aeruginosa* supernatant induces significant depletion of *S. aureus* intracellular ATP (Figure 2.6B).

We found that mutation of *pqsL* (HQNO negative) drastically reduced the capacity of PA14 supernatant to protect *S. aureus* from ciprofloxacin killing, suggesting tolerance to ciprofloxacin killing is mediated by HQNO (Figure 2.6C). Individually, mutations to the biosynthetic pathways for pyocyanin (*phzS*) and hydrogen cyanide (*hcnC)* had no influence on *P. aeruginosa*-conferred protection from ciprofloxacin killing. However, supernatants from a *ΔpqsLphzS* and a respiratory toxin-null mutant (*ΔpqsLphzShcnC)* were further reduced in their capacity to protect *S. aureus* from ciprofloxacin killing (Figures 2.5B, 2.6C). Together, these data demonstrate that *P. aeruginosa* confers protection from ciprofloxacin killing to *S. aureus* through respiration inhibition and depletion of ATP. Further, treatment with HQNO, pyocyanin and HCN at concentrations detected within the sputum of CF patients with active *P. aeruginosa* infection [206,208,214] induced tolerance of *S. aureus* to ciprofloxacin (Figure 2.6D). Surprisingly, similar levels of tolerance were observed for other classes of antibiotics including tobramycin, and vancomycin, with HQNO inducing the most robust tolerance to antibiotic killing (Figure 2.5C,D).

The LasA endopeptidase potentiates vancomycin bactericidal activity against *S. aureus*

The presence of purified HQNO protects *S. aureus* from vancomycin killing (Figure 2.5D). However, *P. aeruginosa* supernatant from the majority of isolates tested significantly potentiated vancomycin killing of *S. aureus* (Figure 2.1C). We hypothesized that, similar to what was observed with *S. aureus* susceptibility to tobramycin, an additional factor present in *P. aeruginosa* supernatant is capable of overcoming the protective effects of HQNO to potentiate vancomycin killing of *S. aureus.* Heat denaturation of PAO1 supernatant completely abrogated the potentiating effect, suggesting the involvement of heat-labile extracellular protein(s) in the phenotype (Figure 2.8A). Bacteriolytic assays revealed that the PAO1 supernatant combined with vancomycin induced dramatic lysis of the population that was absent in the presence of either factor alone (Figure 2.8B). This led us to examine the potential role of the *P. aeruginosa* extracellular lytic enzyme, LasA, in mediating vancomycin killing. LasA cleaves pentaglycine cross bridges in *S. aureus* peptidoglycan and has been shown to attack the cell wall of *S. aureus* during *in vivo* competition[198]. We examined the capacity of supernatant from a PAO1 *lasA* mutant to potentiate vancomycin killing. The *lasA* mutant supernatant did not potentiate killing by vancomycin compared to a 3-log reduction in *S. aureus* cfu in the presence of the PAO1 wild-type supernatant (Figures 2.8A, 2.9A). Similar trends were observed in a *S. aureus* MRSA strain JE-2 (Figure 2.4B). As it was previously shown that *S. aureus* can degrade HQNO[215], the absence of which could result in a more dramatic LasA-dependent potentiation effect in our supernatant experiments, we examined vancomycin killing in a co-culture model where *P. aeruginosa* is present to continually produce HQNO. Again, we found that the

presence of wild-type PAO1 resulted in a 3-Log reduction in cfu following vancomycin challenge, and that this potentiation was not observed in the presence of a PAO1 *lasA* mutant, where we observed 100-fold more survivors at 24h (Figure 2.10).

Next, we measured the levels of LasA in the supernatants of each clinical isolate via western blot and an additional assay developed previously to quantify LasA activity[216](Figures 2.8C, 2.11). 7 of the clinical isolates and both laboratory strains were positive for LasA. Of these, only BC253, the lowest LasA producer, and BC312, a high HQNO producer, did not induce at least a 10-fold increase in killing by vancomycin (Figure 2.1C). Of the 5 LasA negative strains, only one, BC251, significantly potentiated vancomycin killing, although no lysis of the culture was observed (Figure 2.9B). These data suggest that *P. aeruginosa* potentiates the vancomycin killing of *S. aureus* via at least two distinct mechanisms, only one of which is LasA-dependent.

P. aeruginosa **potentiates vancomycin killing in a mouse model of** ***P. aeruginosa/S. aureus*** **co-infection**

Our observation that purified HQNO induces multidrug tolerance in *S. aureus* agrees with recent findings that *P. aeruginosa* protects *S. aureus* biofilm from vancomycin killing[77]. However, we have demonstrated that under planktonic growth conditions the protective effects of *P. aeruginosa* HQNO on *S. aureus* vancomycin susceptibility (Figure 2.5D) can be overcome by the lytic activity of LasA to potentiate vancomycin killing. In order to determine whether the protective effects of HQNO or the potentiating effects of LasA predominated *in vivo*, we adapted a previously described murine model of burn injury for *S. aureus, P. aeruginosa* co-infection[217]. Briefly, groups of mice were inflicted with a 20% total body surface area burn, then after 24h

were infected subcutaneously at the wound site with approximately 10^5 CFU *S. aureus,* HG003 alone or in combination with 10^3 PAO1 or 10^3 PAO1 *lasA*::tet. Mice were then treated daily with vancomycin, and harvested 72h post infection.

LasA has been shown to mediate *P. aeruginosa* epithelial cell invasion and has been shown to be essential for corneal infections[218,219]. Interestingly, in our burn model, it appeared that the presence of PAO1 resulted in a higher burden of *S. aureus*, which is also dependent on *lasA*. However, for this study, we were interested solely on the impact of PAO1 presence on vancomycin sensitivity of *S. aureus*. While we observed no significant vancomycin efficacy in *S. aureus* mono-infected mice, relative to an untreated control group, we observed a 2-Log reduction in *S. aureus* burden following vancomycin treatment in mice co-infected with *P. aeruginosa* PAO1 (Figure 2.12A,B). Furthermore, no potentiation of vancomycin killing was observed in mice co-infected with the PAO1 *lasA* transposon mutant (Figure 2.12 A,B). Importantly, *P. aeruginosa* appeared to be unaffected by vancomycin treatment, and burden was similar for both wild type and PAO1 *lasA::tet* infected mice (Figure 2.13). Finally, we observed that PAO1 transcription of *lasA* is strongly upregulated (~200-fold) during *in vivo* co-infection (Figure 2.12C). Up-regulation of *lasA* transcription was also observed during *P. aeruginosa* monoinfection, suggesting that *lasA* expression is independent of the presence or absence of *S. aureus* during burn wound infection.

Together, these data demonstrate that the presence of *P. aeruginosa* can potentiate vancomycin killing of *S. aureus* during infection through the production of LasA. To our knowledge, these data represent the first evidence of *P. aeruginosa* altering *S. aureus* antibiotic susceptibility *in vivo* and underlines the importance of

deciphering interspecies interactions to improve the antibiotic treatment of polymicrobial infections.

DISCUSSION

Polymicrobial infections are associated with exacerbated morbidity, accelerated disease progression and poor treatment outcome[81,193,220,221]. Antibiotic therapies are often selected to specifically target individual pathogens within a polymicrobial community without consideration of how interspecies interactions may alter a target organism's antibiotic susceptibility. *S. aureus* and *P. aeruginosa* are two major human pathogens that frequently co-exist within chronically colonized patients, and these infections are often impossible to resolve through conventional antibiotic therapy. We find that *P. aeruginosa* dramatically alters the susceptibility of *S. aureus* to the killing activities of commonly used and clinically relevant antibiotics through three distinct pathways governed by rhamnolipids, HQNO, and LasA, and that these molecules are produced at different levels by *P. aeruginosa* clinical isolates resulting in vastly different impacts on antibiotic efficacy against *S. aureus* (Figure 2.14)(Summarized in Table 2.3). We found that *P. aeruginosa* staphylolytic activity correlates with vancomycin potentiation, and that *P. aeruginosa* HQNO production correlates with ciprofloxacin antagonism (Figure 2.15). Correlation analysis with rhamnolipid production is not appropriate as the measurement of biosurfactant activity is qualitative. Overall, our results imply that antibiotic efficacy is strongly influenced by interactions between bacterial species, which may have major implications for future susceptibility determination and antibiotic treatment of polymicrobial infection.

Aminoglycosides are used routinely for the treatment of *P. aeruginosa* infection. Though aminoglycosides are effective against susceptible populations of *S. aureus,* bactericidal activity is limited against anaerobic, small colony variant (SCV), biofilm-associated, or persister subpopulations due in part to decreased respiration and thus PMF-dependent drug uptake[50,149]. Stimulating tobramycin uptake has been proposed as a way to eradicate these recalcitrant populations[149]. We have observed that *P. aeruginosa*-produced rhamnolipids sensitize the entire *S. aureus* population to tobramycin killing, leading to total eradication of otherwise tolerant populations. *P. aeruginosa* rhamnolipids may represent a promising new avenue for potentiating aminoglycoside killing of recalcitrant *S. aureus* and possibly other bacterial populations. Interestingly, a recent study has revealed that *S. aureus* increases tobramycin resistance in *P. aeruginosa* in an *in vitro* biofilm model, further emphasizing the importance of interaction between these organisms in dictating aminoglycoside susceptibility[222].

Vancomycin is a frontline antibiotic in the treatment of MRSA. To exert bactericidal activity against *S. aureus,* vancomycin must specifically bind the D-Ala-D-Ala residues of lipid II during cell wall biosynthesis[43]. However, vancomycin will also bind D-Ala-D-Ala residues of mature peptidoglycan. Thus, vancomycin exhibits limited bactericidal activity against dense populations of *S. aureus* cells due to the increased number of “decoy” targets available in late exponential or stationary phase populations of cells. Our data demonstrate that through LasA, *P. aeruginosa* can restore vancomycin efficacy against otherwise tolerant *S. aureus* populations. In support of this, we found that strains capable of increasing vancomycin lysis of *S. aureus* were LasA

producers while the inert strains, generally, were not. This variance in LasA production may be due to mutations in *lasR*, an activator of *lasA* expression, which acquires mutations at high frequency during chronic *P. aeruginosa* infection[223]. We hypothesize that the combined action of cell wall degradation by LasA and inhibition of *de novo* peptidoglycan biosynthesis by vancomycin leads to cell wall destruction and a potent bactericidal effect.

P. aeruginosa HQNO induces tolerance of *S. aureus* to multiple antibiotic classes through respiration inhibition and depletion of intracellular ATP. Recent work by Orazi *et al*. found that in a bronchial epithelial tissue culture system, *P. aeruginosa* inhibited the killing activity of vancomycin through HQNO[77]. In agreement with these findings, we observed that the addition of exogenous HQNO protects *S. aureus* from vancomycin killing (Figure 2.5D) However, during planktonic growth the protective effect of HQNO was overshadowed by LasA-mediated potentiation of vancomycin killing. Importantly, Orazi et al. performed killing assays in media containing albumin, which has been shown to inhibit LasA production [23, 40]. We were interested in examining whether *P. aeruginosa* antagonized or potentiated vancomycin *in vivo*, and found that *P. aeruginosa* expresses LasA at high levels during infection, and significantly potentiates the activity of vancomycin against *S. aureus*. This effect was abrogated in a *P. aeruginosa lasA* mutant suggesting that LasA plays a role in potentiating vancomycin killing of *S. aureus* during polymicrobial infection.

Similarly, we observed *in vitro* that *P. aeruginosa*-produced rhamnolipids can negate the protective effect of HQNO to restore or even increase *S. aureus* susceptibility to tobramycin killing. The opposing influences of HQNO and rhamnolipids

on aminoglycoside activity against *S. aureus* may have major implications for aminoglycoside treatment of *S. aureus* during co-infection where production of one factor may dominate, leading to inhibition or potentiation of tobramycin activity against *S. aureus*. Indeed, we observed that clinical isolates produce a range of HQNO, LasA and rhamnolipids, and production of each factor determines an isolate's ability to potentiate or antagonize antibiotic killing.

P. aeruginosa strain variation and the impact of this variation on *S. aureus* antibiotic susceptibility suggests that a personalized approach to antibiotic therapy may be necessary to identify the ideal therapy to eradicate infection in an individual patient based on the genotype of *S. aureus* and the genotype of the bacteria it's interacting with. Recent work has demonstrated that within the infectious environment, the production of HQNO, LasA and rhamnolipids is highly variable. *P. aeruginosa* isolates from chronic CF infections frequently harbor mutations associated with decreased quorum sensing activities and increased alginate production[223]. These mutations are attributed to the conversion to a mucoidal phenotype of *P. aeruginosa* that is significantly less competitive with *S. aureus*[224]. *P. aeruginosa* mucoidy is rarely associated with acute infection, thus the impact of *P. aeruginosa* on antibiotic susceptibility of *S. aureus* may differ during acute vs. chronic co-infection. Future studies are necessary to identify genetic hallmarks of *P. aeruginosa* strains that potentiate or antagonize the activities of different antibiotic classes against *S. aureus* towards the goal of improving antibiotic efficacy against currently unresolvable co-infections.

It has long been observed that *S. aureus* is the dominant pathogen in the early life of CF patients with *P. aeruginosa* eventually dominating later in life[225]. It is interesting to consider a possible role of altered antibiotic susceptibility of *S. aureus* contributing to these dynamics, where vancomycin or tobramycin treatment in the presence of LasA or rhamnolipid producing *P. aeruginosa* strains may be particularly efficacious, resulting in a decrease in relative *S. aureus* abundance.

In summary, we characterized 3 distinct *P. aeruginosa* mediated pathways altering *S. aureus* antibiotic susceptibility. HQNO induces a low-energy multidrug tolerant state while LasA and rhamnolipids overcome this tolerance in co-operation with vancomycin and tobramycin respectively. Exploitation of these newly discovered pathways may lead to better prediction of antibiotic efficacy *in vivo* and improved treatments for chronic *S. aureus* infection.

MATERIALS AND METHODS

Ethics Statement

P. aeruginosa CF isolates were provided by an IRB approved biospecimen bank (IRB#02-0948). *P. aeruginosa* burn wound isolates were from a previous study and use was deemed exempt by IRB study number #17-0836. All mice used in the study were maintained under specific pathogen-free conditions in the Animal Association of Laboratory Animal Care-accredited University of North Carolina Department of Laboratory Animal Medicine Facilities. All protocols were approved by the Institutional Animal Care and Use Committee at the University of North Carolina, protocol number 17-141, and all experiments were performed in accordance with the National Institutes

of Health. Animals were anesthetized by inhalation of vaporized isoflurane. A subcutaneous injection of morphine was given prior to burn injury for pain control, and an intraperitoneal injection of lactated Ringer's solution was given immediately after burn injury for fluid resuscitation. Animals were provided morphinated water *ab libitum* and monitored twice a day.

Bacterial strains and growth conditions

S. aureus strains HG003 and JE-2 was cultured aerobically in Mueller-Hinton broth (MHB) at 37°C with shaking at 225 rpm. HG003 is a well-characterized model strain of *S. aureus*, while JE-2 is a well-characterized USA300 *S. aureus* associated with community acquired MRSA infection. For anaerobic growth, overnight cultures were washed twice with PBS and diluted into 5 ml of pre-warmed (37°C) TSB + 100mM MOPS (pH7) to an OD_{600} of 0.05. Cultures were prepared in triplicate in 16x150mm glass tubes containing 1mm stir bars. Following dilution, cultures were immediately transferred into a Coy anaerobic chamber and grown at 37°C with stirring. *P. aeruginosa* strains were grown aerobically in MHB at 37°C with shaking at 225 rpm. Burn wound isolates represent the first positive Pseudomonal wound cultures obtained from 5 unique patients admitted to the NC Jaycee Burn Center between Nov 2015 and April 2016 with a total body surface area burn $\geq$ 20% and/or inhalational injury after obtaining informed consent. Cystic fibrosis isolates were collected from 5 patients at the UNC medical center. Isolates were cultured from sputum or bronchoalveolar lavage (BAL) from patients with cystic fibrosis after obtaining informed consent. All burn and CF isolates were grown on *Pseudomonas* isolation agar (BD Difco) and verified with 16S

ribosomal sequencing using the primer pair 5'-AGTATTGAACTGAAGAGTTTGATCATGG-3' and 5'-CTGAGATCTTCGATTAAGGAGGTGA-3' for PCR amplification.

Strain construction

The PAO1 *lasA* mutant (PW4282 *lasA*-H03::ISlacZ/hah) was from the PAO1 knockout library[226]. PA14 deletion mutants were constructed by singly or sequentially deleting the coding sequences of *rhlA*, *pqsL*, *phzS* and *hcnC*. Briefly, flanking primers were designed to anneal 800-1200bp upstream and downstream of the coding region. The resulting PCR product was inserted into plasmid pEX18Gm in accordance with the NEBuilder HiFi DNA Assembly protocol (New England Biolabs). Mutant alleles were integrated onto the chromosome of PA14 as described previously[227]. Briefly, pEX18Gm containing the in-frame deletion and gene-specific flanking regions was mated into *P. aeruginosa* via *E. coli* S17-λpir. Primary integrants were selected for with gentamycin and irgasan, then grown for 4h in LB without selection to allow for recombination. Dilutions of *P. aeruginosa* were plated on LB containing 8% sucrose for counterselection (loss of plasmid). Deletion strains were confirmed through PCR and sequencing (Genewiz). Plasmid P*pflB::gfp* was constructed as follows, 298bp upstream of the *pflB* coding region was amplified from HG003 genomic DNA using primers flanked with *EcoRI* and *XbaI* sites and cloned upstream of gfp_{UVr} in plasmid pALC1434[228].

Antibiotic survival assays

To prepare sterile supernatants, *S. aureus* and *P. aeruginosa* strains were grown in MHB at 37°C with shaking at 225 rpm for ~20h. The cultures were pelleted and supernatants were passed through a 0.2µm filter. HG003 or JE-2 was grown to ~$5x10^7$ (for cell wall acting antibiotics) or ~$2x10^8$cfu/ml (for all other antibiotics) in 3ml MHB under aerobic or in 5ml TSB + 100mM MOPS under anaerobic conditions. Cells were pre-treated with 0.5ml sterile supernatant (or 0.83ml for anaerobic cultures) and returned to the incubator for a further 30 minutes. A 30-minute pre-exposure was routinely used as we attempted to emulate the situation *in vivo*, where a population that has encountered and reacted to the relevant metabolites is subsequently exposed to antibiotic treatment. Where appropriate, cells were treated with 0.5ml of *P. aeruginosa* culture taken directly from *s*tationary phase (18hr) cultures in place of sterile supernatant. Co-culture experiments were performed in the presence of 5% bovine serum albumin (BSA) to facilitate *S. aureus/P. aeruginosa* co-existence. An aliquot was plated to enumerate cfu before the addition of antibiotics. Antibiotics were added at concentrations similar to the Cmax in humans at recommended dosing; ciprofloxacin 2.34µg/ml[229], tobramycin 58µg/ml[230], vancomycin 50µg/ml[231]. The Cmax of vancomycin is physiologically relevant for bacteremia and infections with good blood supply. The Cmax of vancomycin in serum is likely higher than that reached in the lung during i.v infusion, however, it is certainly within the range experienced during inhaled therapy where clinical trials observed a Cmax of 270 µg/ml in sputum of CF patients. The Cmax of tobramycin is 58 µg/ml. Regarding lung concentrations, work by Ruddy et al. has found that inhaled tobramycin therapy results in sputum concentrations of

between 17.2 and 327.3 μg/ml. The concentration we use is well within this range. Also, this therapy fails to eradicate *P. aeruginosa in vivo* and thus, we believe is physiologically relevant for this study[232]. The ciprofloxacin blood Cmax used in this study is 2.34 μg/ml. This is also well within the physiologically relevant concentration for lung infection where ciprofloxacin concentration is actually higher than corresponding blood serum levels[233].

Ciprofloxacin concentration was increased to 4.68μg/ml when cells were grown in TSB + 100mM MOPS to account for any decrease in pH where ciprofloxacin killing activity is reduced. At indicated times, an aliquot was removed and washed with 1% NaCl. Cells were serially diluted and plated to enumerate survivors. We routinely used two time points to enumerate survivors, 16h and 24h after antibiotic challenge as we previously found that, in *S. aureus*, susceptible cells are killed and a stable sub-population of survivors emerges between 16 and 24h of exposure to antibiotics[26,56]. Where indicated sterile supernatant was heat-inactivated at 95°C for 10 min before addition to culture. Where indicated, pyocyanin 100μM, HQNO 11.5μM, sodium cyanide 150μM or rhamnolipids 10-50μg/ml (50/50 mix of mono- and di-rhamnolipids, Sigma) or L-rhamnose 10-50μg/ml were added in place of supernatant. Concentrations of respiratory toxins represent levels detected in the sputum of cystic fibrosis patients[206,208].

Promoter induction measurement

S. aureus strain HG003 harboring *gfp* promoter plasmid P*pflB::gfp* was grown to

~2x10^8cfu/ml in 3ml MHB containing chloramphenicol 10µg/ml. Cultures were treated with 0.5ml supernatant from HG003, PAO1, PA14 or *P. aeruginosa* clinical isolates as indicated. 200µl culture was added to the wells of a clear bottom, black side 96-well plate. The plate was placed in a Biotek Synergy H1 microplate reader at 37°C with shaking. Absorbance (OD_{600}) and GFP fluorescence (emission 528nm and excitation 485nm) were measured every 1h for 16h. GFP values were divided by OD_{600}.

ATP assays

HG003 was grown to ~2x10^8cfu/ml in 3ml MHB and pre-treated with 0.5ml sterile supernatant from *S. aureus* HG003 or *P. aeruginosa* PAO1 or PA14. ATP levels of the cultures were measured after 1.5h as described previously using a Promega BacTiter Glo kit according to the manufacturer's instructions[26]. *P*-values are indicated.

Vancomycin lysis assay

HG003 was grown to ~2x10^8cfu/ml in 3ml MHB and pre-treated with 0.5ml sterile supernatant from *S. aureus* HG003, *P. aeruginosa* PAO1, PA14 or *P. aeruginosa* clinical isolates as indicated. Cells were incubated for a further 30min before addition of vancomycin 50µg/ml. 200µl aliquots were added to the wells of a clear 96-well plate and placed in a Biotek Synergy H1 microplate reader. Absorbance (OD_{600}) was measured every 1h for 16h.

Western blot analysis of LasA

P. aeruginosa strains were grown in MHB media for ~20h. Cultures were normalized to OD_{600} 2.0, pelleted and supernatants were passed through a 0.2μm filter. Supernatants were boiled in SDS-sample buffer and run on a 4-12% bis-tris acrylamide gel (Invitrogen). Protein was transferred onto a PVDF membrane and LasA was detected using rabbit polyclonal anti-LasA antibodies (LifeSpan BioSciences, Inc.).

Staphylolytic assay

Staphylolytic assay was modified from Grande *et al*.[216]. Briefly, stationary phase *S. aureus* strain HG003 was heat killed at 95c for 20min. Cells were pelleted and resuspended in 20mM Tris-HCl (pH 8.0) at an OD_{595} 0.8-1. *P. aeruginosa* strains were cultured in MHB media for ~20h. Cultures were normalized to OD_{600} 2.0, pelleted and supernatants were passed through a 0.2μm filter. 17μl sterile supernatant was added to a 100μl heat-killed cells. OD_{595} was measured at time 0 and after 2h and % cell lysis was determined. The values shown represent the average of biological triplicates.

Tobramycin-Texas Red Uptake

Tobramycin-Texas Red was made as described previously[27,234]. *S. aureus* strain HG003 was grown to mid-exponential phase and then incubated with or without 30μg/ml rhamnolipids for 30min. Cells were plated to enumerate cfu prior to addition of Texas-Red tobramycin at a final concentration of 58μg/ml. After 1h, an aliquot of cells was removed, washed twice in 1% NaCl and plated to enumerate survivors. The remaining

aliquot was analyzed for Texas Red uptake on a BD Fortessa flow cytometer. 30,000 events were recorded. Figures were generated using FSC Express 6 Flow.

Rhamnolipid Quantification

P. aeruginosa rhamnolipid production was quantified utilizing a drop collapse assay, as previously described[213]. Briefly, clarified supernatants from overnight cultures of *P. aeruginosa* strains were serially diluted (1:1) with de-ionized water plus 0.005% crystal violet for visualization. 25µl aliquots of each dilution were spotted on to the underside of a petri dish plate and tilted to a 90° angle. Surfactant scores represent the reciprocal of the highest dilution at which a collapsed drop migrated down the surface of the plate.

LC-MS/MS quantification of HQNO

500µl aliquots of *P. aeruginosa* supernatant were extracted 3 times with 1ml of ethyl acetate containing 0.01% acetic acid. For each extraction, samples were vortexed for 30 seconds then centrifuged at 15,000xg for 2 minutes. The organic phases were removed and combined in a separate tube and evaporated to dryness in a TurboVap under a gentle stream of nitrogen at 50°C. Dried samples were reconstituted in 250µl acetonitrile and a portion diluted by a factor of 100 prior to analysis by liquid chromatography tandem mass spectrometry (LC-MS/MS). Quantitative analyses were performed on a Quantum Ultra triple quadrupole mass spectrometer (Thermo Scientific, Waltham, MA) equipped with an Acquity ultra performance liquid chromatography (UPLC) system (Waters Corp., Milford, MA). A sample injection volume of 10µl was separated on a 2.1 x 100mm, 1.7µm, CSH™ Fluoro-Phenyl UPLC column (Waters

Corp., Milford, MA) at a flow rate of 250µl per minute and a column temperature of 40°C. Mobile phase solvents consisted of 0.1% acetic acid in deionized water (A) and methanol (B). Separation was achieved with a linear gradient from 30% to 95% B over 5 minutes with a total run time of 10 minutes. Column effluent was diverted to waste from 1-3 and 7-10 minutes, and HQNO eluted at a retention time of 5.8 minutes. The mass spectrometer was operated in positive ion electrospray mode (3000 V; 250°C), and data were acquired by selected reaction monitoring (SRM) in centroid mode using a mass transition of 260.1 to 159.3 m/z and a collision energy of 26 eV.

Burn wound model of *P. aeruginosa/S. aureus* co-infection

Animals were purchased from Taconic Farms and housed in specific pathogen free conditions in the Animal Association of Laboratory Animal Care-accredited at the University of North Carolina's Department of Laboratory Animal Medicine Facilities. All protocols were approved by the Institutional Animal Care and Use Committee at the University of North Carolina, and all experiments were performed in accordance with the National Institutes of Health. Wild type C57BL/6 mice were burned and infected as previously described[217]. Briefly, a 65g copper rod was heated to 100°C and used to create a full-contact burn of approximately 20% of total body surface area through four applications of the rod to the anesthetized animal's dorsal region. In preparing the inoculum, overnight cultures of bacterial strains were subcultured into fresh MHB and grown for 2.5h to mid-exponential phase. An aliquot of each culture was centrifuged and washed with 1ml of PBS + 1% protease peptone. Approximate bacterial density was calculated by absorbance (OD_{600}), and cultures were diluted to obtain the desired

concentration. Inoculum was verified through CFU enumeration. Mice were infected subcutaneously in the mid-dorsal region in unburned skin surrounded by the wound 24h after burn. Mice were administered vancomycin intraperitoneally at 110mg/kg once daily for two days, then sacrificed 48h post-infection. At the time of sacrifice, 5mm tissue biopsy of the bacterial infection site were aseptically removed, homogenized with 3.2mm stainless steel beads and a Bullet Blender (Next Advance; Averill Park, NY) then bacterial burden was enumerated by plating serial dilutions of the homogenates on selective media. Mice that mostly cleared *P. aeruginosa* ($<10^3$ CFU/g tissue) were discounted from analysis.

qRT-PCR

250ul of homogenized tissue was suspended in 1ml of Trizol (ThermoFisher) and frozen at -80^{o}C until extraction. RNA was extracted following manufacturer's protocol. Extracted RNA was DNase treated with 10 units RQ-1 RNase free DNase (Promega) following manufacturer's protocol. RNA was purified after DNase treatment using RNA Clean and Concentrator-25 (Zymo) and eluted in 30µl of H2O, and quantified using a NanoDrop spectrophotometer. 500ng of total RNA was used to generate cDNA using SuperScript II Reverse Transcriptase (ThermoFisher) and Random Primer 9 (NEB) following manufacturer's protocol. Copy number of *lasA* and *gyrA* were quantified using iTaq Universal Sybr Green master mix (Bio-Rad) in 20ul reaction volumes on a Roche LightCycler 96, using the following primer pairs: lasA_RT_5 5'-CCTGTTCCTCTACGGTCGCG-3', lasA_RT_3 5'-GGTTGATGCTGTAGTAGCCG-3',

gyrA_5_RT 5'-GAAGCTGCTCTCCGAATACC-3', gyrA_3_RT 5'-CAGTTCCTCACGGATCACCT-3'.

MIC Assays

MICs were determined using the microdilution method. Briefly, ~5x10^5cfu were incubated with varying concentrations of ciprofloxacin, tobramycin, or vancomycin in a total volume of 200µl MHB in a 96-well plate. Where indicated, 34µl MHB was replaced with sterile *P. aeruginosa* or *S. aureus* supernatant or purified HQNO or rhamnolipids at final concentrations of 11.5µM and 30µg/ml, respectively. MICs were determined following incubation at 37c for 24h.

Statistical Analysis

Statistical data analysis was performed using Prism GraphPad software (San Diego, CA) version 5.0b. Differences in *S. aureus* intracellular ATP concentration or surviving *S. aureus* CFU following *P. aeruginosa* supernatant treatment and antibiotic challenge were compared using a one-way ANOVA with Tukey's multiple comparisons post-test or the Student's t-test where appropriate. Differences in tissue burden following *S. aureus, P. aeruginosa* co-infection were compared with a Mann-Whitney test. Finally, the statistical significance of each correlation analysis was determined with a two-tailed Pearson's chi-squared test. Differences with a p-value ≤ 0.05 were considered significant.

FIGURES

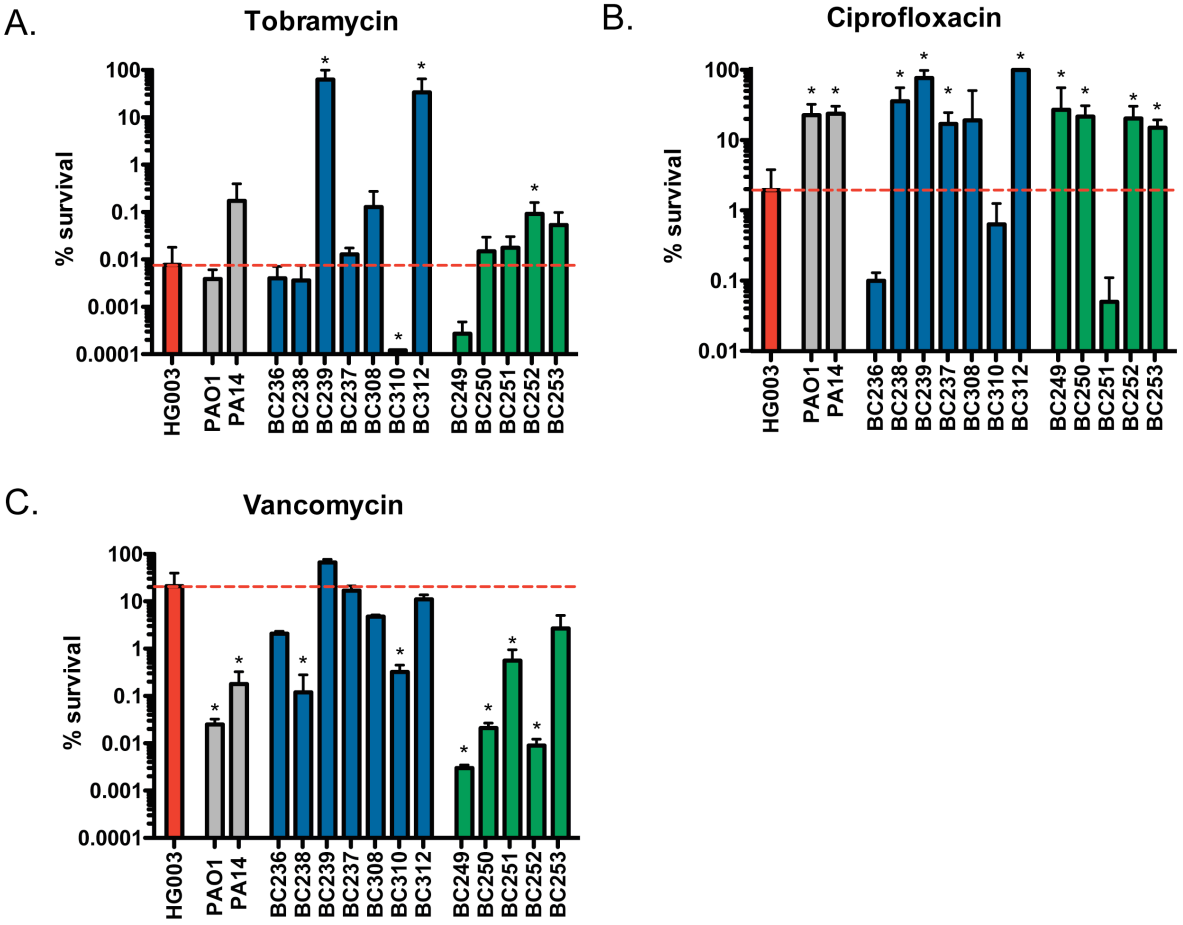

Figure 2.1. *P. aeruginosa* supernatant alters *S. aureus* antibiotic susceptibility. *S. aureus* strain HG003 was grown to mid-exponential phase and exposed to sterile supernatants from *S. aureus* HG003 (red), *P. aeruginosa* laboratory strains PAO1 and PA14 (grey), *P. aeruginosa* CF clinical isolates (blue) or *P. aeruginosa* burn isolates (green) for 30min prior to addition of **(A)** 50µg/ml vancomycin, **(B)** 58µg/ml tobramycin or **(C)** 2.34µg/ml ciprofloxacin - concentrations similar to the Cmax in humans. An aliquot was removed after 24h, washed and plated to enumerate survivors. The dotted red line represents the number of survivors in the control culture. All experiments were performed in biological triplicate and the number of survivors following antibiotic challenge in the presence of *P. aeruginosa* supernatant was compared to the HG003 supernatant-treated control. *$p<0.05$ (one-way ANOVA with Tukey's multiple comparisons post-test analysis of surviving CFU). Error bars represent mean + sd.

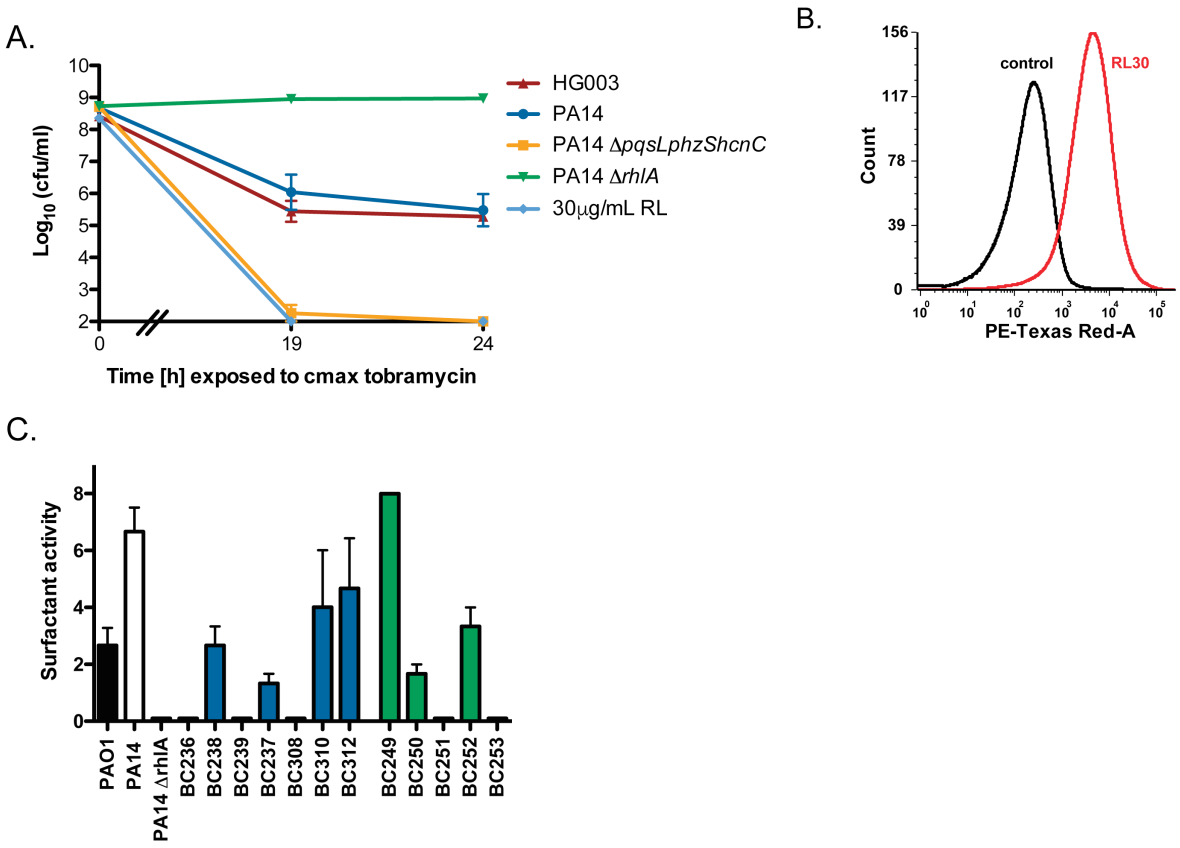

Figure 2.2. *P. aeruginosa* rhamnolipids potentiate aminoglycoside uptake and cell death in *S. aureus*. *S. aureus* HG003 was grown to mid-exponential phase and exposed to **(A)** sterile supernatants from *P. aeruginosa* or *S. aureus* or exogenous addition of rhamnolipids (30μg/ml) before addition of tobramycin 58μg/ml. At indicated times, an aliquot was washed and plated to enumerate survivors. **(B)** Texas Red-conjugated tobramycin was added to *S. aureus* cultures with or without 30μg/ml rhamnolipids. Following 1h, Texas Red-tobramycin uptake was measured by flow cytometry. **(C)** Rhamnolipid production present in the supernatant of *P. aeruginosa* PAO1, PA14, PA14 *ΔrhlA*, CF isolates (blue) or burn isolates (green) were quantified by a drop-collapse assay. Experiments were performed in biological triplicate. Error bars represent mean ± sd.

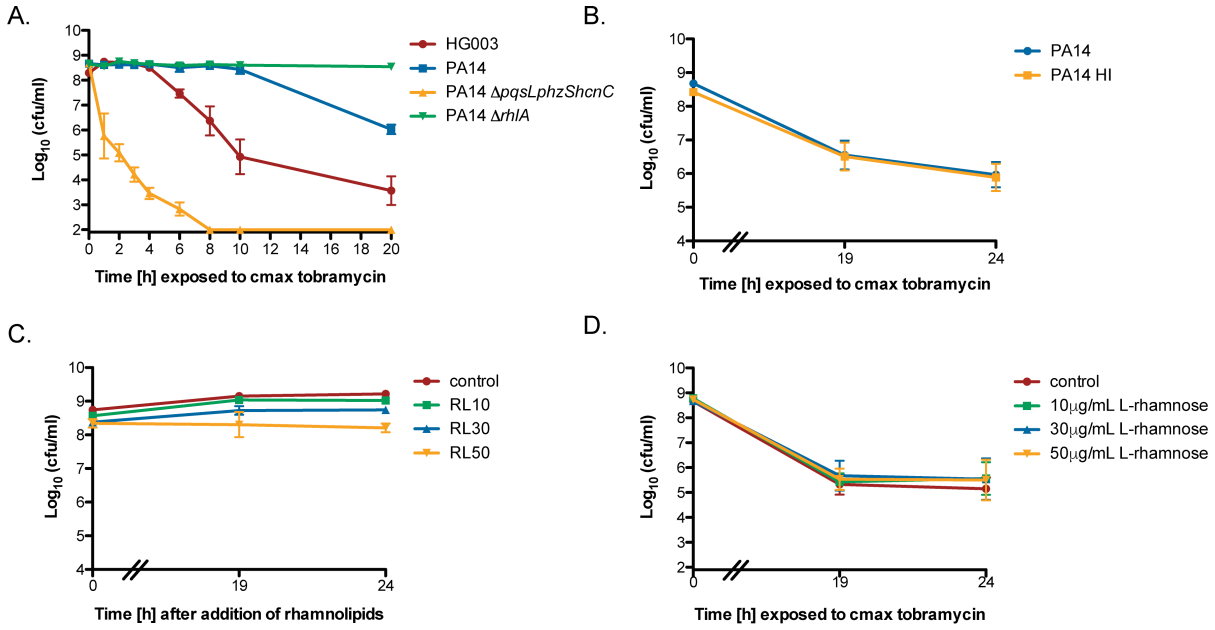

Figure 2.3. Rhamnolipids do not cause cell death in *S. aureus* in the absence of tobramycin. *S. aureus* strain HG003 was grown to mid-exponential phase in MHB media and pre-treated with **(A,B)** sterile supernatants from *P. aeruginosa* PA14 wild type or isogenic mutants, *S. aureus* HG003 or **(D)** L-rhamnose 10-50μg/ml before addition of tobramycin at 58μg/ml. Where indicated, PA14 supernatant was heat inactivated (PA14 HI) at 95c for 10min. **(C,D)** Cultures were treated with exogenous rhamnolipids or L-rhamnose (10-50μg/ml) in the absence of antibiotic. At indicated times, an aliquot was washed and plated to enumerate survivors. Error bars represent mean ± sd.

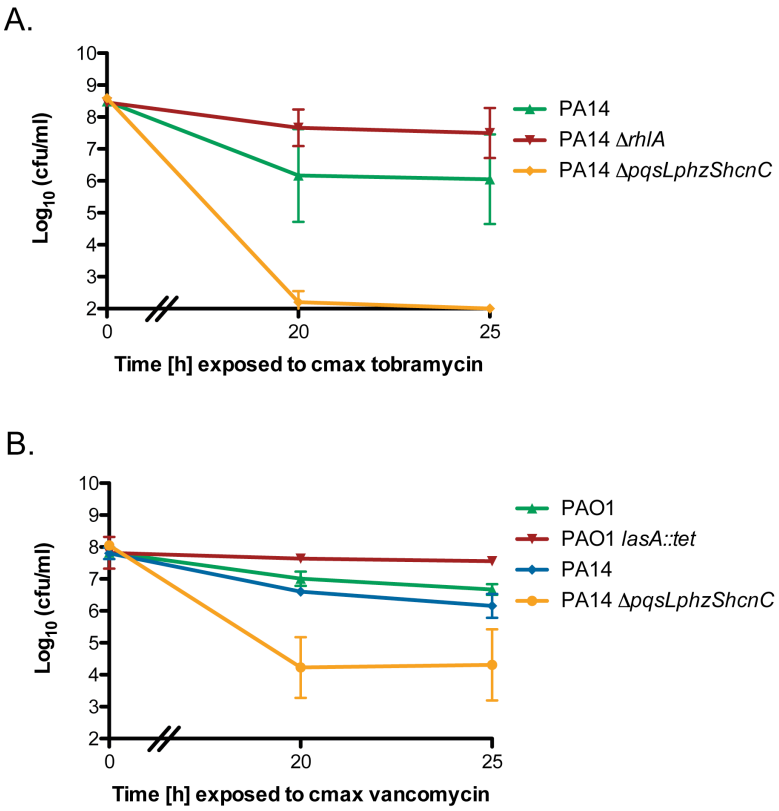

Figure 2.4. Exposure to *P. aeruginosa* supernatant alters methicillin resistant *S. aureus* (MRSA) antibiotic susceptibility. *S. aureus* strain JE-2 was grown to mid-exponential phase and exposed to sterile supernatants from *P. aeruginosa* for 30 mins prior to the addition of **(A)** tobramycin 58µg/ml or **(B)** vancomycin 50 µg/ml. At indicated times, an aliquot was removed, washed and plated to enumerate survivors. All experiments were performed in biological triplicate. Error bars represent mean ± sd.

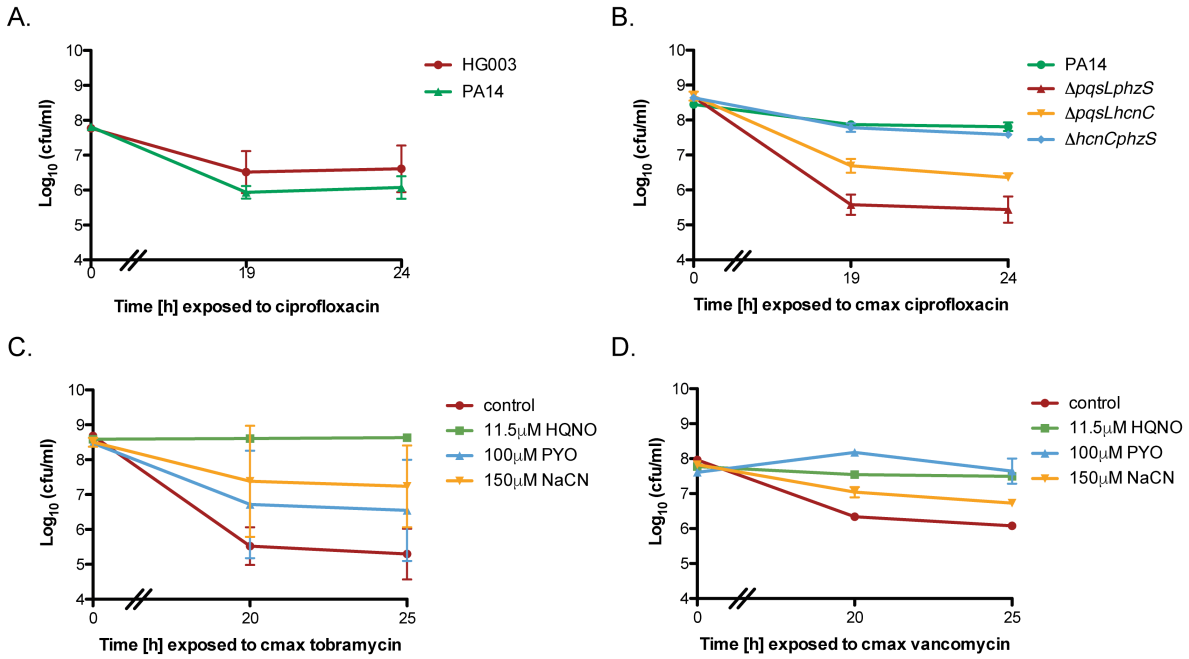

Figure 2.5. *Pseudomonas*-produced toxins inhibit respiration in *S. aureus* and induce antibiotic tolerance. (A) *S. aureus* HG003 was grown to mid-exponential phase in TSB + 100mM MOPS in an anaerobic chamber and pre-treated with sterile supernatants from HG003 or PA14 for 30min before addition of ciprofloxacin. HG003 was grown aerobically to mid-exponential phase in MHB media and pre-treated with **(B)** sterile supernatants from *P. aeruginosa* strains PA14 wild-type or its isogenic mutants or **(C-D)** physiologically relevant concentrations of HQNO, pyocyanin (PYO) or sodium cyanide (NaCN) for 30min prior to antibiotic challenge[206,208]. At indicated times, an aliquot was washed and plated to enumerate survivors. All experiments were performed in biological triplicate. Error bars represent mean ± sd.

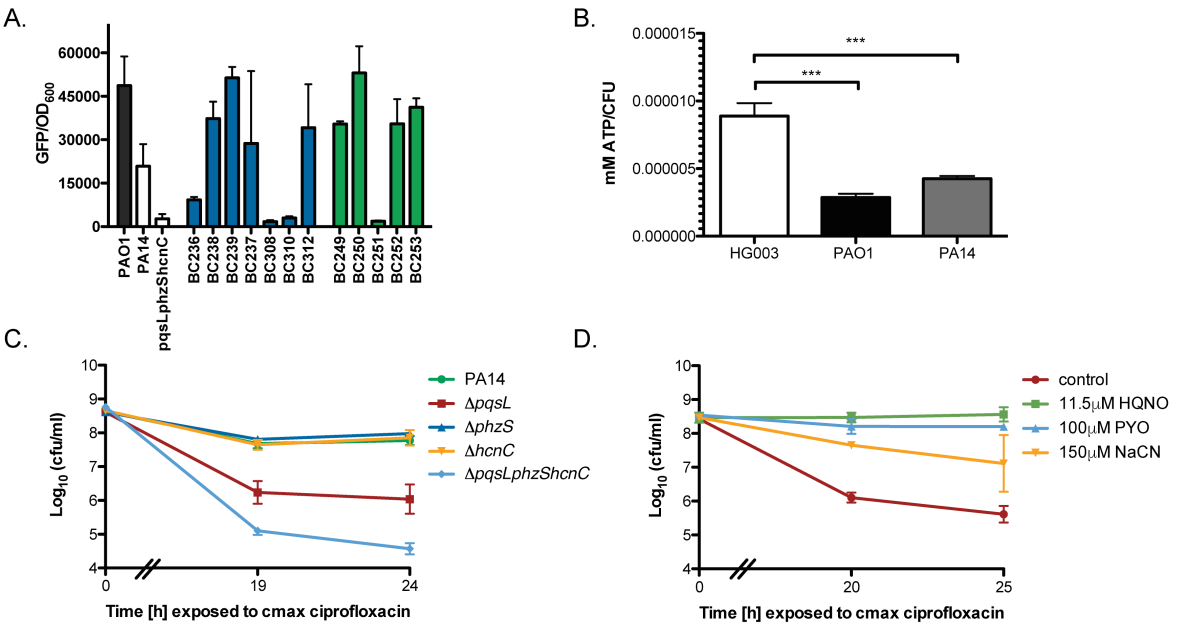

Figure 2.6. *P. aeruginosa* secondary metabolites inhibit *S. aureus* aerobic respiration resulting in a drop in intracellular ATP and protection from ciprofloxacin killing. **(A)** *S. aureus* strain HG003 harboring plasmid P*pflB::gfp* was grown to mid-exponential phase and treated with supernatant from *P. aeruginosa* PAO1, PA14, CF isolates (blue) or burn isolates (green), for 30min. OD_{600} and *gfp* expression levels were determined after 16h using a Biotek Synergy H1 microplate reader. **(B)** Intracellular ATP was measured after 1.5h incubation with supernatant. ****p*<0.0005 (one-way ANOVA with Tukey's multiple comparison post-test). **(C)** *S. aureus* strain HG003 was grown to mid-exponential phase in MHB media and pre-treated with sterile supernatants from *P. aeruginosa* strains PA14 wild-type or its isogenic mutants or **(D)** physiologically relevant concentrations of HQNO, pyocyanin (PYO) or sodium cyanide (NaCN) for 30min prior to antibiotic challenge. At indicated times, an aliquot was washed and plated to enumerate survivors. All experiments were performed in biological triplicate. Error bars represent mean ± sd.

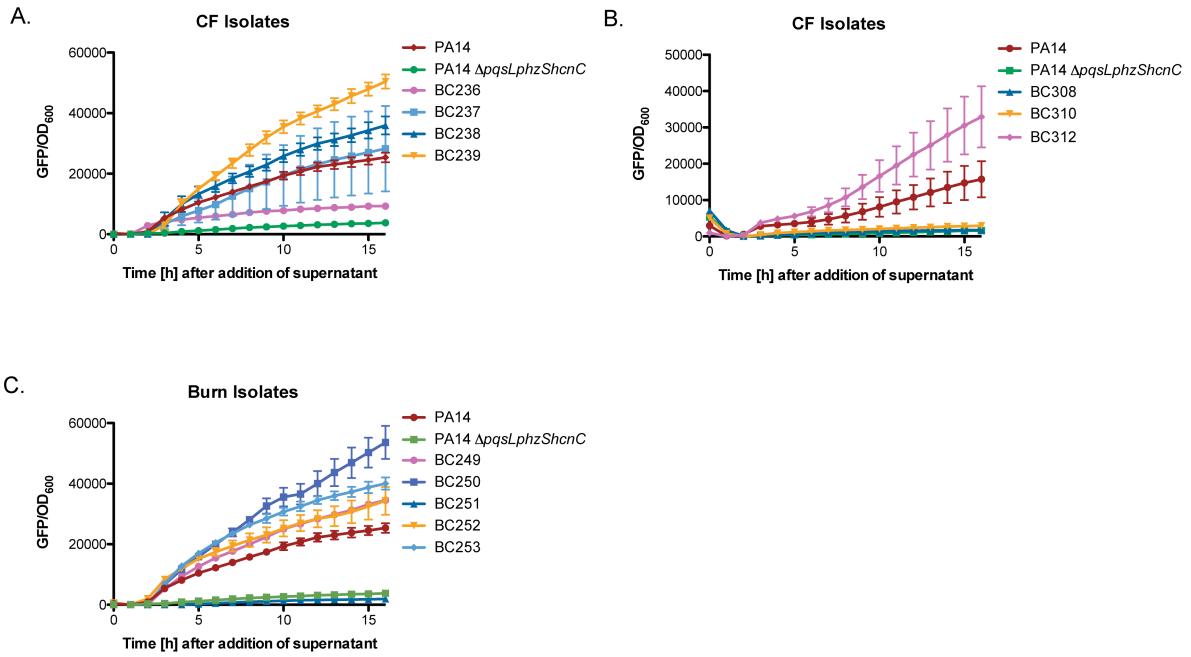

Figure 2.7 *P. aeruginosa* supernatant inhibits *S. aureus* aerobic respiration. (A-C) *S. aureus* strain HG003 harboring plasmid *PpflB::gfp* was grown to mid-exponential phase and treated with supernatant from *P. aeruginosa* clinical isolates or laboratory strains. OD_{600} and *gfp* expression levels were measured every 30 minutes for 16h using a Biotek Synergy H1 microplate reader. All experiments were performed in biological triplicate. Error bars represent mean ± sd.

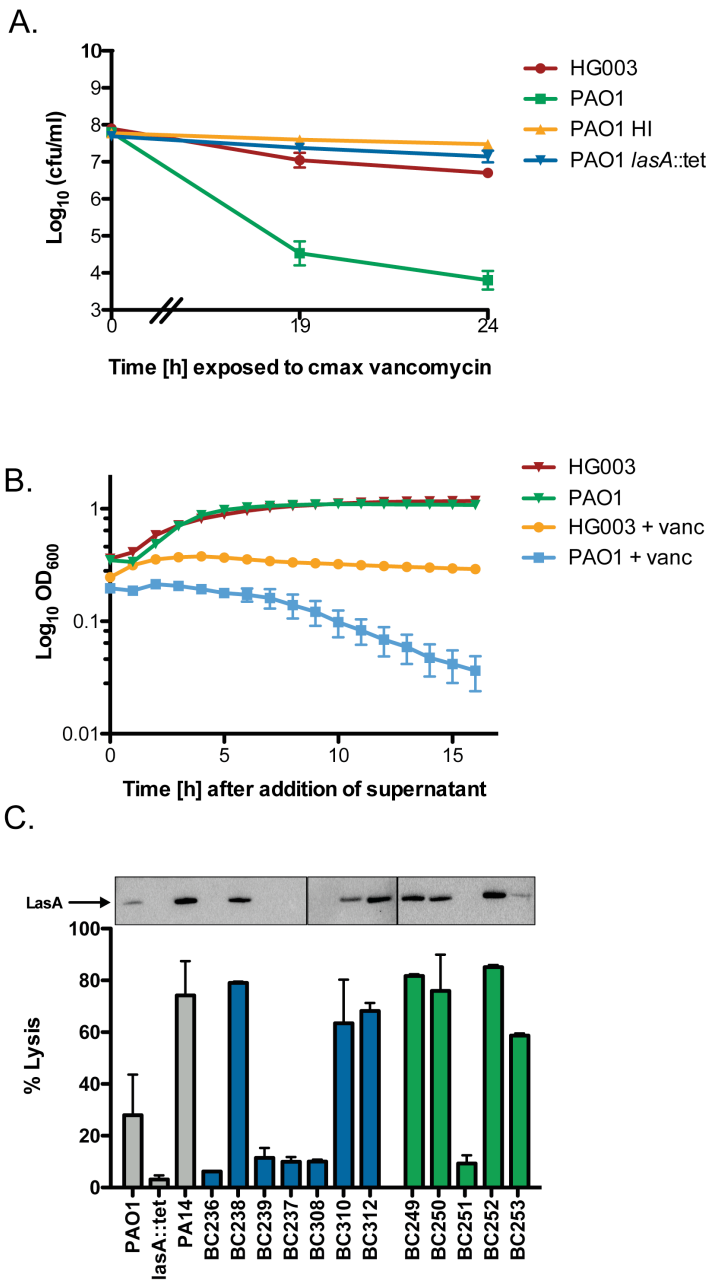

Figure 2.8. *P. aeruginosa* supernatant potentiates killing by vancomycin via the LasA endopeptidase. *S. aureus* HG003 was grown to mid-exponential phase and exposed to sterile supernatants for 30min prior to addition of vancomycin 50µg/ml. Where indicated, PAO1 supernatant was heat inactivated (PAO1 HI) at 95c for 10min. **(A)** At indicated times, an aliquot was removed, washed and plated to enumerate survivors or **(B)** 100µl cells were added to a 96-well plate and lysis was measured at OD_{600} every hour for 16h. **(C)** LasA present in the supernatant of *P. aeruginosa* PAO1, PA14, CF isolates (blue) or burn isolates (green) was quantified by western blot and the ability of each supernatant to lyse heat-killed *S. aureus* HG003 cells after 2h. Error bars represent mean ± sd.

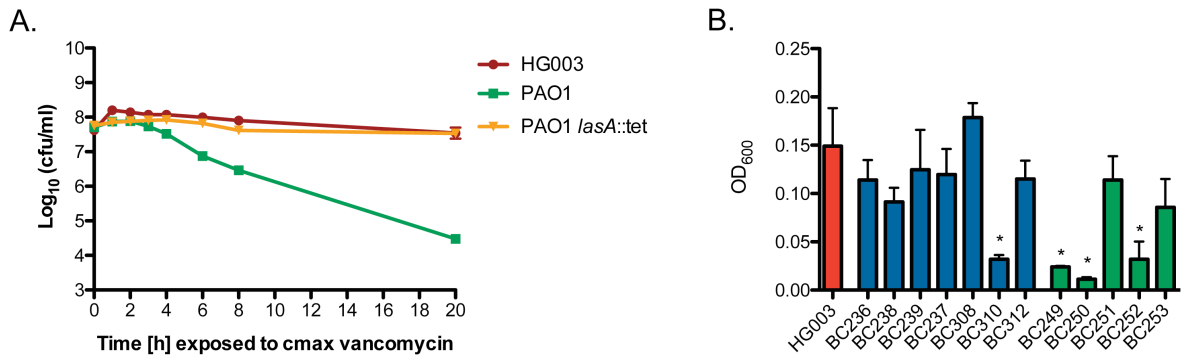

Figure 2.9. *P. aeruginosa* endopeptidase LasA induces lysis in *S. aureus.* *S. aureus* HG003 was grown to mid-exponential phase and exposed to sterile supernatants indicated for 30min prior to addition of vancomycin 50µg/ml. **(A)** At indicated times, an aliquot was removed, washed and plated to enumerate survivors. **(B)** At 24h post antibiotic treatment, the turbidity of cultures treated with supernatant from HG003 (red), *P. aeruginosa* CF isolates (blue), or burn isolates (green) was measured by absorbance at OD_{600}. *$p<0.05$ by one-way analysis of variance (ANOVA) and Tukey's multiple comparisons post-test. All experiments were performed in biological triplicate. Error bars represent mean ± sd.

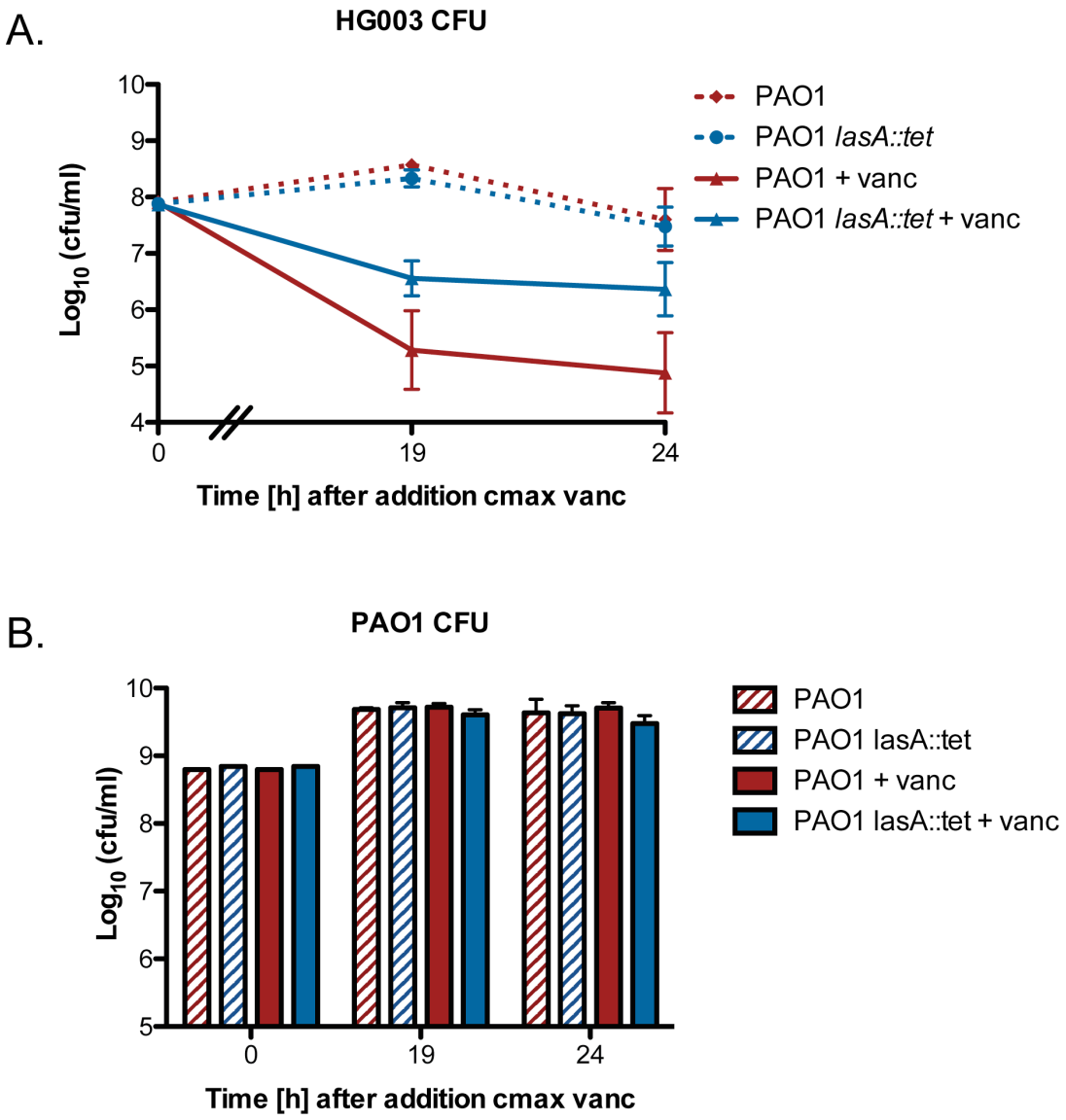

Figure 2.10. *P. aeruginosa* LasA potentiates vancomycin killing of *S. aureus* during *P. aeruginosa/S. aureus* co-culture. *S. aureus* strain HG003 was grown to mid-exponential phase, exposed to 0.5 ml of stationary phase culture from *P. aeruginosa* strains PAO1 or PAO1 *lasA::tet* and 5% BSA for 30 mins prior to addition of vancomycin (50 µg/ml). At indicated times, an aliquot was removed, washed and plated on selective media to enumerate **(A)** *S. aureus* and **(B)** *P. aeruginosa* cells. All experiments were performed in biological triplicate. Error bars represent mean ± sd.

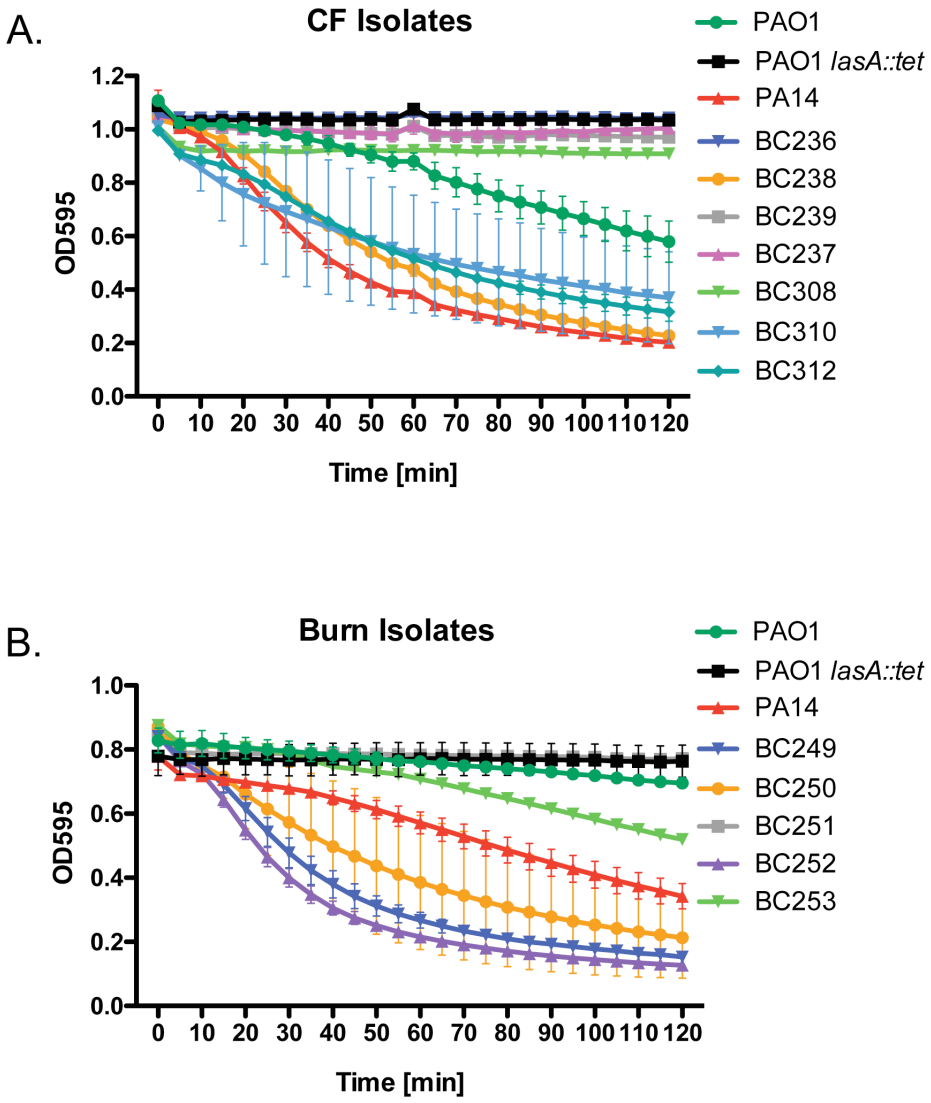

Figure 2.11. *P. aeruginosa* LasA lyses heat-killed *S. aureus*. (A,B) Heat killed *S. aureus* cells were incubated with supernatant from *P. aeruginosa* isolates in a 96-well plate. Lysis of *S. aureus* was monitored by measuring OD_{595} every 5 minutes for 2h. All experiments were performed in biological triplicate. Error bars represent mean ± sd.

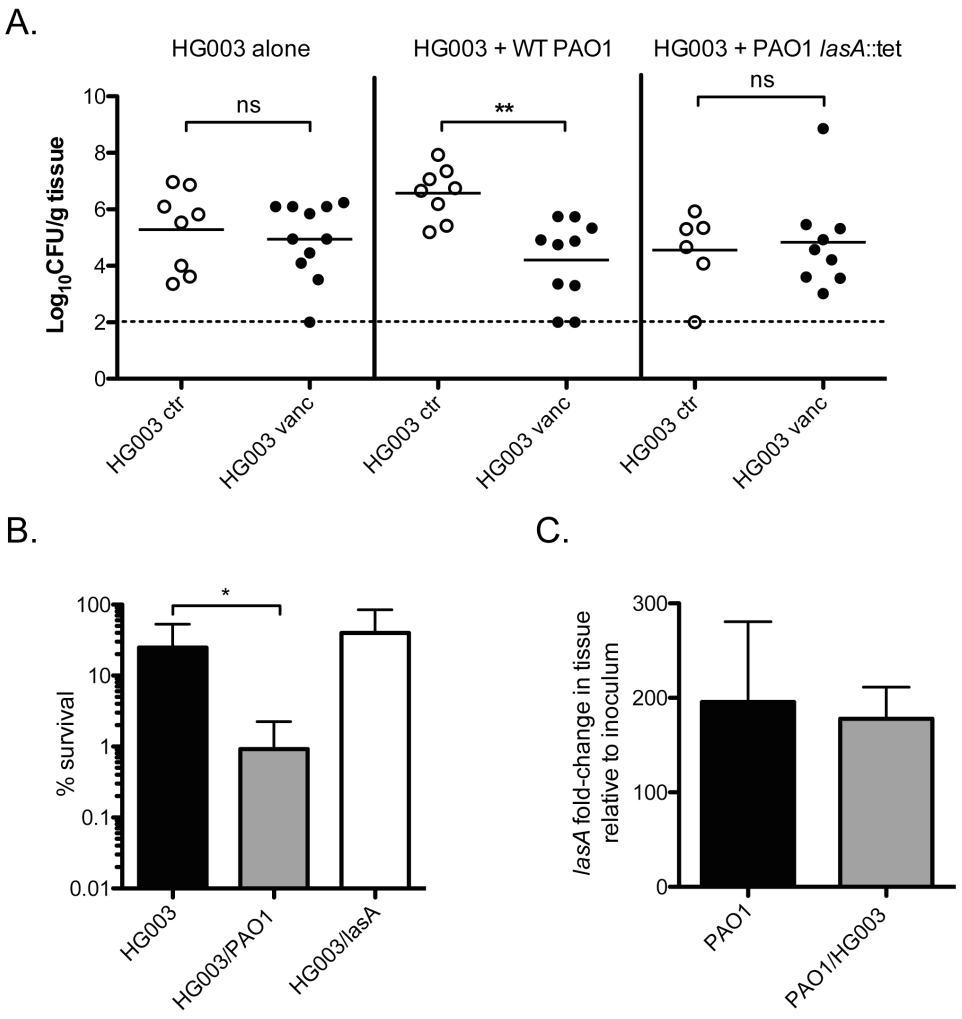

Figure 2.12. *P. aeruginosa* potentiates vancomycin killing of *S. aureus* in a murine model of co-infection. Approximately 1x10^5 CFU *S. aureus* strain HG003 was administered subcutaneously alone or in combination with approximately 1x10^3 CFU *P. aeruginosa* PAO1 or PAO1 *lasA::tn* 24h after burn. Mice were left untreated or administered 110mg/kg vancomycin subcutaneously once daily for two days. Mice were sacrificed 48h post infection. **(A)** Tissue biopsies at the site of infection were harvested, homogenized and *S. aureus* burdens were enumerated on selective media. Data for each group are compiled from two independent experiments. (n=6-10 mice per group) *p<0.05, ***p<0.005 (Mann-Whitney test). **(B)** Relative percentage survival for HG003 in each condition was calculated by dividing the CFU/g tissue of mice treated with vancomycin by the average CFU/g tissue of untreated mice. Maximum percentage survival is 100%. Data for each group are compiled from two independent experiments. **(C)** Expression of *lasA* in tissue from mono- (PAO1 alone) and co-infected (PAO1/HG003) mice relative to the starting inoculum measured by qRT-PCR. *p<0.05 (Student's t test). Error bars represent mean + sd.

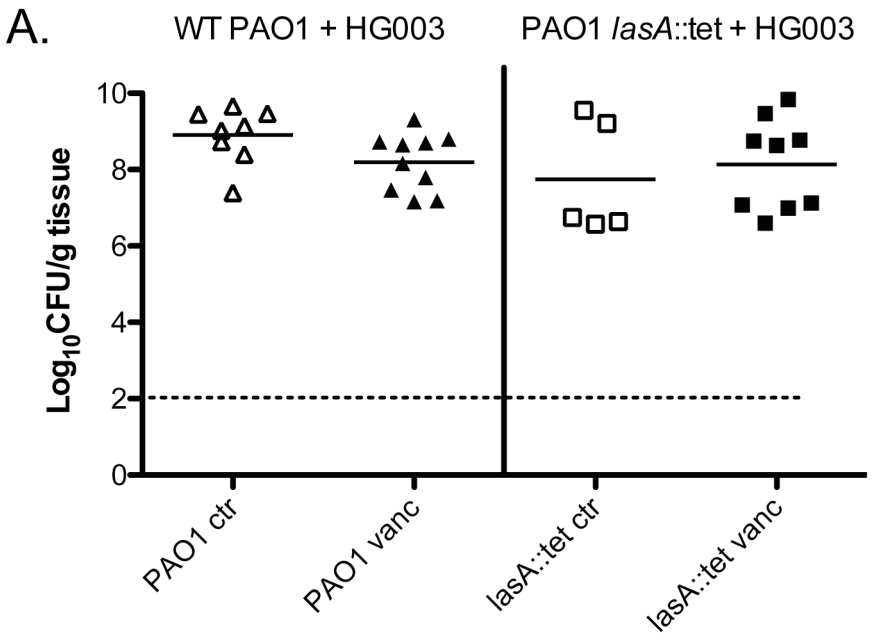

Figure 2.13. Burned mice maintain a high burden of *P. aeruginosa* PAO1 WT and PAO1 *lasA::tet* during co-infection. Approximately $1x10^5$ CFU *S. aureus* strain HG003 was administered subcutaneously alone or in combination with approximately $1x10^3$ CFU *P. aeruginosa* PAO1 or PAO1 *lasA::tn* 24h after burn. Mice were left untreated or administered 110mg/kg vancomycin subcutaneously once daily for two days. Mice were sacrificed 48h post infection. **(A)** Tissue biopsies at the site of infection were harvested, homogenized and *P. aeruginosa* burdens were each enumerated. Data for each group are compiled from two independent experiments.

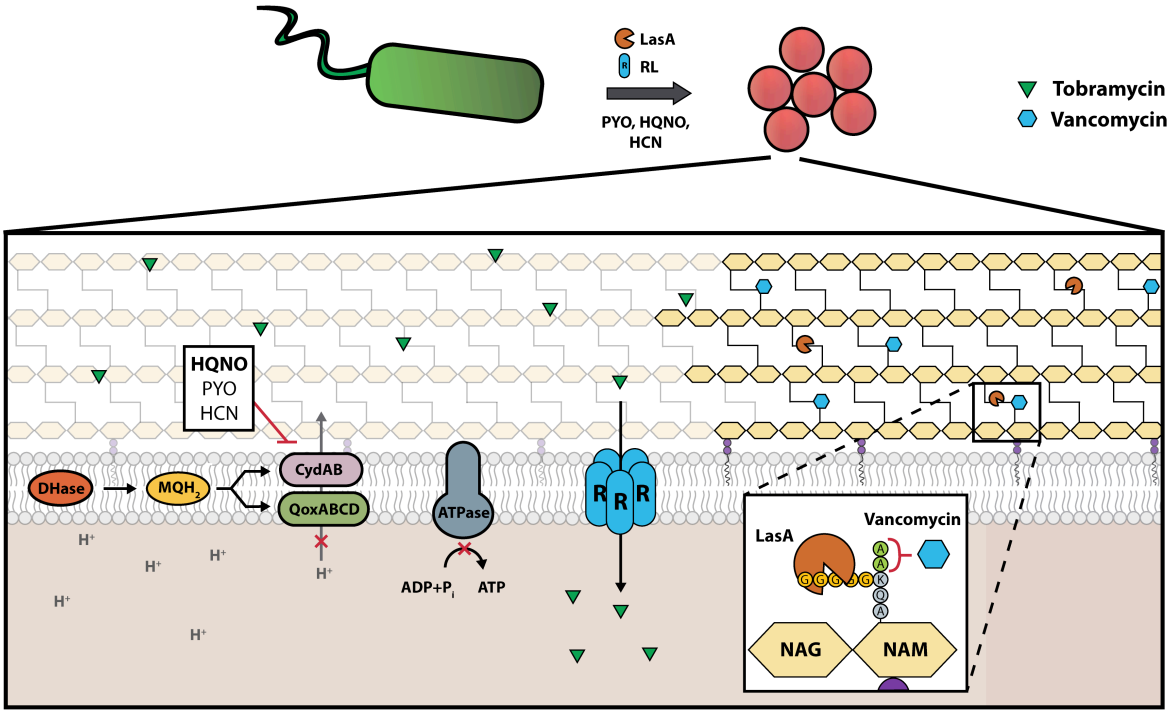

Figure 2.14. *P. aeruginosa* mediated alteration of *S. aureus* antibiotic susceptibility. *P. aeruginosa* exoproducts pyocyanin (PYO), 2-heptyl-4-hydroxyquinoline *N*-oxide (HQNO), and hydrogen cyanide (HCN) inhibit *S. aureus* electron transport, leading to collapse of proton-motive force (PMF) and inhibition of the F_1F_0 ATPase leading to a decrease in *S. aureus* antibiotic susceptibility. Conversely, *P. aeruginosa* rhamnolipids (RL) intercalate into the plasma membrane forming pores that permit aminoglycoside entry into the cell in a PMF-independent manner, while *P. aeruginosa* endopeptidase LasA cleaves pentaglycine crosslinks between peptidoglycan molecules of the cell wall, increasing vancomycin-mediated lysis of *S. aureus*.

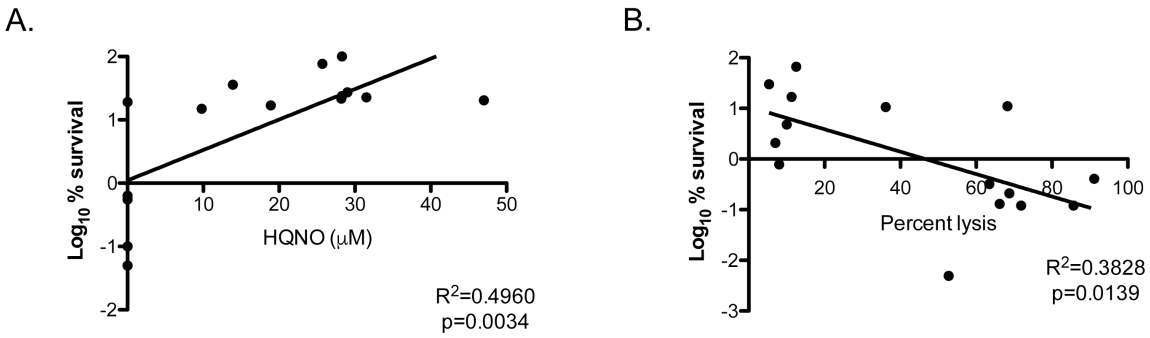

Figure 2.15. Correlation analysis of *P. aeruginosa* exoproduct production and impact on *S. aureus* antibiotic susceptibility. (A) HQNO production (measured by mass spectrometry), and **(B)** lytic activity (measured by staphylolytic assay) of *P. aeruginosa* laboratory strains PAO1 and PA14 and 12 clinical isolates were correlated to the isolate's impact on *S. aureus* susceptibility to **(A)** ciprofloxacin or **(B)** vancomycin. The correlation coefficient and p value for each analysis is shown. Statistical significance was determined using a two-tailed Pearson's chi-squared test.

Table 2.1. LC-MS/MS quantification of HQNO production in *P. aeruginosa* strains

Strain	Conc. (μM)
PAO1	31.5
PA14	28.3
PA14 *ΔpqsL*	ND
BC236	ND
BC237	18.9
BC238	13.9
BC239	25.7
BC308	ND
BC310	ND
BC312	28.3
BC249	29.0
BC250	28.2
BC251	ND
BC252	47.0
BC253	9.8

Table 2.2. Minimum inhibitory concentrations (MIC) of *S. aureus* HG003

Antibiotic	Control	+ HG003 supernatant	PAO1/ PA14 supernatant	PA14 *ΔpqsLphzShcnC*
MIC ciprofloxacin (μg/ml)	0.3	0.3	0.3	-
MIC tobramycin (μg/ml)	0.78	0.78	3.125-6.25	0.39
MIC vancomycin (μg/ml)	1.25	1.25	1.25	-

Antibiotic	Control	10 μg/ml rhamnolipids	30 μg/ml rhamnolipids	50 μg/ml rhamnolipids
MIC tobramycin (μg/ml)	0.78	0.39	0.195	0.0975

Table 2.3. Summary of *P. aeruginosa* isolate phenotypes and resulting impact on HG003 susceptibility to listed antibiotics

Strain	RL	HQNO	LasA	Tobramycin	Ciprofloxacin	Vancomycin
PAO1	+	+	+	nc	↓	↑
PA14	+	+	+	nc	↓	↑
BC236	-	-	-	nc	nc	nc
BC238	+	+	+	nc	↓	↑
BC239	-	+	-	↓	↓	nc
BC237	+	+	-	nc	↓	nc
BC308	-	-	-	nc	nc	nc
BC310	+	-	+	↑	nc	↑
BC312	+	+	+	↓	↓	nc
BC249	+	+	+	nc	↓	↑
BC250	+	+	+	nc	↓	↑
BC251	-	-	-	nc	nc	nc
BC252	+	+	+	nc	↓	↑
BC253	-	+	+	nc	↓	nc

*RL= Rhamnolipid production

CHAPTER 3
CHEMICAL INDUCTION OF AMINOGLYCOSIDE UPTAKE OVERCOMES ANTIBIOTIC TOLERANCE AND RESISTANCE IN *STAPHYLOCOCCUS AUREUS*[1]

Aminoglycoside antibiotics require proton motive force (PMF) for bacterial internalization. In non-respiring populations, PMF drops below the level required for drug influx, limiting the utility of aminoglycosides against strict and facultative anaerobes. We recently demonstrated that rhamnolipids, biosurfactant molecules produced by *Pseudomonas aeruginosa,* potentiate aminoglycoside activity against *Staphylococcus aureus*. Here, we demonstrate that rhamnolipids induce PMF-independent aminoglycoside uptake to restore sensitivity to otherwise tolerant persister, biofilm, small colony variant, and anaerobic populations of *S. aureus*. Furthermore, we show that this approach prevents the rise of resistance, restores sensitivity to highly resistant clinical isolates, and is effective against other Gram-positive pathogens. Finally, while other membrane-acting agents can synergize with aminoglycosides, induction of PMF-independent uptake is uncommon, and distinct to rhamnolipids among several compounds tested. In all, small molecule induction of PMF-independent aminoglycoside uptake circumvents phenotypic tolerance, overcomes genotypic resistance, and expands the utility of aminoglycosides against intrinsically recalcitrant bacterial populations.

[1] Radlinski LC, Rowe SE, Brzozowski R, Wilkinson A, Huang R, Eswara P, Conlon BP. Chemical induction of aminoglycoside uptake overcomes antibiotic tolerance and resistance in *Staphylococcus aureus. Cell Chemical Biology.* 2019 Oct 17;26(10):1355-1364.e4.

IMPORTANCE

The widespread onset of multidrug resistant pathogenic strains, coupled with an evaporating pipeline of new antibiotics reaching market emphasizes the importance of maximizing the efficacy of current antibiotics. As such, novel means for overcoming antibiotic tolerance and re-sensitizing resistant strains are desperately needed to combat infection. Aminoglycosides demonstrate broad-spectrum bactericidal activity against actively growing bacterial populations, but their activity is limited against non-respiring pathogen populations commonly found within the host. This limits the usefulness of this class of antibiotics against difficult-to-treat infections. Our study demonstrates that chemically inducing aminoglycoside uptake by promoting small molecule permeability in the membrane with rhamnolipids overcomes the barriers imposed during PMF depletion to extend the reach of aminoglycosides against recalcitrant pathogen populations. This approach is broadly applicable to Gram-positive pathogens, and sensitizes biofilm, SCV, and anaerobic populations of *S. aureus* to aminoglycoside killing. Furthermore, this combinational therapy demonstrates remarkably potent bactericidal activity against persisters, a bacterial population that is notorious tolerant to killing, regardless of antibiotic class. Chemically inducing PMF-independent aminoglycoside uptake represents a promising new approach for resolving chronic or relapsing infection, improving patient health, and slowing the spread of resistance.

INTRODUCTION

Environmental heterogeneity within a host elicits a spectrum of activities and metabolic states that render a pathogen recalcitrant to antibiotic killing [187]. For the facultative anaerobe, *Staphylococcus aureus,* antibiotic treatment failure occurs in approximately 1 in 5 patients, leading to an estimated 20,000 deaths annually in the United States alone [235]. Paradoxically, clinical isolates from these infections often exhibit sensitivity to administered antibiotics, as measured *in vitro* using minimum inhibitory concentration (MIC) assays [57,236]. This suggests that resistance alone cannot fully account for treatment failure, but rather that environmental factors present *in vivo* may influence the pathogen's susceptibility to antibiotic killing. *S. aureus* frequently colonizes microaerophillic or anaerobic niches during infection of the bone, within an abscess, or in the late-stage cystic fibrosis (CF) lung [114]. The absence of a terminal electron acceptor, such as oxygen or nitrate, pushes *S. aureus* into a fermentative lifestyle associated with diminished PMF and intracellular ATP [109].

Aminoglycosides are broad-spectrum antibiotics that exemplify the disconnect between *in vitro* and *in vivo* antibiotic efficacy. Aminoglycoside internalization is a multi-step process that begins with ionic interaction with the plasma membrane. This association displaces magnesium cations that stabilize the phospholipid bilayer, leading to increased permeability to ionic molecules [237]. This promotes proton motive force (PMF)-mediated aminoglycoside diffusion into the cell, followed by an exponential increase of drug influx as aminoglycosides disrupt translation, and misfolded proteins insert into and further destabilize membrane integrity (Andry 1974; Davis 1987; Taber et al. 1987a). Thus, slow growing or non-respiring bacterial populations can withstand high

levels of aminoglycosides as the initial stage of drug uptake is hindered by diminished PMF [240]. *In vitro,* aminoglycosides are potent killers of growing, respiring bacteria, yet these antibiotics are often dismissed as viable therapeutics for chronic infections because efficacy is severely limited against anaerobic, small colony variant (SCV), biofilm-associated, and persister populations [93,100,119].

The observation that aminoglycoside efficacy is impeded by defects in drug uptake has prompted several groups to pursue novel means for overcoming this barrier. Clinically, aminoglycosides are often prescribed in combination with cell wall-acting antibiotics such as β-lactams [241–243]. β-lactam treatment interferes with peptidoglycan crosslinking at the Gram-positive cell surface[244]. This action has been demonstrated to reduce *S. aureus* cell surface charge, and may promote interaction with positively charged aminoglycosides [50,245]. Though this synergy has been reported *in vitro*, clinical reports documenting this combinational therapy are conflicting [128]. Similarly, groups have investigated other means of stimulating aminoglycoside uptake, including pH-mediated stimulation of Δψ, metabolite-mediated stimulation of PMF in persisters, or the use of other antimicrobial or anti-biofilm peptides and compounds [137,149,246,247]. Apparent synergy has also been reported between aminoglycosides and compounds that destabilize the bacterial membrane, such as antimicrobial lipids and retinoids, however the mechanisms of potentiation are unclear [136,248].

We recently demonstrated that *P. aeruginosa*-produced rhamnolipids synergize with tobramycin to improve efficacy against *S. aureus* [84]. Rhamnolipids are a class of amphiphilic biosurfactants composed of two β-hydroxy fatty acid tails of varying lengths

connected to one or two rhamnose sugar molecules (Figure 3.1A)[200,249]. Previous studies have shown that at high concentrations (>300μg/mL)[250], rhamnolipids exert bactericidal activity against certain Gram-positive species by intercalating into the cytoplasmic membrane and forming pores [210]. Despite demonstrating broad-spectrum antimicrobial activity against Gram-positive pathogens, rhamnolipids are often dismissed as a potential therapeutic because the concentrations necessary to exert bactericidal activity are cytotoxic to host cells. However, here we show that sub-cytotoxic concentrations of rhamnolipids significantly stimulate tobramycin uptake in *S. aureus,* and precipitate rapid and complete sterilization of *S. aureus* cultures. We further demonstrate that small molecule targeting of membrane permeability represents a novel and viable strategy for overcoming aminoglycoside tolerance and resistance in *S. aureus* and other clinically relevant pathogens.

RESULTS

P. aeruginosa rhamnolipids potentiate aminoglycoside killing of *S. aureus*.

Using a mix of mono- and di-rhamnolipid congeners (RL90; AGAE), we first identified a RL concentration that potentiated tobramycin killing without itself exerting bactericidal activity against *S. aureus* (Figure 3.2A), and demonstrated that RL/tobramycin combinational therapy mediates the rapid and total sterilization of *S. aureus* HG003 cultures in a dose-dependent manner (Figure 3.1B). Interestingly, RL treatment did not lead to substantial dissipation of cellular PMF until the applied concentration approached concentrations necessary to inhibit *S. aureus* growth (Figures 3.1C, 3.2A). Other commercially available RL molecules including two purified mono-

rhamnose RL molecules, Rha-C10C10 and Rha-C12C12 (Glycosurf), as well as a purified mix of 90% di-rhamnose RL molecules of various carbon tail lengths (RL95D90; AGAE) similarly potentiated at least a 4-fold increase in tobramycin killing of *S. aureus* (Figure 3.2E). RL concentrations that potentiated aminoglycosides fell well below what were cytotoxic to host cells (Figure 3.3A). Similar potentiation was observed against the MRSA strain JE2 (Figure 3.3B), as well as with the other aminoglycosides including gentamicin, amikacin, neomycin, and kanamycin, demonstrating that RL/aminoglycoside synergy is not strain-dependent, or restricted to tobramycin (Figure 3.3C-F). Rhamnolipids did not potentiate killing by ciprofloxacin, rifampicin or oxacillin, and 30μg/mL rhamnolipids did not change the MIC of ciprofloxacin (0.3125μg/mL), rifampicin (0.008μg/mL), oxacillin (0.5μg/mL), or the bacteriostatic antibiotic tetracycline (0.25μg/mL), suggesting that the synergy observed is specific to aminoglycosides. (Figure 3.3G-I).

Aminoglycosides lack activity against non-respiring bacterial populations, as these cells maintain a low PMF [240]. *S. aureus* frequently experiences oxygen limitation during infection, particularly in biofilms, and biofilm associated *S. aureus* is highly recalcitrant to antibiotics [100]. We hypothesized that rhamnolipids could restore aminoglycoside sensitivity to non-respiring populations of *S. aureus* by facilitating PMF-independent, passive transport. *S. aureus* was grown to mid-exponential phase under anaerobiosis or overnight in conditions that promote biofilm formation, then challenged with the maximum attainable serum concentration (C_{max}, 58μg/mL) of tobramycin [230]. As expected, tobramycin alone was ineffective against anaerobic or biofilm-associated *S. aureus* (Figure 3.1D, E). However, RL/tobramycin combinational therapy led to the

complete sterilization of *S. aureus* HG003 anaerobic cultures within one hour (Figure 3.1D). Similarly, combinational therapy led to approximately a 4-log reduction in biofilm-associated CFU (Figure 3.1E).

S. aureus SCVs are notoriously difficult to treat and are isolated from at least 25% of patients with CF [52]. SCVs are often auxotrophic for the biosynthesis of thiamine, menadione or hemin, and consequently are defective in respiration and resistant to aminoglycosides [51,251,252]. To test whether rhamnolipids could be used to re-sensitize *S. aureus* SCVs to tobramycin killing, we generated a menadione (*menD)* auxotroph in *S. aureus* strain HG003. The *menD* mutant demonstrated high-level resistance (MIC = 50μg/ml) to tobramycin, however rhamnolipids reduced this MIC to 0.0975μg/ml. Similarly, though HG003 *menD* grew unabated in the presence of tobramycin (Figure 3.1F), RL treatment facilitated tobramycin-mediated sterilization of the cultures in a dose-dependent manner (Figure 3.1F). Taken together, these data demonstrate that by bypassing the requirement of PMF for aminoglycoside uptake, rhamnolipids re-sensitize *S. aureus* anaerobic, biofilm, and SCV populations to aminoglycoside killing.

Rhamnolipid/tobramycin combinational therapy eradicates *S. aureus* persisters

Bactericidal antibiotics corrupt active cellular processes such as cell wall or protein synthesis to facilitate killing [253]. Persisters are subpopulations of bacteria that stochastically enter a phenotypically dormant state and can thus tolerate bactericidal concentrations of antibiotics [254]. *S. aureus* persister cell formation is associated with a decrease in intracellular ATP levels [26]. We previously showed that a population-wide

state of antibiotic tolerance can be induced in *S. aureus* by treating cells with potassium arsenate ($AsKO_2$) to reduce ATP levels [26]. As expected, exposing a susceptible population of *S. aureus* to $AsKO_2$ reduced the intracellular ATP concentration of the population, and induced tobramycin tolerance (Figure 3.4A). Conversely, this protective effect was abrogated in the presence of rhamnolipids, suggesting that rhamnolipids allow tobramycin to overcome the level of protection conferred by ATP depletion, and strengthened our conclusion that increasing tobramycin uptake allows us to target low-energy *S. aureus* persister populations.

Aminoglycoside bactericidal activity requires protein synthesis. Consequently, populations demonstrating a decreased rate of translation should be slower to succumb to killing. Chloramphenicol is bacteriostatic antibiotic that inhibits, rather than corrupts, protein synthesis and thus at certain concentrations will cause cessation of growth [253]. We aimed to slow the rate of translation by exposing cells to chloramphenicol and assess the impact on tobramycin/RL killing. We measured translation using a xylose inducible GFP reporter plasmid, pCLON46, to confirm that addition of chloramphenicol to growing *S. aureus* cultures slowed the rate of GFP synthesis (Figure 3.5A). Remarkably, while chloramphenicol treatment protected *S. aureus* from tobramycin killing, tobramycin/RL combinational therapy facilitated eradication of chloramphenicol-treated *S. aureus* cultures, albeit at a diminished rate (Figure 3.4B). Similar results were observed following linezolid pre-treatment (Figure 3.5B). Rhamnolipids also potentiated tobramycin killing in the presence of the protonophore and uncoupling agent, carbonyl cyanide 3-chlorophenylhydrazone (CCCP), which causes collapse of PMF and prevents tobramycin uptake. This confirmed that rhamnolipids facilitate PMF-independent

tobramycin uptake and resensitize PMF-depleted populations to tobramycin killing (Figure 3.4C). Together, these results demonstrate that RL/tobramycin combinational therapy targets persisters by overcoming the requirement of PMF for drug influx and lowering the threshold energy and translation levels required for killing. As low PMF, ATP, and antibiotic target activity represent the primary barriers proposed to reduce to antibiotic efficacy in persisters, RL induction of aminoglycoside uptake may significantly improve treatment of otherwise tolerant persister cell populations.

Rhamnolipids repress the rise of tobramycin resistance, and re-sensitize resistant isolates to killing

Subinhibitory RL concentrations significantly decreased the MIC of tobramycin for *S. aureus* HG003 WT from 0.78 to 0.0975μg/ml. For *S. aureus,* the predominant mechanisms of aminoglycoside resistance include decreased uptake through the adoption of a non-respiring SCV phenotype, or horizontal transfer of an aminoglycoside-modifying enzyme [255]. Because rhamnolipids allow PMF-independent drug uptake, we hypothesized that tobramycin/RL combinational therapy could prevent the rise of tobramycin resistance due to poor drug penetration during long-term tobramycin exposure. To test this, 6 independent *S. aureus* HG003 strains were passaged daily in sub-MIC concentrations of tobramycin with or without 30μg/mL of RL. Serial passage with tobramycin alone led to a 256-500-fold increase in tobramycin MIC, yielding a final MIC of 200μg/ml for HG-1 and HG-2, and 100μg/ml for HG-3 (Figure 3.6A). Conversely, serial passage in tobramycin + rhamnolipids generated a maximum MIC increase to 6.25 or 12.5μg/ml (Figure 3.6A). Two of these strains (HG-4, HG-6) remained below the clinical breakpoint for intravenous tobramycin (8μg/ml). Furthermore, subsequent

treatment with rhamnolipids restored tobramycin susceptibility to resistant mutant strains that arose during passage in tobramycin alone (Figure 3.6B). Together, these findings indicate that when used in combination with aminoglycosides, rhamnolipids slow the rise of aminoglycoside resistance and re-sensitize aminoglycoside resistant isolates to killing.

Patients with CF are routinely administered high doses of inhaled tobramycin therapy (300mg of aerosolized tobramycin twice daily for 28 days, reaching sputum concentrations of 737μg/ml) to reduce *P. aeruginosa* burden during periods of clinical exacerbation [256]. Co-infecting *S. aureus* isolates exposed to inhaled tobramycin therapy can become highly tobramycin resistant. We measured the MIC of tobramycin against a panel of *S. aureus* CF isolates, and found that 6 of 8 isolates grew in concentrations of tobramycin ranging from 800-1600μg/ml (Figure 3.6C). Aminoglycoside-modifying enzymes allow non-SCV *S. aureus* to inactivate intracellular drug and grow in high concentrations of aminoglycosides. All of our resistant isolates were non-SCV, and thus it is likely that these isolates had either acquired an aminoglycoside modifying enzyme or had mutated ribosomal binding sites with lower binding affinity for tobramycin. Regardless of mechanism, we hypothesized that significantly increasing intracellular concentrations of tobramycin with rhamnolipids could overwhelm both mechanisms of resistance to restore some level of susceptibility to these highly resistant isolates. Indeed, we found that rhamnolipids synergized with tobramycin to reduce the MIC 8 to 32-fold among our isolates (Figure 3.6C). Further, rhamnolipids reduced the concentration of tobramycin necessary to inhibit *S. aureus* growth in these isolates to below the clinical achievable concentration following

aerosolized delivery (~673μg/ml per dose)[256] (Figure 3.6C). In all, these findings demonstrate that combinational therapy can slow the rise of resistance in a closed system, and re-sensitize even the most highly resistant clinical isolates.

Rhamnolipids sensitize other Gram-positive pathogens to aminoglycoside killing

We next asked whether targeting membrane permeability to induce aminoglycoside uptake is a valid therapeutic approach against other bacterial pathogens. Consistent with previous findings, we observed that rhamnolipids demonstrated no bactericidal activity, and thus no aminoglycoside-potentiating effects against Gram-negative *Escherichia coli,* presumably due to the presence of an additional outer membrane (Table 3.1)[210]. For Gram-positive species, we found that rhamnolipids lowered the MIC of tobramycin for *Enterococcus faecalis, Bacillus subtilis, Listeria monocytogenes* and *Clostridioides difficile* (Table 3.1). Of note, rhamnolipids reduced the MIC of *C. difficile* from 400μg/ml to under 0.39μg/ml, sensitizing what is otherwise a highly resistant, strictly anaerobic species. Rhamnolipids were ineffective against *Streptococcus pneumoniae.*

Rhamnolipids induce distinct modifications to the *S. aureus* membrane to promote tobramycin uptake

To better understand the molecular mechanism(s) for how rhamnolipids and other cell envelope-acting agents (CEAAs) potentiate aminoglycosides, we selected 3 other putative aminoglycoside adjuvants and compared their impact on *S. aureus* membrane physiology. Antimicrobial monoglycerides such as glycerol monolaurate (GML) target the plasma membrane and were recently demonstrated to synergize with

aminoglycosides against *S. aureus* biofilm [144,248]. Similarly, the retinoid adarotene targets bacterial membranes and synergizes with aminoglycosides against *S. aureus* persisters [136]. Finally, β-lactam/aminoglycoside synergy has long been theorized to occur *in vivo*, with limited *in vitro* support and conflicting clinical reports (Figure 3.7A)[128].

For each compound we attempted to identify a concentration that potentiated tobramycin killing without exerting bactericidal activity alone (Figure 3.2B-D). Treatment with 3.2μg/mL of adarotene and 40μg/mL of GML facilitated 100 to 1000-fold increase in tobramycin killing (Figure 3.8A). Surprisingly we observed that sub-bactericidal concentrations of oxacillin conferred a moderate but significant protective effect against tobramycin (Figure 3.2D, Figure 3.8A). Rhamnolipids were the most powerful potentiator of tobramycin killing, sterilizing cultures to the limit of detection (Figures 3.2A, 3.8A). These findings were supported by traditional checkerboard synergy assays where synergy (FICI ≤ 0.5) was observed between tobramycin and rhamnolipids, GML, and adarotene; but not between tobramycin and oxacillin (Figure 3.9, Table 3.2). We then used flow cytometry to measure changes in Texas Red-conjugated tobramycin uptake following exposure to each CEAA. Strikingly, we found that only RL treatment led to significant changes in tobramycin uptake post antibiotic exposure despite the fact that rhamnolipids, GML and adarotene all potentiated tobramycin killing at these concentrations (Figures 3.8B, 3.7B, C).

We hypothesized that the unique ability of rhamnolipids to promote rapid aminoglycoside influx might stem from how rhamnolipids interact with the bacterial membrane. Aminoglycoside internalization begins with ionic interaction with the cell

surface, followed by PMF-mediated diffusion into the cell [50]. We reasoned that rhamnolipids might promote aminoglycoside uptake by altering membrane charge and/or permeability. Similar to oxacillin, RL treatment decreased *S. aureus* surface charge, and both rhamnolipids and adarotene stimulated a lasting increase in membrane fluidity (Figure 3.7D, E). However, only rhamnolipids significantly stimulated leakage of intracellular ATP into the medium, suggesting that at these concentrations only rhamnolipids induce small molecule permeability of the membrane (Figure 3.7F). Overall, rhamnolipids simultaneously altered surface charge, membrane fluidity, and small molecule permeability, which may explain their unique capacity to stimulate PMF-independent aminoglycoside uptake.

As GML and adarotene did not promote tobramycin influx during the initial phase of tobramycin uptake, we hypothesized that these CEAAs may instead potentiate aminoglycoside killing downstream of initial antibiotic influx. If true, then rhamnolipids alone should restore tobramycin susceptibility to CCCP treated cells, as PMF-depleted cultures exclude aminoglycosides altogether. As expected, CCCP-treatment induced tolerance to tobramycin that was overcome with rhamnolipids (Figure 3.8C). However, combinational therapy with GML, adarotene, or oxacillin were unable to overcome CCCP-mediated PMF depletion, confirming that these compounds do not bypass the initial phase of tobramycin uptake and instead likely synergize with tobramycin after antibiotic has penetrated the cell, possibly by rendering *S. aureus* more sensitive to downstream membrane damage resulting from protein synthesis corruption (Figure 3.8C). Physiologically this distinction is critical, because synergy with GML or adarotene will likely be limited to respiring, high PMF *S. aureus* populations *in vivo.* Indeed, when

grown anaerobically, adarotene no longer potentiated aminoglycoside killing, and the synergy observed for GML was minor compared to the rapid eradication observed following RL treatment (Figure 3.8D).

We used high-resolution fluorescent microscopy to visualize the effects of each compound on the *S. aureus* plasma membrane. We observed that treatment with rhamnolipids at concentrations that potentiate aminoglycoside killing, resulted in a population of viable cells that retained overall shape and membrane morphology, however localization of membrane-associated cell division machinery, measured with the FtsZ proxy, ZapA-GFP, was perturbed, suggesting that rhamnolipids interfere with membrane physiology without completely destabilizing it (Figure 3.8E, Figure 3.7G). Adarotene and GML treatment resulted in membrane clumping indicative of more pronounced membrane destabilization at concentrations that induced tobramycin synergy (Figure 3.8E). All compounds stimulated mislocalization of ZapA-GFP from the membrane (Figure 3.7G). Taken together, these data suggest that rhamnolipids distinctly modify the plasma membrane to induce tobramycin uptake, while the potentiation effects observed from other CEAAs may occur through general destabilization of the membrane during aminoglycoside-induced membrane stress.

DISCUSSION

Aminoglycoside efficacy is limited by the environmental context of infection [187]. Minor fluctuations in nutrient and oxygen availability have dramatic implications for drug penetration, rendering aminoglycosides useless against certain types of infections [50,240]. Here, we demonstrated that inducing PMF-independent aminoglycoside

uptake with rhamnolipids facilitates the eradication of anaerobic, biofilm, SCV and persister populations, represses the rise of aminoglycoside resistance, and restores susceptibility to highly resistant isolates (Figure 3.10). Furthermore, we showed that while other cell membrane-targeting agents can synergize with aminoglycosides, stimulating the initial phase of aminoglycoside influx is rare, and unique to rhamnolipids under these conditions. Consequently, rhamnolipids demonstrated the greatest efficacy as a combinational therapy against aminoglycoside-tolerant *S. aureus*.

The specific mechanisms that induce antibiotic tolerance in the host are poorly understood. *In vitro*, bacterial tolerance is associated with a stochastic or deterministic drop in ATP-dependent antibiotic target activity below the threshold required to facilitate death [26,27]. Aminoglycoside tolerance, however, is further complicated by the fact that PMF-dependent drug influx is also contingent on the metabolic state of the cell. Consequently, it is difficult to delineate between deficiencies in drug penetration or low intracellular ATP when examining an aminoglycoside tolerant population. rhamnolipids remove the prerequisite of PMF for drug influx, and allow us to specifically study the relationship between ATP depletion and aminoglycoside tolerance. Strikingly, we found that rhamnolipids allowed for tobramycin-mediated eradication of *S. aureus* populations exhibiting minimal intracellular ATP and translation activity, suggesting that the primary obstacle to aminoglycoside efficacy lies in drug influx. This is in contrast to other antibiotics that diffuse freely across the membrane or act on the cell surface, where ATP depletion is sufficient to induce tolerance [26]. With these antibiotics, we suggest that the primary barrier to efficacy likely lies in the reduction of active cellular targets such as DNA replication (fluoroquinolones), transcription (rifamycins) or cell wall synthesis (β-

lactams) among tolerant populations. Recent work suggests that “dormant” persister populations maintain low level metabolic activity [257–259]. Although protein synthesis is likely reduced in persisters, our results suggest that the number of active ribosomal targets in these populations is sufficient for aminoglycosides to precipitate cell death if they are accessible to the antibiotic. This is supported by the recent finding that growth-arrested bacterial populations actively synthesize protein for several days after entering stationary phase [260]. By stimulating aminoglycoside influx, rhamnolipids allow us to target and eradicate persister cells with extremely low-level rates of translation.

To date, the molecular details of how rhamnolipids interact with the bacterial membrane are poorly understood. Data from biophysical studies suggest that the inverted cone-like structure that arises from a large polar head group and smaller hydrophilic tail causes rhamnolipids to induce a positive curvature in the membrane that leads to the formation of pores [261]. Indeed, at high bactericidal concentrations, RL treatment causes catastrophic pore formation in *B. subtilis* [210]. We suspect that the subinhibitory RL concentrations used here elicit sufficient membrane destabilization to permit diffusion of aminoglycosides into the cell without inducing bactericidal pore formation and membrane dissolution. This conclusion is supported by the fact that we observed increased small molecule permeability and aminoglycoside uptake, but not total dissipation of PMF when cells were treated with subinhibitory concentrations of rhamnolipids. Importantly, rhamnolipids synergized with aminoglycosides against a panel of Gram-positive pathogens, all of which produce a range of different phospholipid molecules and cell membrane components [139], indicating that this potentiating effect is not unique to the *S. aureus* membrane composition.

Destabilizing the bacterial plasma membrane during aminoglycoside therapy represents a promising approach that is complicated by off-target effects to host cell membranes. While rhamnolipids facilitated tobramycin-mediated eradication of *S. aureus* at concentrations far below what was cytotoxic to host cells, cytotoxicity at higher concentrations may limit the therapeutic potential of these molecules. Furthermore, it remains to be seen whether this therapeutic approach increases the toxicity of aminoglycosides against eukaryotic host cells. An ideal aminoglycoside adjuvant would exhibit broad affinity for the bacterial membrane and limited affinity for eukaryotic membranes. Here we used a commercially available mix of mono- and di-rhamnolipids, however a recent study revealed that chemical derivatization of purified RL congeners significantly alters the antibacterial and cytotoxic properties of these molecules [250]. In particular, semi-synthetic amide RL derivatives demonstrated greatly increased antibacterial activity against *S. aureus.* Furthermore, certain antimicrobial peptides are postulated to disrupt cell membranes via a mechanism that is similar to rhamnolipids [261,262]. In their paper, Lin *et al.* demonstrate that cationic antimicrobial peptides synergize with the macrolide antibiotic azithromycin to potentiate activity against Gram-negative pathogens [59]. Similarly, aminoglycoside/antimicrobial peptide synergism was demonstrated against *Enterococcus faecium* in a murine cutaneous abscess model [137]. In both of these cases the proposed mechanism of potentiation is increased antibiotic uptake. Further investigation to uncover a specific RL derivative or a novel small molecule inducer of permeability that demonstrates minimal cytotoxicity may yield the ideal combinational therapy for targeting recalcitrant bacterial populations within a host. Importantly, however, our findings demonstrate that potential

adjuvants must operate at the initial phase of aminoglycoside uptake to induce PMF-independent influx. Otherwise, compounds that require PMF-mediated aminoglycoside uptake for synergy will fail to clear physiologically relevant PMF-depleted, aminoglycoside tolerant populations.

MATERIALS AND METHODS

Bacterial strains and growth conditions

S. aureus strain HG003 was cultured aerobically in Mueller-Hinton (MHB) or tryptic soy (TSB) broth at 37°C with shaking at 225 rpm. For anaerobic growth, overnight cultures were washed twice with PBS and diluted into 5 ml of pre-warmed (37°C) TSB to an OD_{600} of 0.05. Cultures were prepared in triplicate in 16x150mm glass tubes containing 1mm stir bars. Following dilution, cultures were immediately transferred into a Coy anaerobic chamber and grown at 37°C with stirring. CF isolates were collected from patients at the UNC medical center. Isolates were cultured from sputum or bronchoalveolar lavage (BAL) from patients with CF after obtaining informed consent. HG003 *menD::erm* was generated through transduction using 80α as described previously[263], using a published COL *menD::erm* mutant strain [264] as the donor and HG003 WT was the recipient. A modified version of the *E. coli/S. aureus* cloning vector pEPSA5[265] carrying an erythromycin selection cassette and a xylose-inducible GFP was constructed as follows: pEPSA5 vector was linearized through PCR amplification using primers SR43 and SR44 at the 5’ and 3’ sites immediately flanking the chloramphenicol cassette, which was then replaced with an erythromycin resistance cassette amplified using primers specific to the *bursa aurealis* erythromycin resistant

transposon from the NARSA library (SR41, SR42) [266]. The *gfpuvr* (Clontech)[267] was amplified by primers which added a 5' EcoRI site, 3' KpnI site, and a *sarA* ribosome binding site and spacer. This amplicon was digested with KpnI and EcoRI (NEB) and ligated into similarly digested pEPSA5-erm to yield plasmid pCLON46.

Antibiotic survival assays

HG003 was grown to ~3x10^8cfu/ml in 3ml MHB or in 5ml TSB under aerobic and anaerobic conditions, respectively. An aliquot was plated to enumerate cfu before antibiotic challenge. Tobramycin was added at either the concentration similar to the Cmax in humans at recommended dosing (58µg/ml)[230] or at 20x the MIC (15.6 µg/ml). Non-aminoglycoside antibiotics were added at 20x MIC concentrations as stated. At indicated times, culture aliquots were removed, washed with 1% NaCl, then serially diluted and plated to enumerate survivors. Where indicated, rhamnolipids (RL90, AGAE), GML (Sigma), adarotene (Sigma) or oxacillin (Fisher) was added with antibiotics. For plate-based killing assays, HG003 was grown to ~3x10^8 CFU/mL and 100µl of each culture was seeded into wells of a 96-well plate pre-loaded with 100µL MHB containing 2x the desired concentration of each CEAA +/- 15.6µg/mL tobramycin (final concentration=7.8µg/mL). Plates were incubated with shaking for 24hr at 37°C. Cells were then pelleted, washed, and plated to enumerate survivors.

Biofilm susceptibility assays

Overnight cultures (~18hr) of HG003 were subcultured 1:200 in BHI, seeded in a 96-well microtiter plate and incubated statically at 37°C overnight. After 24hrs, wells were

washed 2x with 1% NaCl and overlaid with 200µl of BHI with or without tobramycin at 58µg/ml +/- rhamnolipids and incubated overnight at 37°C. 24hr later, wells were washed 2x, overlaid with 100µl of 1% NaCl, and sonicated for 10 minutes to disrupt biofilm. Sonicated samples were then serially diluted and plated for CFU enumeration.

ATP assays

HG003 was grown to ~$3x10^8$cfu/ml in 3ml MHB and treated with 5mM sodium arsenate dibasic heptahydrate (Sigma) for 30min +/- 30µg/mL rhamnolipids. ATP levels were measured using a Promega BacTiter Glo kit according to the manufacturer's instructions. For small molecule permeability assays, exponential phase cultures of HG003 were treated with CEAAs for 1hr, then 1mL aliquots of each culture was pelleted and the supernatant used to measure ATP concentration.

Minimum inhibitory concentration (MIC) assays

MICs were determined using the microdilution method. Briefly, ~$5x10^5$cfu were incubated with varying concentrations of tobramycin in a total volume of 200µl MHB in a 96-well plate. MICs were determined following incubation at 37°C for 24hr. MICs were performed in BHI for *E. faecalis* and *L. monocytogenes*, and in BHI supplemented with 2% yeast extract for *C. difficile* to support growth. Where indicated, MICs were performed in the presence of 30µg/ml rhamnolipids. To monitor the rise in spontaneous tobramycin resistant mutants over time, six independent lineages of HG003 were grown in varying concentrations of tobramycin in a 96-well plate. After 24hrs of static incubation at 37°C, wells with the highest concentration of tobramycin that permitted

significant bacterial growth (OD_{600}≥ 0.1) were used to inoculate fresh MHB for the next passage at a bacterial density of approximately $5x10^5$ CFU/mL. Three independent lines (HG1-3) were serially passaged with tobramycin alone, and three lineages (HG4-6) were passaged in tobramycin + RL at 30μg/ml for a total of 31 days. At every third passage, strains were collected and stored at -80°C in a 20% glycerol stock. As a control, the MIC of wild-type HG003 was determined concurrently with each passage of strains HG1-6.

Checkerboard synergy assays

Dual antibiotic synergy was assayed using plate-based checkerboard assay as described previously[268], where 2-fold serial dilutions of each compound added to 2-fold dilutions of tobramycin to create an 8x8 matrix in a 96-well plate. The Fractional Inhibitory Concentration Index (FICI) was calculated as: FICI= (MIC of compound A in combination/MIC compound A alone) + (MIC compound B in combination/MIC compound B alone). FICI ≤ 0.5 = synergy, 0.5 < FICI ≤4 = no interaction, 4<FICI = antagonism.

Texas Red-tobramycin uptake

Texas Red-succinimidyl ester (Invitrogen) was dissolved in high-quality anhydrous *N,N*-dimethylformamide at a final concentration of 20mg/ml. Tobramycin was resuspended in 100mM K_2CO_3, pH 8.5 at a final concentration of 10mg/ml. On ice, 10μl of Texas Red was slowly added to 350μl tobramycin solution at 30 molar excess to allow the conjugation reaction to occur, and to maximize the formation of single-label tobramycin

as described [269]. HG003 was grown to mid-exponential phase and then treated with the indicated compound + Texas Red-tobramycin at a final concentration of 15.6µg/ml. After 1hr, an aliquot of cells was removed, washed twice in 1% NaCl and plated to enumerate survivors. The remaining aliquot was analyzed for Texas Red uptake on a Thermo Fisher Attune NxT flow cytometer. 30,000 events were recorded. Figures were generated using FSC Express 6 Flow.

Membrane potential measurements

Bacterial membrane potential was measured with the BacLight Bacterial Membrane Potential Kit as per the manufacturers instructions. Briefly, overnight cultures of HG003 were subcultured 1:100 in MHB and grown for 3.5 hrs before a 30 min exposure to the indicated concentration of rhamnolipids. Cultures were then diluted 1:100 in 1mL PBS to approximately $1x10^6$ CFU/mL and treated with 30µM $DiOC_2$ for approximately 30 minutes before analysis on a Thermo Fisher Attune NxT flow cytometer. 30,000 events were recorded and relative membrane potential was calculated by taking the ratio of population red and green linear mean fluorescence intensity (MFI) values.

Cytochrome C binding assays

S. aureus surface charge was measured using a modified protocol described previously [270]. HG003 was subcultured 1:100 in TSB and grown 2.5hr at 37°C with shaking prior to a 1hr incubation with indicated compounds. Cells were harvested from 1mL of each cultures normalized to OD_{600}=0.3, then resuspended in 150µL 20mM MOPS pH 7.0. Samples were treated with 200µg/mL of purified cytochrome C (MP Bio) for 10 minutes.

Cells were then pelleted and 100µL of supernatant was transferred to a 96-well plate where absorbance was measured at 530nM.

Laurdan GP Membrane Fluidity

Overnight cultures of HG003 were diluted 1:100 in MHB and grown for 4hrs at 37°C with shaking. Laurdan staining was performed as described[271], and carried out in a 37°C climate-controlled room to ensure stable temperatures. Laurdan was added to each culture at a final concentration of 10µM for 10 min, while shaking in the dark. Cells were harvested by centrifugation in pre-warmed microtubes and washed 4x with pre-warmed wash buffer (137mM NaCl, 2.7mM KCl, 10mM Na_2HPO_4, 0.2% glucose, 1% DMF). Following wash steps, cells were resuspended in wash buffer to an OD_{600}=0.8. 100µL of stained cells were added to 100µL of wash buffer containing 2x the desired concentration of each compound in a pre-warmed black wall, clear bottom plate alongside a baseline control. Fluorescence was measured immediately in 2min intervals over 30mins (excitation: 350nM, emission: 460nM and 500nM. Laurdan GP = $(I_{460}-I_{500})/(I_{460}+I_{500})$.

Eukaryotic cytotoxicity assays

Rhamnolipid cytotoxicity activity was measured for J774A.1 macrophage-like cells using the CellTiter-Blue Cell Viability assay according to the manufacturer's instructions. Briefly, J774A.1 cells were seeded in a black wall, clear bottom 96-well plate at 25,000 cells/well in high-glucose DMEM (Gibco) supplemented with 10% FBS and 2mM L-glutamine, and allowed to incubate overnight at 37°C and 5% CO_2. After 24hr, the

media was removed from wells and replaced with media + the indicated concentration of rhamnolipids and cells were returned to incubate overnight. After 24hr, 100µL of CellTiter-Blue reagent was added to each well and allowed to incubate at 37°C for 2 hours before fluorescence was read at 560/590 nm (excite/emit).

Fluorescent Microscopy

Overnight cultures of *S. aureus* SH1000 harboring a pRB42 plasmid-based cadmium-inducible copy of zapA-gfp [272], were grown at 22°C in tryptic soy broth (TSB) with 5 µg/ml erythromycin (erm) for plasmid maintenance, and then subsequently diluted 1:10 into fresh TSB+erm. Cultures were then grown at 37°C and growth was monitored by the measurement of absorbance. At mid-log phase, when optical density at 600 nm reached 0.5, 1.25 mM cadmium chloride was added to the cultures to induce the expression of zapA-gfp. Cells were then treated with either rhamnolipids (30µg/ml), GML (40µg/ml), adarotene (3.2µg/ml), or oxacillin (0.5µg/ml) for 1 h. Untreated cells and cells treated with DMSO were used as controls. Following the incubation period, 1 ml cells were washed three times in PBS, and then resuspended in 100 ml of PBS containing 1 mg/ml membrane stain (FM6-64). Aliquots of 5 ml culture were pipetted onto a glass bottom dish (MatTek), and sample was covered with a 1% agarose pad. Microscopy was performed at room temperature using a GE Applied Precision DeltaVision Elite deconvolution fluorescence microscope equipped with a Photometrics CoolSnap HQ2 camera.

Quantification and Statistical Analysis

Experiments were performed with three biological replicates from at least two independent experiments when possible. Statistical significance is reported in Figure Legends, and data are presented as mean +/- SD as indicated. All statistical analysis was performed with Graphpad Prism software.

FIGURES

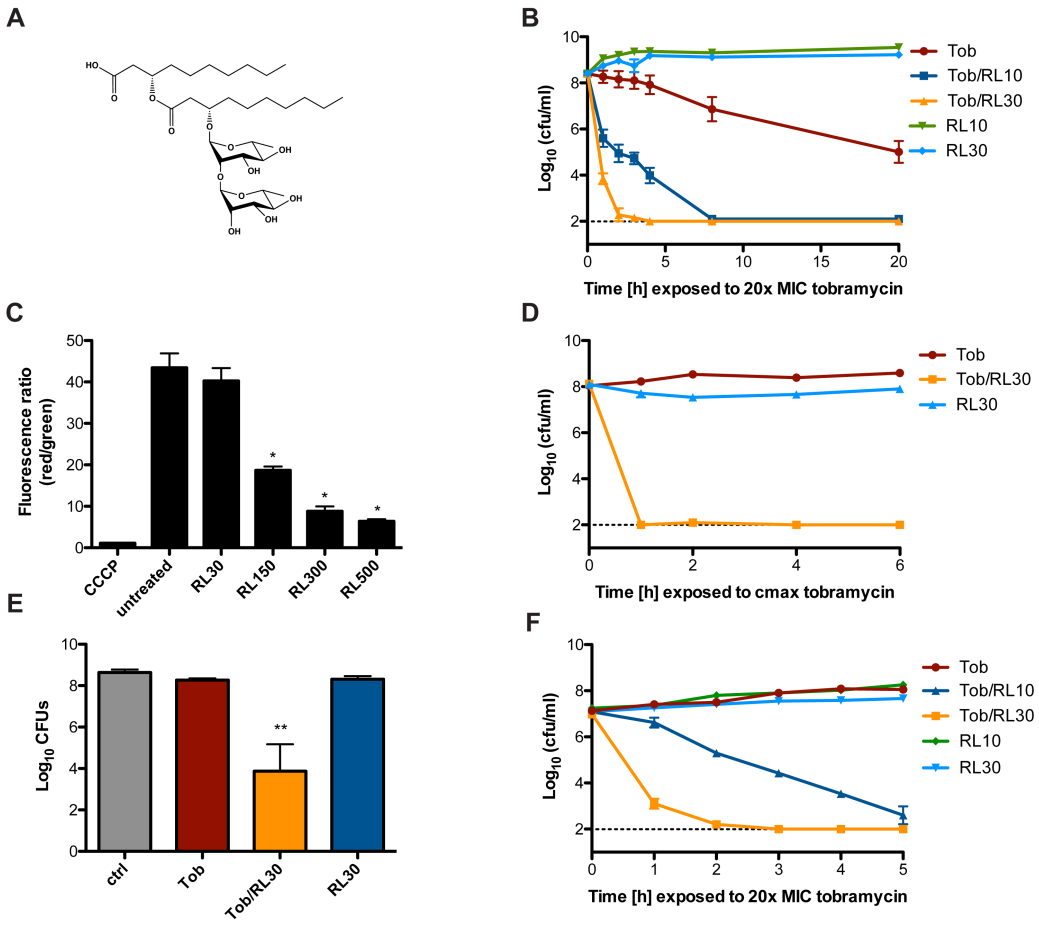

Figure 3.1. Rhamnolipids synergize with aminoglycosides against tolerant *S. aureus* populations. (A) Chemical structure of a representative di-rhamnolipid congener, di-rhamnolipid C10C10. **(B)** *S. aureus* strain HG003 was grown to mid-exponential phase and challenged with 20x the MIC (15.6µg/mL) of tobramycin +/- 10 or 30µg/ml rhamnolipids. Survivors were enumerated at the indicated time points. **(C)** *S. aureus* HG003 membrane potential was measured by calculating the red/green ratio using the population mean fluorescence intensities (MFI) for HG003 incubated with 30µM $DiOC_2(3)$ for 30 minutes. Prior to staining, cells were grown to mid-exponential phase, then treated for 30 minutes with the indicated concentration of rhamnolipids or for 5 minutes with 5µM CCCP as a control. *p<0.05 (One-way ANOVA with Tukey's multiple comparison post test). **(D)** Mid-exponential phase HG003 was challenged with the C_{max} concentration of tobramycin (58µg/mL) +/- 30µg/ml rhamnolipids under anaerobic conditions. Survivors were enumerated at the indicated time points. **(E)** Biofilm-associated *S. aureus* HG003 was challenged with 58µg/mL tobramycin +/- 30µg/ml rhamnolipids for 24 hours prior to CFU enumeration. **(F)** *S. aureus* SCV strain HG003 *menD::tn* was grown to mid-exponential phase and challenged with 15.6µg/mL tobramycin +/- 10 or 30µg/ml rhamnolipids. CFU enumeration occurred at the indicated time points. All experiments were performed in biological triplicate. **p<0.005 (Student's t-test). Error bars represent mean +/- SD. Limit of detection is indicated by the horizontal dashed line.

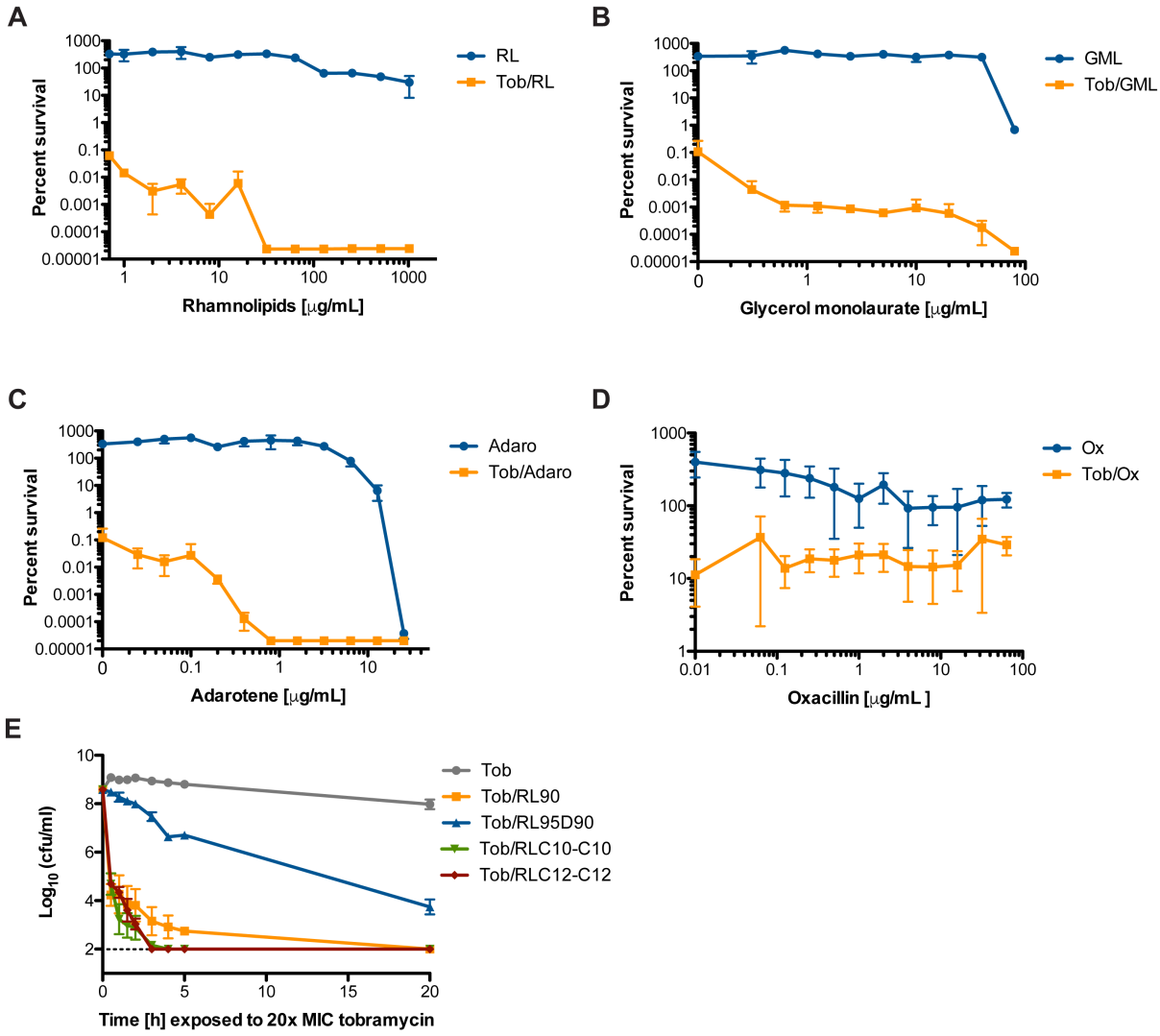

Figure 3.2. Membrane-acting agents potentiate aminoglycoside killing. *S. aureus* HG003 was grown to mid-exponential phase then treated with the indicated concentrations of **(A)** rhamnolipids, **(B)** glycerol monolaurate, **(C)** adarotene, or **(D)** oxacillin +/- 10x the MIC of tobramycin (7.8μg/mL) in a 96-well plate. After 24hr, the wells were washed, and cells were plated to enumerate survivors. (**E)** *S. aureus* strain HG003 was grown to mid-exponential phase and challenged with 15.6μg/mL of tobramycin with or without 30μg/mL of each RL congener. At the indicated time points an aliquot was removed, washed and plated to enumerate survivors. All experiments were performed in biological triplicate. Error bars represent mean +/- SD. Limit of detection is indicated by the horizontal dashed line.

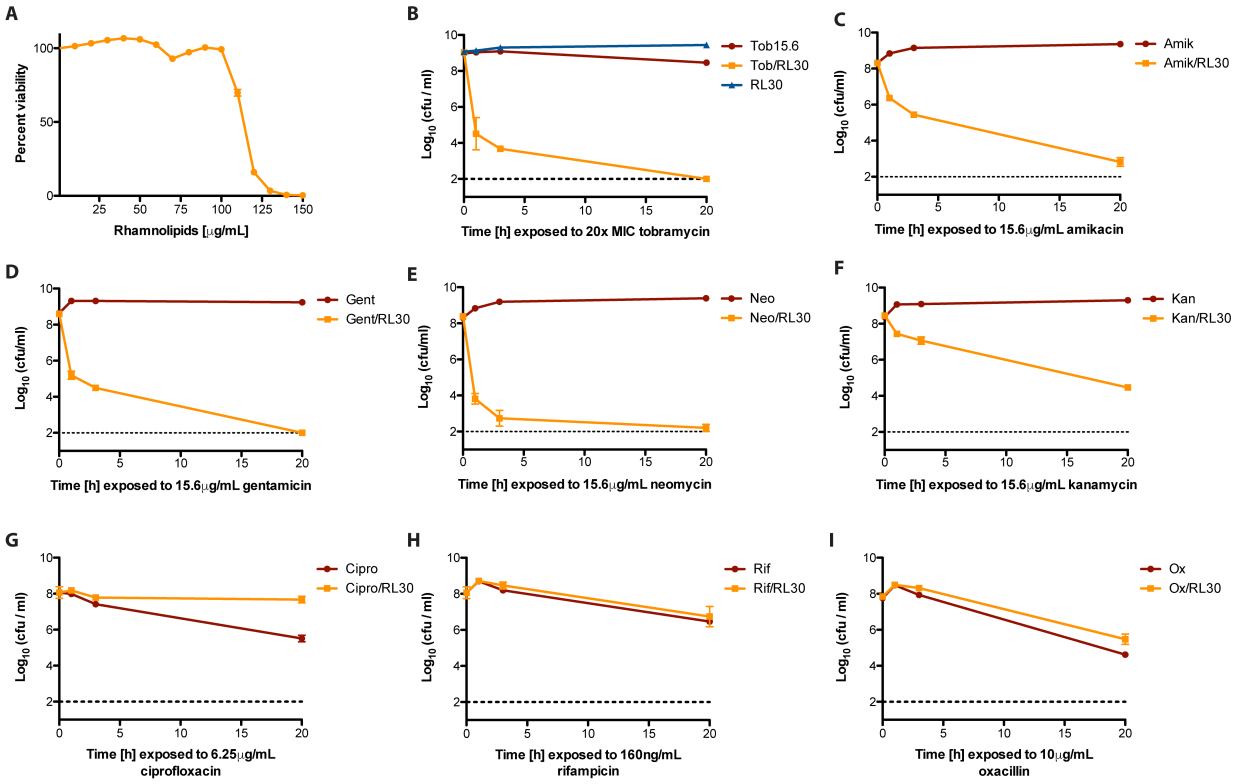

Figure 3.3. Sub-cytotoxic concentrations of rhamnolipids specifically potentiate aminoglycoside killing of *S. aureus*. **(A)** J774.1 macrophage-like cells were treated with the indicated concentrations of rhamnolipids for 24hr before cell viability was determined using a CellTiter Blue cell viability assay. **(B)** *S. aureus* MRSA strain JE2 was grown to mid-exponential phase and challenged with 15.6μg/mL of tobramycin +/- 30μg/mL rhamnolipids. **(C-I)** *S. aureus* strain HG003 was grown to mid-exponential phase and challenged with 15.6μg/mL of **(C)** amikacin, **(D)** gentamicin, **(E)** neomycin, **(F)** kanamycin, **(G)** 6.25 μg/mL ciprofloxacin, **(H)** 160ng/mL rifampicin, or **(I)** 10μg/mL oxacillin +/-30μg/mL rhamnolipids. At the indicated time points an aliquot was removed, washed and plated to enumerate survivors. All experiments were performed in biological triplicate. Error bars represent mean +/- SD. Limit of detection is indicated by the horizontal dashed line.

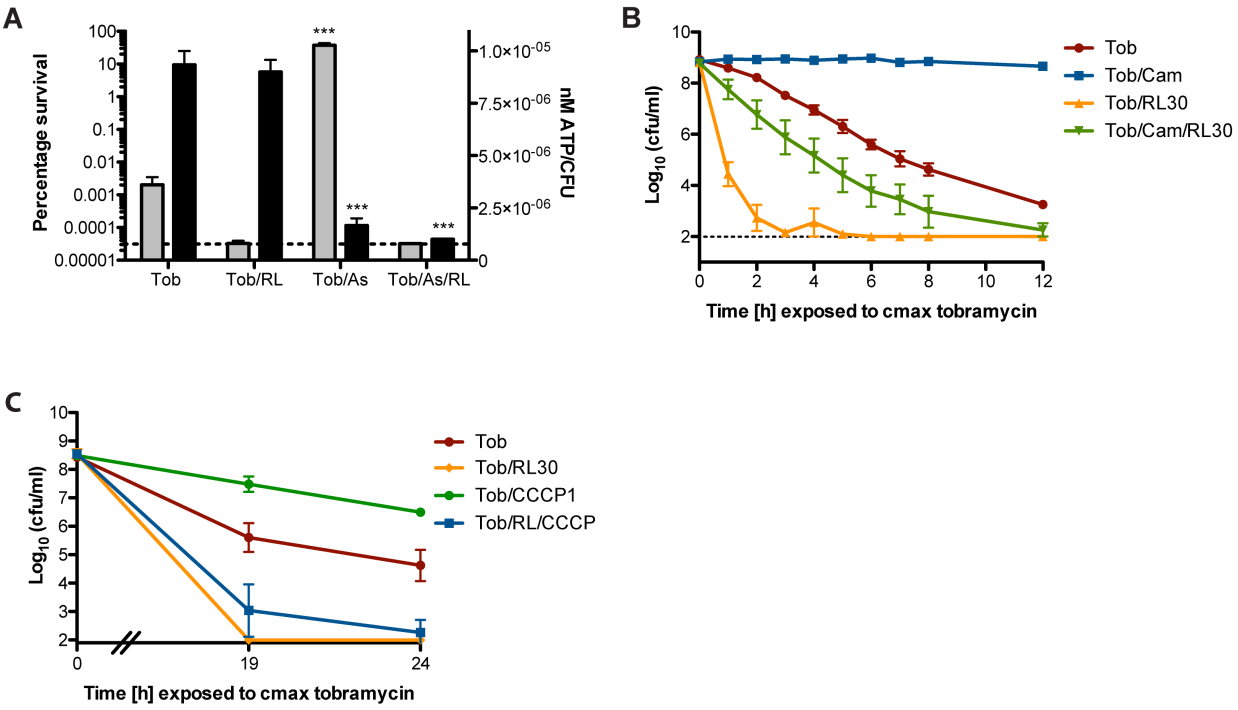

Figure 3.4. Rhamnolipid/aminoglycoside combinational therapy targets *S. aureus* persisters. (A) Mid-exponential phase *S. aureus* strain HG003 was treated with 5mM $AsKO_2$ for 30 min prior to addition of 58µg/mL tobramycin. Intracellular ATP was measured using a BacTiter-Glo cell viability assay immediately prior to antibiotic challenge (black bars). An aliquot of each culture was removed after 24hr, washed, and plated to enumerate survivors (grey bars). ***p<0.005 (Student's t-test, calculated relative to cultures treated with tobramycin alone). **(B, C)** Exponential phase populations of HG003 were exposed to **(B)** 30µg/mL chloramphenicol or **(C)** 1µM CCCP for 30 min prior to challenge with 58µg/mL tobramycin +/- 30µg/ml rhamnolipids. At the indicated time points an aliquot was removed, washed and plated to enumerate survivors. All experiments were performed in biological triplicate. Error bars represent mean +/- SD. Limit of detection is indicated by the horizontal dashed line.

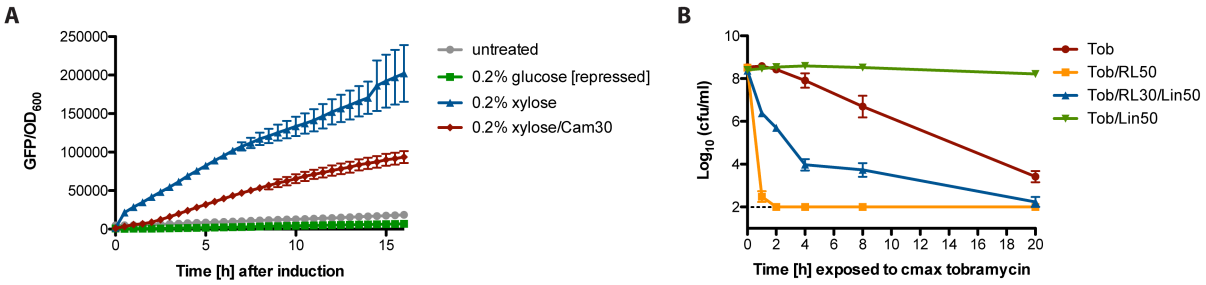

Figure 3.5. Reducing *S. aureus* translation with bacteriostatic translation inhibitors slows the rate of RL/tobramycin killing. (A) Mid-exponential phase populations of *S. aureus* strain HG003 harboring the xylose-inducible gfp reporter plasmid pCLON46 was treated with 30µg/mL chloramphenicol prior to induction with 0.2% xylose. OD_{600} and *gfp* expression levels were determined using a Biotek Synergy H1 microplate reader. **(B)** HG003 was treated with 50µg/mL linezolid for 30 minutes prior to tobramycin challenge in the presence or absence of 30µg/mL rhamnolipids. At the indicated time points an aliquot was removed, washed and plated to enumerate survivors. All experiments were performed in biological triplicate. Error bars represent mean +/- SD. Limit of detection is indicated by the horizontal dashed line.

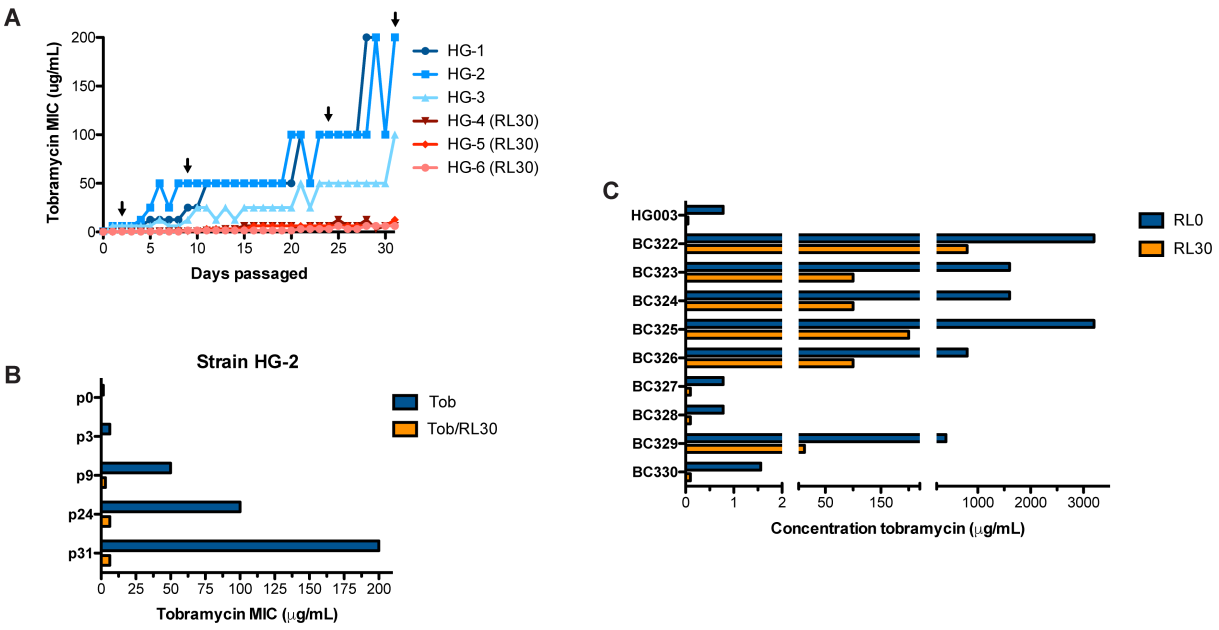

Figure 3.6. Rhamnolipids repress the rise of tobramycin resistance and restore sensitivity to resistant isolates. (A) Six independent lineages of HG003 were passaged daily in subinhibitory concentrations of tobramycin +/- 30μg/mL rhamnolipids and monitored for the spontaneous occurrence of tobramycin resistant mutants through changes in MIC. **(B, C)** Minimum tobramycin concentration necessary to inhibit the growth of **(B)** resistant isolates from passaged strain HG-2 (Figure 3.6A, black arrows) or **(C)** CF clinical isolates, +/- 30μg/mL rhamnolipids.

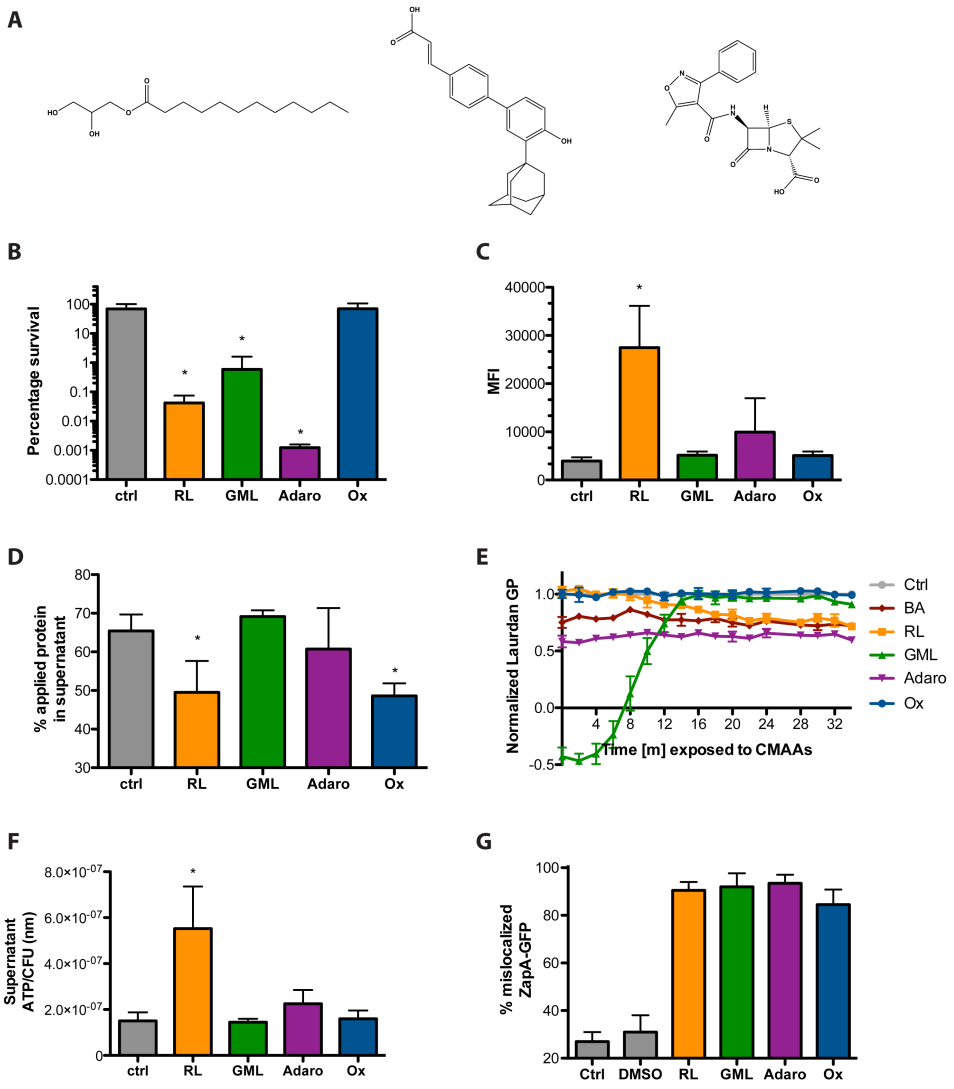

Figure 3.7. Membrane targeting agents can potentiate aminoglycoside killing without improving uptake. (A) The chemical structures of glycerol monolaurate, adarotene, and oxacillin, respectively. **(B)** Percent survival and (**C)** Mean Fluorescence Intensity (MFI) values for *S. aureus* cultures treated with CEAAs + Texas Red-tobramycin **(D)** Changes to *S. aureus* cell surface charge was measured after treatment with each compound through association with positively-charged cytochrome C. **(E)** Changes to *S. aureus* membrane fluidity following treatment with each compound was monitored via Laurdan GP fluorescence. **(F)** Small molecule permeability through the *S. aureus* plasma membrane was assessed 1hr after treatment with each compound by measuring ATP leakage into the supernatant with the BacTiter-Glo cell viability assay. **(G)** *S. aureus* strain SH1000 harboring an inducible P*zapA::gfp* cell division reporter was grown to OD_{600}=0.5, then treated with 30μg/mL rhamnolipids, 40μg/mL GML 3.2μg/mL adarotene, or 0.5μg/mL oxacillin for 1 hr. Changes to membrane morphology and ZapA localization relative to control cultures were visualized using a GE Applied Precision DeltaVision Elite de-convolution fluorescence microscope equipped with a Photometrics CoolSnap HQ2 camera.*p<0.05 (Student's t-test). All experiments were performed in biological triplicate. Error bars represent mean +/- SD.

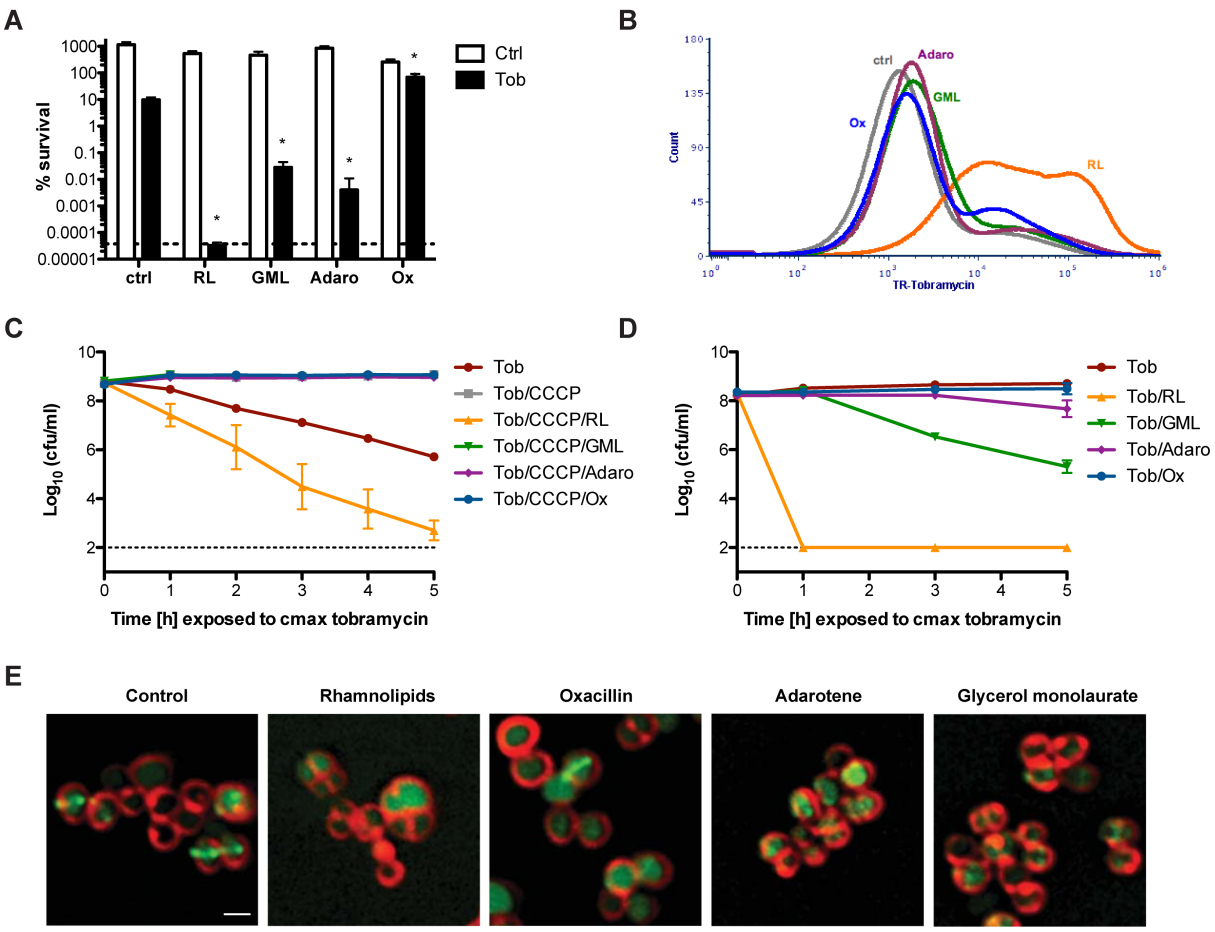

Figure 3.8. Rhamnolipids specifically induce PMF-independent aminoglycoside uptake to resensitize tolerant *S. aureus*. (A) *S. aureus* was grown to mid-exponential phase then challenged with 58µg/mL tobramycin alone, or in combination with 30µg/mL rhamnolipids, 40µg/mL GML, 3.2µg/mL adarotene, or 0.5µg/mL oxacillin (black bars). An aliquot of each culture was removed after 24hr, washed, and plated to enumerate survivors. White bars represent *S. aureus* survivors following 24hr treatment with each cell envelope-acting agent without tobramycin. **(B)** Texas Red-conjugated tobramycin was added to *S. aureus* cultures with our without each compound. Following 1hr, Texas Red-tobramycin uptake was measured by flow cytometry. **(C, D)** *S. aureus* HG003 was **(C)** treated with 1µM CCCP or **(D)** grown anaerobically prior to treatment with 58µg/mL tobramycin +/- each cell envelope acting compound individually. Survivors were enumerated at the indicated time points. **(E)** *S. aureus* strain SH1000 harboring an inducible P*zapA::gfp* cell division reporter was grown to OD_{600}=0.5, then treated with 30 rhamnolipids, 40µg/mL GML 3.2µg/mL adarotene, or 0.5µg/mL oxacillin for 1 hr. Cells were washed, then treated with the membrane dye, FM4-64. Changes to membrane morphology and ZapA localization relative to control cultures were visualized using a GE Applied Precision DeltaVision Elite de-convolution fluorescence microscope equipped with a Photometrics CoolSnap HQ2 camera. Scale bar: 1µm. *p<0.05 (Student's t-test). All experiments were performed in biological triplicate. Error bars represent mean +/- SD.

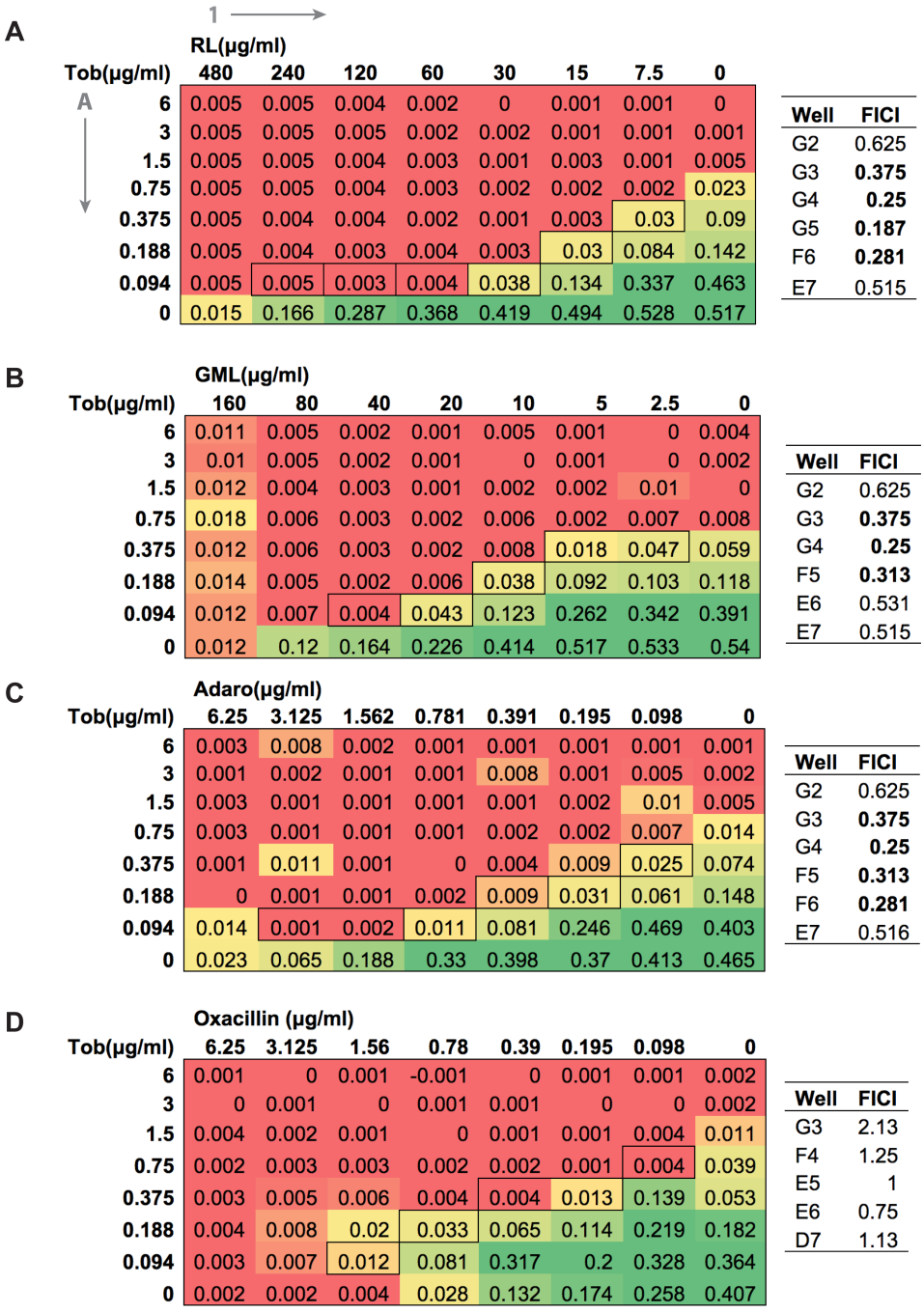

Figure 3.9. Tobramycin and cell envelope-acting agent checkerboard assays. Synergism between tobramycin and **(A)** rhamnolipids, **(B)** glycerol monolaurate, **(C)** adarotene, and **(D)** oxacillin was determined against *S. aureus* HG003 using the checkerboard microdilution method. FICI values were calculated by determining the minimum concentration of each compound necessary to inhibit bacterial growth alone or in combination with tobramycin as described in the main text. Synergy, FICI≤0.5; no interaction, 0.5<FICI<4; antagonism, FICI≥4.

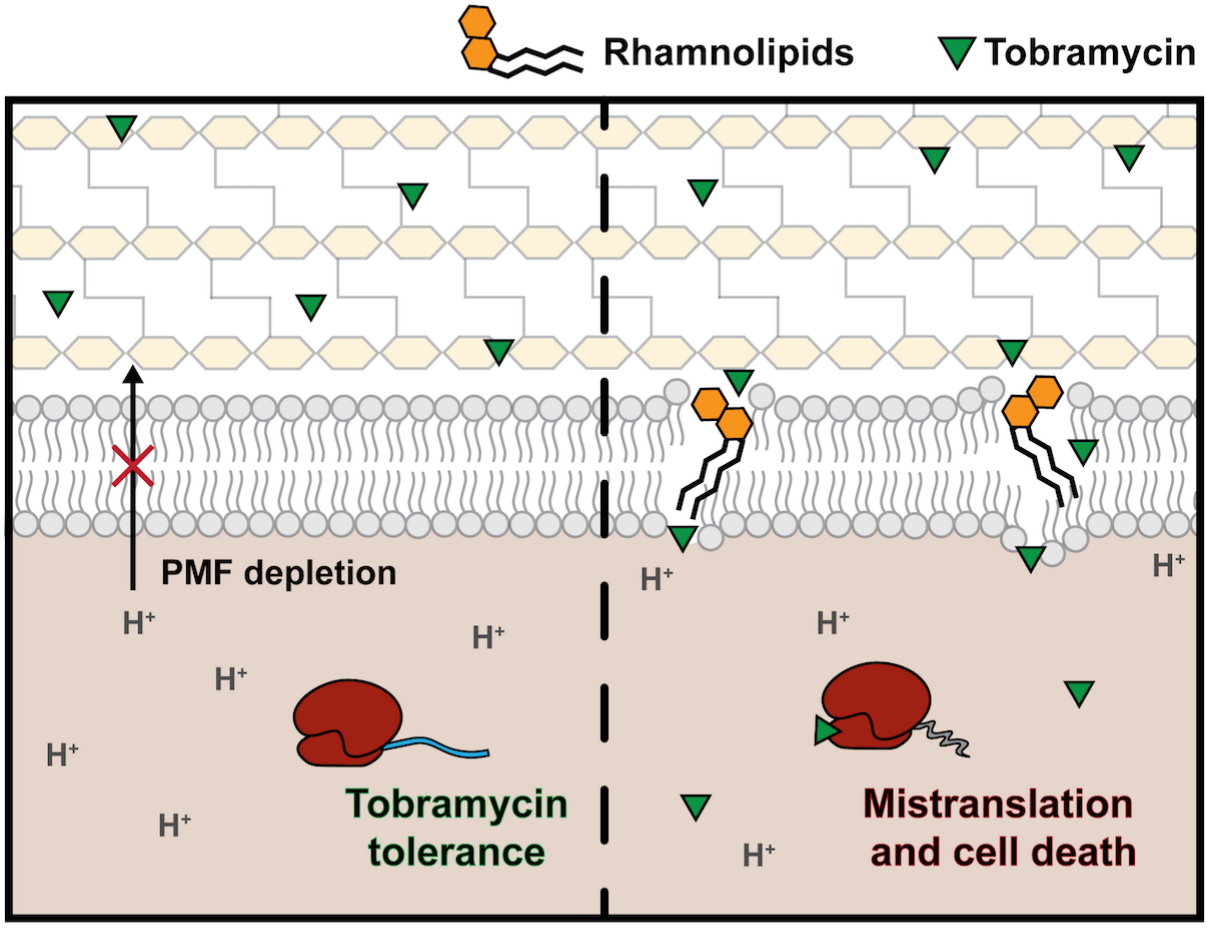

Figure 3.10. Rhamnolipids facilitate PMF-independent aminoglycoside uptake. Aminoglycoside antibiotics such as tobramycin require proton motive force (PMF) for bacterial internalization. In non-respiring populations, bacterial PMF drops below the threshold required for PMF-mediated tobramycin uptake, leading to antibiotic exclusion and subsequent treatment failure. *Pseudomonas aeruginosa*-produced rhamnolipids intercalate into the Gram-positive bacterial membrane to increase membrane permeability to tobramycin and facilitate PMF-independent tobramycin uptake. This restores tobramycin susceptibility to tobramycin resistant and tolerant populations and facilitates rapid bacterial death in otherwise tolerant non-respiring, small colony variant, biofilm-associated, anaerobic and persister-associated *Staphylococcus aureus* populations.

Table 3.1. Tobramycin/rhamnolipid MIC values for other Gram positive and negative bacterial species (µg/mL)

	Tobramycin	Tobramycin + rhamnolipids	Fold change	RL MIC
Gram negative				
Escherichia coli	0.78	0.78	0	>2400
Gram positive				
Bacillus subtilis	0.39	0.0061	64	62.5
Streptococcus pneumoniae	12.5	12.5	0	>2400
Enterococcus faecalis	100	0.78	128	125
Listeria monocytogenes	1.56	0.049	32	125
Clostridioides difficile	400	0.39	1025	31.25

Table 3.2. Fractional inhibitory concentration (FICI[1]) of cell envelope acting agents in combination with tobramycin against *S. aureus* HG003

Compound	$FICI_{max}$	$FICI_{min}$	Synergy
rhamnolipids	0.625	0.1875	YES
Glycerol monolaurate	0.625	0.25	YES
Adarotene	0.625	0.25	YES
Oxacillin	2.125	0.75	NO

[1]FICI ≤ 0.5: synergy, 0.5 < FICI ≤4: no interaction, 4<FICI: antagonism

CHAPTER 4
DEFINING THE METABOLIC PATHWAYS AND HOST-DERIVED CARBON SUBSTRATES REQUIRED FOR *FRANCISELLA TULARENSIS* INTRACELLULAR GROWTH[1]

Francisella tularensis is a Gram negative, facultative intracellular bacterial pathogen and one of the most virulent organisms known. A hallmark of *F. tularensis* pathogenesis is the bacterium's ability to replicate to high densities within the cytoplasm of infected cells in over 250 known host species, including humans. This demonstrates that *F. tularensis* is adept at modulating its metabolism to fluctuating concentrations of host-derived nutrients. The precise metabolic pathways and nutrients utilized by *F. tularensis* during intracellular growth, however, are poorly understood. Here we use systematic mutational analysis to identify the carbon catabolic pathways and host-derived nutrients required for *F. tularensis* intracellular replication. We demonstrate that the glycolytic enzyme phosphofructokinase (PfkA), and thus glycolysis, is dispensable for *F. tularensis* SchuS4 virulence, and highlight the importance of the gluconeogenic enzyme fructose 1,6-bisphosphatase (GlpX). We found that the specific gluconeogenic enzymes that function upstream of GlpX varied based on infection model, indicating that *F. tularensis* alters its metabolic flux according to the nutrients available within its replicative niche. Despite this flexibility, we found that glutamate dehydrogenase (GdhA) and glycerol-3P dehydrogenase (GlpA) are essential for *F. tularensis* intracellular

[1] Radlinski LC, Brunton J, Steele S, Taft-Benz S, Kawula TH. Defining the metabolic pathways and host-derived carbon substrates required for *Francisella tularensis* intracellular growth. *mBio.* 2018 Nov 20;9(6). pii: e01471-18.

replication in all infection models tested. Finally, we demonstrate that host cell lipolysis is required for *F. tularensis* intracellular proliferation, suggesting that host triglyceride stores represent a primary source of glycerol during intracellular replication. Altogether, the data presented here reveal common nutritional requirements for a bacterium that exhibits characteristic metabolic flexibility during infection.

IMPORTANCE

The widespread onset of antibiotic resistance prioritizes the need for novel antimicrobial strategies to prevent the spread of disease. With its low infectious dose, broad host range, and high rate of mortality, *F. tularensis* poses a severe risk to public health and is considered a potential agent for bioterrorism. *F. tularensis* reaches extreme densities within the host cell cytosol, often replicating 1000-fold in a single cell within 24 hours. This remarkable rate of growth demonstrates that *F. tularensis* is adept at harvesting and utilizing host cell nutrients. However, like most intracellular pathogens the types of nutrients utilized by *F. tularensis* and how they are acquired is not fully understood. Identifying the essential pathways for *F. tularensis* replication may reveal new therapeutic strategies for targeting this highly infectious pathogen, and may provide insight for improved targeting of intracellular pathogens in general.

INTRODUCTION

In order to establish a successful infection, intracellular bacterial pathogens must adapt their metabolism to utilize the nutrients available within the host cell, often in direct competition with the host's own metabolic processes and mechanisms for nutrient

sequestration[273]. Nevertheless, many of these microorganisms have evolved dedicated mechanisms to harvest and assimilate essential nutrients to proliferate within this specialized niche[274–276]. Targeted strategies for carbon acquisition and assimilation fuel bacterial replication and often aid in the evasion of host cell defenses[277–279]. Despite their importance, the metabolic pathways and host-derived carbon sources utilized by bacterial pathogens *in vivo* are generally not well understood[165,280].

Metabolites can be directly acquired from the host, salvaged from similar molecules, or synthesized *de novo* using host-derived sources of carbon, nitrogen, sulfur, etc. Bacteria that replicate within the host cell cytosol theoretically have access to the products and intermediates produced during major host metabolic processes that take place within this compartment, including glycolysis and amino acid biosynthesis. The actual concentrations of these products within an infected cell, however, are unclear. Rather, most nutrients are stored within complex structures such as lipid droplets, glycogen and protein, and thus are not immediately available to intracellular pathogens[165].

Many bacteria employ active mechanisms to acquire host-derived carbon during intracellular growth. *Mycobacterium tuberculosis* and *Chlamydia tracomatis*, for instance, associate with host lipid droplets and utilize host-derived lipids for anabolic and catabolic purposes[169,170]. *Salmonella enterica* serovar Typhimurium secretes effector proteins that stimulate the activation of Akt, a major metabolic regulator of host metabolism[166,281]. This in turn stimulates host glycolytic flux, and increases the concentration of glucose within the infected cell[281]. Similar effector molecules actively

alter host vesicular trafficking to direct nutrients to the *Salmonella* containing vacuole[168]. The observation that many pathogens employ active mechanisms to obtain carbon emphasizes that carbon acquisition within the host cell requires complex host-pathogen interactions, which are only beginning to be elucidated.

We previously demonstrated that *F. tularensis* induces host autophagy during infection, and that this pathway provides the pathogen with essential amino acid metabolites[282]. Nevertheless, *F. tularensis* replicates to a considerable degree in the absence of autophagy, indicating that autophagy-derived nutrients are only a subset of the total required to support full *F. tularensis* intracellular proliferation[282]. A transposon mutagenesis screen of *F. tularensis* subspecies *holarctica* LVS revealed that nearly half of the genes identified as essential for proliferation in macrophages encode proteins involved in metabolism or metabolite transport[283]. These proteins include enzymes predicted to facilitate gluconeogenesis, glycerol catabolism, amino acid transport, as well as purine, LPS, and fatty acid biosynthesis. Surprisingly, no glycolytic genes were identified during this screen. Glycolysis is a fundamental metabolic pathway that oxidizes carbohydrates to generate energy and provide precursor metabolites for other biosynthetic pathways. In contrast, the gluconeogenic pathway reverses the reactions of glycolysis during growth on non-glucose carbon substrates to replenish stores of glucose-6P and other essential metabolic intermediates when glucose concentrations are limited. One gene encoding a key gluconeogenic enzyme, *glpX,* was required for efficient intracellular replication[283]. Indeed, *glpX* has repeatedly been identified as an important factor for virulence in genetic screens performed in *F. tularensis* Schu S4 and LVS[284–286]. Furthermore,

recent work by Brissac *et al.* demonstrated that gluconeogenesis is an essential metabolic pathway for *Francisella novicida* and *F. tularensis* LVS during growth in glucose-limiting conditions[287]. These data suggest that *F. tularensis* intracellular proliferation may not be dependent on glycolysis, but rather gluconeogenesis to preferentially assimilate non-glucose carbon substrates within a host cell.

To determine the specific host-derived carbon sources that facilitate rapid *F. tularensis* intracellular proliferation, we aimed to define the essential carbon metabolic pathways and metabolites required for *F. tularensis* intracellular and *in vivo* growth.

RESULTS

Gluconeogenesis, but not glycolysis, is essential for *F. tularensis* intracellular growth and virulence

Unlike most enzymatic reactions of the glycolytic pathway, the conversion between fructose 6-phosphate (F6P) and fructose 1,6-bisphosphate (FBP) is physiologically irreversible, and is catalyzed by enzymes specific to either glycolysis or gluconeogenesis. In *F. tularensis,* the glycolytic enzyme phosphofructokinase (PfkA) converts F6P to FBP, and the gluconeogenic enzyme fructose 1,6-bisphosphatase (GlpX) performs the reverse reaction (Figure 4.1). Deletion of *pfkA* should prevent *F. tularensis* from utilizing glucose or glucose 6-phosphate imported from the host, while deletion of *glpX* should prevent the bacterium from producing F6P during growth on gluconeogenic carbon sources. F6P is a precursor of the pentose phosphate pathway and is used for the *de novo* synthesis of lipopolysaccharide, peptidoglycan, pentose phosphates, and aromatic amino acids. We hypothesized that if glucose represents a

major carbon source for *F. tularensis* within the host cell, then *pfkA* would be essential. Alternatively, if glucose is not a major source of carbon utilized by *F. tularensis*, then the gluconeogenic enzyme *glpX* would be required in order to synthesize sufficient F6P and glucose-6P from alternate carbon sources.

We first sought to confirm the predicted functions of *pfkA* and *glpX* for glycolysis and gluconeogenesis, respectively. Markerless, in-frame deletions were created for *pfkA* and *glpX* in *F. tularensis* subspecies *tularensis* Schu S4, and the deletion strains were grown in defined media with either glycolytic or gluconeogenic carbon substrates. For all broth cultures, *F. tularensis* was grown in Chamberlain's defined media (CDM) containing a low concentration (~3mM) of 13 essential and non-essential amino acids and no other major carbon sources[288]. In this media, wild-type (WT) Schu S4 grew to low, but detectable levels, presumably by assimilating amino acids for protein synthesis or energy production (Figures 4.2A, 4.3A). Indeed, Brissac *et al.* recently demonstrated that supplementation of this media with 30mM of select amino acids (threonine, proline, methionine, lysine, tyrosine, tryptophan, phenylalanine, asparagine or serine) permits varying degrees of *F. novicida* growth*,* suggesting that these amino acids may be utilized as carbon sources [287]. Supplementation with either glucose or glutamate supported robust growth of WT Schu S4 (Figure 4.2A, 4.3A). A *ΔpfkA* mutant grew to WT levels during growth on glutamate, but did not grow on glucose, possibly due to glucose-mediated repression of alternative carbon catabolic pathways (Figure 4.2A). Importantly, though terminal OD_{600} describes the overall capacity of each mutant to grow on different carbon substrates, closer attention to *in vitro* doubling times reveals subtle nuances in how each deletion affects growth. For instance, a *ΔpfkA* mutant

reaches the same OD_{600} as WT Schu S4, but grows at a much slower rate (Figure 4.3B). As expected, the *ΔglpX* mutant grew on a glucose but not glutamate (Figures 4.2A, 4.3C). The growth defects of each mutant were restored to WT levels when the deleted genes were complemented *in trans* (Figures 4.2A, 4.3A-C).

To assess the importance of glycolysis and gluconeogenesis during *F. tularensis* intracellular growth, we utilized a luminescence reporter to monitor intracellular growth as previously described[283], where *F. tularensis* Schu S4 strains harbor a plasmid expressing luciferase enzyme and substrate as well as an addiction system to maintain the plasmid even in the absence of antibiotic selection. As demonstrated previously, an increase in the bacterial burden within the infected cell is directly proportional to an increase in reporter luminescence[283]. BMDMs were infected with WT Schu S4, *ΔpfkA*, or *ΔglpX*, each strain harboring the luminescence reporter. 24 hours post-inoculation, WT Schu S4 and *ΔpfkA* grew to similar levels within the BMDMs, while the growth of *ΔglpX* was reduced approximately 10-fold relative to WT and *ΔpfkA* (Figure 4.2B). These data indicate that gluconeogenesis, but not glycolysis, is necessary for WT levels of *F. tularensis* intracellular growth and suggests that glucose does not represent a major carbon source within macrophage cells.

We hypothesized that the severe intracellular growth defect observed for the *ΔglpX* mutant was due to the mutant's inability to synthesize sufficient levels of F6P and G6P from the catabolism of gluconeogenic carbon substrates. Therefore supplementation with excess glucose should rescue *ΔglpX* mutant growth within cells. J774A.1 cells are a transformed macrophage cell line constitutively expressing c-Myc, and therefore import large quantities of glucose to increase glycolytic flux[289,290]. To

determine if excess glucose could restore the growth defect of the *ΔglpX* mutant, we infected J774A.1 cells with WT Schu S4, *ΔpfkA*, and *ΔglpX*, supplied the infected cells with either high glucose (4.5 g/L) or glucose-free DMEM, and then measured bacterial growth over a 36-hour period. WT Schu S4 and *ΔpfkA* exhibited significant growth with or without glucose supplementation (Figure 4.5A). As expected, the *ΔglpX* mutant strain did not replicate within J774A.1 cells cultured in glucose-free DMEM, however intracellular replication was restored to WT levels with excess glucose (Figure 4.5B).

The rescue of the *ΔglpX* mutant did not occur in primary BMDMs, as all BMDM infections were performed in high glucose (4.5g/L) DMEM (Figure 4.2B). This observation suggests that the reduced level of glucose import and glycolytic flux exhibited by BMDMs, relative to J774A.1 cells, is insufficient to permit *ΔglpX* from acquiring adequate glucose from the host to restore WT growth properties even when glucose is present at high concentrations in the media. To test this, we attempted to rescue growth of *ΔglpX* in BMDMs by treating the host cells with 5-amnoimidazole-4-carboxamide ribonucleotide (AICAR). AICAR is an analog of adenosine monophosphate (AMP) that stimulates activation of the major host metabolic regulator, AMP-dependent protein kinase (AMPK)[291]. When activated, AMPK stimulates glucose uptake and energy production in part by increasing expression of major glucose transporters GLUT1 and GLUT4, and by increasing overall host glycolytic flux[292]. We hypothesized that AICAR treatment of BMDMs cultured in high glucose DMEM would restore *ΔglpX* intracellular growth by stimulating glucose import. Indeed, while AICAR had little impact on the growth of WT Schu S4 within BMDMs (Figure 4.2C), AICAR treatment significantly increased the intracellular growth of *ΔglpX* in BMDMs cultured in

high glucose DMEM (Figure 4.2D). Altogether our results support the conclusion that the inability of the *ΔglpX* mutant to fully assimilate gluconeogenic carbon sources results in attenuated growth during periods of glucose limitation.

We next tested whether *F. tularensis* similarly requires *glpX* and not *pfkA* for replication in a murine model of *F. tularensis* pulmonary infection. Groups of C57BL6/J female mice were infected intranasally with 100 CFU of WT, *ΔpfkA or ΔglpX* Schu S4 strains. Three days post infection, the lungs, livers and spleens of the infected mice were harvested, homogenized, and plated for bacterial enumeration. Organ burdens for the *ΔpfkA* mutant strain were similar to that of WT Schu S4 (Figure 4.2E). However, the number of CFU recovered from the lungs of mice infected with the *ΔglpX* mutant was similar to that of the original inoculum, and below the limit of detection in the liver and spleen (Figure 4.2E). These data align with our observations that *glpX,* and therefore gluconeogenesis, is necessary for *F. tularensis* replication in host cells, while *pfkA* and glycolysis are dispensable.

F. tularensis possesses multiple pathways that supply gluconeogenic substrates to support intracellular growth

Our data suggest that a *ΔglpX* mutant does not produce essential biosynthetic precursors from the nutrients available within the host cell. Since the deletion of *glpX* precludes the utilization of a large number of gluconeogenic carbon sources such as glycerol, pentose sugars, amino acids, lactate, pyruvate, and TCA cycle intermediates, we generated *F. tularensis* mutant strains unable to utilize some of these specific carbon sources. Like the conversion of F6P to FBP, the enzymatic conversion of

pyruvate to phosphoenol pyruvate (PEP) during glycolysis is physiologically irreversible, and must be bypassed during gluconeogenesis. The ATP-dependent decarboxylation of oxaloacetate to PEP is catalyzed by PEP carboxykinase (*pckA*), and is important for growth on carboxylic or amino acids. Alternatively, pyruvate-phosphate dikinase *(ppdK)* converts pyruvate to PEP and is required for growth on pyruvate, lactate and some amino acids. The reactions catalyzed by each enzyme can independently fuel the gluconeogenic pathway to generate essential metabolic precursors necessary for growth. (Figure 4.1)

We generated markerless, in-frame deletions of *ppdK* and *pckA*. Growth characteristics of each mutant were analyzed in defined media with specific glycolytic or gluconeogenic substrates to confirm the metabolic function of each enzyme. Both *ΔppdK* and *ΔpckA* grew to levels similar to WT Schu S4 in CDM supplemented with glucose (Figure 4.4A,B). However, while *ΔpckA* grew to WT levels in CDM with or without excess glutamate, *ΔppdK* had a severe growth defect in CDM and in CDM supplemented with glutamate, similar to the *ΔglpX* mutant (Figure 4.4A,B). These data suggest that during growth in defined media, *F. tularensis* preferentially synthesizes PEP from pyruvate (PpdK) and not oxaloacetate (PckA).

We observed that both *ΔppdK* and *ΔpckA* grew to WT levels within the BMDMs (Figure 4.4C). Furthermore, a *ΔppdKpckA* double mutant replicated to significant levels within these cells, albeit at a slower rate, suggesting that these gluconeogenic pathways are not essential for *F. tularensis* growth within BMDMs (Figure 4.4C). When we infected J774A.1 cells with the *ΔppdK* and *ΔpckA* mutants, we found that *ΔpckA* grew to WT levels within J774A.1 cells cultured with or without glucose supplementation (Figure

4.5C). *ΔppdK,* however, exhibited significantly reduced growth within J774A.1 cells cultured without glucose (Figure 4.5D). Intracellular proliferation of the *ΔppdK* mutant was restored to WT levels upon high glucose supplementation, indicating that *ppdK* may contribute to the assimilation of host-derived carbon in J774A.1 cells.

While we found that the organ burdens of the *ΔppdK* mutant were similar to that of WT Schu S4 in our murine model, we recovered significantly reduced numbers of the *ΔpckA* mutant from the lung, liver and spleen of infected mice (Figure 4.4D). Further, we recovered similar numbers of the *ΔppdKpckA* double mutant relative to the *ΔpckA* single mutant. This indicates that *pckA* is required for optimal replication in a murine model of *F. tularensis* infection but *ppdK* is dispensable (Figure 4.4D).

Amino acids feed the gluconeogenic pathway through the TCA cycle

The attenuation of *ΔpckA* in mice suggests that *F. tularensis* relies on the metabolic pathway catalyzed by PckA during infection. Potential nutrients that can fuel the gluconeogenic pathway through PckA include TCA cycle intermediates or amino acids that feed into the TCA cycle. To discern between these possibilities, we evaluated the importance of glutamate dehydrogenase (*gdhA*) for *F. tularensis* intracellular growth. GdhA catalyzes the reversible oxidative deamination of glutamate to α-ketoglutarate, a TCA cycle intermediate (Figure 4.1). *F. tularensis* is predicted to require GdhA to shuttle several amino acids into the TCA cycle including glutamate, glutamine, proline, arginine, and potentially aspartate and asparagine. Therefore, if *F. tularensis* preferentially catabolizes amino acids and not TCA cycle intermediates, then a *ΔgdhA* mutant would likely be similarly attenuated relative to *ΔpckA* during *in vivo* growth.

To validate the predicted function of *gdhA*, we tested a *ΔgdhA* mutant for growth on glycolytic and gluconeogenic carbon sources in defined media. As expected, we found that *gdhA* was required for growth in CDM or CDM supplemented with glutamate, but not CDM supplemented with glucose (Figure 4.6A). Because *ΔgdhA* grew to significant levels on glucose in defined media lacking glutamate, we reasoned that *gdhA* was dispensable for glutamate synthesis, but required for glutamate assimilation.

The *ΔgdhA* deletion mutant exhibited reduced growth in BMDMs that was restored upon expression of *gdhA in trans* (Figure 4.6B), suggesting that GdhA-mediated carbon assimilation represents an important metabolic pathway during *F. tularensis* replication in BMDMs. When we infected J774A.1 macrophage cells with *ΔgdhA* we found that the defect in bacterial intracellular replication during culture in glucose-free DMEM could be partially rescued with excess glucose, similar to the *ΔglpX* and *ΔppdK* mutants (Figure 4.5E). Similarly, BMDMs cultured in high glucose DMEM and treated with AICAR permitted significant growth of *ΔgdhA* relative to untreated BMDMs (Figure 4.6C). These data suggest that the intracellular growth defect observed for *ΔgdhA* is at least in part due to the ability of this mutant to assimilate sufficient host-derived carbon.

We expected the *ΔgdhA* mutant to be similarly attenuated relative to a *ΔpckA* mutant during growth in mice. Strikingly, when we assessed the requirement of *gdhA* for growth in our murine model of *F. tularensis* pulmonary infection, we found that the CFUs recovered from the lung, liver and spleen of *gdhA*-infected mice were greatly reduced compared to WT, and that the CFUs recovered from the liver and spleen of the mice were reduced approximately 3-fold relative to *ΔpckA* (Figure 4.6D). In addition to fueling

the gluconeogenic pathway, *ΔgdhA*-mediated anaplerosis of the TCA cycle may be essential during infection to supply other essential metabolic precursors (*e.g.* oxaloacetate and/or acetyl-CoA) or to generate reducing power via the use of malic enzyme. This conclusion is consistent with our observation that excess glucose supplementation during growth in J774A.1 or AICAR-treated BMDMs only partially rescued bacterial proliferation of this mutant.

Glycerol catabolism is required for *F. tularensis in vivo* growth

Since *ΔglpX* was more severely attenuated in mice relative to *ΔppdKpckA,* we reasoned that *F. tularensis* may assimilate additional carbon substrates besides those supplied through the gluconeogenic pathways catalyzed by Ppdk and PckA. In *F. tularensis, glpA* (glycerol-3P dehydrogenase) is predicted to be required for the catabolism of glycerol and glycerol-3P (G3P). We used the Targetron gene knockout system modified for use in *Francisella* to disrupt *glpA* in *F. tularensis* Schu S4[293]. Interestingly, we found that the generation of a *ΔglpA* mutant strain was only possible through the simultaneous introduction of a secondary mutation in *glpK* (Figure 4.7A). In *F. tularensis, glpK* is located upstream of *glpA,* and is predicted to encode a kinase responsible for the phosphorylation of glycerol forming G3P during glycerol catabolism (Figure 4.7A). The disruption of G3P dehydrogenase in the presence of a fully functional glycerol kinase can lead to increased concentration of intracellular G3P. In *E. coli,* excess G3P within the cell stimulates the synthesis of the toxic metabolite methylglyoxal[294]. We suspect a similar phenomenon may be responsible for the requirement of a secondary *glpK* mutation in a *F. tularensis ΔglpA* background.

We analyzed the growth properties of the *glpKA* disruption mutant in defined media supplemented with glucose, glycerol or G3P to confirm that *glpA* and *glpK* are required for growth on glycerol and G3P. As expected, the *glpKA* mutant grew to WT levels when cultured with glucose, but not glycerol or G3P (Figure 4.8A). In fact, supplying the *glpKA* mutant with G3P led to significantly lower levels of bacterial replication relative to growth on glycerol or just CDM, possibly due to the toxic buildup of intracellular G3P. We found that growth of the *glpKA* mutant was restored on glycerol and G3P only when these two genes were expressed with the downstream gene, *glpF,* despite the fact that sequencing of the surrounding genes in our *glpKA* mutant revealed no additional mutations in or around the coding sequence for *glpF. glpF* is predicted to encode a glycerol uptake facilitator and may be co-transcribed with glpA (Figure 4.7A). As expected, we observed WT levels of growth on G3P but not glycerol when *glpA* and *glpF*, but not *glpK,* were expressed *in trans* in the *glpKA* mutant (Figure 4.7B), and growth on both glycerol and G3P was restored when the *glpKA* mutant was complemented with *glpKAF in trans* (Figure 4.8A). These findings are summarized in Table 4.1.

The *glpKA* mutant replicated in J774A.1 cells to intermediate levels with or without supplemented glucose, indicating that this mutant can replicate within this cell line, but growth was not fully restored by the addition of excess glucose (Figure 4.5F). We found that the *glpKA* disruption mutant did not replicate within BMDMs (Figure 4.8B). Interestingly, growth within BMDMs was restored to WT levels upon *in trans* expression of *glpA* and *glpF* without *glpK,* suggesting that *F. tularensis* Schu S4 may assimilate G3P and not glycerol during intracellular growth (Figure 4.7C). Growth of the

mutant within BMDMs was similarly restored to WT levels upon complementation of *glpKAF* (Figure 4.8B). Finally, replication of the *glpKA* mutant was significantly increased within BMDMs cultured with AICAR and excess glucose, demonstrating that, similar to the *glpX* mutant, the *glpKA* disruption mutant could be rescued by supplying an alternative carbon source (Figure 4.8C).

We then assessed the importance of glycerol catabolism for *F. tularensis* during growth in mice, and found that the number of CFU recovered from the lungs of mice infected with the *glpKA* disruption mutant was similar to the original inoculum, and below the limit of detection in the livers and spleens of mice (Figure 4.8D). These data suggest that a *glpKA* mutant colonized, but did not proliferate or disseminate in a murine model of *F. tularensis* infection.

Data from our mutational analysis suggest that glycerol represents an essential host-derived source of carbon during *F. tularensis* intracellular growth. However, we could not exclude the alternative possibility that *F. tularensis* attenuation may be due to a toxic buildup of metabolites or disruption of proper metabolic regulatory mechanisms in our mutant strains. To delineate these possibilities we sought to reduce the concentration of available glycerol within BMDMs, and examine the impact on WT *F. tularensis* intracellular proliferation. A significant bulk of host glycerol stores are sequestered as triglycerides in host lipid droplets[295]. During lipolysis, a series of enzymatic reactions free glycerol from cellular triglyceride stores and release it into the cytosol of the host[295,296]. We hypothesized that *F. tularensis* may exploit this process to establish a source of glycerol during intracellular growth. Atglistatin is a selective inhibitor of adipose triglyceride lipase (ATGL), an enzyme responsible for the

first catalytic step of lipolysis[297]. When we infected Atglistatin-treated BMDMs with WT *F. tularensis* we observed that Atglistatin treatment significantly reduced *F. tularensis* intracellular burden in a dose-dependent manner (Figure 4.9A). Importantly, these concentrations were not cytotoxic to BMDMs (Figure 4.10A). To verify these findings, we used Cre-Lox recombination to generate ATGL deficient BMDMs. BMDMs derived from C57Bl6/J or ATGL-flox mice were treated with Cre recombinase gesicles during differentiation. Cre-treated BMDMs isolated from ATGL-flox mice demonstrated approximately 60% knockdown of ATGL expression based on qRT-PCR (Figure 4.10B). This was associated with a significant reduction in *F. tularensis* replication within ATGL knockdown BMDMs (Figure 4.9B). From these data we conclude that host lipolysis is important for sustaining *F. tularensis* growth, and that host-derived glycerol represents a primary source of carbon necessary for fueling *F. tularensis in vivo* replication.

DISCUSSION

Previous work by our group and others highlight the importance of amino acid metabolism for *F. tularensis* replication and virulence [282,298–300]. Furthermore, Brissac et al. recently demonstrated that gluconeogenesis is vital for *F. tularensis* subspecies *holarctica* LVS and *F. novicida* growth during periods of glucose limitation[287]. Here, we have similarly demonstrated that gluconeogenesis is essential for intracellular and *in vivo* growth for the highly virulent *F. tularensis* subspecies *tularensis* Schu S4, while *pfkA,* and thus glycolysis, is dispensable. Additionally, through systematic mutational analysis, we identified specific metabolic pathways essential for *F. tularensis* virulence. We found that *ΔglpX, ΔpckA, ΔgdhA* and *ΔglpA* mutant strains

were attenuated during growth in a mouse model of *F. tularensis* pulmonary infection, suggesting that these pathways may by critical for the efficient assimilation of host-derived carbon. These findings are summarized in Table 4.2.

The metabolic pathways required for *F. tularensis* growth varied based on the infection model. We found that *pckA* was important for growth in mice, while *ppdK* was essential for WT levels of growth within a J774A.1 transformed macrophage cell line. The differential requirements of these genes suggest that *F. tularensis* may utilize alternate gluconeogenic pathways for growth in different environments as the bacterium may preferentially assimilate different host-derived carbon sources, perhaps based on availability. As transformed macrophages undergo altered metabolism relative to primary cells, it is likely that the carbon sources available to *F. tularensis* are distinct within these models. For instance, J774A.1 metabolism is subject to the “Warburg effect” in which these cells significantly increase glucose uptake and aerobic glycolysis, leading to high intracellular concentrations of lactate[301]. *F. tularensis* may exploit this metabolic aberrance and primarily assimilate lactate during replication within these cells. As *ppdK* is required for *F. tularensis* assimilation of lactate (Figure 4.1) this may explain the requirement of *ppdK* specifically in J774A.1 cells.

We found that *ppdk,* and not *pckA,* is essential for growth on glutamate in defined media. *F. tularensis* possesses an additional gluconeogenic enzyme (MaeA, malate dehydrogenase) responsible for the synthesis of pyruvate from malate, which can then be converted to PEP through PpdK (Figure 4.1). Previous work has suggested little or no utilization of the oxidative branch of the pentose phosphate pathway during *F. tularensis* growth[287]. Bypassing the oxidative branch of the pentose phosphate

pathway means that *F. tularensis* must use an alternative mechanism for the generation of the essential cofactor, NADPH. It is possible that the bacterium relies on an $NADP^+$-dependent malic enzyme for the production of NADPH during growth on glutamate defined medium. As the conversion of TCA intermediates to PEP through malic enzyme bypasses PckA but requires PpdK, this would provide a possible explanation for why *ppdK* and not *pckA* is the preferred gluconeogenic pathway during growth on glutamate.

We were surprised to find that a *ΔgdhA* mutant demonstrated significantly reduced growth within a mouse compared to a *ΔppdKpckA* double mutant. If *gdhA* is required solely for gluconeogenic purposes we would expect that these two mutants would be similarly attenuated, as a *ΔppdKpckA* double mutant theoretically halts the gluconeogenic conversion of TCA cycle intermediates to glucose. However, during replication within a mouse, *gdhA* may be additionally required for anaplerosis of the TCA cycle or glutamate biosynthesis. Further, it was recently demonstrated that glutamate import plays a critical role in oxidative stress defense and phagosomal escape during *F. tularensis* infection[299]. Thus, the attenuation of this mutant may be in part due to its inability to withstand oxidative stress within the phagosome to reach the host cell cytosol. However, because growth of *ΔgdhA* can be partially rescued by supplying J774A.1 cells (Figure 4.5E) or AICAR-treated BMDMs (Figure 4.6C) with excess glucose we conclude that this pathway is primarily involved in carbon acquisition during *F. tularensis* intracellular growth.

Unlike *ppdk* and *pckA,* we found that a *glpKA* mutant was attenuated for growth in all models tested, highlighting the importance of glycerol catabolism for *F. tularensis* pathogenesis. Based on the annotated genomic sequence of *F. tularensis* subspecies

tularensis Schu S4, a *ΔglpA* mutant strain cannot assimilate glycerol or G3P[302]. During our investigation we found that disrupting *glpA* in *F. tularensis* Schu S4 resulted in an independent polar mutation in *glpK* that prevented growth on glycerol. As expected, genetic complementation of our *glpA* mutant strain with *glpA,* but not *glpK*, rescued growth on G3P, but not glycerol (Figure 4.7C). However, our partially complemented strain replicated to WT levels within BMDMs, suggesting that within this cell type G3P and not glycerol is available for *F. tularensis* metabolism. This conclusion is consistent with the fact that glycerol is actively phosphorylated by the host to prevent its efflux from the cell. Of note, unlike *F. tularensis* subspecies *tularensis* and *F. novicida, F. tularensis* subspecies *holarctica* can only metabolize G3P and not glycerol. As *F. tularensis* possesses a small decaying genome adapted to an intracellular lifestyle, this may reflect an interesting evolutionary example supporting our prediction that *F. tularensis* specifically metabolizes G3P within the cell[183].

Despite occupying similar niches, intracellular bacterial pathogens have evolved distinct methods to meet their respective nutritional requirements. Many pathogens such as *Salmonella enterica, Legionella pneumophila* and enteroinvasive *Escherichia coli* species preferentially assimilate glucose during intracellular growth[277,303,304]. In contrast, *Shigella flexneri* downregulates genes involved in glucose catabolism and favors the assimilation of C_3 substrates during growth within the cytosol[305]. *Listeria monocytogenes* relies on two major carbon substrates (glycerol and glucose 6-phosphate) to fuel distinct catabolic and anabolic pathways during cytosolic replication[306]. Our data suggest that the primary carbon substrates utilized by *F. tularensis* during intracellular growth varies depending on the model of infection. This is

not surprising, considering that the host range of *F. tularensis* subspecies *tularensis* Schu S4 includes over 250 species, and that within these hosts *F. tularensis* infects numerous cell types including macrophages, dendritic, endothelial and epithelial cells[307]. In order to replicate within such a diverse range of hosts *F. tularensis* must adapt its metabolism to the carbon sources available from the environment, which can vary significantly from host to host, and between cell types. Thus, we suspect that the extraordinary ability of *F. tularensis* to proliferate within such a wide range of hosts is in part due to the pathogen's capability of sensing and adapting to the fluctuating availability of nutrients over the course of its infectious lifestyle.

When available, *F. tularensis* will consume glucose. The intracellular growth defect of the *ΔglpX* mutant in J774A.1 cells was rescued by supplying excess glucose (Figure 4.3B). Further, *F. tularensis* subspecies *holarctica* LVS replication within J774A.1 and THP-1 macrophage cells leads to a significant reduction in host intracellular glucose[287]. However, the nutrient concentrations within these established cell lines do not reflect the physiological conditions encountered by *F. tularensis* during infection, and it is likely that in physiological conditions glucose limitation forces *F. tularensis* to utilize non-glucose carbon substrates. Indeed, a transcriptomic analysis of the *F. tularensis* metabolic network during extracellular and intracellular growth suggests that significant changes in carbohydrate metabolism occur when the pathogen transitions to an intracellular lifestyle[308]. Our data support the proposed model that in the absence of glucose, *F. tularensis* will primarily utilize alternate carbon sources such as amino acids or C_3 substrates derived from the host.

Bacterial metabolic pathways must be coordinated to reduce unnecessary energy expenditure and maximize fitness. In *E. coli,* key branch points in the glycolytic pathway are controlled by feed-forward/feedback inhibition. For instance, the conversion of fructose-6P to fructose-1,6-BP by PfkA is stimulated by ADP and inhibited by the downstream metabolite PEP[309]. Conversely, the reverse reaction (catalyzed by fructose 1,6-bisphosphatase) is inhibited by AMP and glucose-6P[310]. Carbon catabolite repression is poorly understood in *F. tularensis,* however, instances of catabolite repression have been described in other γ-proteobacteria including *Pseudomonas aeruginosa* and *S.* Typhimurium[311]. Therefore it is likely that *F. tularensis* also employs regulatory mechanisms to inhibit the utilization of alternative carbon substrates in the presence of a preferred carbon source such as glucose. We observed significant growth attenuation for a *pfkA* mutant in CDM supplemented with glucose relative to CDM alone or CDM with glutamate. Similar to *E. coli*, the buildup of glucose-6P may allosterically inhibit the activity of GlpX and prevent growth on gluconeogenic carbon sources such as glutamate or other amino acids that are present at low concentrations in the media.

Central carbon metabolism represents arguably the single most important cellular process in the context of bacterial viability and virulence. Energy generation, precursor biosynthesis, virulence factor expression, cell division, etc. are all contingent on a bacterium's ability to acquire and utilize sufficient carbon to fuel these processes. Targeting bacterial catabolic and anabolic pathways is a promising strategy for combating pathogenic organisms such as *F. tularensis.* Indeed, it is well established that *F. tularensis* purine auxotrophs are attenuated during infection, and these mutants

have been suggested as potential candidates for use as a live vaccine[163,164]. Similarly, targeting other essential metabolic pathways such as gluconeogenesis, glycerol catabolism or amino acid catabolism, either through drug or vaccine development, may constitute a means for limiting the spread of this deadly pathogen. Overall, by identifying the specific metabolic pathways and nutrients utilized by *F. tularensis* during intracellular growth our findings begin to unravel the complex host-pathogen relationship exploited by *F. tularensis* during infection and furthers our understanding of *F. tularensis* pathogenicity.

MATERIALS AND METHODS

Bacterial Strains

Francisella tularensis subspecies *tularensis* Schu S4 was obtained from BEI Resources. *F. tularensis* was maintained on solid chocolate agar medium supplemented with 1% IsoVitaleX (Becton-Dickson); modified Mueller-Hinton (MMH) agar supplemented with 1% tryptone, 0.5% NaCl, 0.05% L-cysteine freebase, 1% glucose and 0.00025% Fe pyrophosphate; brain heart infusion (BHI) broth supplemented with 1% IsoVitaleX; Chamerlains Defined Media (CDM); or modified CDM[288]. For selection, each growth medium was supplemented with 10μg/ml kanamycin or 200 μg/ml hygromycin when applicable. All cloning was performed in *Escherichia coli* DH5α and S17-1λpir strains propagated in Luria-Bertani (LB) broth or solid agar supplemented with 50μg/ml kanamycin or 200μg/ml hygromycin when necessary for selection. All cultures were grown at 37°C with aeration.

Cell Culture

J774A.1 (ATCC TIB-67) macrophage-like cells were maintained in Dulbecco's modified Eagle medium (DMEM) supplemented with 4.5 g/liter glucose, 10% fetal bovine serum, 2mM L-glutamine, and 1mM sodium pyruvate. Bone marrow derived macrophages (BMDMs) were generated from C57BL6 mice (Jackson Labs) by flushing bone marrow cells from murine femurs and incubating the recovered cells for 6 days in L929 cell-conditioned DMEM containing 10% fetal bovine serum. Prior to use, non-adherent cells were removed by washing BMDMs with phosphate-buffered saline (PBS), and cells were recovered from untreated plates using 10mM EDTA in PBS. For experiments, BMDMs were maintained in high glucose (4.5g/L) DMEM supplemented with 2mM L-glutamine and 10% fetal bovine serum.

Generating ATGL-Deficient BMDMs

Bone marrow from 8-14 week old C57Bl/6J or ATGL-flox (B6N.129S-Pnpla2^{tm1Eek}/J, Jackson Labs Stock No. 24278) were generated as described above. 5 days after the bone marrow is cultured, 20 ul of Cre Recombinase Gesicles (Takara) were added directly to the culture media on the developing cells. Approximately 36 hours later, the cells were harvested and incubated overnight in tissue culture dishes for experiments. Almost all BMDMs took up detectable levels of the Cre Recombinase Gesicles (data not shown). For the different replicate experiments, the effectiveness of this process on ATGL RNA in the ATGL-flox mice treated with gesicles was 46.7%, 21.5%, and 33.9% of C57Bl/6 mice not exposed to gesicles.

qRT-PCR

BMDMs were seeded at 250,000 cells the night before infection. Immediately prior to infection, Trizol (Life Technologies) was added to a subset of wells. The samples were treated with choloform and centrifuged. The top fraction was mixed with 70% ethanol and RNA was isolated using a RNEasy kit (Qiagen). Samples were then treated with DNase (ThermoFisher). The samples were analyzed using a Sensifast, One-Step PMaster mix kit (Bioline) following the manufacturer's suggested ratio. The primers were based on experiments by Ogasawara *et al.* and verified for use in mice[312]. Briefly, The conditions for the PCR were: 10 min at 45 °C for reverse transcription, 2 min at 95 °C for polymerase activation, 35 cycles with a 95°C denature (10 sec), 55°C anneal (10 sec) and 72°C extension (30 sec). Wells that did not receive template or reverse transcriptase had no amplification in any replicate for any experiment. ATGL: 5′-AGTTCAACCTTCGCAATCTC-3′(sense), 5′-GTCACCCAATTTCCTCTTGG -3′(antisense). B-actin: 5′-ACCTGACAGACTACCTCATG-3′ (sense), 5-ACTCATCGTACTCCTGCTTG-3′ (antisense).

Plasmid Vectors and Bacterial Genetics

Markerless, in-frame deletions were generated through allelic exchange as described for all *F. tularensis* deletion strains except for *glpA*[313]. For allelic exchange, all suicide vectors were constructed from pEDL50, a modified version of the suicide vector pMP812 (Kan^r, *sacB)* containing an origin of transfer for mating into *F. tularensis*[314]. The pEDL50 suicide vector was mated into *F. tularensis* Schu S4 via *E. coli* S17-1λpir by mixing the bacteria on LB agar overnight, then selecting for primary integrants on

chocolate agar with kanamycin (10μg/mL) and polymyxin B (200μg/mL). Kan^r, PMB^r resistant strains were grown overnight in BHI broth without selection to allow for recombination, then plated on chocolate agar containing 10% sucrose for counterselection (loss of plasmid). Deletion strains were confirmed through PCR and sequencing (Genewiz). The *glpA* gene was disrupted using the Targetron system modified for use in *Francisella* species. The Targetron suicide vector was created using primers assigned by the Targetron Primer design program (Sigma). The vector was transformed into *F. tularensis* Schu S4 and the mutant was isolated as described[293]. For complementation of deletion strains, selected genes and their predicted promoters were PCR amplified and ligated into pJB3, a luminescent reporter plasmid derived from the low-copy shuttle, pMP831 that constitutively expresses the *Photorhabdus luminescens luxCDABE* operon from pXB173[283]. Genes lacking an obvious native promoter were cloned into pJB2, a modified version of pJB3 that contains a *pblaB* promoter sequence driving expression of the targeted gene. Suicide and complementation vectors were transformed into *E.coli* S17-1λpir and *F. tularensis,* respectively*. E.coli* S17- λpir was transformed through heat shock. For *F. tularensis* transformation, Schu S4 was grown overnight in CDM, washed 4 times with 0.5M sucrose and electroporated in a 1mm gap cuvette at 2kV, 25μF, and 200Ω. The transformants were allowed to recover for 2 hours in BHI broth at 37°C, then plated on chocolate or MMH agar with appropriate selection.

Growth Curves

Overnight cultures of *F. tularensis* SchuS4 grown in CDM were diluted to an OD_{600} of 0.05 in 200µl of CDM or modified CDM in a 96-well plate (Corning). All CDM was buffered with 50mM MES at pH 6.2 to account for ammonia production during amino acid catabolism in experiments where modified CDM contained amino acids as the primary carbon source. Each major carbon source was added to a final concentration of 0.4%. Cultures were incubated in an Infinite 200M Pro series TECAN plate reader (TECAN) at 37°C with orbital shaking. The OD_{600} was measured every 15 minutes for 48 hours.

Macrophage Infections

Bacterial intracellular growth within J774A.1 or BMDM cells was determined by measuring the luminescence of Schu S4 harboring the luminescence reporter plasmid pJB2 or pJB3 described above. J774A.1 and BMDM cells were plated at $5x10^4$ cells per well in a 96-well white wall, white bottom polystyrene plate (Corning) the night before infection. Each well was inoculated at a multiplicity of infection (MOI) of 100. Following a two-hour infection period, the inoculation medium was removed and replaced with 200µl of media containing 25µg/ml (J774A.1) or 10µg/ml (BMDMs) gentamicin. Luminescence was measured every 15 minutes for 48 hours using an Infinite 200M Pro series TECAN plate reader (TECAN) maintaining constant 37°C temperature and 5% CO_2. To enumerate intracellular bacteria by plating, BMDM tissue culture medium was removed 2 hours post-gentamicin treatment and cells were washed once with PBS before being scraped up, vortexed hard for 1 minute, diluted and plated on chocolate agar. When

applicable, J774A.1 and BMDM cells were cultured in glucose-free, pyruvate-free DMEM (Gibco) supplemented with 10% dialyzed FBS. For the AICAR and Atglistatin experiments, BMDMs were pretreated 2 hours prior to infection with 150μM AICAR (Cayman Chemical), or Atglistain (Cayman Chemical), and this drug concentration was maintained throughout the infection. Atglistatin cytotoxicity was measured using a Vybrant MTT Cell Proliferation Assay Kit (ThermoFisher) following the manufacturer's protocol.

Mouse Infections

Groups of 6-8 week old female C57BL6 mice (Jackson Labs) were inoculated intranasally with 100 CFU of *F. tularensis* Schu S4 wild-type or mutant strains. Infected and control mice were housed in a recirculating air Techniplast system (Techniplast) within a BSL-3 facility. At 3 days post infection, mice were sacrificed and the lungs, livers and spleens were harvested and homogenized using a Biojector (Bioject). The homogenates were serially diluted and plated onto chocolate or MMH agar to quantify organ burdens.

FIGURES

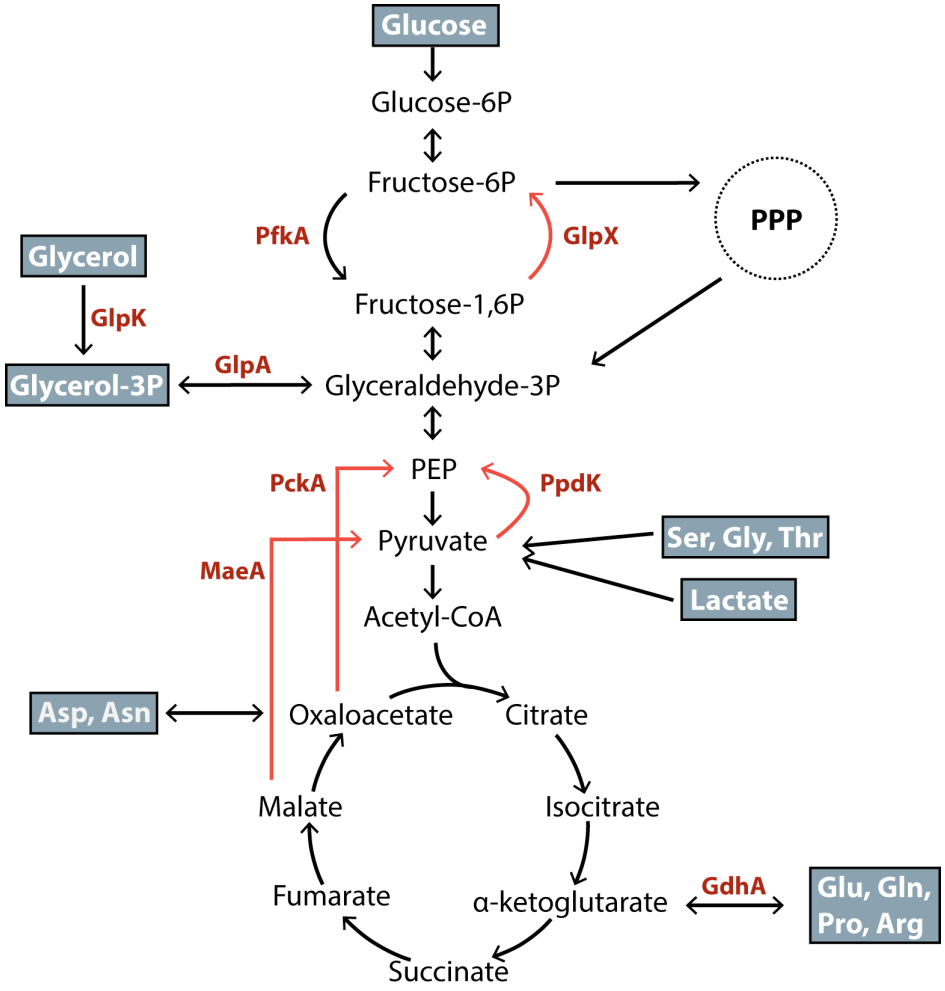

Figure 4.1. An overview of *Francisella tularensis* subsp. *tularensis* Schu S4 central carbon metabolism. Labeled enzymes (red) are predicted to be required for the flux of specific carbon substrates (blue) for *F. tularensis* central carbon metabolism. Orange arrows indicate reactions that are specific to gluconeogenesis. Abbreviations: PPP, pentose phosphate pathway; PEP, phosphoenolpyruvate; Acetyl-CoA, acetyl coenzyme A; PfkA, phosphofructokinase (FTT_0801); GlpX, fructose 1,6-bisphosphatase (FTT_1631); GlpK, glycerol kinase (FTT_0130); GlpA, glycerol 3-phosphate dehydrogenase (FTT_0132); PckA, phosphoenolpyruvate carboxykinase (FTT_0449); PpdK, pyruvate phosphate dikinase (FTT_0250); MaeA, malic enzyme (FTT_0917); GdhA, glutamate dehydrogenase (FTT_0380).

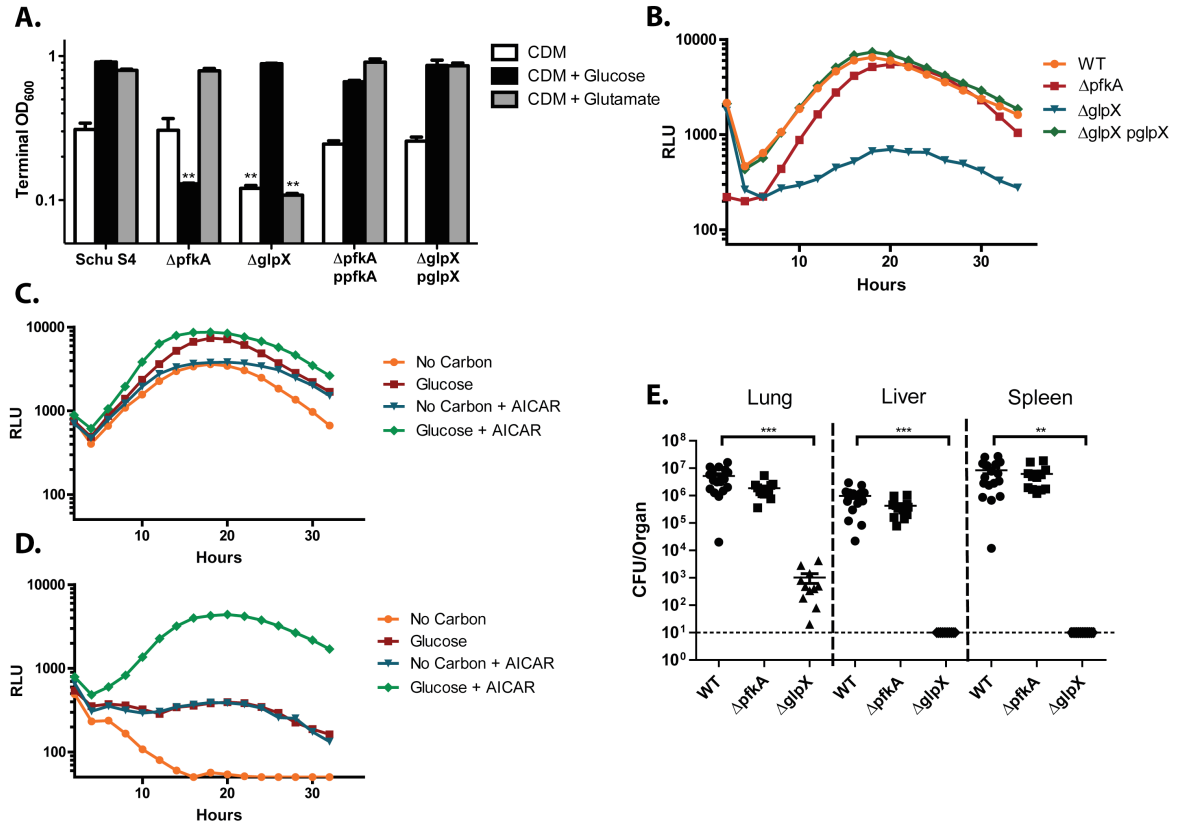

Figure 4.2. *F. tularensis* GlpX is essential for replication on gluconeogenic carbon substrates, within host macrophages, and in a murine model of infection. (A) Terminal OD_{600} of WT Schu S4, *ΔpfkA,* and *ΔglpX* strains after 48 hours of growth in CDM and CDM supplemented with glucose or glutamate at a final concentration of 0.4%. **(B)** Intracellular replication of WT Schu S4, *ΔpfkA, ΔglpX,* and *ΔglpX* p*glpX* in BMDMs as indicated via relative luminescent units (RLU) measured every 15 minutes over a 36-hour period. **(C)** Growth of WT Schu S4, and **(D)** *ΔglpX* in BMDMs cultured with or without 150μM AICAR and/or glucose at a concentration of 4.5g/L. Growth was measured via luminescence read every 15 minutes over 36 hours. All growth curves represent one of three independent experiments and each data point represents the average of three technical triplicates. **(E)** Organ burdens of mice three days post intranasal inoculation with WT Schu S4, and *ΔpfkA,* and *ΔglpX*. Data are pooled from three independent experiments. (**p<0.01, ***p<0.001 as determined by Student's t-test).

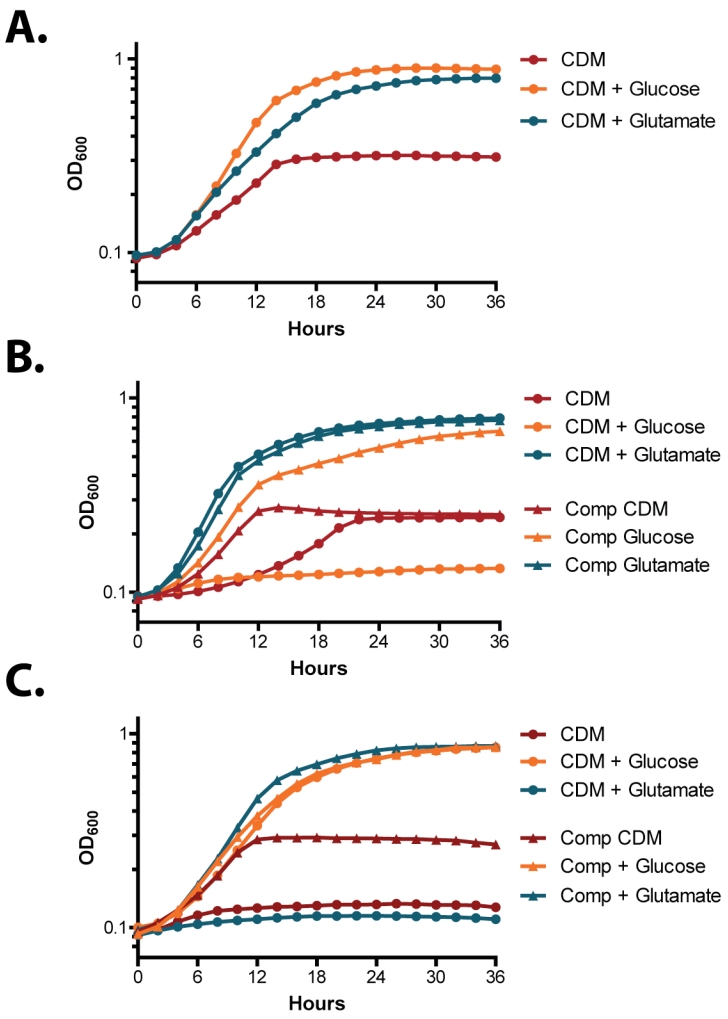

Figure 4.3. Growth kinetics of *F. tularensis ΔpfkA* and *ΔglpX* mutants during growth in CDM, CDM + glucose and CDM + glutamate. (A) WT Schu S4; **(B)** *ΔpfkA, ΔpfkA* p*pfkA*; and **(C)** *ΔglpX, ΔglpX* p*glpX* strains were grown in CDM and CDM supplemented with glucose or glutamate at a final concentration of 0.4%. The OD_{600} was measured every 15 minutes over a 36-hour period. All growth curves represent one of three independent experiments and each data point represents the average of three technical triplicates.

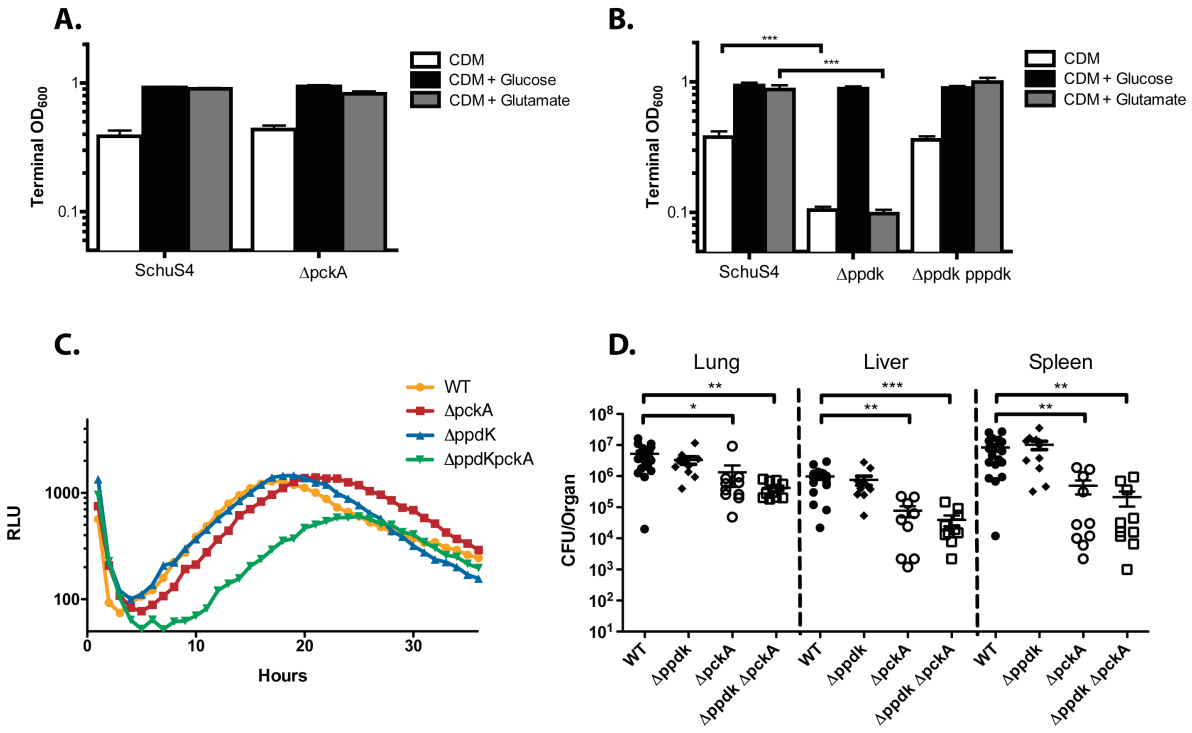

Figure 4.4. Growth of *ΔpckA* and *ΔppdK* in defined media, host cells and in a murine model of infection. Terminal OD_{600} of **(A)** *ΔpckA* and **(B)** *ΔppdK* and *ΔppdK* p*ppdK* after 48 hours of growth in CDM and CDM supplemented with glucose or glutamate at a final concentration of 0.4%. Data are pooled from three triplicate wells from three independent experiments (mean +/- SD). **(C)** The intracellular growth kinetics of *ΔpckA, ΔppdK* and *ΔppdKpckA* cultured in high glucose (4.5g/L) DMEM as indicated via RLU measured every 15 minutes over a 36-hour period. The data shown represent three independent experiments and each data point represents the average of three technical replicates. **(D)** Organ burdens of mice three days post intranasal inoculation with WT Schu S4, *ΔppdK, ΔpckA,* or *ΔppdKpckA* mutants. Data are pooled from three independent experiments (*p<0.05, **p<0.01, ***p<0.001 as determined by Student's t-test).

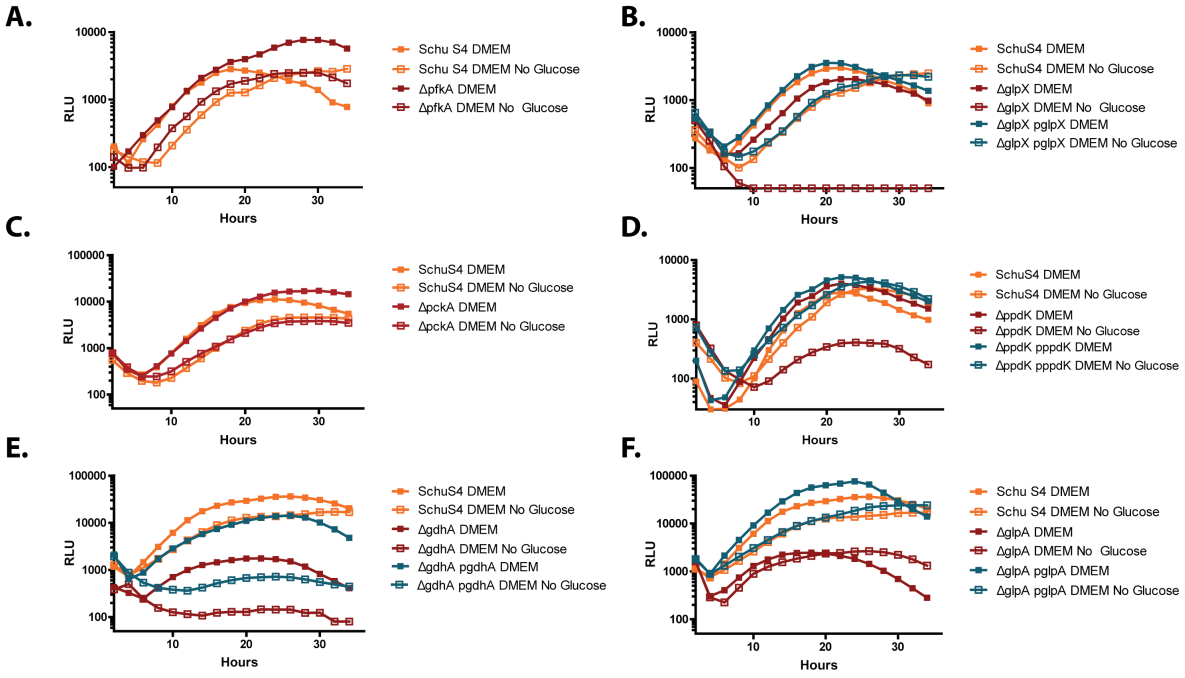

Figure 4.5. Intracellular growth characteristics of *F. tularensis* Schu S4 and mutant strains in J774A.1 macrophage cells. Representative intracellular bacterial growth kinetics of **(A)** *ΔpfkA*; **(B)** *ΔglpX*, *ΔglpX* p*glpX*; **(C)** *ΔpckA;* **(D)** *ΔppdK*, *Δppdk* p*ppdK*; **(E)** *ΔgdhA, ΔgdhA* p*gdhA*; and **(F)** *ΔglpKA, ΔglpKA* p*glpAF* deletion strains carrying a LUX reporter for intracellular growth within J774A.1 macrophage cells cultured with and without glucose. Luminescence was measured every 15 minutes over a 36-hour period and each point represents the average of three technical replicates. Each panel is a representative of at least 2 independent experiments.

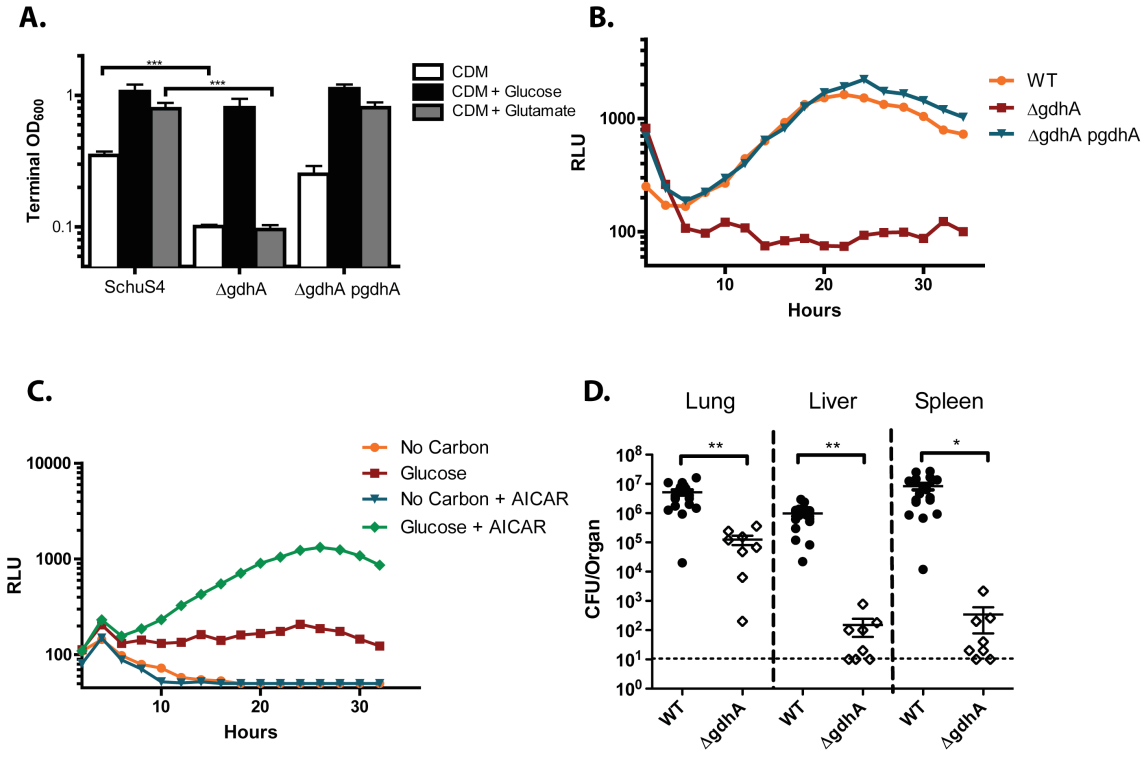

Figure 4.6. GdhA fuels gluconeogenesis by shuttling carbon into the TCA cycle. **(A)** Terminal OD_{600} of *ΔgdhA* after 48 hours of growth in CDM and CDM supplemented with glucose or glutamate at a final concentration of 0.4%. Data are pooled from three triplicate wells from three independent experiments (mean +/- SD). **(B)** The intracellular growth kinetics of WT Schu S4, *ΔgdhA* and *ΔgdhA* p*gdhA* within BMDMs as indicated via RLU measured every 15 minutes over a 36-hour period. **(C)** *ΔgdhA* strains expressing the LUX reporter of intracellular growth in BMDMs cultured with or without 150μM AICAR and/or glucose at a concentration of 4.5g/L. All growth curves represent one of three independent experiments and each data point represents the average of three technical triplicates. **(D)** Organ burdens of mice three days post intranasal inoculation with WT Schu S4, or the *ΔgdhA* mutant. Data are pooled from three independent experiments (*p<0.05, **p<0.01, ***p<0.001 as determined by Student's t-test).

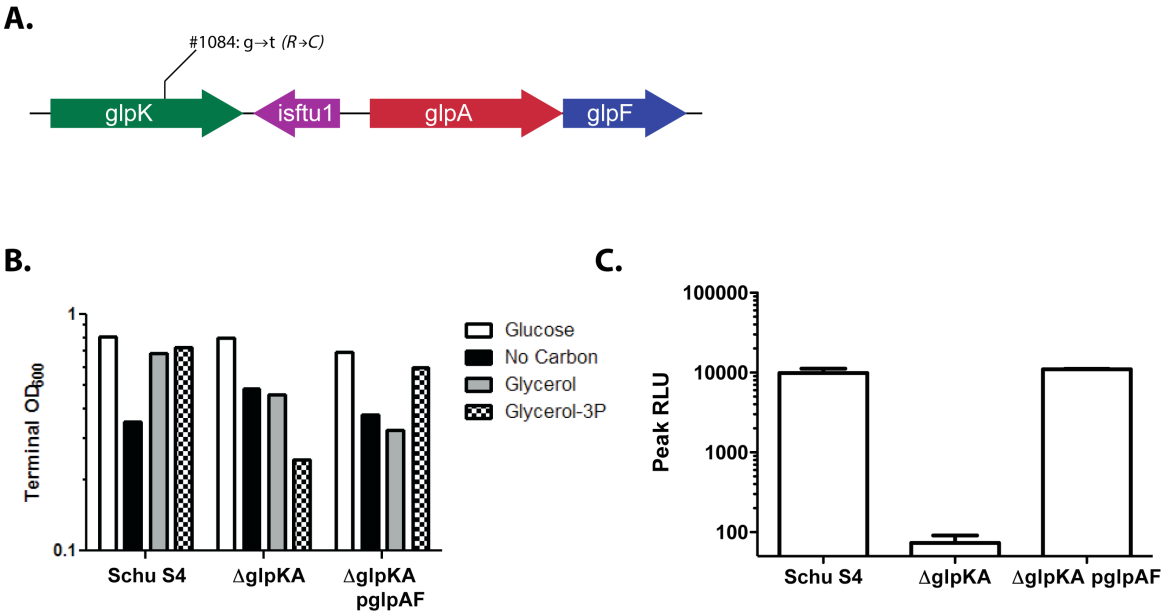

Figure 4.7. GlpA, but not GlpK, is required for growth on glycerol-3P and in BMDMs. (A) Schematic representing the coding regions for *glpK, glpA* and *glpF* including the location of the missense substitution mutation (resulting in an arginine to cysteine substitution) introduced at position #1084 in glpK during the generation of the *glpA* insertion mutant. *(glpK*- glycerol kinase, *isftu1*- insertion sequence element, *glpA*- glycerol-3P dehydrogenase, *glpF*- glycerol uptake facilitator). **(B)** Terminal OD_{600} of WT Schu S4, the *glpKA* insertion mutant, and corresponding p*glpAF* complemented strain grown in CDM and CDM supplemented with glucose, glycerol or G3P after 48 hours of growth. **(C)** Terminal RLU values for BMDMs infected with WT Schu S4, *ΔglpKA, or ΔglpKA* p*glpAF* strains harboring a LUX reporter for intracellular growth. The panel is representative of two independent experiments and data shown are averages of from three triplicate wells (mean +/- SD). Data are pooled from three triplicate wells from three independent experiments (mean +/- SD).

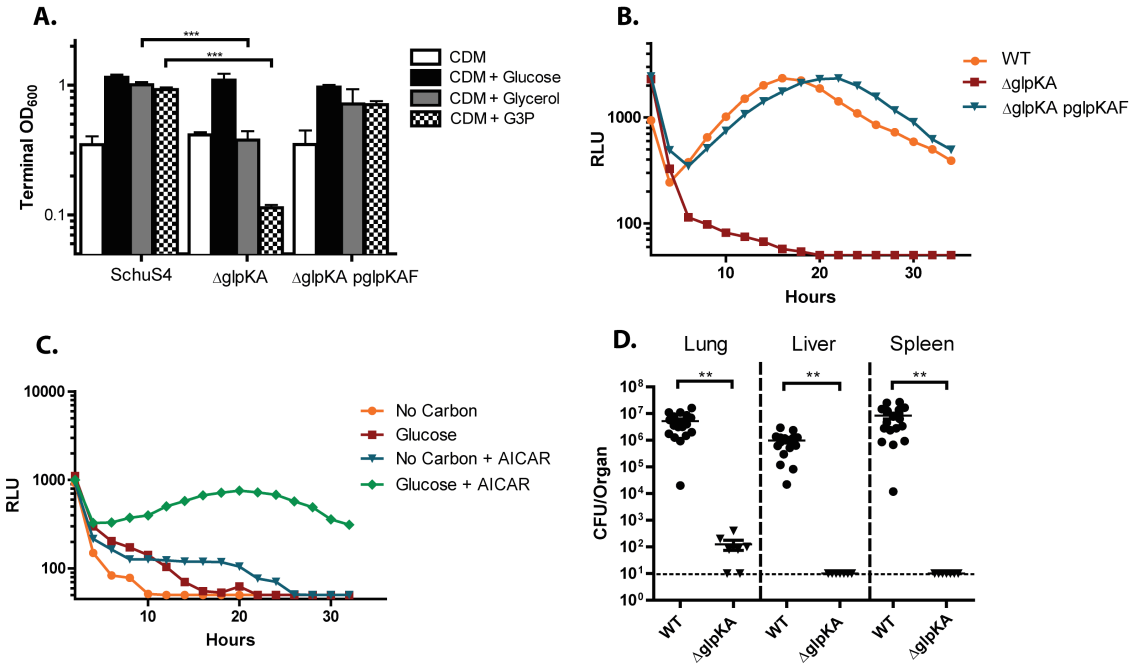

Figure 4.8. Glycerol metabolism is essential for *F. tularensis* intracellular replication. (A) Terminal OD_{600} of WT Schu S4, the *glpKA* insertion mutant, and corresponding p*glpKAF* complemented strain grown in CDM and CDM supplemented with glucose, glycerol or G3P after 48 hours of growth. Data are pooled from three triplicate wells from three independent experiments (mean +/- SD). **(B)** Growth curve of WT Schu S4, the *glpKA* mutant and the *glpKAF* complemented strain harboring the LUX reporter within BMDMs. Intracellular bacterial growth was measured via luminescence (RLU), read every 15 minutes over a 36-hour period. **(C)** Growth of *ΔglpA* expressing the LUX reporter of intracellular growth in BMDMs cultured with or without 150μM AICAR and/or glucose at a concentration of 4.5g/L. All growth curves represent one of three independent experiments and each data point represents the average of three technical triplicates. **(D)** Organ burdens of mice three days post intranasal inoculation with WT Schu S4, and the *glpKA* insertional mutant. Data are pooled from three independent experiments (*p<0.05, **p<0.01, ***p<0.001 as determined by Student's t-test).

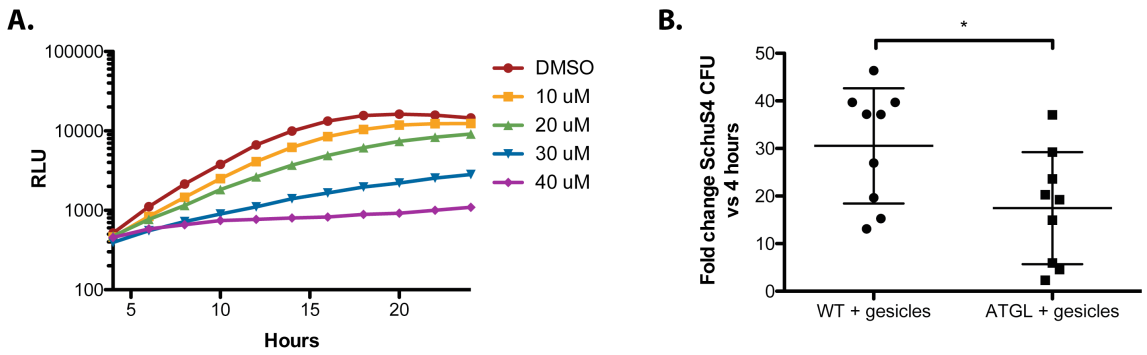

Figure 4.9. Active host cell lipolysis is required for efficient *F. tularensis* intracellular replication. (A) Growth curve of WT Schu S4 harboring a LUX reporter within BMDMs cultured in high glucose (4.5g/L) DMEM with our without Atglistatin at indicated concentrations. Intracellular bacterial growth was measured via luminescence (RLU), read every 15 minutes over a 24-hour period. Data represent the mean pooled from 3 replicates in 3 independent experiments. **(B)** Fold change in WT Schu S4 burden between 24 and 4 hours post-infection of WT and ATGL knockdown BMDMs. Data are pooled from three independent experiments (*p<0.05, **p<0.01, ***p<0.001 as determined by Student's t-test).

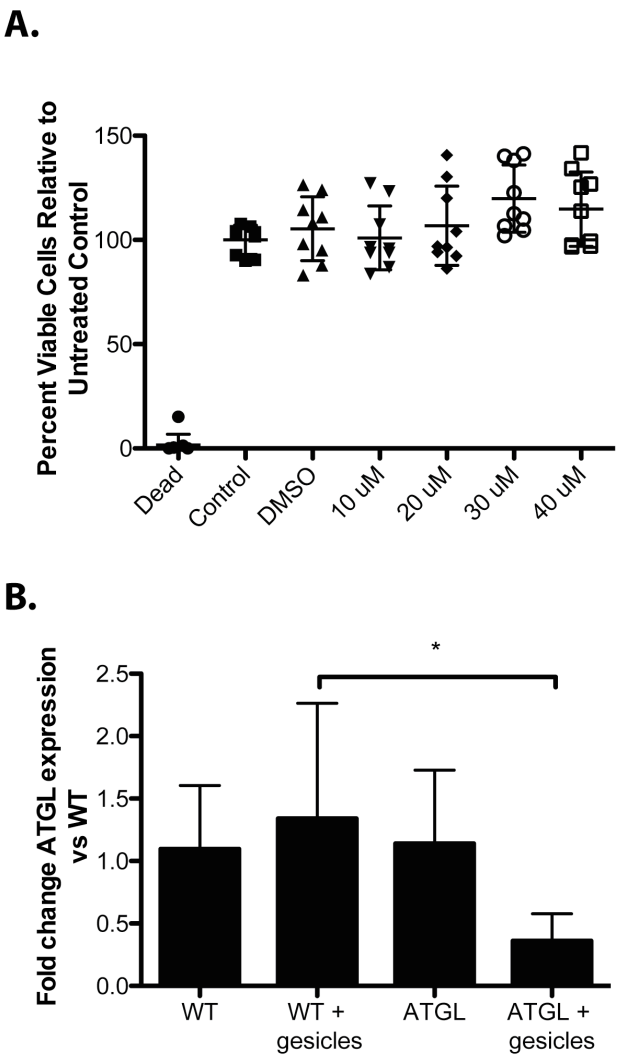

Figure 4.10. ATGL inhibition reduces *F. tularensis* growth within BMDMs without cytotoxicity. (A) BMDMs were treated with various concentrations of Atglistatin or vehicle control and allowed to incubate for 36 hours before BMDM cytotoxicity was measured using a Vybrant MTT Assay. Data are pooled from three triplicate wells from three independent experiments (mean +/- SD). **(B).** qRT-PCR quantification of ATGL expression in WT or ATGL knockdown BMDMs in the presence or absence of Cre recombinase-containing gesicles. Data are represented as fold change relative to wild type. Data are pooled from three triplicate wells from three independent experiments (mean +/- SD) (*$p<0.01$ by Student's t test).

Table 4.1 Growth of Schu S4 and *glpKA* strains in broth, BMDMs or J774A.1 cells

	CDM	CDM + Glucose	CDM + Glycerol	CDM + G3P	BMDM	J774A.1
WT	+	++	++	++	++	++
ΔglpKA	+	++	-	-	-	+
ΔglpKA p*glpAF*	+	++	-	++	++	+
ΔglpKA p*glpKAF*	+	++	++	++	++	+

Table 4.2. Summary table of Schu S4 WT and mutant strain growth in described infection models

	CDM	CDM + Glucose	CDM + Glutamate	CDM + Glycerol-3P	BMDM	J774A.1	C57 BL6/J
WT	+	++	++	++	++	++	++
ΔpfkA	+	-	++	*n/a*	++	++	++
ΔglpX	-	++	-	*n/a*	-	-	-
ΔpckA	+	++	++	*n/a*	++	++	+
ΔppdK	-	++	-	*n/a*	++	+	++
ΔgdhA	-	++	-	*n/a*	-	-	+
ΔglpKA	+	++	*n/a*	-	-	+	-

CHAPTER 5
SUMMARY OF RESULTS AND DISCUSSION

Antibiotic treatment failure is a complex, multifaceted issue that imposes a heavy burden on global public health. Conventional views surmise that bacterial resistance alone can explain treatment failure, and that developing new broad-spectrum therapeutics will prevent the spread of deadly pathogenic strains. Economically, however, the risk associated with antibiotic development is high, and profitability low. Consequently, the number of new antibiotics reaching market has plummeted while the number of reported cases of infection by resistant pathogens continues to increase exponentially[1,2,315]. Unlike drugs for chronic illnesses (e.g. diabetes, heart disease), antibiotic regimens are relatively short (typically days to weeks), often curative, and overuse of the drug renders it useless. New therapeutics also face steep hurdles prior to FDA approval and commercialization that require a significant investment of time and money[316]. Together, these factors have led to a steep decline in new antibiotic development.

To prevent the coming antibiotic ‘apocalypse’ prophesized by clinicians and researchers alike, we must look to alternative means for eradicating difficult-to-treat bacterial populations within the host before these populations develop resistance mechanisms that render our current arsenal useless. First and foremost, we must understand how and why our treatments fail to resolve chronic and relapsing bacterial

infection in the absence of genetically heritable resistance mechanisms. Second, we must develop new therapeutics that exploit the molecular mechanisms underlying antibiotic tolerance in order to resensitize tolerant populations to antibiotic killing. Finally, we must develop specialized approaches for resolving infections by bacterial populations that are innately recalcitrant to broad-spectrum antibiotic action due to the niche they occupy within the host. The aim of this thesis was to identify factors present in the complex infection environment that alter antibiotic efficacy in order to overcome and exploit relevant mechanisms of antibiotic antagonism and potentiation, respectively.

SUMMARY- CHAPTER 2: INTERSPECIES INTERACTION DURING POLYMICROBIAL INFECTION ALTERS *S. AUREUS* PHYSIOLOGY AND SUSCEPTIBILITY TO ANTIBIOTICS.

Within complex polymicrobial communities, inter- and intra- species interactions can influence the pathogenicity and antibiotic susceptibility of individual organisms. *Staphylococcus aureus* is commonly co-isolated with the opportunistic pathogen *Pseudomonas aeruginosa*, and these co-infections are generally more virulent and/or more difficult to treat than infections caused by either pathogen alone[220,317,318]. The interaction between *S. aureus* and *P. aeruginosa* is complex, with *P. aeruginosa* producing a number of molecules that interfere with *S. aureus* growth, metabolism, and cellular homeostasis including HQNO, rhamnolipids, and the endopeptidase LasA[197,198,200]. In Chapter 2 we investigated the impact of *P. aeruginosa/S. aureus* interaction on *S. aureus* antibiotic susceptibility. We observed that the bactericidal activities of three major classes of antibiotics were altered by the presence of *P. aeruginosa* secreted exoproducts and aimed to determine the mechanism(s) by which

P. aeruginosa alters *S. aureus* antibiotic susceptibility.

Adaptation to the CF lung during chronic infection promotes significant heterogeneity in virulence factor production among clinical *P. aeruginosa* isolates[319,320]. Consequently, *P. aeruginosa* production of HQNO, rhamnolipids and LasA varies drastically among isolates, with some isolates overproducing these factors and some isolates producing none at all[84,224]. Production of HQNO by *P. aeruginosa* isolates correlated perfectly with protection from ciprofloxacin killing. Through mutational analysis and exogenous addition of clinically relevant concentrations of HQNO, we demonstrated that HQNO induces a multidrug-tolerant state in *S. aureus* by inhibiting respiration and depleting intracellular ATP levels. We then demonstrated that subinhibitory concentrations of *P. aeruginosa* rhamnolipids potentiated tobramycin killing of *S. aureus* by destabilizing the membrane to induce tobramycin influx, and that this combinational therapy facilitated the rapid eradication of *S. aureus* persisters. Furthermore, *P. aeruginosa* isolates that were strong producers of rhamnolipids significantly potentiated tobramycin killing of *S. aureus*, thus demonstrating that the presence of *P. aeruginosa* can positively and negatively influence *S. aureus* tobramycin susceptibility via the differential production of rhamnolipids and HQNO, respectively.

Finally, we observed that *P. aeruginosa* supernatant from many of our isolates significantly potentiated vancomycin killing of *S. aureus.* The *P. aeruginosa* secreted endopeptidase, LasA, cleaves pentaglycine cross bridges in *S. aureus* peptidoglycan[198]. Supernatant from a *lasA* transposon mutant lost the ability to potentiate vancomycin activity, implicating LasA in this phenotype. Quantification of LasA activity in *P. aeruginosa* clinical isolates demonstrated a strong correlation

between LasA activity and vancomycin potentiation, and we further developed a murine burn wound model of *P. aeruginosa*/*S. aureus* infection to demonstrate that the presence of *P. aeruginosa* increases *S. aureus* susceptibility to vancomycin in a LasA dependent manner. In all, the data presented in Chapter 2 demonstrate that interaction with *P. aeruginosa* has a major, and varying impact on *S. aureus* antibiotic susceptibility, and suggested that therapeutic outcome of *S. aureus* infection may depend on the activity of co-infecting *P. aeruginosa* strains.

Interspecies interaction may play an underappreciated role in dictating antibiotic treatment outcome.

Though studies of bacterial pathogenesis and antibiotic susceptibility are conventionally performed in isolation, recent strides in understanding the infection environment suggest that polymicrobial infections are extremely common [321–323]. Exploratory 16S sequencing studies of the skin, respiratory passages, intestinal lumen, and urinary tract have revealed that these niches are rife with microorganisms of the mammalian microbiome[324]. Pathogen colonization of these niches therefore cannot occur without extensive interaction with both the resident microflora and other co-infecting pathogens. Members of a polymicrobial community are subject to a variety ecological pressures that may alter cellular physiology and metabolism of individual microorganisms. These include nutrient competition, metabolic cross feeding, and exposure to microbial-produced signaling or antimicrobial molecules [80,325–327]. Studying a pathogen in the context of its microbial interaction network reveals subtle factors that may influence antibiotic susceptibility that go otherwise unnoticed when studied in isolation[72,328]. Identifying key interspecies interactions that improve or

impair antibiotic action will advance our understanding of antibiotic efficacy, and help us to move away from common reductionist approaches to susceptibility testing.

The polymicrobial CF lung environment presents an interesting opportunity to explore how extrinsic ecological factors influence antibiotic treatment outcome. Throughout this thesis work we have primarily focused on *P. aeruginosa/S. aureus,* however the CF lung is a complex microbial environment colonized by several core genera including (but not limited to) *Streptococcus, Stenotrophomonas, Prevotella, Veillonella, Neisseria* and *Porphorymonas*[329]*.* It is unlikely that antibiotic antagonizing or potentiating interactions within the CF lung are limited to the examples discussed in Chapter 2. Further investigation may reveal other ways that polymicrobial interaction alters antibiotic efficacy in this environment. For instance, aminoglycoside resistance-encoding genes (e.g. aminoglycoside-modifying enzymes, AME) are typically located on mobile genetic elements such as plasmids or transposons[330]. The formation of polymicrobial biofilm increases the frequency of horizontal gene transfer (HGT) by increasing bacterial rates of conjugation[331–333]. Enzymatic aminoglycoside deactivation allows *S. aureus* to proliferate in the presence of antibiotic without the fitness cost of adopting a SCV lifestyle, thus there is likely a strong selective pressure for AME acquisition in this environment*.* Indeed, in Chapter 3 we observed that 75% of our *S. aureus* CF isolates were resistant to extreme concentrations of tobramycin (MICs ranged from .78µg/mL- 3.2mg/mL), and none of these isolates were SCVs. Thus, infection by a single AME-expressing microorganism may lead to the acquisition of aminoglycoside resistance among co-infecting pathogens.

CF exacerbation and lung deterioration corresponds with an outgrowth of *P.*

aeruginosa[334,335]. Patients receive high-dose regimens of inhaled tobramycin therapy that reach concentrations of approximately 737μg per gram of sputum[336]. In children suffering from acute infection, inhaled tobramycin is sufficient to eradicate *P. aeruginosa* from the CF lung[337]. However, as they mature, adult patients inevitably become chronically colonized by *P. aeruginosa*, and these infections are almost impossible to clear, even when isolates are genetically susceptible to tobramycin killing[338,339]. At this stage, the same therapy that once resolved infection in children is used merely to reduce *P. aeruginosa* burden and palliate disease during periods of exacerbation. It is unclear why high-dose tobramycin therapy no longer resolves chronic *P. aeruginosa* infection in CF adults. Treatment failure could result from poor drug penetration through the thick mucus layers that build up over time within the CF lung[340]. Alternatively, impaired aminoglycoside uptake following bacterial respiration inhibition may promote treatment failure. CF disease progression is associated with deteriorating lung function partially due to chronic neutrophil influx and pro-inflammatory activity[341]. Aberrant neutrophil degranulation and macrophage activities during chronic inflammation increase the concentration of respiration inhibitors (e.g. NO□) within CF lung tissue, and may inadvertently induce transient tolerance to aminoglycosides among infecting populations[62,342]. Interspecies microbial interactions could also contribute to progressive treatment failure. *P. aeruginosa*-produced respiration inhibitors have long been known to induce transient aminoglycoside tolerance in *S. aureus*[53]. As antibiotic deactivation by a single bacterial species can lead to the *de facto* resistance of the entire community[73,74,328], it is possible that the proliferation of AME-expressing populations within this

environment may contribute to the stable lung colonization of *P. aeruginosa* over time as the expansion of an AME-expressing population could reduce the concentration of aminoglycosides present in the sputum.

The finding that *P. aeruginosa*-secreted exoproducts alter *S. aureus* antibiotic susceptibility may have broad implications for improving CF patient health, as these co-infections are common and notoriously difficult to treat[220]. However, one major caveat of the study described in Chapter 2 is that the bulk of the experimentation was performed *in vitro* on planktonic cultures. Future studies are necessary to probe these interactions in the context of the CF lung. This will address many unanswered questions prompted by our study, including whether these two organisms interact within this environment, and whether these interactions are relevant for the physiological conditions of the CF lung (i.e. does respiration inhibition influence *S. aureus* fitness in response to antibiotic challenge, or does *S. aureus* already exist in a non-respiring state in this niche?). A recent *ex vivo* study examining *S. aureus, P. aeruginosa* spatial organization in explanted lung tissue suggested that mixed communities of these two pathogens can be found together in the CF lung[202]. Further studies have used peptide nucleic acid (PNA) fluorescence in situ hybridization (FISH) techniques to characterize the spatial organization of *P. aeruginosa/S. aureus* aggregates in expectorated CF sputum[343]. The authors of this study observed that both pathogens reside primarily in separate monospecies aggregates with minimal inter-aggregate mixing between microcolonies. In the absence of physical cell-to-cell contact, diffusible secreted exoproducts may represent the primary mediator of interspecies interaction. However, the question remains whether the *P. aeruginosa* exoproducts discussed in

Chapter 2 significantly influence *S. aureus* physiology within this environment. The biggest challenge to answering this question is the current lack of a suitable model of CF lung disease capable of fostering long-term *P. aeruginosa/S. aureus* co-infection[344].

Much attention has recently been placed on understanding trends in *P. aeruginosa* phenotypic and genotypic adaptation to the lung environment [220,224,319,320]. The results from these studies suggest that *P. aeruginosa* virulence factor production is highly variable between early and late stage CF infection. As clinicians and researchers continue to collect data describing the phenotypic and genotypic adaptations that accompany chronic *P. aeruginosa* lung colonization, an alternative approach to assessing the relevance of *P. aeruginosa/S. aureus* co-infection on antibiotic treatment outcome may be through retrospective study. Future projects in the lab could contrast antibiotic treatment outcome with *P. aeruginosa* phenotypic characterization of pertinent exoproduct production to determine if, for instance, *P. aeruginosa* production of rhamnolipids correlates with improved resolution of *S. aureus* by aminoglycosides. The results from such studies may improve antibiotic-mediated resolution of chronic co-infections.

SUMMARY- CHAPTER 3: RHAMNOLIPIDS INDUCE PMF-INDEPENDENT AMINOGLYCOSIDE UPTAKE TO RESTORE SENSITIVITY TO TOLERANT AND RESISTANT *S. AUREUS* POPULATIONS.

Non-respiring bacterial populations are inherently tolerant to aminoglycoside antibiotics that require PMF for bacterial internalization[50]. *S. aureus* frequently colonizes microaerophillic or anaerobic niches during infection of the bone, within an

abscess, or in the late-stage cystic fibrosis lung[103]. Thus, aminoglycoside efficacy is limited against anaerobic, SCV, biofilm-associated, and persister subpopulations of *S. aureus* due to decreased respiration and decreased PMF-dependent drug uptake. In Chapter 3 we further explored the ability of aminoglycoside/rhamnolipid combinational therapy to restore antibiotic susceptibility to resistant and tolerant *S. aureus* populations.

We demonstrated that subinhibitory, non-cytotoxic concentrations of rhamnolipids induce aminoglycoside uptake in the absence of PMF. By bypassing the PMF requirement for drug influx, rhamnolipids restore aminoglycoside sensitivity to otherwise tolerant persister, biofilm, SCV, and anaerobic populations of *S. aureus*. Strikingly, in most cases rhamnolipid/aminoglycoside combinational therapy led to the complete and rapid sterilization of these populations that are otherwise completely tolerant to aminoglycoside killing. Furthermore, we demonstrated that this combinational therapy prevents the rise of tobramycin resistance, restores sensitivity to highly resistant *S. aureus* clinical isolates, and is effective against other aminoglycoside resistant, Gram-positive pathogens such as *Listeria monocytogenes, Enterococcus faecalis,* and *Clostridium difficile*. Further, while we observed that other membrane-targeting compounds synergize with tobramycin, only rhamnolipids stimulated PMF-independent uptake under these conditions and thus were the strongest potentiators of aminoglycoside activity.

Destabilizing membrane activity during aminoglycoside therapy is a promising approach for targeting recalcitrant populations.

The biggest foreseeable barrier preventing implementation rhamnolipid/aminoglycoside combinational therapy is that high concentrations of

rhamnolipids are cytotoxic to host cells[250]. Other RL congeners differ structurally, and we observed that changes in carbon tail length or number of rhamnose sugar moieties alter tobramycin potentiating activity (Figure 3.2E) and hemolytic and cytotoxic effects on host cells indicating that there may be room to develop a modified rhamnolipid congener. Furthermore, trends in cytotoxicity between prokaryotic and eukaryotic cells do not always align as there are distinct differences in prokaryotic and eukaryotic membrane composition[139]. Future investigation into the practicality of using rhamnolipids has an antibiotic adjuvant should begin by identifying a specific congener that exhibits maximal tobramycin-potentiating activity and minimal eukaryotic cytotoxicity. It is also possible that the optimum adjuvant for improving aminoglycoside uptake may not be a rhamnolipid molecule, but instead another small molecule capable of inducing PMF-independent aminoglycoside uptake. A small molecule screen that assesses bacterial aminoglycoside uptake under conditions of respiration inhibition would be ideal for identifying putative adjuvant candidates.

The finding that rhamnolipids resensitize tolerant and resistant Gram-positive bacterial species to aminoglycoside killing came from a single study of interspecies interaction, and suggests that future screening of other competitive microbial interactions in the presence of antibiotics may reveal novel antibiotic sensitizers with clinical relevance. Rhamnolipid biosurfactants not only potentiate aminoglycoside uptake in *S. aureus,* but in other important Gram-positive pathogens as well. For *C. difficile* in particular, 30µg/mL of rhamnolipids reduced the MIC of tobramycin over 1000-fold (Table 3.1), rendering what is considered an aminoglycoside-resistant pathogen completely susceptible to killing. Further, biosurfactant production is not

unique to *P. aeruginosa.* Indeed, many other glycolipid molecules with properties similar to rhamnolipids have been characterized from various *Mycobacterium, Corynebacterium,* and *Candida* species[345]. If other glycolipid molecules improve antibiotic penetrance across the bacterial membrane, the broad implications of microbial biosurfactant production during polymicrobial infection will require further investigation. Further, within and without the host, bacteria produce an extensive array of secondary metabolites in order to survive within densely populated microbial environments. Mono- vs. pairwise culturing of competitive species under conditions that induce secondary metabolite production and in the presence of antibiotic could prove a fruitful approach for identifying new molecules for sensitizing tolerant populations to antibiotic killing.

Identifying the underlying mechanism(s) of antibiotic tolerance may reveal new paths to eradication.

Intrinsically tolerant bacterial populations often tolerate multiple classes of antibiotics with distinct mechanisms of action. This has led many to believe that there exists a single molecular mechanism that pushes bacteria into an antibiotic tolerant state. Because slow-growing and metabolically dormant bacteria tolerate antibiotic killing, it has long been proposed that bacterial persisters reflect a stochastic decline towards cell death[346]. Indeed, until recently it was believed that aberrations in toxin-antitoxin (TA) module expression or stringent response activation represented the primary drivers of population heterogeneity that lead to persister cell formation[347]. However, neither TA expression nor stringent response activity contribute to persister formation in *S. aureus*[26]*.* Instead, *S. aureus* persister cell formation is associated with stochastic entrance into a stationary phase-like, low energy state which may result from

stochastic variations in TCA cycle enzyme expression[29]. These findings have prompted a “low energy” hypothesis proposing that persister formation is a direct result of ATP depletion[26]. In support of this, many of the TA-mediated mechanisms of persister cell formation originally described induce tolerance by depleting intracellular ATP. For instance, overexpression of the TisB toxin in *E. coli* leads to disruption of the membrane and dissipation of PMF[348]. This inhibits ATP production through the F_1F_0 ATPase and induces a metabolically dormant, antibiotic tolerant state[349]. However, instead of being the sole mechanism of bacterial persister formation as was once proposed, TA and stringent response aberrations may simply represent a small subset of molecular interactions that fall under the much larger category of induced tolerance through ATP depletion.

Recently, however, several groups have questioned the conclusion that ATP depletion and metabolic dormancy represent the underlying cause of antibiotic tolerance. Pontes *et al.* demonstrated that *Salmonella* cultures treated with the bacteriostatic antibiotic chloramphenicol tolerate ciprofloxacin and cefotaxime challenge while maintaining high intracellular ATP concentrations[36]. Similarly, within infected macrophages, *S.* Typhimurium persisters were demonstrated to exist in a metabolically active, non-growing state[35]. These intracellular populations were shown to be transcriptionally and translationally active, but tolerant to killing by β-lactam antibiotics[35]. Based on these findings some claim that ATP-depletion cannot be the underlying mechanism driving antibiotic tolerance, and we agree. Instead, we propose that in the same way that TA module activation promotes antibiotic tolerance by inducing ATP depletion, ATP depletion drives antibiotic tolerance by reducing antibiotic

target activity. Antibiotic target inhibition is not restricted to ATP depletion, thus this model accommodates ATP-independent determinants of antibiotic tolerance.

As with cancer, where many extrinsic factors like carcinogens, radiation, or viral infection can elicit a similar state of uncontrolled growth, we propose that many extrinsic factors in the host can decrease antibiotic target activity to promote tolerance. Sometimes this occurs through ATP depletion, and sometimes not. For the cases described above, it is logical to conclude that treating *Salmonella* with chloramphenicol (a translation inhibitor) will result in increased intracellular ATP concentrations, as protein synthesis is an energy-demanding process. However, as chloramphenicol is a bacteriostatic antibiotic that inhibits bacterial growth and replication, chloramphenicol-treated cells are no longer replicating DNA or synthesizing new cell wall. Thus, these populations will no longer be susceptible to killing by antibiotics that corrupting active DNA (ciprofloxacin) or cell wall (cefotaxime) biosynthesis. Similarly, though Stapels *et al.* demonstrated that transcriptionally and translationally active, non-dividing *Salmonella* are tolerant to β-lactam antibiotics, it remains to be seen whether these populations are tolerant to antibiotics that specifically target transcription or translation in this state.

Conversely, data presented in Chapter 3 demonstrated that inducing PMF-independent aminoglycoside uptake allowed for the eradication of ATP-depleted *S. aureus* populations. Arsenate treatment depletes *S. aureus* intracellular ATP levels and pushes the population into a non-dividing state that is completely tolerant to ciprofloxacin killing[26]. Recently, Pu *et al* demonstrated that non-growing, ATP-depleted persister cells maintain low levels of translation[257]. This may explain why

ATP-depleted persister cells are tolerant to ciprofloxacin (DNA synthesis) but not aminoglycosides (protein synthesis) as these cells are no longer dividing but are still synthesizing new protein. Together, these findings support our hypothesis that antibiotic tolerance occurs when target activity is inhibited and that populations remain susceptible when antibiotics can access active targets, independent of ATP levels. Understanding which metabolic processes are active in persisters will improve our ability to treat these populations.

Shifting attention away from strictly considering the factors that deplete intracellular ATP levels and towards the factors that influence antibiotic target activity may reveal how other extrinsic factors present within the host contribute to antibiotic treatment failure. For instance, many core bacterial processes are facilitated by metal-dependent metalloenzymes[350]. Within the host, the concentrations of transition metals like iron, zinc, manganese, etc. are tightly regulated through host mechanisms of sequestration[351]. It is possible that metal starvation by the host may inadvertently lead to antibiotic tolerance in infecting bacterial populations by reducing target activity. For example, host calprotectin readily binds excess zinc in the host as a form of nutritional immunity against invading pathogens[352]. Bacteria require zinc for a number of important cellular processes including the binding of zinc-dependent transcription factors during RNA synthesis. We have observed that zinc starvation through exposure to the heavy metal chelator TPEN inhibits transcription in *S. aureus in vitro* cultures, and that this reduction corresponds to a population-wide induction of tolerance to rifampicin (unpublished data). Importantly, ATP levels following TPEN treatment is approximately twice that of untreated, rifampicin sensitive cultures, suggesting that target inactivation

through zinc starvation induces antibiotic tolerance through an ATP-independent mechanism, perhaps through the slowing of bacterial transcription. Future studies in the lab will determine the precise mechanism by which zinc starvation induces antibiotic tolerance, as well as if zinc concentration influence antibiotic susceptibility within the host.

SUMMARY- CHAPTER 4 *FRANCISELLA TULARENSIS* UTILIZES NON-GLUCOSE CARBON SUBSTRATES TO FUEL RAPID INTRACELLULAR PROLIFERATION.

Intracellular pathogens are sheltered from both host- and antibiotic- mediated mechanisms of killing that occur in the extracellular space. Identifying and inhibiting the pathways these pathogens use to modify the intracellular niche to survive within this environment is a promising approach to target these populations when other antibiotics fail. However, for most pathogens the bacterial metabolic pathways and host-derived nutrients required for intracellular proliferation are poorly understood. In Chapter 4, we used systematic mutational analysis to identify the carbon catabolic pathways and host-derived nutrients required for intracellular replication of the BSL-3 *F. tularensis* strain, SchuS4. We demonstrated that the glycolytic enzyme phosphofructokinase (PfkA), and thus glycolysis, is dispensable for *F. tularensis* SchuS4 virulence, and highlighted the importance of the gluconeogenic enzyme fructose 1,6-bisphosphatase (GlpX). We found that the specific gluconeogenic enzymes that function upstream of GlpX varied based on infection model, indicating that *F. tularensis* alters its metabolic flux according to the nutrients available within its replicative niche. For instance, pyruvate-phosphate dikinase (PpdK)-mediated conversion of pyruvate to PEP (required for growth on lactate) was required for growth within J774A.1 transformed macrophages but not within

primary cells or a mouse. Transformed cell lines produce significant concentrations of lactate through aerobic glycolysis[281], and this availability may dictate the preferred metabolic pathway, perhaps through catabolite repression. Despite this flexibility, we found that glutamate dehydrogenase (GdhA) and glycerol 3-phosphate dehydrogenase (GlpA) are essential for *F. tularensis* intracellular replication in all infection models tested. Finally, we used the small molecule inhibitor, Atglistatin, and ATGL knockdown BMDMs to demonstrate that host cell lipolysis is required for *F. tularensis* intracellular proliferation, suggesting that host triglyceride stores may inadvertently fuel *F. tularensis* intracellular replication. These findings reveal new therapeutic strategies for targeting this highly infectious pathogen and may provide insight for improved targeting of intracellular pathogens in general.

Disrupting niche modification to target recalcitrant pathogen populations.

In identifying factors required for *F. tularensis* intracellular replication in Chapter 4, we began to unravel the complex host-microbe interactions that occur during *F. tularensis* infection. We identified the gluconeogenic pathway as well as glycerol and glutamate catabolism as essential for *F. tularensis* intracellular proliferation. However, these central metabolic pathways are equally essential to host cell metabolism, and as such, direct targeting of these pathways may have undesired effects on host health. Instead, we propose that disrupting *F. tularensis* re-programming of host metabolism is a more practical approach to limiting pathogen growth.

Bacterial strategies for obtaining host-derived trace metals such as iron are relatively well defined. Previous studies have identified an array of siderophores,

hemoglobin-binding modules or active transport system that scavenge and import precious iron from the host[276,353,354]. However, to date, relatively few active carbon acquisition mechanisms are described for intracellular bacterial pathogens. A few examples include *M. tuberculosis* secretion of lipases that free up fatty acids from host lipid droplets, and *S.* Typhimurium secreted protein effector molecules that redirect vesicular trafficking of nutrients to the *Salmonella*-containing vacuole[168,170]. As carbon acquisition is essential to intracellular replication, there are likely many other unidentified mechanisms by which intracellular pathogens actively modulate this environment to derive nutrients.

Following intracellular invasion, *F. tularensis* subverts host xenophagy and hijacks host metabolism through the secretion of various effector molecules that aid in establishing a permissive niche[355,356]. This includes inhibiting phagosome acidification, inhibiting reactive oxygen species generation by the host, and inducing host cell autophagy to provide free amino acids[282,357–359]. *F. tularensis* intracellular replication occurs in the presence of host autophagy inhibitors[282], suggesting that the pathogen consumes additional nutrients besides host autophagy-derived amino acids. We observed that inhibition of host cell lipolysis reduced *F. tularensis* intracellular burden. It is possible that commandeering both host lipolysis and autophagy provides *F. tularensis* with the bulk of the host-derived carbon necessary for replication. Future studies by the lab will determine whether treating cells simultaneously with autophagy inhibitors (e.g. 3-methyladenine) and lipolysis inhibitors (e.g Atglistatin) are sufficient to abrogate *F. tularensis* replication within the host.

Future screening of host-acting compounds against *F. tularensis* infected macrophages may reveal new therapeutics that reduce intracellular permissibility to *F. tularensis* replication. Many viral and bacterial pathogens manipulate host signaling through the major metabolic regulators AMP-activated protein kinase (AMPK)[360]. AMPK is a major eukaryotic regulator of energy homeostasis that responds to an increase in ADP:ATP ratios by stimulating nutrient acquisition and reducing energy consuming processes within the cell[361]. Previously we observed that *F. tularensis* infection stimulates host AMPK activation, and that $AMPK^{-/-}$ host cells do not support wild-type levels of *F. tularensis* growth (unpublished data). Furthermore, in Chapter 4 we observed that stimulating AMPK activation with an AMP analogue (AICAR) rescued the intracellular growth defects observed for *ΔglpX, ΔgdhA,* and *ΔglpKA* mutants. As this rescue only occurred when cells were cultured in excess glucose, AICAR presumably restored the viability of these mutants by increasing host glucose uptake and availability thus subverting the growth defect caused by inhibiting these metabolic pathways. Additionally, AMPK activation triggers host cell autophagy, and autophagy-derived amino acids support *F. tularensis* intracellular replication[282,361]. Together these results suggest that inhibiting *F. tularensis*-mediated AMPK activation may represent an alternative approach for reducing intracellular burden by decreasing the availability of free nutrients. Future *in vivo* experiments will explore whether pharmacologically inhibiting *F. tularensis* activation of AMPK reduces bacterial virulence and burden within a host.

One potential caveat of inhibiting *F. tularensis* nutrient acquisition during intracellular replication is that this approach will presumably reduce the metabolic

activity of the pathogen and may inadvertently render it tolerant to subsequent antibiotic challenge. The extreme intracellular growth rate of *F. tularensis* likely contributes to its broad susceptibility to antibiotics and may explain why even aminoglycosides that normally penetrate poorly into the intracellular space are effective at clearing *F. tularensis* following long-term treatment. Antibiotic tolerance is poorly understood for *F. tularensis,* and few studies have probed the clinical relevance of *F. tularensis* persister formation. As *F. tularensis* is adept at inhibiting host-mediated clearance during intracellular replication, future studies are required to determine how long an energy-starved population of *F. tularensis* can persist within the intracellular space in order to prevent selection for persister populations that perpetuate relapsing infection following cessation of treatment.

REFERENCES

[1] **Payne DJ, Gwynn MN, Holmes DJ, Pompliano DL.** Drugs for bad bugs: Confronting the challenges of antibacterial discovery. Nat Rev Drug Discov 2007;6:29–40. doi:10.1038/nrd2201.

[2] **Silver LL**. Challenges of antibacterial discovery. Clin Microbiol Rev 2011;24:71–109. doi:10.1128/CMR.00030-10.

[3] **McKeegan KS, Borges-Walmsley MI, Walmsley AR**. Microbial and viral drug resistance mechanisms. Trends Microbiol 2002;10. doi:10.1016/S0966-842X(02)02429-0.

[4] **Centers for Disease Control and Prevention (CDC)**. Antibiotic Resistance Threats in the United States, 2019. 2019.

[5] **Mulcahy LR, Isabella VM, Lewis K**. Pseudomonas aeruginosa Biofilms in Disease. Microb Ecol 2013;68:1–12. doi:10.1007/s00248-013-0297-x.

[6] **Fauvart M, de Groote VN, Michiels J**. Role of persister cells in chronic infections: Clinical relevance and perspectives on anti-persister therapies. J Med Microbiol 2011;60:699–709. doi:10.1099/jmm.0.030932-0.

[7] **LaFleur MD, Qi Q, Lewis K**. Patients with long-term oral carriage harbor high-persister mutants of Candida albicans. Antimicrob Agents Chemother 2010;54:39–44. doi:10.1128/AAC.00860-09.

[8] **Brauner A, Fridman O, Gefen O, Balaban NQ**. Distinguishing between resistance, tolerance and persistence to antibiotic treatment. Nat Rev Microbiol 2016;14:320–30. doi:10.1038/nrmicro.2016.34.

[9] **Michiels JE, Van den Bergh B, Verstraeten N, Michiels J**. Molecular mechanisms and clinical implications of bacterial persistence. Drug Resist Updat 2016;29:76–89. doi:10.1016/j.drup.2016.10.002.

[10] **Conlon BP**. *Staphylococcus aureus* chronic and relapsing infections: Evidence of a role for persister cells. BioEssays 2014;36:991–6. doi:10.1002/bies.201400080.

[11] **Fisher RA, Gollan B, Helaine S**. Persistent bacterial infections and persister cells. Nat Rev Microbiol 2017;15:453–64. doi:10.1038/nrmicro.2017.42.

[12] **Fridman O, Goldberg A, Ronin I, Shoresh N, Balaban NQ**. Optimization of lag time underlies antibiotic tolerance in evolved bacterial populations. Nature 2014;513:418–21. doi:10.1038/nature13469.

[13] **Levin-Reisman I, Ronin I, Gefen O, Braniss I, Shoresh N, Balaban NQ**. Antibiotic tolerance facilitates the evolution of resistance. Science (80-) 2017;355(6327):826-830. doi: 10.1126/science.aaj2191

[14] **Liu J, Gefen O, Ronin I, Bar-Meir M, Balaban NQ**. Effect of tolerance on the evolution of antibiotic resistance under drug combinations. Science 2020;367:200–4. doi:10.1126/science.aay3041.

[15] **Bakkeren E, Huisman JS, Fattinger SA, Hausmann A, Furter M, Egli A, et al.** Salmonella persisters promote the spread of antibiotic resistance plasmids in the gut. Nature 2019;573:276–80. doi:10.1038/s41586-019-1521-8.

[16] **Claudi B, Spröte P, Chirkova A, Personnic N, Zankl J, Schürmann N, et al.** Phenotypic variation of salmonella in host tissues delays eradication by antimicrobial chemotherapy. Cell 2014;158:722–33. doi:10.1016/j.cell.2014.06.045.

[17] **Helaine S, Cheverton AM, Watson KG, Faure LM, Matthews SA, Holden DW**. Internalization of Salmonella by Macrophages Induces Formation of Nonreplicating Persisters. Science (80-) 2014;343:204–8. doi:10.1126/science.1244705.

[18] **Diard M, Sellin ME, Dolowschiak T, Arnoldini M, Ackermann M, Hardt WD**. Antibiotic treatment selects for cooperative virulence of salmonella typhimurium. Curr Biol 2014;24:2000–5. doi:10.1016/j.cub.2014.07.028.

[19] **Kohanski MA, Dwyer DJ, Collins JJ**. How antibiotics kill bacteria: from targets to networks. Nat Rev Microbiol 2010;8:423–35. doi:10.1038/nrmicro2333.

[20] **Davies J, Gorini L, Davis BD**. Misreading of RNA codewords induced by aminoglycoside antibiotics. Mol Pharmacol 1965;1:93–106.

[21] **Drlica K, Malik M, Kerns RJ, Zhao X**. Quinolone-mediated bacterial death. Antimicrob Agents Chemother 2008;52:385–92. doi:10.1128/AAC.01617-06.

[22] **Bigger JW**. Treatment of Staphylococcal infections with penicillin by intermittent sterilisation . Lancet 1944;244:497–500. doi:10.1016/S0140-6736(00)74210-3.

[23] **Balaban NQ, Helaine S, Lewis K, Ackermann M, Aldridge B, Andersson DI, et al.** Definitions and guidelines for research on antibiotic persistence. Nat Rev Microbiol 2019;17:441–8. doi:10.1038/s41579-019-0196-3.

[24] **Balaban NQ, Merrin J, Chait R, Kowalik L, Leibler S**. Bacterial Persistence as a Phenotypic Switch. Science 2004; 10;305(5690):1622-5.

[25] **van den Bergh B, Fauvart M, Michiels J**. Formation, physiology, ecology,

evolution and clinical importance of bacterial persisters. FEMS Microbiol Rev 2017;41:219–51. doi:10.1093/femsre/fux001.

[26] **Conlon BP, Rowe SE, Gandt AB, Nuxoll AS, Donegan NP, Zalis EA, et al.** Persister formation in Staphylococcus aureus is associated with ATP depletion. Nat Microbiol 2016;1:16051. doi:10.1038/nmicrobiol.2016.51.

[27] **Shan Y, Brown Gandt A, Rowe SE, Deisinger JP, Conlon BP, Lewis K**. ATP-Dependent Persister Formation in Escherichia coli. MBio 2017;8:e02267-16. doi:10.1128/mBio.02267-16.

[28] **Crane RK, Lipmann F**. The Effect of Arsenate on Aerobic Phosphorylation. J Biol Chem. 1953 Mar;201(1):235-43.

[29] **Zalis EA, Nuxoll AS, Manuse S, Clair G, Radlinski LC, Conlon BP, et al.** Stochastic variation in expression of the tricarboxylic acid cycle produces persister cells. MBio 2019;10. doi:10.1128/mBio.01930-19.

[30] **Nguyen D, Joshi-Datar A, Lepine F, Bauerle E, Olakanmi O, Beer K, et al.** Active starvation responses mediate antibiotic tolerance in biofilms and nutrient-limited bacteria. Science 2011;334:982–6. doi:10.1126/science.1211037.

[31] **Gutierrez A, Jain S, Bhargava P, Hamblin M, Lobritz MA, Collins JJ**. Understanding and Sensitizing Density-Dependent Persistence to Quinolone Antibiotics. Mol Cell 2017;68:1147-1154.e3. doi:10.1016/j.molcel.2017.11.012.

[32] **Rowe SE, Wagner NJ, Li L, Beam JE, Wilkinson AD, Radlinski LC, et al.** Reactive oxygen species induce antibiotic tolerance during systemic Staphylococcus aureus infection. Nat Microbiol 2019. doi:10.1038/s41564-019-0627-y.

[33] **Bernier SP, Lebeaux D, DeFrancesco AS, Valomon A, Soubigou G, Coppée J-Y, et al.** Starvation, Together with the SOS Response, Mediates High Biofilm-Specific Tolerance to the Fluoroquinolone Ofloxacin. PLoS Genet 2013;9:e1003144. doi:10.1371/journal.pgen.1003144.

[34] **Spoering AL, Lewis K**. Biofilms and planktonic cells of Pseudomonas aeruginosa have similar resistance to killing by antimicrobials. J Bacteriol 2001;183:6746–51. doi:10.1128/JB.183.23.6746-6751.2001.

[35] **Stapels DAC, Hill PWS, Westermann AJ, Fisher RA, Thurston TL, Saliba AE, et al.** Salmonella persisters undermine host immune defenses during antibiotic treatment. Science (80-) 2018;362:1156–60. doi:10.1126/science.aat7148.

[36] **Pontes MH, Groisman EA**. Slow growth determines nonheritable antibiotic resistance in Salmonella enterica. Sci Signal. 2019 Jul 30;12(592). pii: eaax3938.

doi: 10.1126/scisignal.aax3938.

[37] **Jager NGL, van Hest RM, Lipman J, Roberts JA, Cotta MO**. Antibiotic exposure at the site of infection: principles and assessment of tissue penetration. Expert Rev Clin Pharmacol 2019;12:623–34. doi:10.1080/17512433.2019.1621161.

[38] **Landersdorfer CB, Bulitta JB, Kinzig M, Holzgrabe U, Sörgel F**. Penetration of antibacterials into bone: Pharmacokinetic, pharmacodynamic and bioanalytical considerations. Clin Pharmacokinet 2009;48:89–124. doi:10.2165/00003088-200948020-00002.

[39] **Thabit AK, Fatani DF, Bamakhrama MS, Barnawi OA, Basudan LO, Alhejaili SF**. Antibiotic penetration into bone and joints: An updated review. Int J Infect Dis 2019;81:128–36. doi:10.1016/j.ijid.2019.02.005.

[40] **Wistrand-Yuen E, Knopp M, Hjort K, Koskiniemi S, Berg OG, Andersson DI**. Evolution of high-level resistance during low-level antibiotic exposure. Nat Commun 2018;9. doi:10.1038/s41467-018-04059-1.

[41] **Zhu K, Chen S, Sysoeva TA, You L**. Universal antibiotic tolerance arising from antibiotic-triggered accumulation of pyocyanin in Pseudomonas aeruginosa. PLOS Biol 2019;17:e3000573. doi:10.1371/journal.pbio.3000573.

[42] **Stevens DL**. The Role of Vancomycin in the Treatment Paradigm. Clin Infect Dis 2006;42:S51–7. doi:10.1086/491714.

[43] **Reynolds PE**. Structure, biochemistry and mechanism of action of glycopeptide antibiotics. Eur J Clin Microbiol Infect Dis 1989;8:943–50. doi:10.1007/BF01967563.

[44] **Gardete S, Tomasz A, Tomasz A, Pinho M, Ramirez M, Albrecht V**. Mechanisms of vancomycin resistance in Staphylococcus aureus. vol. 124. American Society for Clinical Investigation; 2014. doi:10.1172/JCI68834.

[45] **Rose WE, Poppens PT**. Impact of biofilm on the in vitro activity of vancomycin alone and in combination with tigecycline and rifampicin against Staphylococcus aureus. J Antimicrob Chemother 2009;63:485–8. doi:10.1093/jac/dkn513.

[46] **Sakoulas G, Eliopoulos GM, Moellering RC, Wennersten C, Venkataraman L, Novick RP, et al.** Accessory gene regulator (agr) locus in geographically diverse Staphylococcus aureus isolates with reduced susceptibility to vancomycin. Antimicrob Agents Chemother 2002;46:1492–502. doi:10.1128/AAC.46.5.1492-1502.2002.

[47] **Ling LL, Schneider T, Peoples AJ, Spoering AL, Engels I, Conlon BP, et al.** A

new antibiotic kills pathogens without detectable resistance. Nature 2015;517:455–9. doi:10.1038/nature14098.

[48] **Homma T, Nuxoll A, Gandt AB, Ebner P, Engels I, Schneider T, et al.** Dual targeting of cell wall precursors by teixobactin leads to cell lysis. Antimicrob Agents Chemother 2016;60:6510–7. doi:10.1128/AAC.01050-16.

[49] **Tulkens PM**. Intracellular pharmacokinetics and localization of antibiotics as predictors of their efficacy against intraphagocytic infections. Scand J Infect Dis Suppl 1990;74:209–17.

[50] **Taber HW, Mueller JP, Miller PF, Arrow AS**. Bacterial uptake of aminoglycoside antibiotics. Microbiol Rev 1987;51:439–57.

[51] **Schaaff F, Bierbaum G, Baumert N, Bartmann P, Sahl H-G**. Mutations are involved in emergence of aminoglycoside-induced small colony variants of Staphylococcus aureus. Int J Med Microbiol 2003;293:427–35. doi:10.1078/1438-4221-00282.

[52] **Proctor RA, Kahl B, von Eiff C, Vaudaux PE, Lew DP, Peters G**. Staphylococcal small colony variants have novel mechanisms for antibiotic resistance. Clin Infect Dis 1998;27 Suppl 1:S68-74.

[53] **Hoffman LR, Déziel E, D'Argenio DA, Lépine F, Emerson J, McNamara S, et al.** Selection for Staphylococcus aureus small-colony variants due to growth in the presence of Pseudomonas aeruginosa. Proc Natl Acad Sci U S A 2006;103:19890–5. doi:10.1073/pnas.0606756104.

[54] **Smith AL, Fiel SB, Mayer-Hamblett N, Ramsey B, Burns JL**. Susceptibility testing of Pseudomonas aeruginosa isolates and clinical response to parenteral antibiotic administration: Lack of association in cystic fibrosis. Chest 2003;123:1495–502. doi:10.1378/chest.123.5.1495.

[55] **Gillham MI, Sundaram S, Laughton CR, Haworth CS, Bilton D, Foweraker JE**. Variable antibiotic susceptibility in populations of Pseudomonas aeruginosa infecting patients with bronchiectasis. J Antimicrob Chemother 2009;63:728–32. doi:10.1093/jac/dkp007.

[56] **Keren I, Kaldalu N, Spoering A, Wang Y, Lewis K**. Persister cells and tolerance to antimicrobials. FEMS Microbiol Lett 230:13–8. doi:10.1016/S0378-1097(03)00856-5.

[57] **Sakoulas G, Moise-Broder PA, Schentag J, Forrest A, Moellering RC, Eliopoulos GM**. Relationship of MIC and bactericidal activity to efficacy of vancomycin for treatment of methicillin-resistant Staphylococcus aureus bacteremia. J Clin Microbiol 2004;42:2398–402. doi:10.1128/JCM.42.6.2398-

2402.2004.

[58] **Sakoulas G, Okumura CY, Thienphrapa W, Olson J, Nonejuie P, Dam Q, et al.** Nafcillin enhances innate immune-mediated killing of methicillin-resistant Staphylococcus aureus. J Mol Med 2014;92:139–49. doi:10.1007/s00109-013-1100-7.

[59] **Lin L, Nonejuie P, Munguia J, Hollands A, Olson J, Dam Q, et al**. Azithromycin Synergizes with Cationic Antimicrobial Peptides to Exert Bactericidal and Therapeutic Activity Against Highly Multidrug-Resistant Gram-Negative Bacterial Pathogens. EBioMedicine 2015;2:690. doi:10.1016/J.EBIOM.2015.05.021.

[60] **Kumaraswamy M, Lin L, Olson J, Sun C-F, Nonejuie P, Corriden R, et al.** Standard susceptibility testing overlooks potent azithromycin activity and cationic peptide synergy against MDR *Stenotrophomonas maltophilia*. J Antimicrob Chemother 2016;71:1264–9. doi:10.1093/jac/dkv487.

[61] **Band VI, Crispell EK, Napier BA, Herrera CM, Tharp GK, Vavikolanu K, et al**. Antibiotic failure mediated by a resistant subpopulation in Enterobacter cloacae. Nat Microbiol 2016;1. doi:10.1038/nmicrobiol.2016.53.

[62] **McCollister BD, Hoffman M, Husain M, Vázquez-Torres A**. Nitric oxide protects bacteria from aminoglycosides by blocking the energy-dependent phases of drug uptake. Antimicrob Agents Chemother 2011;55:2189–96. doi:10.1128/AAC.01203-10.

[63] **Dörr T, Lewis K, Vulić M**. SOS response induces persistence to fluoroquinolones in Escherichia coli. PLoS Genet 2009;5:e1000760. doi:10.1371/journal.pgen.1000760.

[64] **Ouadrhiri Y, Scorneaux B, Sibille Y, Tulkens PM**. Mechanism of the intracellular killing and modulation of antibiotic susceptibility of Listeria monocytogenes in THP-1 macrophages activated by gamma interferon. Antimicrob Agents Chemother 1999;43:1242–51. doi:10.1128/aac.43.5.1242.

[65] **Barcia-Macay M, Seral C, Mingeot-Leclercq MP, Tulkens PM, Van Bambeke F**. Pharmacodynamic evaluation of the intracellular activities of antibiotics against Staphylococcus aureus in a model of THP-1 macrophages. Antimicrob Agents Chemother 2006;50:841–51. doi:10.1128/AAC.50.3.841-851.2006.

[66] **Wendte JM, Ponnusamy D, Reiber D, Blair JL, Clinkenbeard KD**. In vitro efficacy of antibiotics commonly used to treat human plague against intracellular Yersinia pestis. Antimicrob Agents Chemother 2011;55:3752–7. doi:10.1128/AAC.01481-10.

[67] **Bongers S, Hellebrekers P, Leenen LPH, Koenderman L, Hietbrink F**.

Intracellular penetration and effects of antibiotics on staphylococcus aureus inside human neutrophils: A comprehensive review. Antibiotics 2019;8. doi:10.3390/antibiotics8020054.

[68] **Surewaard BGJ, Deniset JF, Zemp FJ, Amrein M, Otto M, Conly J, et al.** Identification and treatment of the Staphylococcus aureus reservoir in vivo. J Exp Med 2016;213:1141–51. doi:10.1084/jem.20160334.

[69] **Lehar SM, Pillow T, Xu M, Staben L, Kajihara KK, Vandlen R, et al.** Novel antibody-antibiotic conjugate eliminates intracellular S. aureus. Nature 2015;527:323–8. doi:10.1038/nature16057.

[70] **Rosales C, Uribe-Querol E**. Phagocytosis: A Fundamental Process in Immunity. Biomed Res Int 2017;2017. doi:10.1155/2017/9042851.

[71] **Liu Y, Tan S, Huang L, Abramovitch RB, Rohde KH, Zimmerman MD, et al.** Immune activation of the host cell induces drug tolerance in Mycobacterium tuberculosis both in vitro and in vivo. J Exp Med 2016;213:809–25. doi:10.1084/jem.20151248.

[72] **De Vos MGJ, Zagorski M, McNally A, Bollenbach T**. Interaction networks, ecological stability, and collective antibiotic tolerance in polymicrobial infections. Proc Natl Acad Sci U S A 2017;114:10666–71. doi:10.1073/pnas.1713372114.

[73] **Sorg RA, Lin L, van Doorn GS, Sorg M, Olson J, Nizet V, et al.** Collective Resistance in Microbial Communities by Intracellular Antibiotic Deactivation. PLOS Biol 2016;14:e2000631. doi:10.1371/journal.pbio.2000631.

[74] **Medaney F, Dimitriu T, Ellis RJ, Raymond B.** Live to cheat another day: Bacterial dormancy facilitates the social exploitation of β-lactamases. ISME J 2016;10:778–87. doi:10.1038/ismej.2015.154.

[75] **Andersson DI, Levin BR.** The biological cost of antibiotic resistance. Curr Opin Microbiol 1999;2:489–93. doi:10.1016/S1369-5274(99)00005-3.

[76] **Szilágyi A, Boza G, Scheuring I**. Analysis of stability to cheaters in models of antibiotic degrading microbial communities. J Theor Biol 2017;423:53–62. doi:10.1016/j.jtbi.2017.04.025.

[77] **Orazi G, O'Toole GA**. Pseudomonas aeruginosa alters Staphylococcus aureus sensitivity to vancomycin in a biofilm model of cystic fibrosis infection. MBio 2017;8. doi:10.1128/mBio.00873-17.

[78] **Leung V, Lévesque CM**. A stress-inducible quorum-sensing peptide mediates the formation of persister cells with noninherited multidrug tolerance. J Bacteriol 2012;194:2265–74. doi:10.1128/JB.06707-11.

[79] **Möker N, Dean CR, Tao J**. Pseudomonas aeruginosa increases formation of multidrug-tolerant persister cells in response to quorum-sensing signaling molecules. J Bacteriol 2010;192:1946–55. doi:10.1128/JB.01231-09.

[80] **Vega NM, Allison KR, Samuels AN, Klempner MS, Collins JJ**. Salmonella typhimurium intercepts Escherichia coli signaling to enhance antibiotic tolerance. Proc Natl Acad Sci U S A 2013;110:14420–5. doi:10.1073/pnas.1308085110.

[81] **Armbruster CE, Hong W, Pang B, Weimer KED, Juneau RA, Turner J, et al.** Indirect Pathogenicity of Haemophilus influenzae and Moraxella catarrhalis in Polymicrobial Otitis Media Occurs via Interspecies Quorum Signaling. MBio 2010;1:e00102-10-e00102-19. doi:10.1128/mBio.00102-10.

[82] **Costerton JW, Cheng KJ, Geesey GG, Ladd TI, Nickel JC, Dasgupta M, et al.** Bacterial Biofilms in Nature and Disease. Annu Rev Microbiol 1987;41:435–64. doi:10.1146/annurev.mi.41.100187.002251.

[83] **Kean R, Rajendran R, Haggarty J, Townsend EM, Short B, Burgess KE, et al.** Candida albicans Mycofilms Support Staphylococcus aureus Colonization and Enhances Miconazole Resistance in Dual-Species Interactions. Front Microbiol 2017;8. doi:10.3389/fmicb.2017.00258.

[84] **Radlinski L, Rowe SE, Kartchner LB, Maile R, Cairns BA, Vitko NP, et al.** Pseudomonas aeruginosa exoproducts determine antibiotic efficacy against Staphylococcus aureus. PLOS Biol 2017;15:e2003981. doi:10.1371/journal.pbio.2003981.

[85] **Radlinski LC, Rowe SE, Brzozowski R, Wilkinson AD, Huang R, Eswara P, et al.** Chemical Induction of Aminoglycoside Uptake Overcomes Antibiotic Tolerance and Resistance in Staphylococcus aureus. Cell Chem Biol 2019;26:1355-1364.e4. doi:10.1016/j.chembiol.2019.07.009.

[86] **Tunney MM, Field TR, Moriarty TF, Patrick S, Doering G, Muhlebach MS, et al.** Detection of Anaerobic Bacteria in High Numbers in Sputum from Patients with Cystic Fibrosis. Am J Respir Crit Care Med 2008;177:995–1001. doi:10.1164/rccm.200708-1151OC.

[87] **Sen CK**. Wound healing essentials: Let there be oxygen. Wound Repair Regen 2009;17:1–18. doi:10.1111/j.1524-475X.2008.00436.x.

[88] **Park MK, Myers RAM, Marzella L**. Oxygen Tensions and Infections: Modulation of Microbial Growth, Activity of Antimicrobial Agents, and Immunologic Responses. Clin Infect Dis 1992;14:720–40. doi:10.1093/clinids/14.3.720.

[89] **White BK, Mende K, Weintrob AC, Beckius ML, Zera WC, Lu D, et al.**

Epidemiology and antimicrobial susceptibilities of wound isolates of obligate anaerobes from combat casualties. Diagn Microbiol Infect Dis 2016;84:144–50. doi:10.1016/j.diagmicrobio.2015.10.010.

[90] **Freeman CD, Klutman NE, Lamp KC**. Metronidazole. A therapeutic review and update. Drugs 1997;54:679–708. doi:10.2165/00003495-199754050-00003.

[91] **Bryan LE, Van Den Elzen HM**. Effects of membrane-energy mutations and cations on streptomycin and gentamicin accumulation by bacteria: a model for entry of streptomycin and gentamicin in susceptible and resistant bacteria. Antimicrob Agents Chemother 1977;12:163–77. doi:10.1128/AAC.12.2.163.

[92] **Lobritz MA, Belenky P, Porter CBM, Gutierrez A, Yang JH, Schwarz EG, et al.** Antibiotic efficacy is linked to bacterial cellular respiration. Proc Natl Acad Sci U S A 2015;112:8173–80. doi:10.1073/pnas.1509743112.

[93] **Garcia LG, Lemaire S, Kahl BC, Becker K, Proctor RA, Denis O, et al.** Antibiotic activity against small-colony variants of Staphylococcus aureus: review of in vitro, animal and clinical data. J Antimicrob Chemother 2013;68:1455–64. doi:10.1093/jac/dkt072.

[94] **Painter KL, Strange E, Parkhill J, Bamford KB, Armstrong-James D, Edwards AM**. Staphylococcus aureus adapts to oxidative stress by producing H2O2-resistant small-colony variants via the SOS response. Infect Immun 2015;83:1830–44. doi:10.1128/IAI.03016-14.

[95] **Leimer N, Rachmühl C, Palheiros Marques M, Bahlmann AS, Furrer A, Eichenseher F, et al.** Nonstable *Staphylococcus aureus* Small-Colony Variants Are Induced by Low pH and Sensitized to Antimicrobial Therapy by Phagolysosomal Alkalinization. J Infect Dis 2016;213:305–13. doi:10.1093/infdis/jiv388.

[96] **Eng RH, Padberg FT, Smith SM, Tan EN, Cherubin CE**. Bactericidal effects of antibiotics on slowly growing and nongrowing bacteria. Antimicrob Agents Chemother 1991;35:1824–8.

[97] **Amato SM, Brynildsen MP**. Nutrient Transitions Are a Source of Persisters in Escherichia coli Biofilms. PLoS One 2014;9:e93110. doi:10.1371/journal.pone.0093110.

[98] **Stewart PS, Franklin MJ**. Physiological heterogeneity in biofilms. Nat Rev Microbiol 2008;6:199–210. doi:10.1038/nrmicro1838.

[99] **Borriello G, Richards L, Ehrlich GD, Stewart PS**. Arginine or nitrate enhances antibiotic susceptibility of Pseudomonas aeruginosa in biofilms. Antimicrob Agents Chemother 2006;50:382–4. doi:10.1128/AAC.50.1.382-384.2006.

[100] **Waters EM, Rowe SE, O'Gara JP, Conlon BP**. Convergence of Staphylococcus aureus Persister and Biofilm Research: Can Biofilms Be Defined as Communities of Adherent Persister Cells? PLOS Pathog 2016;12:e1006012. doi:10.1371/journal.ppat.1006012.

[101] **Uhlemann AC, Otto M, Lowy FD, DeLeo FR**. Evolution of community- and healthcare-associated methicillin-resistant Staphylococcus aureus. Infect Genet Evol 2014;21:563–74. doi:10.1016/j.meegid.2013.04.030.

[102] **van Belkum A, Melles DC, Nouwen J, van Leeuwen WB, van Wamel W, Vos MC, et al.** Co-evolutionary aspects of human colonisation and infection by Staphylococcus aureus. Infect Genet Evol 2009;9:32–47. doi:10.1016/j.meegid.2008.09.012.

[103] **David MZ, Daum RS**. Community-associated methicillin-resistant Staphylococcus aureus: Epidemiology and clinical consequences of an emerging epidemic. Clin Microbiol Rev 2010;23:616–87. doi:10.1128/CMR.00081-09.

[104] **Lowy FD**. Staphylococcus aureus infections. N Engl J Med 1998;339:2026. doi:10.1056/nejm199812313392716.

[105] **Johnson LB, Almoujahed MO, Ilg K, Maolood L, Khatib R**. Staphylococcus aureus bacteremia: Compliance with standard treatment, long-term outcome and predictors of relapse. Scand J Infect Dis 2003;35:782–9. doi:10.1080/00365540310016682.

[106] **Fowler VG, Boucher HW, Corey GR, Abrutyn E, Karchmer AW, Rupp ME, et al.** Daptomycin versus standard therapy for bacteremia and endocarditis caused by Staphylococcus aureus. N Engl J Med 2006;355:653–65. doi:10.1056/NEJMoa053783.

[107] **Yoon YK, Kim JY, Park DW, Sohn JW, Kim M**J. Predictors of persistent methicillin-resistant Staphylococcus aureus bacteraemia in patients treated with vancomycin. J Antimicrob Chemother 2010;65:1015–8. doi:10.1093/jac/dkq050.

[108] **Kullar R, Davis SL, Levine DP, Rybak MJ**. Impact of vancomycin exposure on outcomes in patients with methicillin-resistant staphylococcus aureus bacteremia: Support for consensus guidelines suggested targets. Clin Infect Dis 2011;52:975–81. doi:10.1093/cid/cir124.

[109] **Balasubramanian D, Harper L, Shopsin B, Torres VJ**. Staphylococcus aureus pathogenesis in diverse host environments. Pathog Dis 2017;75. doi:10.1093/femspd/ftx005.

[110] **Heinemann M, Kümmel A, Ruinatscha R, Panke S**. In silico genome-scale

reconstruction and validation of the Staphylococcus aureus metabolic network. Biotechnol Bioeng 2005;92:850–64. doi:10.1002/bit.20663.

[111] **Leibig M, Liebeke M, Mader D, Lalk M, Peschel A, Götz F**. Pyruvate formate lyase acts as a formate supplier for metabolic processes during anaerobiosis in Staphylococcus aureus. J Bacteriol 2011;193:952–62. doi:10.1128/JB.01161-10.

[112] **Richardson AR, Libby SJ, Fang FC**. A nitric oxide-inducible lactate dehydrogenase enables Saphylococcus aureus to resist innate immunity. Science (80-) 2008;319:1672–6. doi:10.1126/science.1155207.

[113] **Fuchs S, Pané-Farré J, Kohler C, Hecker M, Engelmann S**. Anaerobic gene expression in Staphylococcus aureus. J Bacteriol 2007;189:4275–89. doi:10.1128/JB.00081-07.

[114] **Tong SYC, Davis JS, Eichenberger E, Holland TL, Fowler VG, Jr**. Staphylococcus aureus infections: epidemiology, pathophysiology, clinical manifestations, and management. Clin Microbiol Rev 2015;28:603–61. doi:10.1128/CMR.00134-14.

[115] **LaPlante KL, Mermel LA**. In vitro activities of telavancin and vancomycin against biofilm-producing Staphylococcus aureus, S. epidermidis, and Enterococcus faecalis strains. Antimicrob Agents Chemother 2009;53:3166–9. doi:10.1128/AAC.01642-08.

[116] **Cogan NG**. Effects of persister formation on bacterial response to dosing. J Theor Biol 2006;238:694–703. doi:10.1016/j.jtbi.2005.06.017.

[117] **Cogan NG, Brown J, Darres K, Petty K**. Optimal control strategies for disinfection of bacterial populations with persister and susceptible dynamics. Antimicrob Agents Chemother 2012;56:4816–26. doi:10.1128/AAC.00675-12.

[118] **Cogan NG, Szomolay B, Dindos M**. Effect of Periodic Disinfection on Persisters in a One-Dimensional Biofilm Model. Bull Math Biol 2013;75:94–123. doi:10.1007/s11538-012-9796-z.

[119] **Lechner S, Lewis K, Bertram R**. Staphylococcus aureus persisters tolerant to bactericidal antibiotics. J Mol Microbiol Biotechnol 2012;22:235–44. doi:10.1159/000342449.

[120] **Glombiewski JA, Nestoriuc Y, Rief W, Glaesmer H, Braehler E**. Medication Adherence in the General Population. PLoS One 2012;7:e50537. doi:10.1371/journal.pone.0050537.

[121] **Pieters J**. Mycobacterium tuberculosis and the Macrophage: Maintaining a Balance. Cell Host Microbe 2008;3:399–407. doi:10.1016/j.chom.2008.05.006.

[122] **Nahid P, Dorman SE, Alipanah N, Barry PM, Brozek JL, Cattamanchi A, et al.** Executive Summary: Official American Thoracic Society/Centers for Disease Control and Prevention/Infectious Diseases Society of America Clinical Practice Guidelines: Treatment of Drug-Susceptible Tuberculosis. Clin Infect Dis 2016;63:853–67. doi:10.1093/cid/ciw566.

[123] **Tola HH, Tol A, Shojaeizadeh D, Garmaroudi G**. Tuberculosis treatment non-adherence and lost to follow up among TB patients with or without HIV in developing countries: A systematic review. Iran J Public Health 2015;44:1–11.

[124] **MacNeil A, Glaziou P, Sismanidis C, Maloney S, Floyd K**. Global Epidemiology of Tuberculosis and Progress Toward Achieving Global Targets — 2017. MMWR Morb Mortal Wkly Rep 2019;68:263–6. doi:10.15585/mmwr.mm6811a3.

[125] **Doern CD**. When does 2 plus 2 equal 5? A review of antimicrobial synergy testing. J Clin Microbiol 2014;52:4124–8. doi:10.1128/JCM.01121-14.

[126] **Bhat S, Fujitani S, Potoski BA, Capitano B, Linden PK, Shutt K, et al.** Pseudomonas aeruginosa infections in the Intensive Care Unit: can the adequacy of empirical β-lactam antibiotic therapy be improved? Int J Antimicrob Agents 2007;30:458–62. doi:10.1016/j.ijantimicag.2007.05.022.

[127] **Grasela TH, Welage LS, Walawander CA, Timm EG, Pelter MA, Poirier TI, et al.** A nationwide survey of antibiotic prescribing patterns and clinical outcomes in patients with bacterial pneumonia. DICP, Ann Pharmacother 1990;24:1220–5. doi:10.1177/106002809002401215.

[128] **Tamma PD, Cosgrove SE, Maragakis LL**. Combination therapy for treatment of infections with gram-negative bacteria. Clin Microbiol Rev 2012;25:450–70. doi:10.1128/CMR.05041-11.

[129] **Fischbach MA**. Combination therapies for combating antimicrobial resistance. Curr Opin Microbiol 2011;14:519–23. doi:10.1016/j.mib.2011.08.003.

[130] **Miller MH, Feinstein SA, Chow RT**. Early effects of β-lactams on aminoglycoside uptake, bactericidal rates, and turbidimetrically measured growth inhibition in Pseudomonas aeruginosa. Antimicrob Agents Chemother 1987;31:108–10. doi:10.1128/AAC.31.1.108.

[131] **Giamarellou H, Zissis NP, Tagari G, Bouzos J**. In vitro synergistic activities of aminoglycosides and new β-lactams against multiresistant Pseudomonas aeruginosa. Antimicrob Agents Chemother 1984;25:534–6. doi:10.1128/AAC.25.4.534.

[132] **Vestergaard M, Paulander W, Marvig RL, Clasen J, Jochumsen N, Molin S, et**

al. Antibiotic combination therapy can select for broad-spectrum multidrug resistance in Pseudomonas aeruginosa. Int J Antimicrob Agents 2016;47:48–55. doi:10.1016/j.ijantimicag.2015.09.014.

[133] **Bernal P, Molina-Santiago C, Daddaoua A, Llamas MA**. Antibiotic adjuvants: Identification and clinical use. Microb Biotechnol 2013;6:445–9. doi:10.1111/1751-7915.12044.

[134] **Rolinson GN**. Naturally-occurring β-lactamase inhibitors with antibacterial activity. J Antibiot (Tokyo) 1976;29:668–9. doi:10.7164/antibiotics.29.668.

[135] **Kitahara T, Koyama N, Matsuda J, Aoyama Y, Hirakata Y, Kamihira S, et al.** Antimicrobial activity of saturated fatty acids and fatty amines against methicillin-resistant Staphylococcus aureus. Biol Pharm Bull 2004;27:1321–6. doi:10.1248/bpb.27.1321.

[136] **Kim W, Zhu W, Hendricks GL, Van Tyne D, Steele AD, Keohane CE, et al.** A new class of synthetic retinoid antibiotics effective against bacterial persisters. Nature 2018;556:103–7. doi:10.1038/nature26157.

[137] **Pletzer D, Mansour SC, Hancock REW**. Synergy between conventional antibiotics and anti-biofilm peptides in a murine, sub-cutaneous abscess model caused by recalcitrant ESKAPE pathogens. PLOS Pathog 2018;14:e1007084. doi:10.1371/journal.ppat.1007084.

[138] **Hurdle JG, O'Neill AJ, Chopra I, Lee RE**. Targeting bacterial membrane function: An underexploited mechanism for treating persistent infections. Nat Rev Microbiol 2011;9:62–75. doi:10.1038/nrmicro2474.

[139] **Sohlenkamp C, Geiger O**. Bacterial membrane lipids: diversity in structures and pathways. FEMS Microbiol Rev 2016;40:133–59. doi:10.1093/femsre/fuv008.

[140] **Silverman JA, Perlmutter NG, Shapiro HM**. Correlation of daptomycin bactericidal activity and membrane depolarization in Staphylococcus aureus. Antimicrob Agents Chemother 2003;47:2538–44. doi:10.1128/AAC.47.8.2538-2544.2003.

[141] **Straus SK, Hancock REW**. Mode of action of the new antibiotic for Gram-positive pathogens daptomycin: Comparison with cationic antimicrobial peptides and lipopeptides. Biochim Biophys Acta - Biomembr 2006;1758:1215–23. doi:10.1016/j.bbamem.2006.02.009.

[142] **Nakatsuji T, Kao MC, Fang JY, Zouboulis CC, Zhang L, Gallo RL, et al.** Antimicrobial property of lauric acid against propionibacterium acnes: Its therapeutic potential for inflammatory acne vulgaris. J Invest Dermatol 2009;129:2480–8. doi:10.1038/jid.2009.93.

[143] **Schlievert PM, Peterson ML**. Glycerol Monolaurate Antibacterial Activity in Broth and Biofilm Cultures. PLoS One 2012;7:e40350. doi:10.1371/journal.pone.0040350.

[144] **Yoon B, Jackman J, Valle-González E, Cho N-J**. Antibacterial Free Fatty Acids and Monoglycerides: Biological Activities, Experimental Testing, and Therapeutic Applications. Int J Mol Sci 2018;19:1114. doi:10.3390/ijms19041114.

[145] **Gupta S, Bhatia G, Sharma A, Saxena S**. Host defense peptides: An insight into the antimicrobial world. J Oral Maxillofac Pathol 2018;22:239–44. doi:10.4103/jomfp.JOMFP_113_16.

[146] **Conlon BP, Nakayasu ES, Fleck LE, LaFleur MD, Isabella VM, Coleman K, et al.** Activated ClpP kills persisters and eradicates a chronic biofilm infection. Nature 2013;503:365–70. doi:10.1038/nature12790.

[147] **Li DHS, Chung YS, Gloyd M, Joseph E, Ghirlando R, Wright GD, et al.** Acyldepsipeptide antibiotics induce the formation of a structured axial channel in ClpP: A model for the ClpX/ClpA-bound state of ClpP. Chem Biol 2010;17:959–69. doi:10.1016/j.chembiol.2010.07.008.

[148] **Lee BG, Park EY, Lee KE, Jeon H, Sung KH, Paulsen H, et al.** Structures of ClpP in complex with acyldepsipeptide antibiotics reveal its activation mechanism. Nat Struct Mol Biol 2010;17:471–8. doi:10.1038/nsmb.1787.

[149] **Allison KR, Brynildsen MP, Collins JJ**. Metabolite-enabled eradication of bacterial persisters by aminoglycosides. Nature 2011;473:216–20. doi:10.1038/nature10069.

[150] **Prax M, Mechler L, Weidenmaier C, Bertram R**. Glucose Augments Killing Efficiency of Daptomycin Challenged Staphylococcus aureus Persisters. PLoS One 2016;11:e0150907. doi:10.1371/journal.pone.0150907.

[151] Committee opinion No. 485: Prevention of early-onset group B streptococcal disease in newborns. Obstet Gynecol 2011;117:1019–27. doi:10.1097/AOG.0b013e318219229b.

[152] **Lerminiaux NA, Cameron ADS**. Horizontal transfer of antibiotic resistance genes in clinical environments. Can J Microbiol 2019;65:34–44. doi:10.1139/cjm-2018-0275.

[153] **Theriot CM, Koenigsknecht MJ, Carlson PE, Hatton GE, Nelson AM, Li B, et al.** Antibiotic-induced shifts in the mouse gut microbiome and metabolome increase susceptibility to Clostridium difficile infection. Nat Commun 2014;5. doi:10.1038/ncomms4114.

[154] **Steele S, Radlinski L, Taft-Benz S, Brunton J, Kawula TH**. Trogocytosis-associated cell to cell spread of intracellular bacterial pathogens. Elife 2016;5. doi:10.7554/eLife.10625.

[155] **Melander RJ, Zurawski D V., Melander C**. Narrow-spectrum antibacterial agents. Medchemcomm 2018;9:12–21. doi:10.1039/c7md00528h.

[156] **Litvak Y, Byndloss MX, Tsolis RM, Bäumler AJ**. Dysbiotic Proteobacteria expansion: a microbial signature of epithelial dysfunction. Curr Opin Microbiol 2017;39:1–6. doi:10.1016/j.mib.2017.07.003.

[157] **Lopez CA, Miller BM, Rivera-Chávez F, Velazquez EM, Byndloss MX, Chávez-Arroyo A, et al.** Virulence factors enhance Citrobacter rodentium expansion through aerobic respiration. Science (80-) 2016;353:1249–53. doi:10.1126/science.aag3042.

[158] **Byndloss MX, Olsan EE, Rivera-Chávez F, Tiffany CR, Cevallos SA, Lokken KL, et al.** Microbiota-activated PPAR-γ signaling inhibits dysbiotic Enterobacteriaceae expansion. Science (80-) 2017;357:570–5. doi:10.1126/science.aam9949.

[159] **Rousseaux C, El-Jamal N, Fumery M, Dubuquoy C, Romano O, Chatelain D, et al.** The 5-aminosalicylic acid antineoplastic effect in the intestine is mediated by PPARγ. Carcinogenesis 2013;34:2580–6. doi:10.1093/carcin/bgt245.

[160] **Hu Y, Helm JS, Chen L, Ginsberg C, Gross B, Kraybill B, et al.** Identification of selective inhibitors for the glycosyltransferase murg via high-throughput screening. Chem Biol 2004;11:703–11. doi:10.1016/j.chembiol.2004.02.024.

[161] **Goldman R, Kohlbrenner W, Lartey P, Pernet A.** Antibacterial agents specifically inhibiting lipopolysaccharide synthesis. Nature 1987;329:162–4. doi:10.1038/329162a0.

[162] **Barh D, Tiwari S, Jain N, Ali A, Santos AR, Misra AN, et al.** In silico subtractive genomics for target identification in human bacterial pathogens. Drug Dev Res 2011;72:162–77. doi:10.1002/ddr.20413.

[163] **Pechous R, Celli J, Penoske R, Hayes SF, Frank DW, Zahrt TC**. Construction and characterization of an attenuated purine auxotroph in a Francisella tularensis live vaccine strain. Infect Immun 2006;74:4452–61. doi:10.1128/IAI.00666-06.

[164] **Pechous RD, McCarthy TR, Zahrt TC**. Working toward the future: insights into Francisella tularensis pathogenesis and vaccine development. Microbiol Mol Biol Rev 2009;73:684–711. doi:10.1128/MMBR.00028-09.

[165] **Eisenreich W, Dandekar T, Heesemann J, Goebel W**. Carbon metabolism of intracellular bacterial pathogens and possible links to virulence. Nat Rev Microbiol 2010;8:401–12. doi:10.1038/nrmicro2351.

[166] **Knodler LA, Finlay BB, Steele-Mortimer O**. The Salmonella Effector Protein SopB Protects Epithelial Cells from Apoptosis by Sustained Activation of Akt. J Biol Chem 2005;280:9058–64. doi:10.1074/jbc.M412588200.

[167] **Gillmaier N, Götz A, Schulz A, Eisenreich W, Goebel W, Muñoz-Elías E, et al.** Metabolic Responses of Primary and Transformed Cells to Intracellular Listeria monocytogenes. PLoS One 2012;7:e52378. doi:10.1371/journal.pone.0052378.

[168] **Kuhle V, Abrahams GL, Hensel M**. Intracellular Salmonella enterica Redirect Exocytic Transport Processes in a Salmonella Pathogenicity Island 2-Dependent Manner. Traffic 2006;7:716–30. doi:10.1111/j.1600-0854.2006.00422.x.

[169] **Cocchiaro JL, Kumar Y, Fischer ER, Hackstadt T, Valdivia RH**. Cytoplasmic lipid droplets are translocated into the lumen of the Chlamydia trachomatis parasitophorous vacuole. Proc Natl Acad Sci 2008;105:9379–84. doi:10.1073/pnas.0712241105.

[170] **Daniel J, Maamar H, Deb C, Sirakova TD, Kolattukudy PE**. Mycobacterium tuberculosis Uses Host Triacylglycerol to Accumulate Lipid Droplets and Acquires a Dormancy-Like Phenotype in Lipid-Loaded Macrophages. PLoS Pathog 2011;7:e1002093. doi:10.1371/journal.ppat.1002093.

[171] **Verjans GM, Ringrose JH, van Alphen L, Feltkamp TE, Kusters JG**. Entrance and survival of Salmonella typhimurium and Yersinia enterocolitica within human B- and T-cell lines. Infect Immun 1994;62:2229–35.

[172] **Vazquez-Terres A, Jones-Carson J, Bäumler AJ, Falkow S, Valdivia R, Brown W, et al.** Extraintestinal dissemination of Salmonella by CD18-expressing phagocytes. Nature 1999;401:804–8. doi:10.1038/44593.

[173] **Mörner T**. The ecology of tularaemia. Rev Sci Tech 1992;11:1123–30. doi:10.20506/rst.11.4.657.

[174] **Hall JD, Craven RR, Fuller JR, Pickles RJ, Kawula TH**. Francisella tularensis Replicates within Alveolar Type II Epithelial Cells In Vitro and In Vivo following Inhalation. Infect Immun 2007;75:1034–9. doi:10.1128/IAI.01254-06.

[175] **Hall JD, Woolard MD, Gunn BM, Craven RR, Taft-Benz S, Frelinger JA, et al.** Infected-host-cell repertoire and cellular response in the lung following inhalation of Francisella tularensis Schu S4, LVS, or U112. Infect Immun 2008;76:5843–52. doi:10.1128/IAI.01176-08.

[176] **McCaffrey RL, Allen L-AH**. Francisella tularensis LVS evades killing by human neutrophils via inhibition of the respiratory burst and phagosome escape . J Leukoc Biol 2006;80:1224–30. doi:10.1189/jlb.0406287.

[177] **Qin A, Mann BJ**. Identification of transposon insertion mutants of Francisella tularensis tularensis strain Schu S4 deficient in intracellular replication in the hepatic cell line HepG2. BMC Microbiol 2006;6. doi:10.1186/1471-2180-6-69.

[178] **Chong A, Wehrly TD, Nair V, Fischer ER, Barker JR, Klose KE, et al.** The early phagosomal stage of Francisella tularensis determines optimal phagosomal escape and Francisella pathogenicity island protein expression. Infect Immun 2008;76:5488–99. doi:10.1128/IAI.00682-08.

[179] **Steele S, Brunton J, Ziehr B, Taft-Benz S, Moorman NN, Kawula T, et al.** Francisella tularensis Harvests Nutrients Derived via ATG5-Independent Autophagy to Support Intracellular Growth. PLoS Pathog 2013;9:e1003562. doi:10.1371/journal.ppat.1003562.

[180] **Dennis DT, Inglesby T V., Henderson DA, Bartlett JG, Ascher MS, Eitzen E, et al.** Tularemia as a biological weapon: Medical and public health management. J Am Med Assoc 2001;285:2763–73. doi:10.1001/jama.285.21.2763.

[181] **Saslaw S, Eigelsbach HT, Prior JA, Wilson HE, Carhart S.** Tularemia vaccine study. II. Respiratory challenge. Arch Intern Med 1961;107:702–14. doi:10.1001/archinte.1961.03620050068007.

[182] **Saslaw S, Eigelsbach HT, Wilson HE, Prior JA, Carhart S.** Tularemia vaccine study. I. Intracutaneous challenge. Arch Intern Med 1961;107:689–701. doi:10.1001/archinte.1961.03620050055006.

[183] **Champion MD, Zeng Q, Nix EB, Nano FE, Keim P, Kodira CD, et al.** Comparative Genomic Characterization of Francisella tularensis Strains Belonging to Low and High Virulence Subspecies. PLoS Pathog 2009;5:e1000459. doi:10.1371/journal.ppat.1000459.

[184] **Levin BR, Rozen DE**. Non-inherited antibiotic resistance. Nat Rev Microbiol 2006;4:556–62. doi:10.1038/nrmicro1445.

[185] **Kubicek-Sutherland JZ, Lofton H, Vestergaard M, Hjort K, Ingmer H, Andersson DI**. Antimicrobial peptide exposure selects for Staphylococcus aureus resistance to human defence peptides. J Antimicrob Chemother 2017;72:115–27. doi:10.1093/jac/dkw381.

[186] **Kong EF, Tsui C, Kucharíková S, Andes D, Van Dijck P, Jabra-Rizk MA**. Commensal Protection of Staphylococcus aureus against Antimicrobials by Candida albicans Biofilm Matrix. MBio 2016;7:e01365-16.

doi:10.1128/mBio.01365-16.

[187] **Radlinski L, Conlon BP**. Antibiotic efficacy in the complex infection environment. Curr Opin Microbiol 2018;42:19–24. doi:10.1016/J.MIB.2017.09.007.

[188] **Weimer KED, Juneau RA, Murrah KA, Pang B, Armbruster CE, Richardson SH, et al.** Divergent mechanisms for passive pneumococcal resistance to β-Lactam antibiotics in the presence of Haemophilus influenzae. J Infect Dis 2011;203:549–55. doi:10.1093/infdis/jiq087.

[189] **Brook I**. The role of beta-lactamase-producing-bacteria in mixed infections. BMC Infect Dis 2009;9. doi:10.1186/1471-2334-9-202.

[190] **Nicoloff H. H, Andersson DI**. Indirect resistance to several classes of antibiotics in cocultures with resistant bacteria expressing antibiotic-modifying or -degrading enzymes. J Antimicrob Chemother 2016;71:100–10. doi:10.1093/jac/dkv312.

[191] **Gjødsbøl K, Christensen JJ, Karlsmark T, Jørgensen B, Klein BM, Krogfelt KA**. Multiple bacterial species reside in chronic wounds: a longitudinal study. Int Wound J 2006;3:225–31. doi:10.1111/j.1742-481X.2006.00159.x.

[192] **Pastar I, Nusbaum AG, Gil J, Patel SB, Chen J, Valdes J, et al**. Interactions of Methicillin Resistant Staphylococcus aureus USA300 and Pseudomonas aeruginosa in Polymicrobial Wound Infection. PLoS One 2013;8:e56846. doi:10.1371/journal.pone.0056846.

[193] **Hendricks KJ, Burd TA, Anglen JO, Simpson AW, Christensen GD, Gainor BJ**. Synergy between Staphylococcus aureus and Pseudomonas aeruginosa in a rat model of complex orthopaedic wounds. J Bone Joint Surg Am 2001;83-A:855–61.

[194] **Duan K, Dammel C, Stein J, Rabin H, Surette MG**. Modulation of Pseudomonas aeruginosa gene expression by host microflora through interspecies communication. Mol Microbiol 2003;50:1477–91.

[195] **Nguyen AT, Jones JW, Cámara M, Williams P, Kane MA, Oglesby-Sherrouse AG**. Cystic Fibrosis Isolates of Pseudomonas aeruginosa Retain Iron-Regulated Antimicrobial Activity against Staphylococcus aureus through the Action of Multiple Alkylquinolones. Front Microbiol 2016;7:1171. doi:10.3389/fmicb.2016.01171.

[196] **Filkins LM, Graber JA, Olson DG, Dolben EL, Lynd LR, Bhuju S, et al.** Coculture of Staphylococcus aureus with Pseudomonas aeruginosa Drives S. aureus towards Fermentative Metabolism and Reduced Viability in a Cystic Fibrosis Model. J Bacteriol 2015;197:2252–64. doi:10.1128/JB.00059-15.

[197] **Machan ZA, Taylor GW, Pitt TL, Cole PJ, Wilson R**. 2-Heptyl-4-hydroxyquinoline N-oxide, an antistaphylococcal agent produced by Pseudomonas aeruginosa. J Antimicrob Chemother 1992;30:615–23.

[198] **Kessler E, Safrin M, Olson JC, Ohman DE**. Secreted LasA of Pseudomonas aeruginosa is a staphylolytic protease. J Biol Chem 1993;268:7503–8.

[199] **Bharali P, Saikia JP, Ray A, Konwar BK**. Rhamnolipid (RL) from Pseudomonas aeruginosa OBP1: A novel chemotaxis and antibacterial agent. Colloids Surfaces B Biointerfaces 2013;103:502–9. doi:10.1016/J.COLSURFB.2012.10.064.

[200] **Haba E, Pinazo A, Jauregui O, Espuny MJ, Infante MR, Manresa A**. Physicochemical characterization and antimicrobial properties of rhamnolipids produced by Pseudomonas aeruginosa 47T2 NCBIM 40044. Biotechnol Bioeng 2003;81:316–22. doi:10.1002/bit.10474.

[201] **Baldan R, Cigana C, Testa F, Bianconi I, De Simone M, Pellin D, et al.** Adaptation of Pseudomonas aeruginosa in Cystic Fibrosis Airways Influences Virulence of Staphylococcus aureus In Vitro and Murine Models of Co-Infection. PLoS One 2014;9:e89614. doi:10.1371/journal.pone.0089614.

[202] **Wakeman CA, Moore JL, Noto MJ, Zhang Y, Singleton MD, Prentice BM, et al.** The innate immune protein calprotectin promotes Pseudomonas aeruginosa and Staphylococcus aureus interaction. Nat Commun 2016;7. doi:10.1038/ncomms11951.

[203] **Smith AC, Rice A, Sutton B, Gabrilska R, Wessel AK, Whiteley M, et al.** Albumin inhibits Pseudomonas aeruginosa quorum sensing and alters polymicrobial interactions. Infect Immun 2017;85. doi:10.1128/IAI.00116-17.

[204] **Read RC, Roberts P, Munro N, Rutman A, Hastie A, Shryock T, et al.** Effect of Pseudomonas aeruginosa rhamnolipids on mucociliary transport and ciliary beating. J Appl Physiol 1992;72:2271–7.

[205] **Kownatzki R, Tümmler B, Döring G**. Rhamnolipid of Pseudomonas aeruginosa in sputum of cystic fibrosis patients. Lancet 1987;329:1026–7. doi:10.1016/S0140-6736(87)92286-0.

[206] **Barr HL, Halliday N, Cámara M, Barrett DA, Williams P, Forrester DL, et al.** Pseudomonas aeruginosa quorum sensing molecules correlate with clinical status in cystic fibrosis. Eur Respir J 2015;46:1046–54. doi:10.1183/09031936.00225214.

[207] **O'Brien S, Williams D, Fothergill JL, Paterson S, Winstanley C, Brockhurst MA**. High virulence sub-populations in Pseudomonas aeruginosa long-term cystic fibrosis airway infections. BMC Microbiol 2017;17. doi:10.1186/s12866-017-0941-

6.

[208] **Hunter RC, Klepac-Ceraj V, Lorenzi MM, Grotzinger H, Martin TR, Newman DK**. Phenazine content in the cystic fibrosis respiratory tract negatively correlates with lung function and microbial complexity. Am J Respir Cell Mol Biol 2012;47:738–45. doi:10.1165/rcmb.2012-0088OC.

[209] **Mates SM, Eisenberg ES, Mandel LJ, Patel L, Kaback HR, Miller MH**. Membrane potential and gentamicin uptake in Staphylococcus aureus. Proc Natl Acad Sci U S A 1982;79:6693–7.

[210] **Sotirova A V., Spasova DI, Galabova DN, Karpenko E, Shulga A**. Rhamnolipid–Biosurfactant Permeabilizing Effects on Gram-Positive and Gram-Negative Bacterial Strains. Curr Microbiol 2008;56:639–44. doi:10.1007/s00284-008-9139-3.

[211] **Bjarnsholt T, Jensen PØ, Jakobsen TH, Phipps R, Nielsen AK, Rybtke MT, et al.** Quorum Sensing and Virulence of Pseudomonas aeruginosa during Lung Infection of Cystic Fibrosis Patients. PLoS One 2010;5:e10115. doi:10.1371/journal.pone.0010115.

[212] **Lépine F, Milot S, Déziel E, He J, Rahme LG**. Electrospray/mass spectrometric identification and analysis of 4-hydroxy-2-alkylquinolines (HAQs) produced by Pseudomonas aeruginosa. J Am Soc Mass Spectrom 2004;15:862–9. doi:10.1016/j.jasms.2004.02.012.

[213] **Jain DK, Collins-Thompson DL, Lee H, Trevors JT**. A drop-collapsing test for screening surfactant-producing microorganisms. J Microbiol Methods 1991;13:271–9. doi:10.1016/0167-7012(91)90064-W.

[214] **Ryall B, Davies JC, Wilson R, Shoemark A, Williams HD**. Pseudomonas aeruginosa, cyanide accumulation and lung function in CF and non-CF bronchiectasis patients 2008;32(3):740-7. doi:10.1183/09031936.00159607.

[215] **Thierbach S, Birmes FS, Letzel MC, Hennecke U, Fetzner S**. Chemical Modification and Detoxification of the Pseudomonas aeruginosa Toxin 2-Heptyl-4-hydroxyquinoline N-Oxide by Environmental and Pathogenic Bacteria. ACS Chem Biol 2017;12:2305–12. doi:10.1021/acschembio.7b00345.

[216] **Grande KK, Gustin JK, Kessler E, Ohman DE**. Identification of critical residues in the propeptide of LasA protease of Pseudomonas aeruginosa involved in the formation of a stable mature protease. J Bacteriol 2007;189:3960–8. doi:10.1128/JB.01828-06.

[217] **Neely CJ, Kartchner LB, Mendoza AE, Linz BM, Frelinger JA, Wolfgang MC, et al.** Flagellin treatment prevents increased susceptibility to systemic bacterial

infection after injury by inhibiting anti-inflammatory IL-10+ IL-12- neutrophil polarization. PLoS One 2014;9. doi:10.1371/journal.pone.0085623.

[218] **Cowell BA, Twining SS, Hobden JA, Kwong MSF, Fleiszig SMJ**. Mutation of lasA and lasB reduces Pseudomonas aeruginosa invasion of epithelial cells. Microbiology 2003;149:2291–9. doi:10.1099/mic.0.26280-0.

[219] **White CD, Alionte LG, Cannon BM, Caballero AR, O'Callaghan RJ, Hobden JA.** Corneal virulence of LasA protease - Deficient Pseudomonas aeruginosa PAO1. Cornea 2001;20:643–6. doi:10.1097/00003226-200108000-00017.

[220] **Limoli DH, Yang J, Khansaheb MK, Helfman B, Peng L, Stecenko AA, et al.** Staphylococcus aureus and Pseudomonas aeruginosa co-infection is associated with cystic fibrosis-related diabetes and poor clinical outcomes. Eur J Clin Microbiol Infect Dis 2016;35:947–53. doi:10.1007/s10096-016-2621-0.

[221] **Burmølle M, Webb JS, Rao D, Hansen LH, Sørensen SJ, Kjelleberg S**. Enhanced biofilm formation and increased resistance to antimicrobial agents and bacterial invasion are caused by synergistic interactions in multispecies biofilms. Appl Environ Microbiol 2006;72:3916–23. doi:10.1128/AEM.03022-05.

[222] **Beaudoin T, Yau YCW, Stapleton PJ, Gong Y, Wang PW, Guttman DS, et al.** Staphylococcus aureus interaction with Pseudomonas aeruginosa biofilm enhances tobramycin resistance. Npj Biofilms Microbiomes 2017;3. doi:10.1038/s41522-017-0035-0.

[223] **Hoffman LR, Kulasekara HD, Emerson J, Houston LS, Burns JL, Ramsey BW, et al.** Pseudomonas aeruginosa lasR mutants are associated with cystic fibrosis lung disease progression. J Cyst Fibros 2009;8:66–70. doi:10.1016/J.JCF.2008.09.006.

[224] **Limoli DH, Whitfield GB, Kitao T, Ivey ML, Davis MR, Grahl N, et al.** Pseudomonas aeruginosa Alginate Overproduction Promotes Coexistence with Staphylococcus aureus in a Model of Cystic Fibrosis Respiratory Infection. MBio 2017;8. doi:10.1128/mBio.00186-17.

[225] **LiPuma JJ**. The changing microbial epidemiology in cystic fibrosis. Clin Microbiol Rev 2010;23:299–323. doi:10.1128/CMR.00068-09.

[226] **Held K, Ramage E, Jacobs M, Gallagher L, Manoil C**. Sequence-verified two-allele transposon mutant library for Pseudomonas aeruginosa PAO1. J Bacteriol 2012;194:6387–9. doi:10.1128/JB.01479-12.

[227] **Hoang TT, Karkhoff-Schweizer RR, Kutchma AJ, Schweizer HP**. A broad-host-range F1p-FRT recombination system for site-specific excision of chromosomally-located DNA sequences: Application for isolation of unmarked

Pseudomonas aeruginosa mutants. Gene 1998;212:77–86. doi:10.1016/S0378-1119(98)00130-9.

[228] **Cheung AL, Nast CC, Bayer AS**. Selective activation of sar promoters with the use of green fluorescent protein transcriptional fusions as the detection system in the rabbit endocarditis model. Infect Immun 1998;66:5988–93.

[229] **Szałek E, Kamińska A, Gozdzik-Spychalska J, Grześkowiak E, Batura-Gabryel H**. The PK/PD index (CMAX/MIC) for ciprofloxacin in patients with cystic fibrosis. Acta Pol Pharm 2011;68:777–83.

[230] **Burkhardt O**. Once-daily tobramycin in cystic fibrosis: better for clinical outcome than thrice-daily tobramycin but more resistance development? J Antimicrob Chemother 2006;58:822–9. doi:10.1093/jac/dkl328.

[231] **Barcia-Macay M, Lemaire S, Mingeot-Leclercq MP, Tulkens PM, Van Bambeke F**. Evaluation of the extracellular and intracellular activities (human THP-1 macrophages) of telavancin versus vancomycin against methicillin-susceptible, methicillin-resistant, vancomycin-intermediate and vancomycin-resistant Staphylococcus aureus. J Antimicrob Chemother 2006;58:1177–84. doi:10.1093/jac/dkl424.

[232] **Ruddy J, Emerson J, Moss R, Genatossio A, McNamara S, Burns JL, et al.** Sputum tobramycin concentrations in cystic fibrosis patients with repeated administration of inhaled tobramycin. J Aerosol Med Pulm Drug Deliv 2013;26:69–75. doi:10.1089/jamp.2011.0942.

[233] **Rohweddei R, Bergan T, Caruso E, Thorsteinsson SB, Torre HD, Scholl H**. Penetration of ciprofloxacin and metabolites into human lung, bronchial and pleural tissue after 250 and 500 mg oral ciprofloxacin. Chemotherapy 1991;37:229–38. doi:10.1159/000238860.

[234] **Sundin DP, Meyer C, Dahl R, Geerdes A, Sandoval R, Molitoris BA**. Cellular mechanism of aminoglycoside tolerance in long-term gentamicin treatment. Am J Physiol 1997;272:C1309-18.

[235] **Kourtis AP, Hatfield K, Baggs J, Mu Y, See I, Epson E, et al.** *Vital Signs:* Epidemiology and Recent Trends in Methicillin-Resistant and in Methicillin-Susceptible *Staphylococcus aureus* Bloodstream Infections — United States. MMWR Morb Mortal Wkly Rep 2019;68:214–9. doi:10.15585/mmwr.mm6809e1.

[236] **Walraven CJ, North MS, Marr-Lyon L, Deming P, Sakoulas G, Mercier R-C**. Site of infection rather than vancomycin MIC predicts vancomycin treatment failure in methicillin-resistant Staphylococcus aureus bacteraemia. J Antimicrob Chemother 2011;66:2386–92. doi:10.1093/jac/dkr301.

[237] **Hancock RE, Raffle VJ, Nicas TI**. Involvement of the outer membrane in gentamicin and streptomycin uptake and killing in Pseudomonas aeruginosa. Antimicrob Agents Chemother 1981;19:777–85. doi:10.1128/aac.19.5.777.

[238] **Andrey K, Bockrath RC**. Dihydrostreptomycin accumulation in E. coli. Nature 1974;251:534–6. doi:10.1038/251534a0.

[239] **Davis BD**. Mechanism of bactericidal action of aminoglycosides. Microbiol Rev 1987;51:341–50.

[240] **Bryan LE, Kowand SK, Van Den Elzen HM**. Mechanism of aminoglycoside antibiotic resistance in anaerobic bacteria: Clostridium perfringens and Bacteroides fragilis. Antimicrob Agents Chemother 1979;15:7–13.

[241] **Eliopoulos GM**. Synergism and antagonism. Infect Dis Clin North Am 1989;3:399–406.

[242] **Scaglione F, Dugnani S, Demartini G, Arcidiacono MM, Cocuzza CE, Fraschini F**. Bactericidal Kinetics of an in vitro Infection Model of Once-Daily Ceftriaxone plus Amikacin against Gram-Positive and Gram-Negative Bacteria. Chemotherapy 1995;41:239–46. doi:10.1159/000239351.

[243] **Rhodes A, Evans LE, Alhazzani W, Levy MM, Antonelli M, Ferrer R, et al.** Surviving Sepsis Campaign: International Guidelines for Management of Sepsis and Septic Shock: 2016. Intensive Care Med 2017;43:304–77. doi:10.1007/s00134-017-4683-6.

[244] **Wise EM, Park JT, Park JT**. Penicillin: its basic site of action as an inhibitor of a peptide cross-linking reaction in cell wall mucopeptide synthesis. Proc Natl Acad Sci U S A 1965;54:75–81. doi:10.1073/pnas.54.1.75.

[245] **Mehta S, Singh C, Plata KB, Chanda PK, Paul A, Riosa S, et al.** β-Lactams increase the antibacterial activity of daptomycin against clinical methicillin-resistant Staphylococcus aureus strains and prevent selection of daptomycin-resistant derivatives. Antimicrob Agents Chemother 2012;56:6192–200. doi:10.1128/AAC.01525-12.

[246] **Farha MA, Verschoor CP, Bowdish D, Brown ED**. Collapsing the Proton Motive Force to Identify Synergistic Combinations against Staphylococcus aureus. Chem Biol 2013;20:1168–78. doi:10.1016/j.chembiol.2013.07.006.

[247] **Lebeaux D, Chauhan A, Létoffé S, Fischer F, de Reuse H, Beloin C, et al.** pH-Mediated Potentiation of Aminoglycosides Kills Bacterial Persisters and Eradicates In Vivo Biofilms. J Infect Dis 2014;210:1357–66. doi:10.1093/infdis/jiu286.

[248] **Hess DJ, Henry-Stanley MJ, Wells CL**. Antibacterial synergy of glycerol monolaurate and aminoglycosides in Staphylococcus aureus biofilms. Antimicrob Agents Chemother 2014;58:6970–3. doi:10.1128/AAC.03672-14.

[249] **Haba E, Pinazo A, Pons R, Pérez L, Manresa A**. Complex rhamnolipid mixture characterization and its influence on DPPC bilayer organization. Biochim Biophys Acta - Biomembr 2014;1838:776–83. doi:10.1016/J.BBAMEM.2013.11.004.

[250] **Aleksic I, Petkovic M, Jovanovic M, Milivojevic D, Vasiljevic B, Nikodinovic-Runic J, et al.** Anti-biofilm Properties of Bacterial Di-Rhamnolipids and Their Semi-Synthetic Amide Derivatives. Front Microbiol 2017;8:2454. doi:10.3389/fmicb.2017.02454.

[251] **Lannergard J, von Eiff C, Sander G, Cordes T, Seggewiss J, Peters G, et al.** Identification of the Genetic Basis for Clinical Menadione-Auxotrophic Small-Colony Variant Isolates of Staphylococcus aureus. Antimicrob Agents Chemother 2008;52:4017–22. doi:10.1128/AAC.00668-08.

[252] **Proctor RA, von Eiff C, Kahl BC, Becker K, McNamara P, Herrmann M, et al.** Small colony variants: a pathogenic form of bacteria that facilitates persistent and recurrent infections. Nat Rev Microbiol 2006;4:295–305. doi:10.1038/nrmicro1384.

[253] **Kohanski MA, Dwyer DJ, Collins JJ.** How antibiotics kill bacteria: from targets to networks. Nat Rev Microbiol 2010;8:423–35. doi:10.1038/nrmicro2333.

[254] **Lewis K**. Persister Cells. Annu Rev Microbiol 2010;64:357–72. doi:10.1146/annurev.micro.112408.134306.

[255] **Vakulenko SB, Mobashery S**. Versatility of aminoglycosides and prospects for their future. Clin Microbiol Rev 2003;16:430–50.

[256] **Chmiel JF, Aksamit TR, Chotirmall SH, Dasenbrook EC, Elborn JS, LiPuma JJ, et al.** Antibiotic management of lung infections in cystic fibrosis. I. The microbiome, methicillin-resistant Staphylococcus aureus, gram-negative bacteria, and multiple infections. Ann Am Thorac Soc 2014;11:1120–9. doi:10.1513/AnnalsATS.201402-050AS.

[257] **Pu Y, Zhao Z, Li Y, Zou J, Ma Q, Zhao Y, et al.** Enhanced Efflux Activity Facilitates Drug Tolerance in Dormant Bacterial Cells. Mol Cell 2016;62:284–94. doi:10.1016/j.molcel.2016.03.035.

[258] **Lechner S, Prax M, Lange B, Huber C, Eisenreich W, Herbig A, et al.** Metabolic and transcriptional activities of Staphylococcus aureus challenged with high-doses of daptomycin. Int J Med Microbiol 2014;304:931–40. doi:10.1016/j.ijmm.2014.05.008.

[259] **Prax M, Bertram R**. Metabolic aspects of bacterial persisters. Front Cell Infect Microbiol 2014;4. doi:10.3389/FCIMB.2014.00148.

[260] **Gefen O, Fridman O, Ronin I, Balaban NQ**. Direct observation of single stationary-phase bacteria reveals a surprisingly long period of constant protein production activity. PNAS 2014;111. doi:10.1073/pnas.1314114111.

[261] **Ortiz A, Teruel JA, Espuny MJ, Marqués A, Manresa Á, Aranda FJ**. Effects of dirhamnolipid on the structural properties of phosphatidylcholine membranes. Int J Pharm 2006;325:99–107. doi:10.1016/j.ijpharm.2006.06.028.

[262] **Hallock KJ, Lee D-K, Ramamoorthy A**. MSI-78, an Analogue of the Magainin Antimicrobial Peptides, Disrupts Lipid Bilayer Structure via Positive Curvature Strain. Biophys J 2003;84:3052–60. doi:10.1016/S0006-3495(03)70031-9.

[263] **Grosser MR, Richardson AR**. Method for Preparation and Electroporation of S. aureus and S. epidermidis, Humana Press, New York, NY; 2014, p. 51–7. doi:10.1007/7651_2014_183.

[264] **Joshi GS, Spontak JS, Klapper DG, Richardson AR**. ACME encoded speG abrogates the unique hypersensitivity of Staphylococcus aureus to exogenous polyamines. Mol Microbiol 2011;82:9. doi:10.1111/J.1365-2958.2011.07809.X.

[265] **Forsyth RA, Haselbeck RJ, Ohlsen KL, Yamamoto RT, Xu H, Trawick JD, et al.** A genome-wide strategy for the identification of essential genes in Staphylococcus aureus. Mol Microbiol 2002;43:1387–400. doi:10.1046/j.1365-2958.2002.02832.x.

[266] **Bae T, Banger AK, Wallace A, Glass EM, Aslund F, Schneewind O, et al.** Staphylococcus aureus virulence genes identified by bursa aurealis mutagenesis and nematode killing. Proc Natl Acad Sci 2004;101:12312–7. doi:10.1073/pnas.0404728101.

[267] **Kahl BC, Goulian M, van Wamel W, Herrmann M, Simon SM, Kaplan G, et al.** Staphylococcus aureus RN6390 replicates and induces apoptosis in a pulmonary epithelial cell line. Infect Immun 2000;68:5385–92.

[268] **Orhan G, Bayram A, Zer Y, Balci I.** Synergy tests by E test and checkerboard methods of antimicrobial combinations against Brucella melitensis. J Clin Microbiol 2005;43:140–3. doi:10.1128/JCM.43.1.140-143.2005.

[269] **Sandoval R, Leiser J, Molitoris BA**. Aminoglycoside antibiotics traffic to the Golgi complex in LLC-PK1 cells. J Am Soc Nephrol 1998;9.

[270] **Peschel A, Otto M, Jack RW, Kalbacher H, Jung G, Götz F**. Inactivation of the

dlt operon in Staphylococcus aureus confers sensitivity to defensins, protegrins, and other antimicrobial peptides. J Biol Chem 1999;274:8405–10. doi:10.1074/JBC.274.13.8405.

[271] **Scheinpflug K, Krylova O, Strahl H**. Measurement of Cell Membrane Fluidity by Laurdan GP: Fluorescence Spectroscopy and Microscopy. Methods Mol. Biol., vol. 1520, Humana Press, New York, NY; 2017, p. 159–74. doi:10.1007/978-1-4939-6634-9_10.

[272] **Eswara PJ, Brzozowski RS, Viola MG, Graham G, Spanoudis C, Trebino C, et al.** An essential Staphylococcus aureus cell division protein directly regulates FtsZ dynamics. Elife 2018;7. doi:10.7554/eLife.38856.

[273] **Weinberg ED**. Nutritional immunity. Host's attempt to withold iron from microbial invaders. JAMA 1975;231:39–41.

[274] **Cassat JE, Skaar EP**. Metal ion acquisition in Staphylococcus aureus: overcoming nutritional immunity. Semin Immunopathol 2012;34:215–35. doi:10.1007/s00281-011-0294-4.

[275] **Eisenreich W, Heesemann J, Rudel T, Goebel W**. Metabolic Adaptations of Intracellullar Bacterial Pathogens and their Mammalian Host Cells during Infection ("Pathometabolism"). Microbiol Spectr 2015;3. doi:10.1128/microbiolspec.MBP-0002-2014.

[276] **Lindgren H, Honn M, Golovlev I, Kadzhaev K, Conlan W, Sjostedt A**. The 58-Kilodalton Major Virulence Factor of Francisella tularensis Is Required for Efficient Utilization of Iron. Infect Immun 2009;77:4429–36. doi:10.1128/IAI.00702-09.

[277] **Lundberg BE, Wolf RE, Dinauer MC, Xu Y, Fang FC**. Glucose 6-phosphate dehydrogenase is required for Salmonella typhimurium virulence and resistance to reactive oxygen and nitrogen intermediates. Infect Immun 1999;67:436–8.

[278] **Gobert AP, McGee DJ, Akhtar M, Mendz GL, Newton JC, Cheng Y, et al.** Helicobacter pylori arginase inhibits nitric oxide production by eukaryotic cells: a strategy for bacterial survival. Proc Natl Acad Sci U S A 2001;98:13844–9. doi:10.1073/pnas.241443798.

[279] **Bryk R, Lima CD, Erdjument-Bromage H, Tempst P, Nathan C, Nathan C, et al.** Metabolic enzymes of mycobacteria linked to antioxidant defense by a thioredoxin-like protein. Science 2002;295:1073–7. doi:10.1126/science.1067798.

[280] **Eisenreich W, Heesemann J, Rudel T, Goebel W**. Metabolic host responses to infection by intracellular bacterial pathogens. Front Cell Infect Microbiol 2013;3:24. doi:10.3389/fcimb.2013.00024.

[281] **Yin C, Qie S, Sang N**. Carbon source metabolism and its regulation in cancer cells. Crit Rev Eukaryot Gene Expr 2012;22:17–35.

[282] **Steele S, Brunton J, Ziehr B, Taft-Benz S, Moorman N, Kawula T**. Francisella tularensis Harvests Nutrients Derived via ATG5-Independent Autophagy to Support Intracellular Growth. PLoS Pathog 2013;9. doi:10.1371/journal.ppat.1003562.

[283] **Brunton J, Steele S, Miller C, Lovullo E, Taft-Benz S, Kawula T**. Identifying Francisella tularensis genes required for growth in host cells. Infect Immun 2015;83:3015–25. doi:10.1128/IAI.00004-15.

[284] **Kadzhaev K, Zingmark C, Golovliov I, Bolanowski M, Shen H, Conlan W, et al.** Identification of Genes Contributing to the Virulence of Francisella tularensis SCHU S4 in a Mouse Intradermal Infection Model. PLoS One 2009;4:e5463. doi:10.1371/journal.pone.0005463.

[285] **Su J, Yang J, Zhao D, Kawula TH, Banas JA, Zhang J-R**. Genome-wide identification of Francisella tularensis virulence determinants. Infect Immun 2007;75:3089–101. doi:10.1128/IAI.01865-06.

[286] **Maier TM, Pechous R, Casey M, Zahrt TC, Frank DW**. In vivo Himar1-based transposon mutagenesis of Francisella tularensis. Appl Environ Microbiol 2006;72:1878–85. doi:10.1128/AEM.72.3.1878-1885.2006.

[287] **Brissac T, Ziveri J, Ramond E, Tros F, Kock S, Dupuis M, et al**. Gluconeogenesis, an essential metabolic pathway for pathogenic Francisella. Mol Microbiol 2015;98:518–34. doi:10.1111/mmi.13139.

[288] **Chamberlain RE**. Evaluation of live Tularemia vaccine prepared in a chemically defined medium. Appl Microbiol 1965;13:232–5.

[289] **Fan K, Barendsen N, Sensenbrenner L, Chen BD**. Deregulation of granulocyte-macrophage colony-stimulating factor (GM-CSF) receptor in murine macrophage cell line J774A.1. J Cell Physiol 1993;154:535–42. doi:10.1002/jcp.1041540312.

[290] **Dang C V, Le A, Gao P**. MYC-induced cancer cell energy metabolism and therapeutic opportunities. Clin Cancer Res 2009;15:6479–83. doi:10.1158/1078-0432.CCR-09-0889.

[291] **Corton JM, Gillespie JG, Hawley SA, Hardie DG**. 5-Aminoimidazole-4-Carboxamide Ribonucleoside. A Specific Method for Activating AMP-Activated Protein Kinase in Intact Cells? Eur J Biochem 1995;229:558–65. doi:10.1111/j.1432-1033.1995.0558k.x.

[292] **Hardie DG, Ross FA, Hawley SA**. AMPK: a nutrient and energy sensor that

maintains energy homeostasis. Nat Rev Mol Cell Biol 2012;13:251–62. doi:10.1038/nrm3311.

[293] **Rodriguez SA, Davis G, Klose KE**. Targeted gene disruption in Francisella tularensis by group II introns. Methods 2009;49:270–4. doi:10.1016/j.ymeth.2009.04.011.

[294] **Ackerman RS, Cozzarelli NR, Epstein W**. Accumulation of toxic concentrations of methylglyoxal by wild-type Escherichia coli K-12. J Bacteriol 1974;119:357–62.

[295] **Zimmermann R, Lass A, Haemmerle G, Zechner R**. Fate of fat: The role of adipose triglyceride lipase in lipolysis. Biochim Biophys Acta - Mol Cell Biol Lipids 2009;1791:494–500. doi:10.1016/J.BBALIP.2008.10.005.

[296] **Schweiger M, Eichmann TO, Taschler U, Zimmermann R, Zechner R, Lass A**. Measurement of lipolysis. Methods Enzymol 2014;538:171–93. doi:10.1016/B978-0-12-800280-3.00010-4.

[297] **Mayer N, Schweiger M, Romauch M, Grabner GF, Eichmann TO, Fuchs E, et al.** Development of small-molecule inhibitors targeting adipose triglyceride lipase. Nat Chem Biol 2013;9:785–7. doi:10.1038/nchembio.1359.

[298] **Gesbert G, Ramond E, Tros F, Dairou J, Frapy E, Barel M, et al**. Importance of Branched-Chain Amino Acid Utilization in Francisella Intracellular Adaptation. Infect Immun 2015;83:173–83. doi:10.1128/IAI.02579-14.

[299] **Ramond E, Gesbert G, Rigard M, Dairou J, Dupuis M, Dubail I, et al**. Glutamate utilization couples oxidative stress defense and the tricarboxylic acid cycle in Francisella phagosomal escape. PLoS Pathog 2014;10:e1003893. doi:10.1371/journal.ppat.1003893.

[300] **Gesbert G, Ramond E, Rigard M, Frapy E, Dupuis M, Dubail I, et al**. Asparagine assimilation is critical for intracellular replication and dissemination of *F rancisella*. Cell Microbiol 2014;16:434–49. doi:10.1111/cmi.12227.

[301] **Weinhouse S, Warburg O, Burk D, Shade AL.** On Respiratory Impairment in Cancer Cells. Science (80-) 1956;124(3215):269-70.

[302] **Larsson P, Oyston PCF, Chain P, Chu MC, Duffield M, Fuxelius H-H, et al.** The complete genome sequence of Francisella tularensis, the causative agent of tularemia. Nat Genet 2005;37:153–9. doi:10.1038/ng1499.

[303] **Eylert E, Herrmann V, Jules M, Gillmaier N, Lautner M, Buchrieser C, et al.** Isotopologue profiling of Legionella pneumophila: role of serine and glucose as carbon substrates. J Biol Chem 2010;285:22232–43. doi:10.1074/jbc.M110.128678.

[304] **Götz A, Eylert E, Eisenreich W, Goebel W**. Carbon metabolism of enterobacterial human pathogens growing in epithelial colorectal adenocarcinoma (Caco-2) cells. PLoS One 2010;5:e10586. doi:10.1371/journal.pone.0010586.

[305] **Lucchini S, Liu H, Jin Q, Hinton JCD, Yu J**. Transcriptional adaptation of Shigella flexneri during infection of macrophages and epithelial cells: insights into the strategies of a cytosolic bacterial pathogen. Infect Immun 2005;73:88–102. doi:10.1128/IAI.73.1.88-102.2005.

[306] **Grubmüller S, Schauer K, Goebel W, Fuchs TM, Eisenreich W**. Analysis of carbon substrates used by Listeria monocytogenes during growth in J774A.1 macrophages suggests a bipartite intracellular metabolism. Front Cell Infect Microbiol 2014;4:1–14. doi:10.3389/fcimb.2014.00156.

[307] **Keim P, Johansson A, Wagner DM**. Molecular Epidemiology, Evolution, and Ecology of Francisella. Ann N Y Acad Sci 2007;1105:30–66. doi:10.1196/annals.1409.011.

[308] **Raghunathan A, Shin S, Daefler S, McLendon M, Apicella M, Allen L, et al.** Systems approach to investigating host-pathogen interactions in infections with the biothreat agent Francisella. Constraints-based model of Francisella tularensis. BMC Syst Biol 2010;4:118. doi:10.1186/1752-0509-4-118.

[309] **Uyeda K.** Phosphofructokinase. Adv Enzymol Relat Areas Mol Biol 1979;48:193–244.

[310] **Hines JK, Kruesel CE, Fromm HJ, Honzatko RB**. Structure of inhibited fructose-1,6-bisphosphatase from Escherichia coli: distinct allosteric inhibition sites for AMP and glucose 6-phosphate and the characterization of a gluconeogenic switch. J Biol Chem 2007;282:24697–706. doi:10.1074/jbc.M703580200.

[311] **Warner JB, Lolkema JS**. CcpA-dependent carbon catabolite repression in bacteria. Microbiol Mol Biol Rev 2003;67:475–90. doi:10.1128/MMBR.67.4.475-490.2003.

[312] **Ogasawara J, Sakurai T, Kizaki T, Ishibashi Y, Izawa T, Sumitani Y, et al.** Higher Levels of ATGL Are Associated with Exercise-Induced Enhancement of Lipolysis in Rat Epididymal Adipocytes. PLoS One 2012;7:e40876. doi:10.1371/journal.pone.0040876.

[313] **LoVullo ED, Sherrill LA, Perez LL, Pavelka MS**. Genetic tools for highly pathogenic Francisella tularensis subsp. tularensis. Microbiology 2006;152:3425–35. doi:10.1099/mic.0.29121-0.

[314] **LoVullo ED, Molins-Schneekloth CR, Schweizer HP, Pavelka MS**. Single-copy chromosomal integration systems for Francisella tularensis. Microbiology 2009;155:1152–63. doi:10.1099/mic.0.022491-0.

[315] **Ventola CL**. The antibiotic resistance crisis: causes and threats. P T J 2015;40:277–83.

[316] **Piddock LJV**. The crisis of no new antibiotics-what is the way forward? Lancet Infect Dis 2012;12:249–53. doi:10.1016/S1473-3099(11)70316-4.

[317] **Rosenbluth DB, Wilson K, Ferkol T, Schuster DP**. Lung function decline in cystic fibrosis patients and timing for lung transplantation referral. Chest 2004;126:412–9. doi:10.1378/chest.126.2.412.

[318] **Maliniak ML, Stecenko AA, McCarty NA**. A longitudinal analysis of chronic MRSA and Pseudomonas aeruginosa co-infection in cystic fibrosis: A single-center study. J Cyst Fibros 2016;15:350–6. doi:10.1016/j.jcf.2015.10.014.

[319] **Jorth P, Staudinger BJ, Wu X, Bruce JE, Yahr TL, Singh Correspondence PK, et al.** Regional Isolation Drives Bacterial Diversification within Cystic Fibrosis Lungs. Cell Host Microbe 2015;18:307–19. doi:10.1016/j.chom.2015.07.006.

[320] **Winstanley C, O'Brien S, Brockhurst MA**. Pseudomonas aeruginosa Evolutionary Adaptation and Diversification in Cystic Fibrosis Chronic Lung Infections. Trends Microbiol 2016;24:327–37. doi:10.1016/j.tim.2016.01.008.

[321] **Smith H. The role of microbial interactions in infectious disease**. Philos Trans R Soc Lond B Biol Sci 1982;297:551–61. doi:10.1098/rstb.1982.0060.

[322] **Hajishengallis G, Liang S, Payne MA, Hashim A, Jotwani R, Eskan MA, et al.** Low-abundance biofilm species orchestrates inflammatory periodontal disease through the commensal microbiota and complement. Cell Host Microbe 2011;10:497–506. doi:10.1016/j.chom.2011.10.006.

[323] **Stacy A, McNally L, Darch SE, Brown SP, Whiteley M**. The biogeography of polymicrobial infection. Nat Rev Microbiol 2016;14:93–105. doi:10.1038/nrmicro.2015.8.

[324] **Knight R, Callewaert C, Marotz C, Hyde ER, Debelius JW, McDonald D, et al.** The Microbiome and Human Biology. Annu Rev Genomics Hum Genet 2017;18:65–86. doi:10.1146/annurev-genom-083115-022438.

[325] **Fredrickson AG, Stephanopoulos G**. Microbial competition. Science (80-) 1981;213:972–9. doi:10.1126/science.7268409.

[326] **Wintermute EH, Silver PA**. Emergent cooperation in microbial metabolism. Mol

Syst Biol 2010;6:407. doi:10.1038/msb.2010.66.

[327] **Price-Whelan A, Dietrich LEP, Newman DK**. Rethinking “secondary” metabolism: Physiological roles for phenazine antibiotics. Nat Chem Biol 2006;2:71–8. doi:10.1038/nchembio764.

[328] **Yurtsev EA, Conwill A, Gore J**. Oscillatory dynamics in a bacterial cross-protection mutualism. Proc Natl Acad Sci U S A 2016;113:6236–41. doi:10.1073/pnas.1523317113.

[329] **Van Der Gast CJ, Walker AW, Stressmann FA, Rogers GB, Scott P, Daniels TW, et al.** Partitioning core and satellite taxa from within cystic fibrosis lung bacterial communities. ISME J 2011;5:780–91. doi:10.1038/ismej.2010.175.

[330] **Ramirez MS, Tolmasky ME**. Aminoglycoside modifying enzymes. Drug Resist Updat 2010;13:151–71. doi:10.1016/j.drup.2010.08.003.

[331] **Hausner M, Wuertz S**. High rates of conjugation in bacterial biofilms as determined by quantitative in situ analysis. Appl Environ Microbiol 1999;65:3710–3.

[332] **Savage VJ, Chopra I, O’Neill AJ**. Staphylococcus aureus biofilms promote horizontal transfer of antibiotic resistance. Antimicrob Agents Chemother 2013;57:1968–70. doi:10.1128/AAC.02008-12.

[333] **Maheshwari M, Ahmad I, Althubiani AS**. Multidrug resistance and transferability of blaCTX-M among extended-spectrum β-lactamase-producing enteric bacteria in biofilm. J Glob Antimicrob Resist 2016;6:142–9. doi:10.1016/j.jgar.2016.04.009.

[334] **Regelmann WE, Elliott GR, Warwick WJ, Clawson CC**. Reduction of sputum Pseudomonas aeruginosa density by antibiotics improves lung function in cystic fibrosis more than do bronchodilators and chest physiotherapy alone. Am Rev Respir Dis 1990;141:914–21. doi:10.1164/ajrccm/141.4_Pt_1.914.

[335] **Smith AL, Redding G, Doershuk C, Goldmann D, Gore E, Hilman B, et al.** Sputum changes associated with therapy for endobronchial exacerbation in cystic fibrosis. J Pediatr 1988;112:547–54. doi:10.1016/S0022-3476(88)80165-3.

[336] **Chmiel JF, Davis PB**. State of the art: why do the lungs of patients with cystic fibrosis become infected and why can’t they clear the infection? Respir Res 2003;4:8. doi:10.1186/1465-9921-4-8.

[337] **Stanojevic S, Waters V, Mathew JL, Taylor L, Ratjen F**. Effectiveness of inhaled tobramycin in eradicating pseudomonas aeruginosa in children with cystic fibrosis. J Cyst Fibros 2014;13:172–8. doi:10.1016/j.jcf.2013.09.002.

[338] **Govan JR, Deretic V**. Microbial pathogenesis in cystic fibrosis: mucoid Pseudomonas aeruginosa and Burkholderia cepacia. Microbiol Mol Biol Rev 1996;60.

[339] **Ramsey BW, Pepe MS, Quan JM, Otto KL, Montgomery AB, Williams-Warren J, et al.** Intermittent administration of inhaled tobramycin in patients with cystic fibrosis. N Engl J Med 1999;340:23–30. doi:10.1056/NEJM199901073400104.

[340] **Ramphal R, Lhermitte M, Filliat M, Roussel P**. The binding of anti-pseudomonal antibiotics to macromolecules from cystic fibrosis sputum. J Antimicrob Chemother 1988;22:483–90. doi:10.1093/jac/22.4.483.

[341] **Khan MA, Ali ZS, Sweezey N, Grasemann H, Palaniyar N**. Progression of cystic fibrosis lung disease from childhood to adulthood: Neutrophils, neutrophil extracellular trap (NET) formation, and NET degradation. Genes (Basel) 2019;10. doi:10.3390/genes10030183.

[342] **Belvisi M, Barnes PJ, Larkin S, Yacoub M, Tadjkarimi S, Williams TJ, et al.** Nitric oxide synthase activity is elevated in inflammatory lung disease in humans. Eur J Pharmacol 1995;283:255–8. doi:10.1016/0014-2999(95)00421-g.

[343] **Rudkjøbing VB, Thomsen TR, Alhede M, Kragh KN, Nielsen PH, Johansen UR, et al.** The microorganisms in chronically infected end-stage and non-end-stage cystic fibrosis patients. FEMS Immunol Med Microbiol 2012;65:236–44. doi:10.1111/j.1574-695X.2011.00925.x.

[344] **Semaniakou A, Croll RP, Chappe V**. Animal models in the pathophysiology of cystic fibrosis. Front Pharmacol 2019;9. doi:10.3389/fphar.2018.01475.

[345] **Desai JD, Banat IM**. Microbial Production of Surfactants and Their Commercial Potential. vol. 61. 1997.

[346] **Nyström T**. Conditional senescence in bacteria: Death of the immortals. Mol Microbiol 2003;48:17–23. doi:10.1046/j.1365-2958.2003.03385.x.

[347] **Page R, Peti W**. Toxin-antitoxin systems in bacterial growth arrest and persistence. Nat Chem Biol 2016;12:208–14. doi:10.1038/nchembio.2044.

[348] **Unoson C, Wagner EGH**. A small SOS-induced toxin is targeted against the inner membrane in Escherichia coli. Mol Microbiol 2008;70:258–70. doi:10.1111/j.1365-2958.2008.06416.x.

[349] **Dörr T, Vulić M, Lewis K**. Ciprofloxacin causes persister formation by inducing the TisB toxin in Escherichia coli. PLoS Biol 2010;8:e1000317. doi:10.1371/journal.pbio.1000317.

[350] **Andreini C, Bertini I, Cavallaro G, Holliday GL, Thornton JM**. Metal ions in biological catalysis: From enzyme databases to general principles. J Biol Inorg Chem 2008;13:1205–18. doi:10.1007/s00775-008-0404-5.

[351] **Becker KW, Skaar EP**. Metal limitation and toxicity at the interface between host and pathogen. FEMS Microbiol Rev 2014;38:1235–49. doi:10.1111/1574-6976.12087.

[352] **Damo SM, Kehl-Fie TE, Sugitani N, Holt ME, Rathi S, Murphy WJ, et al.** Molecular basis for manganese sequestration by calprotectin and roles in the innate immune response to invading bacterial pathogens. Proc Natl Acad Sci U S A 2013;110:3841–6. doi:10.1073/pnas.1220341110.

[353] **Spirig T, Malmirchegini GR, Zhang J, Robson SA, Sjodt M, Liu M, et al.** Staphylococcus aureus uses a novel multidomain receptor to break apart human hemoglobin and steal its heme. J Biol Chem 2013;288:1065–78. doi:10.1074/jbc.M112.419119.

[354] **Noinaj N, Easley NC, Oke M, Mizuno N, Gumbart J, Boura E, et al.** Structural basis for iron piracy by pathogenic Neisseria. Nature 2012;483:53–61. doi:10.1038/nature10823.

[355] **Eshraghi A, Kim J, Walls AC, Ledvina HE, Miller CN, Ramsey KM, et al.** Secreted Effectors Encoded within and outside of the Francisella Pathogenicity Island Promote Intramacrophage Growth. Cell Host Microbe 2016;20:573–83. doi:10.1016/j.chom.2016.10.008.

[356] **Clemens DL, Lee BY, Horwitz MA**. The Francisella Type VI secretion system. Front Cell Infect Microbiol 2018;8:121. doi:10.3389/fcimb.2018.00121.

[357] **Clemens DL, Lee BY, Horwitz MA**. Virulent and avirulent strains of Francisella tularensis prevent acidification and maturation of their phagosomes and escape into the cytoplasm in human macrophages. Infect Immun 2004;72:3204–17. doi:10.1128/IAI.72.6.3204-3217.2004.

[358] **Mohapatra NP, Soni S, Rajaram MVS, Dang PM-C, Reilly TJ, El-Benna J, et al.** Francisella Acid Phosphatases Inactivate the NADPH Oxidase in Human Phagocytes . J Immunol 2010;184:5141–50. doi:10.4049/jimmunol.0903413.

[359] **McCaffrey RL, Schwartz JT, Lindemann SR, Moreland JG, Buchan BW, Jones BD, et al.** Multiple mechanisms of NADPH oxidase inhibition by type A and type B Francisella tularensis . J Leukoc Biol 2010;88:791–805. doi:10.1189/jlb.1209811.

[360] **Brunton J, Steele S, Ziehr B, Moorman N, Kawula T**. Feeding Uninvited Guests: MTOR and AMPK Set the Table for Intracellular Pathogens. PLoS

Pathog 2013; 9(10):e1003552. doi:10.1371/journal.ppat.1003552.

[361] **Inoki K, Kim J, Guan K-L**. AMPK and mTOR in Cellular Energy Homeostasis and Drug Targets. Annu Rev Pharmacol Toxicol 2012;52:381–400. doi:10.1146/annurev-pharmtox-010611-134537.